

**REGULATION OF BIOCHEMICAL AND MORPHOLOGICAL  
FEATURES OF CHEMICAL- AND RECEPTOR-MEDIATED  
APOPTOSIS IN JURKAT T CELLS**

Thesis submitted for the degree of  
Doctor of Philosophy  
at the University of Leicester

by

Victoria Louise Johnson BSc (Leicester)  
Department of Biochemistry  
University of Leicester

**August 2000**

UMI Number: U138439

All rights reserved

INFORMATION TO ALL USERS

The quality of this reproduction is dependent upon the quality of the copy submitted.

In the unlikely event that the author did not send a complete manuscript and there are missing pages, these will be noted. Also, if material had to be removed, a note will indicate the deletion.



UMI U138439

Published by ProQuest LLC 2013. Copyright in the Dissertation held by the Author.  
Microform Edition © ProQuest LLC.

All rights reserved. This work is protected against  
unauthorized copying under Title 17, United States Code.



ProQuest LLC  
789 East Eisenhower Parkway  
P.O. Box 1346  
Ann Arbor, MI 48106-1346

# **REGULATION OF BIOCHEMICAL AND MORPHOLOGICAL FEATURES OF CHEMICAL- AND RECEPTOR-MEDIATED APOPTOSIS IN JURKAT T-CELLS**

Victoria L. Johnson, Centre for Mechanisms of Human Toxicity,  
University of Leicester

Evidence suggests that the signalling events which occur after apoptotic stimulation, define two basic mechanisms for the induction of apoptosis. The first is dependent on signalling via the mitochondria and the second is dependent upon signalling directly from the death receptors. After induction of apoptosis, there is a convergence in signalling at the level of caspase activation and subsequent biochemical and morphological changes. Therefore the efficacy of various inhibitors of apoptosis is dependent upon the initiating signal. In order to understand the apoptotic pathway, the mechanisms by which these inhibitors regulate chemical- and receptor-mediated apoptosis must be understood. The anti-apoptotic oncoprotein, Bcl-2, was shown to inhibit both staurosporine and Fas-mediated apoptosis in a manner which was partially dependent upon the level of Bcl-2 protein expressed. During both staurosporine and Fas-induced apoptosis Bcl-2 acted downstream of caspase-8 activation. High levels of Bcl-2 expression did not effectively inhibit apoptosis induced by anti-Fas but inhibited AICD by inhibiting the secretion of sFasL at a level above caspase-8 activation. The peptide based caspase inhibitor z-VAD-FMK resulted in a novel nuclear morphological change, characterized by partially condensed nuclear morphology and could be dissociated from the externalisation of PS, HMW DNA fragmentation and preceded the appearance of a condensed nuclear morphology during staurosporine-induced apoptosis. Furthermore, the appearance of the partially condensed nuclear morphology was independent of effector caspases. The nuclear morphological change occurred downstream of cytochrome c release, disruption of mitochondrial membrane potential and could be inhibited by Bcl-2. Finally the role of caspase-3 and DFF40/45 were examined in staurosporine- and Fas-mediated apoptosis. Using the MCF-7 cell line, it was found that caspase-3 and DFF40/45 were dispensable for the formation of HMW DNA fragments. Furthermore, the serine protease inhibitor, TPCK which has been previously shown to inhibit oligonucleosomal-length DNA fragmentation, was found to exert this effect by acting downstream of DFF40 activation.

## **Acknowledgements**

The work presented in this thesis was carried out in the Centre for Mechanisms of Human Toxicity, University of Leicester and funded by the Medical Research Council. I would like to thank the MRC for financial support and the opportunity for travel to international meetings. I would also like to thank NORFA for generously providing me with the opportunities to attend regular conferences and present my work to distinguished audiences. I would like to begin by taking this opportunity to thank the many friends and colleagues who have made my time in Leicester, and the completion of my PhD such a rewarding experience.

First and foremost I would like to express my gratitude to my supervisor Dr. Sek Chow who has given me this chance to prove myself. I thank him for his truly excellent supervision and guidance. It has been a great honour to work with such a dedicated scientist. I hope that some of his vast knowledge and expertise will show itself in my future scientific work.

I would especially like to thank Professor John Eriksson, Dr. George Kass, Dr. John Jenkins and Dr. Colin Hewitt for their faith in my abilities, their friendly support and encouragement and the experience of rewarding collaborative work. I would also like to thank Tim Holmstrom, Stefanie Tran, Richard Jones and Richard Cooper.

There are many people who have supported me during my time at Leicester. I would like to thank those in my department, past and present, who have advised, encouraged, listened and been true friends, namely Wendy Merrison, Melanie Leech, William Coward, Gail Walker, Kirk Bedford, Gwen Draycott, Melanie Gould, Tracey Wright, Matthew Scullion, Christopher Hatton, Dave Brown and Stanley Ko, without whom it would have been literally impossible to write this thesis. It has been a pleasure working with them all.

At this point I would like to thank my new supervisor at the University of Manchester, Dr. Stephen Taylor, for the opportunity to further my scientific career and his patience and understanding during the completion of this work. I am looking forward to making excellent discoveries under his guidance. I would also like to thank my new colleagues and friends who have so far made my time in Manchester an enjoyable one.

To my many other friends who deserve special mention, particularly those from St.James, who have watched over me and been like a second family during my time in Leicester. I owe them a great deal and thank them heartily for their care and encouragement. I must particularly thank Margaret and Arnold Terry, Rev. Glynn Richerby, Ian and Annette Jones, Susan Hockings, Graham Jagger, Thomas Moore and Victoria Felstead. They have been my home from home and the base from which I have been able to grow as a whole person and not just as a scientist.

I would like to thank my family who are my life's sure foundation; their support and love has always been unconditional and their belief in me has helped me believe in myself. They have taught me the importance of keeping my feet on the ground and coping with life's worries and troubles by laughing and remembering the bigger picture. I dedicate this work to them and Mr Ross Graham FRCVS who lived his life standing for scientific truth and integrity, I hope to emulate his philosophy.

Finally I would like to thank God, to whom my life is dedicated.

## **ORIGINAL PUBLICATIONS**

V.L.Johnson, S.C.W.Ko, T.H.Holmstrom, J.E.Eriksson and S.C.Chow (2000). Effector caspases are dispensable for the early morphological changes during chemical-induced apoptosis. *Journal of Cell Science* 113, 2941-2953.

S.C.W.Ko, V.L.Johnson and S.C.Chow (2000). Functional characterization of Jurkat T cells rescued from CD95/Fas-induced apoptosis through the inhibition of caspases. *Biochemical and Biophysical Research Communications* 270, 1009-1015.

V.L.Johnson, I.R.Cooper, J.R.Jenkins and S.C.Chow (1999). Effects of differential overexpression of Bcl-2 on apoptosis, proliferation and telomerase activity in Jurkat T cells. *Experimental Cell Research* 252, 175-184.

R.A.Jones, V.L.Johnson, R.H.Hinton, G.G.Poirier, S.C.Chow and G.E.N.Kass (1999). Liver Poly(ADP-ribose) polymerase is resistant to cleavage by caspases. *Biochemical and Biophysical Research Communications* 256, 436-441.

R.A.Jones, V.L.Johnson, N.R.Buck, M.Dobrota, R.H.Hinton, S.C.Chow and G.E.N.Kass (1998). Fas-mediated apoptosis in mouse hepatocytes involves the processing and activation of caspases. *Hepatology* 27, 1632-1642.

T.H.Holmström, S.E.F.Tran, V.L.Johnson, N.G.Ahn, S.C.Chow and J.E.Eriksson (1999). Inhibition of mitogen-activated kinase signalling sensitizes HeLa cells to Fas receptor-mediated apoptosis. *Molecular and Cellular Biology* 19, 5991-6002.

T.H. Holmström, I. Schmitz, T.S.Söderstrom, M.Poukkula, V.L.Johnson, S.C.Chow, P.H.Krammer and J.E Eriksson (2000). MAPK/ERK signalling in activated T cells inhibits CD95/Fas-mediated apoptosis downstream of DISC assembly. *EMBO J.* 19, 5418-5428.

## Abbreviations

Ac-YVAD-CMK	<i>N</i> -acetyl-Tyr-Val-Ala-Asp-fluoromethylketone
AFC	7-amino-4-trifluoromethylcoumarin
AICD	activation induced cell death
AIF	apoptosis inducing factor
AMC	7-amino-4-methylcoumarin
Anti-Fas	human anti-Fas R antibody
Apaf-1	apoptotic protease activating factor-1
BH1-4	Bcl-2 homology domains 1-4
CAGE	conventional agarose gel electrophoresis
CARD	caspase recruitment domain
DD	death domain
DED	death effector domain
DFF	DNA fragmentation factor
DISC	death inducing signalling complex
DR	death receptor
ER	endoplasmic reticulum
FACS	fluorescence activated cell sorting
FADD	Fas associated death domain
FasL	Fas ligand
FIGE	field inversion gel electrophoresis
FITC	fluorescein-5-isothiocyanate
gld	generalised lymphoproliferative disorder
HMW	high molecular weight
HRP	horse radish peroxidase
ICE	interleukin 1 $\beta$ converting enzyme
IL-1 $\beta$	interleukin 1 $\beta$
IPTG	isopropyl $\beta$ -D-thiogalactosidase
IAP	inhibitor of apoptosis protein
LB	luria bertani
Lpr	lymphoproliferative
MAB	modified annexin buffer

MTS	3-45-dimethylthiazol-2-yl)-5-(3-carboxymethoxyphenyl)-2-(4-sulphonyl)-2H-tetrazolium, inner salt.
NF-AT	nuclear factor of activated T cells
NF-κB	nuclear factor κB
PAGE	polyacrylamide gel electrophoresis
PARP	poly(ADP)ribose polymerase
PBS	phosphate buffered saline
PHA	phytohaemagglutinin
PI	propidium iodide
PKC	protein kinase c
PMS	phenazine methosulfate
PS	phosphatidyl serine
PT	permeability transition
RIP	receptor interacting protein
SDS	sodium dodecyl sulphate
sFasL	soluble Fas ligand
SLE	systemic lupus erythematosus
Sts	staurosporine
TBS	tris-buffered saline
TG	thapsigargin
TNF	tumour necrosis factor
TNF-R1	tumour necrosis factor receptor 1
TRAIL	tumour necrosis factor-related apoptosis-inducing ligand
TPA	tetradecanoylphorbol-13-acetate
TPEN	N,N,N',N'-tetrakis(2-pyridylmethyl)ethylenediamine
TPCK	N-tosyl-L-phenylalanine chloromethylketone
TMRE	tetramethylrhodamineethyl ester (TMRE)
z-DEVD-FMK	benzyloxycarbonyl-Asp-Glu-Val-Asp fluoromethylketone
z-VAD-FMK	benzyloxycarbonyl-Val-Ala-Asp(OMe)fluoromethylketone

# CONTENTS

<b>Chapter One</b> .....	1
<b>Introduction</b> .....	2
1.1 Historical perspective .....	2
1.2 Forms of cell death, necrosis and apoptosis.....	3
1.3 Hallmarks of apoptosis.....	5
1.4 The genetic control of apoptosis.....	6
1.5 Mammalian homologues of <i>ced-3</i> , the caspases.....	7
1.5.1 Properties of the caspases.....	10
1.5.2 Prodomain length and sequence- <i>initiator and effector caspases</i> .....	11
1.5.3 Group I caspases.....	13
1.5.4 Group II caspases.....	13
1.5.5 Group III caspases.....	14
1.5.6 Substrate specificity of caspases.....	14
1.5.7 Caspases substrates.....	15
1.5.8 Inhibition of caspases.....	16
1.5.8.1 Naturally occurring caspase inhibitors, Crm-A, p35, IAP's.....	16
1.5.8.2 Peptide based caspase inhibitors.....	17
1.6 Apaf-1, the <i>ced-4</i> homologue .....	19
1.7 Mammalian homologues of <i>ced-9</i> , the <i>Bcl-2</i> family of oncoproteins.....	20
1.7.1 Structure and function of the Bcl-2 family of oncoproteins.....	21
1.7.2 Determination of cell fate by Bcl-2 family ratios.....	23
1.7.3 Localization of Bcl-2.....	24
1.7.4 Membrane channel function of Bcl-2.....	25
1.7.5 Further functions of Bcl-2.....	26
1.8 Induction of apoptosis.....	26
1.8.1 Induction of apoptosis via the mitochondria.....	26
1.8.2 Mitochondria and the permeability transition pore.....	27
1.8.3 Bcl-2 and the mitochondria.....	29
1.8.4 Receptor-mediated apoptosis.....	30
1.8.5 Role of Fas/FasL in disease.....	32
1.8.6 Apoptosis signalling through Fas.....	33
1.9 Aims and objectives.....	35

<b>Chapter Two</b>	36
<b>Materials and Methods</b>	36
<b>2.1 Cell Culture techniques</b>	37
2.1.1 Culture of Jurkat T cells	37
2.1.2 Culture of MCF-7 cells	37
2.1.3 Treatment of cells	37
<b>2.2 Biochemical assays</b>	38
2.2.1 Electrophoretic analysis of protein	38
2.2.1.1 Background	38
2.2.1.2 Preparation of gel buffers	39
2.2.1.3 Preparation of the lower resolving gel and Upper stacking gel	40
2.2.1.4 Preparation of samples for SDS PAGE	41
2.2.1.5 Determination of protein concentrations using the Biorad protein assay	42
2.2.1.6 SDS Polyacrylamide gel electrophoresis	42
2.2.1.7 Coomassie blue staining of protein in SDS polyacrylamide gels	42
2.2.2 Western transfer and immunodetection procedures	43
2.2.2.1 Immunodetection procedures	44
2.2.2.2 Washing and blocking buffers	44
2.2.2.3 Immunodetection of transferred protein	46
2.2.2.4 Double-immunodetection procedure	47
2.2.2.5 Analysis of sFasL secretion by Dot Blotting	47
2.2.3 DNA fragmentation analysis	48
2.2.3.1 Analysis of DNA fragmentation into oligonucleosomal -length fragments by convention agarose gel electrophoresis	48
2.2.3.2 Background	48
2.2.3.3 Preparation of agarose gel	48
2.2.3.4 Sample preparation	49
2.2.3.5 Field Inversion Gel Electrophoresis (FIGE) for analysis of HMW DNA fragments	49
2.2.3.6 Background	49

2.2.3.7	Preparation of cell samples in agarose plugs .....	50
2.2.3.8	Preparation of FIGE agarose gel.....	50
2.2.4	Column purification of His <sub>6</sub> tagged proteins using metal affinity resin.....	51
2.2.5	<i>In vitro</i> DFF nuclease assay.....	52
2.2.6	Analysis of cytochrome c release into cytosol during apoptosis.....	52
2.2.6.1	Optimisation of cell lysis using streptolysin O.....	53
2.2.7	Measurement of caspase enzymatic activity using fluorogenic substrates.....	55
2.2.7.1	Preparation of cell lysates.....	55
<b>2.3</b>	<b>Molecular Biology techniques.....</b>	<b>58</b>
2.3.1	Small scale preparation of plasmid DNA (mini-prep).....	58
2.3.2	Preparation of agarose gel and restriction enzyme digests.....	58
2.3.3	Generation and purification of bacterially expressed DFF protein complexes.....	59
2.3.3.1	Transformation of competent E.coli with PET-15b-DFF vector.....	59
2.3.3.2	Induction of DFF45 and His <sub>6</sub> tagged DFF40 protein expression in E.coli.....	60
<b>2.4</b>	<b>Cell Biology techniques.....</b>	<b>61</b>
2.4.1	Generation of Jurkat E6.1 cell clones overexpressing Bcl-2/Bcl-xl by electroporation.....	61
2.4.1.1	Preparation of conditioned media.....	61
2.4.1.2	Limiting dilution of transfected Jurkat cells.....	62
2.4.1.3	Expansion of clones derived from a single cell.....	62
2.4.2	Techniques for cellular fluorescence staining.....	64
2.4.2.1	Assessment of apoptosis by Hoechst 33358.....	64
2.4.2.2	Annexin V-FITC/Hoechst 33358 double staining.....	65
2.4.2.3	Detection of mitochondrial membrane depolarization using TMRE.....	65
2.4.2.4	Staining for cell surface antigens-FasL (non-permeabilized cells).....	66
2.4.2.5	Intracellular staining for FasL (permeabilized cells).....	66
2.4.2.6	Analysis of cell growth kinetics.....	67

2.4.2.7 Cell cycle analysis.....	67
2.4.2.8 Electron microscopy.....	67
2.4.2.9 Assessment of cell viability.....	68
<b>Chapter Three.....</b>	<b>69</b>
<b>Effect of differential Bcl-2 overexpression on chemical- and receptor-mediated apoptosis in Jurkat T cells.....</b>	<b>69</b>
3.1 Introduction.....	70
3.2 Results.....	73
3.2.1 Generation of stable Jurkat T cell clones overexpressing Bcl-2 and Bcl-xl.....	73
3.2.2 Induction of apoptosis in wild type Jurkat T cells using staurosporine and anti-Fas.....	77
3.2.3 Time dependent activation of caspase in wild type Jurkat T cells after treatment with staurosporine or anti-Fas.....	79
3.2.4 Effect of differential overexpression of Bcl-2 on staurosporine- and Fas-induced apoptosis in Jurkat T cell clones.....	83
3.2.5 Effect of differential overexpression of Bcl-2 on caspase processing during staurosporine- and Fas-mediated apoptosis.....	86
3.2.6 Effect of Bcl-2 overexpression on the time-dependent processing of caspase-8 and caspase-3 during staurosporine- and anti-Fas-mediated apoptosis.....	88
3.2.7 Effect of Bcl-2 overexpression on cell proliferation.....	92
3.3 Discussion.....	94
<b>Chapter Four.....</b>	<b>98</b>
<b>Effect of Bcl-2 overexpression on activation-induced cell death in Jurkat T cells.....</b>	<b>99</b>
4.1 Introduction.....	99
4.2 Results.....	101
4.2.1 Effect of Bcl-2 overexpression on AICD in Jurkat T cells.....	101
4.2.2 Processing of caspase-8 and -3 during AICD in Bcl-2 overexpressing Jurkat T cells.....	104

4.2.3	Effect of Bcl-2 on FasL expression.....	106
4.2.4	Release of soluble FasL into the culture supernatants of treated wild type Jurkat cells.....	109
4.2.5	Release of sFasL into the culture supernatants of treated Bcl-2 overexpressing Jurkat T cell clones.....	111
4.3	Discussion.....	114
<b>Chapter Five.....</b>		<b>117</b>
<b>Effector caspase-independent nuclear morphological changes during chemical-induced apoptosis in Jurkat T cells.....</b>		<b>117</b>
5.1	Introduction.....	118
5.2	Results.....	120
5.2.1	Observation of a novel nuclear morphological change in staurosporine-treated Jurkat cells in the presence of caspase inhibitors.....	120
5.2.2	Ultrastructural characterization of partially condensed nuclear morphology.....	129
5.2.3	Dissociation of partially condensed nuclei from DNA fragmentation.....	130
5.2.4	Dissociation of partially condensed nuclear morphology from PS externalization and loss of cell volume.....	132
5.2.5	Caspase processing in Jurkat cells with a partially condensed nuclear morphology.....	137
5.2.6	Processing of caspase-3 to the p20 fragment correlates with the formation of the partially condensed nuclear morphology.....	144
5.2.7	Caspase-3 is dispensable for the formation of the partially condensed nuclear morphology.....	147
5.2.8	The partially condensed nuclear morphology occurs downstream of the mitochondrial release of cytochrome c.....	149
5.2.9	The partially condensed nuclear morphology occurs downstream of mitochondrial membrane depolarisation and is inhibited by Bcl-2.....	153
5.2.10	Induction of the partially condensed nuclear morphology in Jurkat cells by other chemical stimuli.....	158

5.3	Discussion .....	160
<b>Chapter Six</b> .....		<b>165</b>
<b>Role of caspase-3 and DFF40/45 in high molecular weight and oligonucleosomal-length DNA fragmentation during apoptosis</b> .....		<b>166</b>
6.1	Introduction .....	166
6.2	Results .....	168
6.2.1	Caspase-3 is not required for high molecular weight DNA fragmentation during staurosporine-induced apoptosis .....	168
6.2.2	Partial cleavage of DFF40/45 correlates to lack of oligonucleosomal-length DNA fragmentation .....	174
6.2.3	Effect of TPCK on apoptosis in Jurkat T cells .....	176
6.2.4	Effect of TPCK on HMW and oligonucleosomal-length DNA fragmentation in Fas-treated Jurkat cells .....	178
6.2.5	Effect of TPCK on HMW and oligonucleosomal-length DNA fragmentation in staurosporine-treated Jurkat cells .....	178
6.2.6	Effect of TPCK on caspase-3 processing and the cleavage of PARP and DEVD-AFC during Fas- and staurosporine-mediated apoptosis .....	182
6.2.7	Effect of TPCK on DFF45 cleavage during Fas- and staurosprine-mediated apoptosis .....	186
6.2.8	<i>In vitro</i> assay to determine the effect of TPCK on DFF40 activity .....	189
6.3	Discussion .....	193
<b>Chapter Seven</b> .....		<b>196</b>
7.0	General Discussion .....	197
7.1	Future work .....	202
<b>Chapter Eight</b> .....		<b>203</b>
8.0	References .....	204

## INDEX OF FIGURES

<b>Chapter One</b> .....	1
<b>Introduction</b> .....	2
<b>Figure 1.1</b> Genetic pathway for programmed cell death in <i>C.elegans</i> .....	6
<b>Figure 1.2</b> Schematic diagram of an archetypal caspase, showing large and small subunits divided by a linker region.....	10
<b>Figure 1.3</b> Schematic diagram of caspase family structure.....	12
<b>Figure 1.4</b> Design of tetrapeptide-based caspase inhibitors.....	18
<b>Figure 1.5</b> Summary of anti-apoptotic and pro-apoptotic members of the Bcl-2 oncoprotein family showing the Bcl-2 homology domains BH1, BH2, BH3 and BH4.....	22
<b>Figure 1.6</b> Determination of cell fate by anti-apoptotic and pro-apoptotic Bcl-2 family ratios.....	24
<b>Figure 1.7</b> Model for mitochondrial involvement in apoptosis.....	28
<b>Figure 1.8</b> Schematic representing structures of human Fas and FasL.....	31
<b>Figure 1.9</b> Modes of Fas/FasL interaction resulting in apoptosis.....	32
<b>Figure 1.10</b> Model for receptor mediated apoptosis.....	34
<b>Chapter Two</b> .....	36
<b>Materials and Methods</b>	
<b>Figure 2.1</b> Assembly of transfer sandwich for western blotting.....	43
<b>Figure 2.2</b> Determination of cell lysis by streptolysin O.....	54
<b>Figure 2.3</b> Determination of optimal A) protein concentration and B) DEVD substrate concentration for caspase-3 fluorogenic enzyme assay.....	57
<b>Chapter Three</b> .....	68
<b>Effect of differential Bcl-2 overexpression on chemical- and receptor -mediated apoptosis in Jurkat T cells</b> .....	69
<b>Figure 3.1</b> Effect of overexpression of Bcl-2 and Bcl-xl on cell viability in Jurkat T cells after treatment with staurosporine and anti-Fas.....	75

<b>Figure 3.2</b>	Expression of Bcl-2 protein levels in Bcl-2 transfected Jurkat T cell clones.....	76
<b>Figure 3.3</b>	Dose-response and time-course showing effects of staurosporine on A) apoptosis and B) viability in wild type Jurkat T cells.....	78
<b>Figure 3.4</b>	Time-dependent processing of caspase-2, -3, -7 and -8 in wild type Jurkat T cells (clone E6.1) in response to staurosporine.....	81
<b>Figure 3.5</b>	Time-dependent processing of caspase-2, -3, -7 and -8 in wild type Jurkat T cells in response to anti-Fas.....	82
<b>Figure 3.6A</b>	Effect of differential overexpression of Bcl-2 in Jurkat T cells on staurosporine-induced apoptosis.....	84
<b>Figure 3.6B</b>	Effect of differential overexpression of Bcl-2 in Jurkat T cells on anti-Fas-induced apoptosis.....	85
<b>Figure 3.7</b>	Processing of caspase-2, -3, -7, and -8 in Jurkat T cells clones overexpressing Bcl-2 after treatment with either staurosporine or anti-Fas.....	87
<b>Figure 3.8</b>	Effect of Bcl-2 on staurosporine- and Fas-mediated caspase-3 and caspase-8 processing.....	90
<b>Figure 3.9</b>	Inhibition of anti-Fas-induced caspase-2, -3, -7 and -8 processing in Jurkat T cells by z-VAD-FMK.....	91
<b>Figure 3.10</b>	Decreased cell proliferation in Jurkat T cell clones overexpressing Bcl-2.....	93
<b>Chapter Four</b>	.....	98
<b>Effect of Bcl-2 overexpression on activation- induced cell death in Jurkat T cells</b>	.....	98
<b>Figure 4.1A</b>	Effect of Bcl-2 overexpression on AICD in Jurkat T cells.....	102
<b>Figure 4.1B</b>	Effect of Bcl-2 overexpression on Jurkat T cell viability during AICD.....	103
<b>Figure 4.2</b>	Effect of Bcl-2 overexpression on caspase-8 and caspase-3 processing during AICD in Jurkat T cells.....	105
<b>Figure 4.3</b>	Relative levels of constitutive FasL expression in Bcl-2	

	overexpressing Jurkat T cell clones .....	107
<b>Figure 4.4</b>	Localization of FasL constitutively expressed in Bcl-2 overexpressing Jurkat T cell clones.....	108
<b>Figure 4.5</b>	Preliminary dot-blot to determine the optimum volume ( $\mu$ l) of cell culture supernatant required for sFasL detection.....	110
<b>Figure 4.6</b>	Dot blot showing the secretion of sFasL in cell culture supernatants of treated Jurkat T cell clones overexpressing Bcl-2.....	112
<b>Figure 4.7</b>	Analysis of sFasL secretion into the culture supernatants during AICD in Jurkat T cell clones overexpressing Bcl-2.....	113
 <b>Chapter Five</b> .....		117
	<b>Effector caspase-independent nuclear morphological change during chemical-induced apoptosis in Jurkat T cells</b> .....	117
<b>Figure 5.1</b>	Distinct nuclear morphological changes in Jurkat T cells treated with staurosporine in the absence or presence of z-VAD-FMK.....	121
<b>Figure 5.2</b>	Effect of various concentrations of caspase inhibitors on staurosporine-treated Jurkat cells.....	124
<b>Figure 5.3</b>	Partially condensed nuclear morphology represents an early event during staurosporine-induced apoptosis.....	125
<b>Figure 5.4A</b>	The partially condensed nuclear morphological change represents an early event in staurosporine-induced apoptosis in Jurkat T cells.....	126
<b>Figure 5.4B</b>	Jurkat T cells with a partially condensed nuclear morphology became fully apoptotic after the removal of extracellular staurosporine and z-VAD-FMK.....	127
<b>Figure 5.5</b>	Ultra-structural analysis of Jurkat cells with partially condensed nuclear morphology.....	128
<b>Figure 5.6</b>	Effect of caspase inhibitors on chromatin cleavage in staurosporine-treated Jurkat T cells.....	131
<b>Figure 5.7A</b>	Effect of caspase inhibitors on binding of Annexin V-FITC in Jurkat T cells treated with staurosporine.....	134

<b>Figure 5.7B</b>	Flow cytometric analysis of annexin V-FITC binding in Jurkat T cells treated with staurosporine in the absence or presence of caspase inhibitors.....	135
<b>Figure 5.8</b>	Flow cytometric analysis of cell volume in Jurkat T cells treated with staurosporine in the absence or presence of caspase inhibitors.....	136
<b>Figure 5.9A</b>	Caspase processing in Jurkat T cells with a partially condensed nuclear morphology.....	140
<b>Figure 5.9B</b>	Effect of caspase inhibitors on z-VEID-AMC cleavage in staurosporine-treated Jurkat cells.....	141
<b>Figure 5.9C</b>	Cleavage of PARP in Jurkat T cells treated with staurosporine in the presence or absence of caspase inhibitors.....	142
<b>Figure 5.10</b>	Effect of caspase inhibitors on z-DEVD-AFC cleavage in staurosporine-treated Jurkat cells.....	143
<b>Figure 5.11A</b>	Effect of high concentrations of z-VAD-FMK on staurosporine-treated Jurkat cells.....	145
<b>Figure 5.11B</b>	Effect of high concentrations of z-VAD-FMK on caspase-3 processing in staurosporine-treated Jurkat T cells.....	146
<b>Figure 5.12</b>	Partially condensed nuclear morphology in MCF-7 cells treated with staurosporine.....	148
<b>Figure 5.13</b>	Cytochrome c release during staurosporine-induced apoptosis.....	151
<b>Figure 5.14</b>	Effect of caspase inhibitors on staurosporine-induced cytochrome c release in cells with partially condensed nuclear morphology.....	152
<b>Figure 5.15A</b>	Effect of caspase inhibitors on mitochondrial membrane potential in cells with partially condensed nuclear morphology.....	155
<b>Figure 5.15B</b>	Effect of high concentrations of z-VAD-FMK on mitochondrial membrane potential.....	156
<b>Figure 5.16</b>	Effect of Bcl-2 on the formation of a partially condensed nuclear morphology.....	157

<b>Chapter Six</b> .....	165
<b>Role of caspase-3 and DFF40/45 in oligonucleosomal-length and high molecular weight DNA fragmentation during apoptosis</b> .....	165
<b>Figure 6.1</b> Absence of caspase-3 in MCF-7 cells.....	170
<b>Figure 6.2</b> Comparison of staurosporine-induced apoptotic morphology in MCF-7 and Jurkat T cells.....	171
<b>Figure 6.3</b> Comparison of staurosporine-induced apoptosis and cell viability in MCF-7 and Jurkat T cells.....	172
<b>Figure 6.4</b> Comparison of oligonucleosomal-length and HMW DNA cleavage in MCF-7 and Jurkat T cells.....	173
<b>Figure 6.5</b> Effect of staurosporine on DFF45 and caspase-7 processing in MCF-7 and Jurkat T cells.....	175
<b>Figure 6.6</b> Effect of TPCK on receptor-mediated and chemical-induced apoptosis in Jurkat T cells.....	177
<b>Figure 6.7</b> Effect of TPCK on the formation of HMW and oligonucleosomal-length DNA fragments in anti-Fas-treated Jurkat T cells.....	180
<b>Figure 6.8</b> Effect of TPCK on formation of HMW and oligonucleosomal-length DNA fragments in staurosporine-treated Jurkat T cells.....	181
<b>Figure 6.9</b> Effect of TPCK on caspase-3 processing and PARP cleavage in Fas-treated Jurkat T cells.....	183
<b>Figure 6.10</b> Effect of TPCK on caspase-3 processing and PARP cleavage in staurosporine-treated Jurkat T cells.....	184
<b>Figure 6.11</b> Effect of TPCK on Ac-DEVD-AFC cleavage in Fas- and staurosporine-treated Jurkat T cells.....	185
<b>Figure 6.12</b> Effect of TPCK on DFF45 processing during Fas-mediated apoptosis.....	187
<b>Figure 6.13</b> Effect of TPCK on DFF45 processing during staurosporine-mediated apoptosis.....	188
<b>Figure 6.14</b> Induction of DFF40/45 expression from bacterial cultures.....	190

<b>Figure 6.15</b>	<i>Invitro</i> assay for DFF40/45 nuclease activity.....	191
<b>Figure 6.16</b>	Determination of recombinant caspase-3 enzymatic activity by measurement of DEVD-AFC cleavage.....	192
<b>Figure 6.17</b>	Temporal scheme for the potential role of TPCK in the regulation of DFF40/45 activity and HMW and oligonucleosomal-length DNA fragmentation .....	194

## **INDEX OF TABLES**

### **Chapter One**

Table 1.1 Distinctions between apoptosis and necrosis.....4

Table 1.2 Caspase characteristics and classifications.....9

### **Chapter Two**

Table 2.1 Preparation of lower resolving gel and upper stacking gel.....41

Table 2.2 Antibodies used for immunodetection procedures.....45

Table 2.3 Tables representing probability of obtaining a single cell clone .....63

### **Chapter Five**

Table 5.1 Induction of pre-apoptotic nuclei in Jurkat cells treated with  
etoposide or TPEN in the presence of z-VAD-FMK.....159

**CHAPTER ONE**  
**INTRODUCTION**

## **1.0 Introduction**

### **1.1 Historical perspective**

The survival and efficient functioning of any multicellular organism is highly dependent upon the rate of cell proliferation and cell death (Ellis et al., 1991; Raff, 1992). Under normal physiological conditions, these processes are in a state of homeostasis. However, when this delicate balance is disturbed it may result in, or be the result of, a variety of disorders in which the body cannot maintain this equilibrium within a population of cells. Although much is known about the mechanisms of cell proliferation, the relevance of cell death to normal physiological mechanisms and the pathogenesis of disease were underrated until recently when the full implications of aberrant cell death were realised (Thompson, 1995). The observation of a physiological deletion of specific cells in the context of the whole organism was first noted during the 1950's and 1960's in studies on vertebrate development (Glucksmann, 1951; Saunders J.W, 1966). In contrast to the violent form of cell death observed in response to tissue injury, the 'programmed cell death' observed was protracted, ordered and appeared to be genetically predetermined and an essential contributing factor to successful embryogenic maturation (Saunders J.W, 1966; Hammar and Mottet, 1971). Programmed Cell Death is the term applied to cell death in a developmental environment. It serves to sculpt and shape tissues, organs and even whole organisms (Kerr et al., 1972; Waring et al., 1991). It is responsible for palatal fusion, interdigital web deletion, development of the nervous system and the fine tuning of the immune system (Glucksmann, 1951; Pratt and Martin, 1975; Jacobson et al., 1997b). The phenomenon was later characterized morphologically in a seminal study by Kerr, Wyllie and Currie in 1972 and the process by which these programmed cell deaths occurred was termed 'Apoptosis', a word derived from the ancient Greek for 'falling off' and sometimes applied to the loss of damaged or dying leaves from trees. Once the process had been characterized morphologically (Kerr et al., 1972; Alles et al., 1991) it was possible to conclude that apoptosis may play a part in the development and functioning of almost all organisms (Arends and Wyllie, 1991).

## 1.2 Forms of cell death, necrosis and apoptosis

There are two major forms of cell death, necrosis and apoptosis (Buja et al., 1993). Both serve to rid the body of damaged or unwanted cells but can be distinguished as two separate arms of a highly evolved defence mechanism against varied pathological insults. Necrosis is often the result of acute irreversible physical damage, particularly to the cellular membrane, or severe trauma such as ischaemia. The effects of such an insult render the cell incapable of maintaining fluid balance due to a sudden influx of ions and water interfering with ATP synthesis and severely disrupting the intracellular environment (Cohen, 1993). This results in gross cellular swelling and enlargement of intracellular organelles such as the endoplasmic reticulum and mitochondria (Kroemer et al., 1998). The process does not depend on *de novo* synthesis of protein and is independent of ATP (Leist et al., 1999). It is for this reason that necrosis is often thought of as being passive. Other effects include the clumping of chromatin into ill-defined aggregates and random cleavage of DNA. Necrosis usually affects an area of tissue or a population of cells and eventually results in cell lysis, triggering an inflammatory response (Gerschenson and Rotello, 1992).

In contrast, apoptosis occurs asynchronously in individual cells which receive the stimuli to initiate an internally encoded suicide program where, for whatever reason, there is a default decision to die often requiring the expenditure of ATP (Liu et al., 1996; Richter et al., 1996; Tsujimoto, 1997). It is for this reason that apoptosis represents an active form of cellular suicide. Apoptosis, in contrast to necrosis, is a highly ordered and efficient process during which the cell is neatly disposed. Cell death is discrete; rather than swelling and inciting an inflammatory response, the cell shrinks and undergoes a form of internal autodigestion (Kerr, 1971). The stimuli for apoptosis are diverse and can originate from two potential sources; either extracellular, such as environmental factors, cell-cell interactions, cell-substrate interactions, hormones and growth factors; or intracellular sources including metabolic state, genotype, developmental history or cell damage (Williams et al., 1992).

**Table 1.1 Distinctions between apoptosis and necrosis**

<b>Apoptosis</b>	<b>Necrosis</b>
Physiological stimuli	Pathological stimuli
Affects scattered individual cells	Affects tracts of contiguous cells
Late stage swelling of organelles	Very early swelling of organelles
Cytoplasm and cell volume decrease	Cytoplasm and cell volume increase
Convolution of nuclear outline and breakdown (Karyorrhexis)	Disappearance (Karyolysis)
Sharply defined chromatin compaction and margination	Chromatin marginates as small ill defined aggregates
Cell fragments forming apoptotic bodies	Cell ruptures, swelling and disintegration
Cell fragments are phagocytosed	Cell contents are released

Adapted from (Gerschenson and Rotello, 1992)

The apoptotic cell can be clearly distinguished by a series of well defined morphological and biochemical changes (Kerr et al., 1972; Wyllie, 1980a). After recognition of a stimulatory signal a series of overlapping morphological changes occur (Cohen, 1993). The cell volume decreases dramatically, cytoplasmic organelles become compact and the cytoskeleton is disrupted (Gerschenson and Rotello, 1992). There is a reduction in nuclear size, condensation of chromatin to the nuclear periphery and nucleolar disintegration. Specialized surface structures are lost and the cell adopts a smooth surface. There is surface membrane 'blebbing' - a loss of membrane integrity and the nucleus and cytoplasm begin to fragment. The cell becomes a cluster of smooth, rounded apoptotic bodies. Specific cell surface molecules are externalized and signal to complementary molecules on phagocytes and macrophages which instigate clearance (Savill et al., 1993; Devitt et al., 2000), thus avoiding leakage of their potentially dangerous contents into the cellular environment. Finally, usually within the phagosome of an ingesting cell there is degeneration of residual nuclear and cytoplasmic structures and in culture this is seen as complete rupture and disappearance, where organelles become indistinguishable.

### 1.3 Hallmarks of Apoptosis.

By studying the biochemistry of apoptosis it is possible to recognise two distinct stages in the process (Steller, 1995). Firstly, after recognition of the external or internally derived signal, the cell becomes committed to death. At this point, there are no morphological changes and the cell can still enter division before the onset of apoptosis (Lazebnik et al., 1993). The second 'execution' phase is the point at which the hallmark features of apoptosis become distinguishable and apoptosis can be completed (Earnshaw, 1995). Many of these hallmarks can be used as a method for identifying and distinguishing apoptosis from necrosis. Commonly used features include nuclear condensation and the fragmentation of nuclear DNA into 180-200bp length fragments which can be observed as a laddering pattern upon conventional agarose gel electrophoresis of apoptotic cells (Wyllie, 1980a). This process is mediated by DFF45 (DNA Fragmentation Factor)/ICAD (Inhibitor of Caspase-activated DNase) which is inactivated during apoptosis to release the active nuclease activity of DFF40/CAD (Caspase-activated DNase) (Liu et al., 1997; Enari et al., 1998). Cleavage of the 116kDa DNA repair enzyme PARP to a characteristic 85kDa fragment is also a common feature of many forms of apoptosis (Lazebnik et al., 1994). However, the relevance of PARP cleavage to the apoptotic phenotype remains unclear (Nosseri et al., 1994). The externalization of phosphatidylserine (PS) to the outer leaflet of the plasma membrane can also serve as an exclusive marker for apoptosis. It can be detected using FITC-conjugated Annexin V, which in the presence of calcium ions, adheres to the externalized PS emitting a green fluorescence which can be quantified (Martin et al., 1995). The externalization of PS represents a dramatic reorganization of the plasma membrane culminating in the redistribution of many phospholipids which may act as markers for phagocyte recognition and apoptotic cell clearance (Savill et al., 1993; Fadok et al., 2000).

## 1.4 The Genetic control of apoptosis

To further elucidate the molecular mechanisms of apoptosis it was necessary to identify the genes that were involved in the process. Much of the preliminary work in identifying the genes responsible for apoptosis was carried out in the nematode worm *Caenorhabditis elegans* and provided evidence for an evolutionary conserved apoptotic pathway (Ellis and Horvitz, 1986; Ellis et al., 1991; Yuan, 1996). As a model organism the nematode had the advantage of having a well characterized developmental history during which a defined number of cells were observed to undergo programmed cell death. During *C.elegans* development 131 of its 1090 cells succumb to apoptosis. Therefore it was possible to trace the lineage of each cell throughout maturation. Mutations were studied and lead to the identification of 14 different genes, which could directly influence cell death (Ellis and Horvitz, 1986; Steller, 1995) (Figure 1.1). Three genes *ced-3*, *ced-4* and *ced-9* (*ced- cell death defective*) were found to be essential at the execution phase of the apoptotic pathway. The discovery of these genes has provided a molecular framework for cell death in many experimental systems (Chinnaiyan et al., 1997).

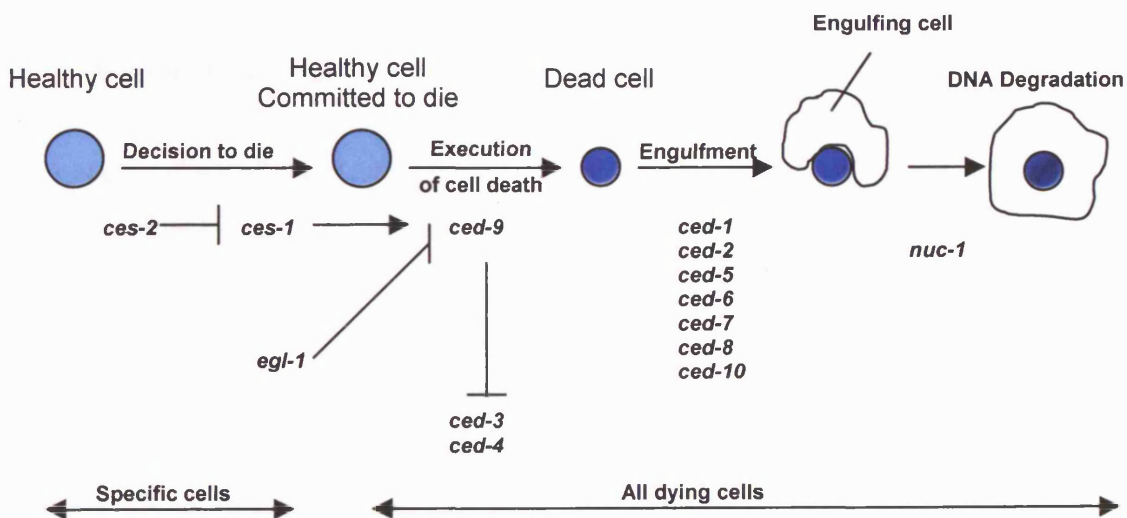


**Figure 1.1 Genetic pathway for programmed cell death in *C.elegans*.** Mutations in 14 different genes have been shown to affect specific stages of programmed cell death in *C.elegans*. Three genes *ced-3*, *ced-4* and *ced-9* affect the execution of the death program. *Ced-3* and *ced-4* promote, and *ced-9* prevents cell death. Adapted from (Steller, 1995).

Both *ced-3* and *ced-4* were found to be essential for cell death to occur. If either gene was inactivated, cells that normally died by apoptosis survived (Chinnaiyan et al., 1997; Wu et al., 1997b) and transfection of *ced-3* into a variety of cell types induced apoptosis (Yuan et al., 1993). The *ced-9* gene antagonizes the function of *ced-3* and *ced-4* by protecting cells from death (Hengartner et al., 1992; Hengartner and Horvitz, 1994; Spector et al., 1997). In *ced-9* loss of function mutants, cells that normally live undergo programmed cell death early in development. Conversely, *ced-9* gain of function mutants prevent cells from dying (Hengartner and Horvitz, 1994). *Ced-3*, *ced-4* and *ced-9* were all found to have highly related mammalian homologues whose functions had profound effects on apoptosis. The cloning of *ced-3* led to the observation that it encoded a putative protease that was related to the mammalian interleukin-1  $\beta$  converting enzyme (ICE) and was the first identified member of a new family of cysteine proteases, or caspases (Nicholson et al., 1995; Thornberry and Molineaux, 1995; Tewari et al., 1995b). The mammalian *ced-4* homologue was identified as APAF-1 (Apoptotic protease activating factor-1) (Zou et al., 1997; Vaux, 1997; Wu et al., 1997b) and the *ced-9* protein was found to have significant homology to members of the Bcl-2 oncoprotein family (Vaux et al., 1988; Hengartner et al., 1992; Hengartner and Horvitz, 1994).

### 1.5 Mammalian homologues of *ced-3*, *the caspases*

The gene product of *ced-3* was found to have 28% sequence identity to the mammalian protein interleukin-1  $\beta$  converting enzyme (ICE), which proteolytically cleaves pro-interleukin-1  $\beta$  (pro-IL-1 $\beta$ ) to its active mature form (Thornberry et al., 1992; Cerretti et al., 1992; Yuan et al., 1993). In addition, overexpression of ICE in fibroblasts provided compelling evidence for its involvement in apoptosis (Miura et al., 1993). These initial findings resulted in the subsequent discovery of a number of proteases with similar properties (Van de Craen et al., 1997). It soon became apparent that ICE represented a large family of cysteine proteases with distinct roles in inflammation and apoptosis (Cohen, 1997). These include ICH-1/ NEDD-2 (Kumar et al., 1994), CPP32/Yama/apopain (Fernandez-Alnemri et al., 1994; Tewari et al., 1995b; Casciola-Rosen et al., 1996), ICERel-II/TX/ICH-2 (Faucheu et al., 1995; Kamens et al., 1995), ICERel-III/TY/ICH-3 (Munday et al., 1995; Faucheu et al., 1996), Mch2 (Fernandes Alnemri et al., 1995), Mch3/ICE-LAP3/CMH-1 (Fernandes Alnemri et al., 1995; Duan et

al., 1996), FLICE1/MACH1/Mch5 (Boldin et al., 1995; Muzio et al., 1996), ICE-LAP6/Mch6 (Duan et al., 1996; Srinivasula et al., 1996b) and FLICE2/Mch4 (Fernandes-Alnemri et al., 1996; Vincenz and Dixit, 1997) (Table 1.2). Because many ICE/CED-3-like proteases were simultaneously identified and cloned by different groups, the identity of each caspase became swamped in an array of names and classifications. Therefore to consolidate the research in this area a common nomenclature was assigned based on the specificity of the enzymes for specifically cleaving substrates after an aspartic acid residue, hence the name 'Caspase' for cysteinyl aspartate specific protease (Alnemri et al., 1996). Later studies identified caspase-3 as being the mammalian ced-3 homologue and its central role in apoptosis was illustrated in caspase-3 deficient mice (Nicholson et al., 1995; Kuida et al., 1996). The caspase-3/ CPP32 deficient mice were generated by homologous recombination using a targeting vector where the catalytically active QACRG site was replaced with a neomycin resistance gene. The resulting mice were smaller than their littermates and displayed serious brain defects as a result of decreased neuronal apoptosis (Kuida et al., 1996).

**Table 1.2 Caspase characteristics and classifications**

CASPASE (MW) <sup>*</sup>	Other names	Optimal tetrapeptide preferences (P <sub>1</sub> -P <sub>4</sub> ) <sup>a</sup>	Group Classification <sup>b</sup>	Prodomain Length <sup>c</sup>	Role/Function	Active Subunits (MW) <sup>*</sup>	References
Caspase-1 (45kDa)	ICE, CED-3	(W/Y/F)EHD	I	Long, CARD	Inflammation	20/10kDa	(Thornberry et al., 1992)
Caspase-2 (51kDa)	ICH-1, NEDD-2	DXXD	II	Long, CARD	Initiator/effector	20/12 kDa	(Kumar et al., 1994)
Caspase-3 (32kDa)	CPP32, Apopain, Yama	DEXD	II	Short	Effector	17/12kDa	(Fernandes-Alnemri et al., 1994; Nicholson et al., 1996, Tewari et al.,1995)
Caspase-4 (43kDa)	ICErel-II, TX, ICH-2	(W/L/F)EHD	I	Long, CARD	Inflammation	20/10kDa	(Facheu et al., 1995)
Caspase-5 (48kDa)	ICErel-III, TY, ICH-3	(W/L/F)EHD	I	Long	Inflammation	20/10kDa	(Munday et al., 1995)
Caspase-6 (34kDa)	Mch2	(V/E/I)EXD	III	Short	Effector	18/11kDa	(Fernandes-Alnemri et al., 1995)
Caspase-7 (35kDa)	Mch3, ICE-LAP3, CMH-1	DEXD	II	Short	Effector	20/12kDa	(Boldin et al., 1996) (Duan et al., 1996)
Caspase-8 (55kDa)	FLICE-1, MACH1, Mch5	(L/V/D)EXD	III	Long, DED	Initiator	18/11 kDa	(Boldin et al., 1995)
Caspase-9 (45kDa)	ICE-LAP6, Mch6	(I/V/L)EXD	III	Long, CARD	Initiator	17/10 kDa	(Fernandes-Alnemri et al., 1996)
Caspase-10 (55kDa)	FLICE2, Mch4	XEXD	III	Long, DED	Initiator	17/12 kDa	(Vincenz and Dixit., 1997)
mCaspase-11(42kDa)	mICH-3 (murine)		I	Long	Inflammation	20/10 kDa	(Wang et al., 1996)
mCaspase-12 (50kDa)	mICH-4 (murine)		I	Long	Apoptosis	20/10kDa	(Van de Craen et al., 1997)
Caspase-13	ERICE		I	Long	Effector	20/10kDa	(Humke et al., 1998)
Caspase-14 (29.5kDa)	MICE		I	Short	Effector?		(Van de Craen et al., 1998)
<b>Invertebrate Caspases</b>							
CED-3 (56kDa)		DEXD	I	Long, CARD	Effector/Initiator	17/14kDa	(Ellis et al., 1996)
DCP-1 (36kDa)	Drosophila caspase-1	unknown	I	Short	Effector/Initiator	22/13kDa	

Adapted from Kidd., 1998, Wolf and Green., 1999.

\* MW-Molecular Weight

<sup>a</sup> X-denotes broad subsite amino acid specificity

<sup>b</sup> According to substrate preference

<sup>c</sup> Determinant of initiator/effector functions

### 1.5.1 Properties of the caspases

Caspases are synthesized as inactive proenzymes, which require proteolytic cleavage events to process them to the active enzyme (Thornberry et al., 1992; Nicholson and Thornberry, 1997). All of the caspase family members share a basic structure, consisting of a variable length N-terminal prodomain, a large subunit of ~20kDa and a small C-terminal subunit of ~10kDa (Walker et al., 1994; Cohen, 1997) (Figure 1.2). A pentapeptide motif, QACXG, where X represents R, Q or G, surrounds an active site cysteine residue and is found within the large subunit of all caspases (Thornberry et al., 1992). The large subunit is itself linked to the small C-terminal subunit via an interdomain linker region (Thornberry and Lazebnik, 1998). Activation of caspases requires cleavage at specific aspartate cleavage sites, which are found between the prodomain and large subunit and within the linker region (Cohen, 1997).

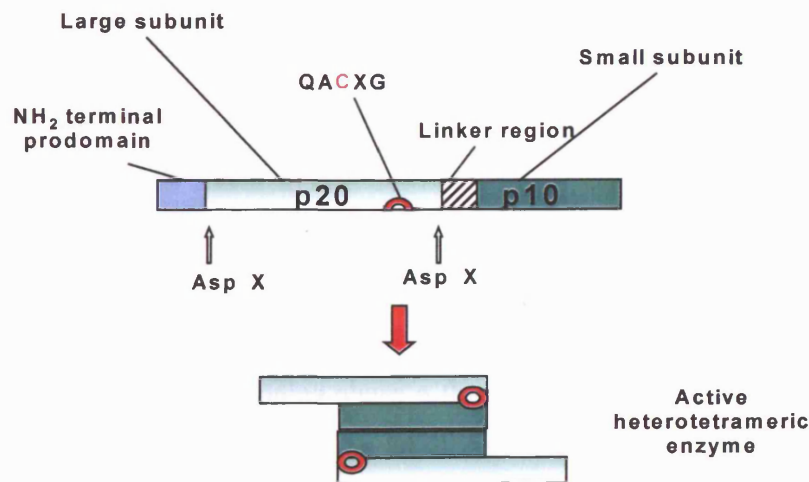


**Figure 1.2 Schematic diagram of an archetypal caspase, showing large and small subunits divided by a linker region.** Activation requires proteolytic cleavage between domains and removal of the prodomain. The large and small subunits associate to form heterodimers and the crystal structure of caspase-1 and caspase-3 reveal that the heterodimers associate to form a tetramer with two active sites. A conserved QACXG pentapeptide motif surrounds the active site cysteine residue.

This suggests a mechanism of autoproteolytic activity between caspases, which are thought to act in an amplifying proteolytic cascade (Hirata et al., 1998). Cleavage of caspases at these conserved sequences releases the prodomain and subunits resulting in the formation of two ~p10/~p20 heterodimers which associate to form an active heterotetramer (Thornberry et al., 1992; Walker et al., 1994; Wilson et al., 1994). There are two main differences within caspase protein structure, which contribute to diversity in function of family members. The first is prodomain length and sequence which is variable between caspases (23-216 amino acids) and can to some extent, determine hierarchy within the caspase cascade (Cryns and Yuan, 1998) (Figure 1.3). The second structural feature which affects caspase function, is substrate binding site specificity (Talanian et al., 1997; Thornberry et al., 1997). Taken together these features provide an integrated view of caspase function during the onset and execution of apoptosis (Wolf and Green, 1999).

### **1.5.2 Prodomain length and sequence -*initiator and effector caspases***

Caspases with long prodomains, such as caspase-2, -8, -9 and -10, tend to function at the apex of the cascade as 'initiators' in response to death inducing stimuli (Cohen, 1997; Ashkenazi and Dixit, 1998). Recent studies have suggested an important role for adapter protein-mediated-oligomerization of procaspases with long prodomains during apoptosis (Zhang et al., 1998; Li and Yuan, 1999). There are two types of prodomain dependent upon the presence of either a DED (death effector domain) or CARD (caspase recruitment domain) which are necessary for caspase interactions with other family members and other proteins of the apoptotic machinery (Li and Yuan, 1999; Aravind et al., 1999). NMR studies have shown that these domains share a three dimensional  $\alpha$ -helical structure and bind other molecules containing CARD or DED domains by hydrophilic or hydrophobic interactions, respectively (Chou et al., 1998; Eberstadt et al., 1998; Li and Yuan, 1999). Such motifs mediate protein-protein interactions between DED and CARD motifs found in adapter molecules such as FADD/MORT-1 (Fas-associating protein with a death domain) (Boldin et al., 1995; Chinnaiyan et al., 1995) and RAIDD (Receptor interacting

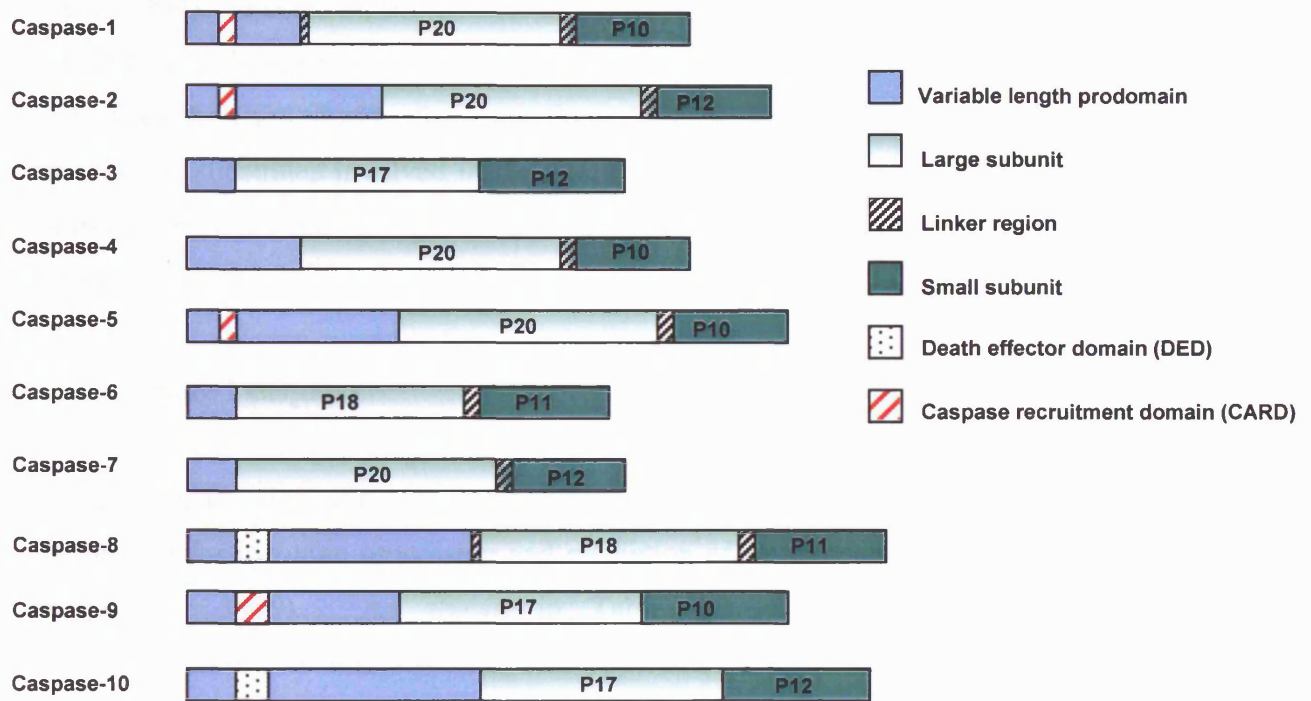


**Figure 1.3 Schematic diagram of caspase family structure.** Caspase pro-enzymes are represented showing the variable length prodomain containing DED and CARD motifs which influence initiator and effector functions. Caspases with long prodomains such as caspase-8, -9 and -10 tend to function as initiators at the apex of the caspase cascade whilst those such as caspase-3, -6 and -7 act as effectors. Adapted from Cohen, (1997).

protein RIP-associated ICH-1/CED-3-homologous protein with a death domain) (Duan and Dixit, 1997). The prodomains of procaspases-2 and -9, contain CARDS whereas the prodomains of procaspase-8 and -10 contain DED's (Li and Yuan, 1999). Procaspase-9 activation is mediated by Apaf-1, which also contains a CARD motif. Apaf-1 binds cytochrome c and subsequently recruits procaspase-9 causing oligomerization and activation (Li et al., 1997; Srinivasula et al., 1998). In contrast, procaspase-8 activation is mediated via its DED by FADD and subsequent recruitment to the death inducing signalling complex (DISC) at the receptor (Medema et al., 1997). Thus, the association between long prodomain caspases and adapter molecules via DED and CARD motifs establishes a link between death inducing stimuli and activation of downstream 'effector' caspases, such as caspase-3, -6 and -7. The prodomains either recruit the caspase to the activated death receptor complex or promote the formation of cytosolic apoptosis-inducing

complexes which can then activate downstream effector caspases (Whyte, 1996; Wolf and Green, 1999). In contrast, the effector caspases generally have short prodomains and lack the DED and CARD motifs found in initiator caspases (Wolf and Green, 1999) (Figure 1.3). They function during the execution phase of apoptosis and are able to cleave intracellular substrates involved in the maintenance of cell structure, inactivate apoptotic inhibitory proteins and deregulate normal protein function (Thornberry and Lazebnik, 1998).

### 1.5.3 Group I caspases

Group I caspases, including caspase-1, -4, -5, -11 and -13, represent activities that may be responsible for cytokine processing and mediation of inflammation, (Cohen, 1997; Wolf and Green, 1999). As shown in Table 1.2, Caspase-1, -4 and -5 prefer aromatic/hydrophobic amino acids in the P<sub>4</sub> position and share the preferential tetrapeptide sequence WEHD. This correlates well with the preferential processing of pro-interleukin-1 $\beta$  by caspase-1 at Asp<sup>116</sup>-Ala<sup>117</sup> to produce 17.5kDa cytokine (Thornberry et al., 1992; Cerretti et al., 1992; Kuida et al., 1995; Li et al., 1995). Caspase-4 and -5 differ from caspase-1 in their substrate specificities and are less capable of cleaving pro-interleukin-1 $\beta$ , implying a dependence not only on tetrapeptide sequence, but also tertiary protein structure in relation to enzyme function (Munday et al., 1995). Caspase-4 may be involved in the maturation of caspase-1 (Faucheu et al., 1995); and it is interesting to note that both caspase-1 and -4 contain CARDs, suggesting an upstream function for these enzymes in cytokine processing in inflammation (Gu et al., 1997). Group I caspases generally have long prodomains with the exception of the recently discovered caspase-14 which is proposed to be the first short prodomain member of the group I subfamily (Hu et al., 1998).

### 1.5.4 Group II caspases

Group II caspases include ced-3 and caspases-2, -3, and -7, and show a substrate specificity of optimal recognition sequence DEXD, requiring Asp in the P<sub>4</sub> position for efficient catalysis (Thornberry et al., 1997). With the exception of caspase-2, Group II caspases generally have short prodomains consistent with their function as 'effector'

caspases (Green, 1998). They are largely responsible for targeting specific cellular substrates and the ordered breakdown of cellular structures and gross morphological changes during apoptosis. Caspase-3 and -7 substrate specificities are almost indistinguishable although in most systems caspase-3 appears to be the major enzyme responsible for cellular substrate cleavage during apoptosis (Tewari et al., 1995b; Thornberry et al., 1997; Woo et al., 1998; Zheng et al., 1998). Both caspase-3 and -7 are able to cleave PARP at a DEVD motif (Kaufmann et al., 1993; Lazebnik et al., 1994) but may also co-operate to cleave the same substrate, for example DFF45, at different sites (Tang and Kidd, 1998).

### **1.5.5 Group III caspases**

Group III caspases include caspases-6, -8, -9 and -10. The group III caspases do not have a requirement for specific residues in the P<sub>4</sub> position but have preference for amino acids with larger aliphatic side chains such as leucine or valine (Talanian et al., 1997; Thornberry et al., 1997; Cryns and Yuan, 1998). The tetrapeptide motif preferred by group III caspases is (L/V)EXD (Thornberry et al., 1997). Caspase-6 is the only group III member to have a short prodomain and functions as an effector caspase cleaving nuclear lamins at the sequence VEID (Srinivasula et al., 1996b; Cohen, 1997; Ashkenazi and Dixit, 1998). Of the group III caspases, caspase-8, -9 and -10 have long prodomains containing DED and CARD motifs and tend to act as initiators in the caspase cascade (Green, 1998). One important feature of these group III caspases, which correlates well to their general function as upstream initiators, is their ability to cleave and so activate, group II caspases at aspartate cleavage sites (Thornberry et al., 1997; Stennicke et al., 1998).

### **1.5.6 Substrate specificity of caspases**

Substrate cleavage by caspases is dependent upon the binding between a highly conserved, positively charged P<sub>1</sub> subsite within the caspase and the presence of a negatively charged aspartate residue, in the P<sub>1</sub> position of the substrate (Sleath et al., 1990; Howard et al., 1991). Therefore, caspases are targeted to cleave specifically after an aspartate residue. However, caspases also require the recognition of at least four further residues N-terminal to the cleavage site for complete activity (Thornberry et al., 1997). The absolute

requirement for Aspartate in the P<sub>1</sub> position is accompanied by the potential for a variety of residues in the P<sub>2</sub>-P<sub>4</sub> positions, although the P<sub>4</sub> position can also be a critical determinant of specificity for certain caspases (Sleath et al., 1990; Thornberry et al., 1997). The overall effect of this subsite variety, is a family of caspases with differing specificities for tetrapeptide recognition motifs within any given substrate, thereby preventing the indiscriminate cleavage of cellular proteins. Based upon work using a positional scanning substrate combinatorial library (PSSCL), caspases can be broadly categorized into three functionally related groups according to their tetrapeptide preference (Talanian et al., 1997; Thornberry et al., 1997) (Table 1.2)

### 1.5.7 Caspase substrates

During apoptosis, specific proteins within the cell are targeted for proteolytic cleavage by effector caspases. The proteins cleaved by effector caspases can be broadly categorized as either being inactive pro-apoptotic proteins or proteins that promote the apoptotic phenotype, components of the cytoskeleton and other cellular structures, inhibitors of apoptosis or proteins involved in the cell cycle (Cryns and Yuan, 1998; Wolf and Green, 1999). Cleavage by caspases at specific residues can result in the activation of latent pro-apoptotic proteins, such as PKC $\delta$  and  $\theta$  (Emoto et al., 1995; Datta et al., 1997), MEKK-1 (Cardone et al., 1997), PAK2 (Rudel and Bokoch, 1997; Lee et al., 1997) and other pro-caspases. The recently identified DFF45/ICAD is the inhibitory partner of DFF/CAD, a nuclease responsible for the cleavage of nuclear DNA into oligonucleosomal length fragments (Liu et al., 1997). During apoptosis DFF45/ICAD is cleaved by caspase-3 (Janicke et al., 1998b) to release the active DFF40/CAD which cleaves chromatin (Sakahira et al., 1998; Enari et al., 1998; Liu et al., 1998).

A second class of substrates includes those proteins involved in maintaining the structural integrity of the nucleus and cytoskeleton and DNA repair. Examples of such proteins include, nuclear lamins (Lazebnik et al., 1995; Rao et al., 1996), a microfilament component Gas2 (Brancolini et al., 1995),  $\beta$  and  $\gamma$  catenins (Brancolini et al., 1997; Schmeiser et al., 1998), Nuclear Matrix proteins (NuMa) (Gueth-Hallonet et al., 1997), actin and  $\alpha$ -fodrin (Janicke et al., 1998a), and gelsolin (Kothakota et al., 1997). Cleavage of proteins involved in DNA repair during apoptosis, such as PARP and DNA dependent

protein kinase<sub>cs</sub>, ensures that inefficient repair of critically damaged DNA is prevented and may also facilitate DNA degradation (Casciola-Rosen et al., 1996; Song et al., 1996). One of the most well used markers for apoptosis is the cleavage of the 116kDa DNA repair enzyme PARP, to an 85kDa fragment by caspase-3 (Kaufmann et al., 1993; Lazebnik et al., 1994; Tewari et al., 1995b). Although its precise function remains uncertain, recent studies have suggested that cleavage of PARP by caspase-3 may cause the relinquishing of poly(ADP-ribosyl)ation-induced inhibition of nuclear proteins. This could then trigger key apoptotic steps by releasing specific proteins, including p53, from the nucleus (Simbulan-Rosenthal et al., 1998).

Caspases can also target anti-apoptotic proteins such as Bcl-2 and Bcl-xl. Cleavage of Bcl-2 and Bcl-xl produce pro-apoptotic c-terminal fragments which can themselves have pro-apoptotic activity (Cheng et al., 1997; Clem et al., 1998; Grandgirard et al., 1998). In addition, apoptotic agonists, such as Bid (Luo et al., 1998; Li et al., 1998) and p28Bap31 (Ng et al., 1997) can be targeted and activated by caspases. The ability of caspases to critically disable the cell is further exemplified by reports showing that caspases can target proteins specifically associated with the cell cycle such as cyclin dependent kinases, cdc2 and cdk2 (Shi et al., 1994), cdc27 and weel, which show similar cleavage profiles to PARP during Fas- and staurosporine-mediated apoptosis (Zhou et al., 1998) and Rb (Janicke et al., 1996). However, the exact functional significance of cell cycle associated protein cleavage events during apoptosis remains unclear (Evan et al., 1995).

### **1.5.8 Inhibition of caspases**

#### **1.5.8.1 Naturally occurring caspase inhibitors, Crm-A, p35, IAP's**

The identification of naturally occurring caspase inhibitors has stemmed from the study of virus infection. In order to propagate, viruses evade the normal apoptotic responses mounted by the host in response to infection (Smith et al., 1994; Shen and Shenk, 1995). At least three classes of viral caspase inhibitors have been described and include Crm-A, p35 and IAPs (Thornberry and Lazebnik, 1998). Crm-A (Cytokine response modifier A) is a cowpox virus serpin of 38kDa and aids viral infection by inhibiting host inflammatory responses and apoptosis (Ray et al., 1992; Gagliardini et al., 1994; Howard et al., 1995). It particularly inhibits receptor-mediated apoptosis, by acting as a pseudo-substrate for active

caspases, including caspase-1, -4, -6 and -8, and remaining tightly bound to the active site following proteolysis at an LVAD motif (Komiyama et al., 1994; Zhou et al., 1997). The baculovirus p35 protein also acts by being cleaved at specific residues, blocking further caspase activity by tight binding at the active site (Clem et al., 1991). The p35 gene product inhibits apoptosis in insects, mammals and nematodes, suggesting an evolutionary conserved pathway (Rabizadeh et al., 1993; Hay et al., 1994; Sugimoto et al., 1994). It was discovered as the result of a viral gene mutation causing death in the host (Clem et al., 1991). p35 inhibits a wider range of caspases than Crm-A, including caspase-1, -2, -3, -4 and those of the group II subfamily (Bump et al., 1995; Xue and Horvitz, 1995). Although mammalian homologues of crm-A and p35 have not been identified a number of mammalian IAP's have been identified which contain at least one baculoviral IAP repeat (BIR) which are sufficient and necessary for function and have similar anti-apoptotic functions (Takahashi et al., 1998). The IAP family of inhibitors were discovered due to their ability to functionally complement p35 in mutant viruses (Crook et al., 1993; Clem and Miller, 1994). In contrast, members of the mammalian IAP family are endogenously expressed cellular proteins conserved across many species (Hay et al., 1995). The first human IAP, neuronal apoptosis inhibitory protein (NAIP), was identified as having deletions in patients with spinal muscular atrophy, a disorder where motoneurone depletion is observed as a result of excessive apoptosis (Roy et al., 1995). Further human IAPs include c-IAP1, c-IAP2, x-IAP and survivin (Rothe et al., 1995; Duckett et al., 1996; Liston et al., 1996; Ambrosini et al., 1997). IAP's have been shown to inhibit apoptosis at the level of distal effector caspases such as caspase-3 and -7 as well as upstream targets such as caspase-9 (Xue and Horvitz, 1995; Hay et al., 1995; Deveraux et al., 1997; Roy et al., 1997; Deveraux et al., 1998). Most recently the IAP survivin has been shown to be involved in the mitotic spindle checkpoint and therefore may have a role in signalling between aberrant mitosis and default entry into apoptosis (Li et al., 1998)

### **1.5.9 Peptide based caspase inhibitors**

Initially the use of synthetic peptide inhibitors was aimed at dissecting the signalling and enzymatic activity of caspases (Thornberry et al., 1997) but their potential use as a drug model for treatment of diseases where apoptosis is in excess, has also been recognised and shown to be effective in animal models of stroke, ischaemia and other neurodegenerative

disorders (Nicholson, 1996; Yakovlev et al., 1997; Hara et al., 1997). Peptide inhibitors consist of 3 to 4 amino acids whose sequence mimics that of the P<sub>1</sub>-P<sub>4</sub> caspase substrate sites coupled to aldehyde, nitrile or ketone moieties (Figure 1.4). For example, caspase-3 targets cellular substrates such as PARP and U1-70K, which contain DXXD cleavage sites. Thus caspase-3 and other group II caspases can be effectively inhibited with peptide inhibitors such as z-DEVD-FMK (Asp-Glu-Val-Asp-fluoromethylketone).

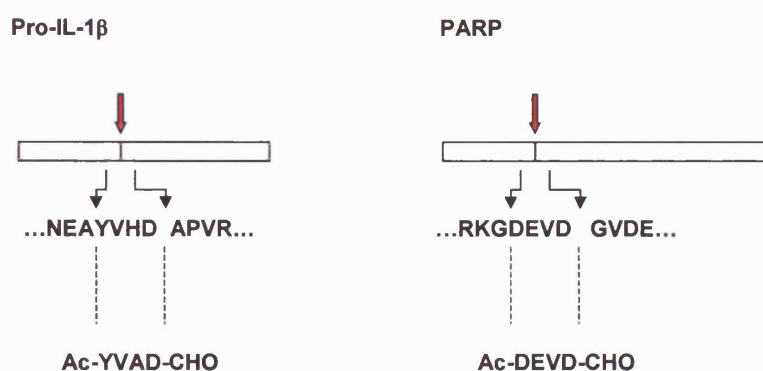


**Figure 1.4 Design of tetrapeptide-based caspase inhibitors.** The P<sub>4</sub>-P<sub>1</sub> tetrapeptide motifs recognised by caspase-1 and caspase-3 in pro-IL-1 $\beta$  and PARP respectively are used as templates for specific inhibitors of caspase-1 and -3. Adapted from Nicholson, (1996).

The peptide aldehydes, nitriles and ketones are potent caspase inhibitors which undergo nucleophilic addition of the catalytic cysteine to form thiohemiacetals, thioimidates and thiohemiketals, respectively (Thornberry et al., 1992; Thornberry and Molineaux, 1995). One of the most widely used caspase inhibitors is z-VAD-FMK (benzyloxycarbonyl-Val-Ala-Asp(OMe)fluoromethylketone) which, after expulsion of the carboxylate leaving group, is able to form an irreversible thiomethylketone adduct with the active site cysteine residue (Thornberry et al., 1994; Nicholson, 1996). z-VAD-FMK is a broad-range, cell permeable caspase inhibitor, and the ability of this particular inhibitor to enter the cell is further facilitated by the presence of the benzyl-oxycarbonyl and OMe groups (Cohen, 1997). z-VAD-FMK is effective in inhibiting many forms of apoptosis in various systems by potentially blocking apical caspase activities (Chow et al., 1995; MacFarlane et al., 1997; Longthorne and Williams, 1997). Other commonly used peptide-based caspase inhibitors include, Ac-YVAD-CMK (acetyl-Tyr-Val-Ala-Asp-fluoromethylketone), a

caspase-1 based inhibitor and VEID-FMK (acetyl-Val-Glu-Ile-Asp-fluoromethylketone), a caspase-6 specific inhibitor which mimics the preferred VEID substrate sequence preference of caspase-6. The use of these inhibitors, amongst others, has been integral in defining caspase function and enzymatic activity in *in vitro* and *in vivo* systems (Chow et al., 1995). Because caspases play such a fundamental role during the initiation and execution phase of apoptosis, it is not so radical to propose that inhibition of this caspase activity would in itself, be sufficient to prevent the morphological features of apoptosis. Indeed, in certain circumstances this appears to be the case (Longthorne and Williams, 1997; Ko et al., 2000).

## 1.6 Apaf-1, the *Ced-4* homologue

In the *C.elegans* model of apoptosis, it was found that the *ced-4* gene interacted with both *ced-3* and *ced-9* therefore linking the caspases and the Bcl-2 family of proteins (Jacobson, 1997a). This observation provided a molecular framework for apoptosis which suggested that *ced-9* inhibited the apoptotic activity of *ced-3* and *ced-4* (Chinnaiyan et al., 1997; Spector et al., 1997; Wu et al., 1997a). Furthermore, *ced-4* was found to be involved in the activation of *ced-3*, via an interaction with the *ced-3* prodomain, in the presence of ATP (Chinnaiyan et al., 1997). In addition to this, *ced-4* and *ced-9* were also found to interact and therefore prevent the pro-apoptotic action of *ced-4* on *ced-3*. The *ced-4* mammalian homologue remained elusive until the discovery of a cytosolic 130kd protein, which was involved in cytochrome c mediated caspase activation (Zou et al., 1997). The protein shared 21% identity and 53% similarity with the NH2 terminal prodomain of *ced-3* and 22% identity and 48% similarity to *ced-4*. The protein was designated Apaf-1 (apoptotic protease activating factor-1) and was necessary for the activation of caspase-3 by cytochrome c. The 'initiator' caspase-9 also interacts with Apaf-1 to form a functional Apaf-1/caspase-9 complex or 'apoptosome', which initiates the caspase cascade (Hu et al., 1998b). Recruitment of procaspase-9 is mediated by a CARD domain and results in stoichiometric 1:1 binding between Apaf-1 and the prodomain of procaspase-9 (Zou et al., 1999). Procaspase-3 can then be activated by recruitment to the complex or dissociation of active caspase-9. Apaf-1 acts downstream of the *ced-9*/Bcl-2 family which block the release of cytochrome c from mitochondria (Kluck et al., 1997; Yang et al., 1997). Bcl-2 family members, such as Bcl-xl and Diva have also been shown to bind Apaf-1, thus

preventing caspase-9 activation (Pan et al., 1998; Inohara et al., 1998; Hu et al., 1998a). This observation neatly parallels the interaction of ced-4 and ced-9 in *C.elegans* (Hengartner, 1997; Hengartner, 1998). However, a controversial recent report suggests that association between Apaf-1 and Bcl-2 family members, does not occur *in vivo* and regulation may instead involve an indirect action of Bcl-2 homologues on Apaf-1 function (Moriishi et al., 1999). Apaf-1 is ubiquitously expressed with high levels of expression in tissues prone to apoptotic activity such as adult spleen, peripheral blood leukocytes and foetal brain, kidney and lung (Zou et al., 1997). Apaf-1 knockout mice exhibit neurone accumulation, facial abnormalities and delayed recession of interdigital webbing. Cells from these animals were also resistant to varied apoptotic stimuli suggesting a central role for Apaf-1 in the mediation of many forms of apoptosis (Cecconi et al., 1998; Yoshida et al., 1998).

### 1.7 Mammalian homologues of Ced-9, the Bcl-2 family of oncoproteins

The Bcl-2 protein was first discovered as the result of an interchromosomal translocation event resulting in a t (14:18) (q32: q21) breakpoint, often used as a cytogenetic/molecular marker for follicular B-cell lymphomas (Tsujiimoto et al., 1985; Cleary et al., 1986; Bakhshi et al., 1995). Translocation results in the positioning of the Bcl-2 gene adjacent to the IgG heavy chain locus and thus under its transcriptional control. Overexpression of Bcl-2 was later found to be a common feature of many types of follicular lymphomas, leukaemia's and carcinomas of breast, prostate, ovary, colon and lung (Pezzella et al., 1990; Zutter et al., 1991; McDonnell and Korsmeyer, 1991; Ikegaki et al., 1994; Hague et al., 1994; Leek et al., 1994; Watson et al., 1996). The Wilms tumour suppressor gene WT1 has been shown to interact with the bcl-2 promoter and thus transcriptionally upregulate Bcl-2 expression contributing to oncogenesis by inhibiting apoptosis (Mayo et al., 1999). In a clinical context, the overexpression or up regulation of Bcl-2 may affect the sensitivity of certain patients to chemotherapy (Jäättelä, 1999). In contrast to the oncogenic functions of p53, Ras, Myc and Abl, which contribute to proliferation, Bcl-2 was proposed to be the founder member of a new category of oncogenes which are responsible for preventing cell death. (Korsmeyer, 1992). Bcl-2 was found to increase viability in haematopoietic cell lines upon growth factor withdrawal (Vaux et al., 1988; Nunez et al., 1990; Deng and Podack, 1993), affect T-cell death in transfected T-cell hybridomas and thymocytes from

transgenic mice (Strasser et al., 1991; Sentman et al., 1991) and protect cells from a variety of apoptotic insults (Jäättelä et al., 1995; Estoppey et al., 1997). Bcl-2 is unable to induce tumourigenicity alone (Vaux et al., 1988), but contributes to transformation by acting in co-operation with other oncogenes such as c-myc (Evan et al., 1992). Bcl-2 is also able to prevent apoptosis induced by c-myc and p53 and therefore may render cells susceptible to further mutations, leading to transformation (Bissonnette et al., 1992). The wider implications of the *C.elegans* model for apoptosis were realised when the Bcl-2 gene was discovered to have significant homology to ced-9 (23%) (Hengartner et al., 1992), and represent a large family of proteins which contained both anti- and pro-apoptotic members (Adams and Cory, 1998). This complexity highlights the need to efficiently regulate apoptosis in the context of the multicellular organism and protect against the potential of aberrant cell death, which could contribute to neoplasia, malignancy and many other diseases.

### 1.7.1 Structure and function of the Bcl-2 family of oncoproteins

Since the discovery of Bcl-2, many homologous interacting proteins have been identified which are related by virtue of several conserved Bcl-2 homology (BH1, BH2, BH3 and BH4) domains (Figure 1.5). These domains contribute significantly to binding between family members and induction of apoptosis (Yin et al., 1994; Zhang et al., 1995; Hunter et al., 1996; Huang et al., 1998). Family members can be divided into those with a) anti-apoptotic/pro-survival functions, such as Bcl-2, Bcl-xl, Bcl-w, Mcl-1, A1, Ced-9 and the adenoviral E1B 19K, b) pro-apoptotic functions with homology to Bax, including Bak and Bok, and c) pro-apoptotic functions with a conserved BH3 domain including Bcl-x<sub>s</sub>, Bad, Bik, Bid and the nematode Egl-1 (Conradt and Horvitz, 1998). The conserved BH1, BH2 and BH3 domains have been shown to be essential for dimerization between family members and influence the repression of cell death (Yin et al., 1994; Chittenden et al., 1995; Zhang et al., 1995). The dimerization between Bcl-2/Bcl-xl and pro-apoptotic BH3 containing members, such as Bax, is mediated primarily by the formation of a long hydrophobic cleft between the BH1, BH2 and BH3 domains of Bcl-2/Bcl-xl to which a BH3 amphipathic helix can bind (Muchmore et al., 1996; Sattler et al., 1997; Adams and Cory, 1998).

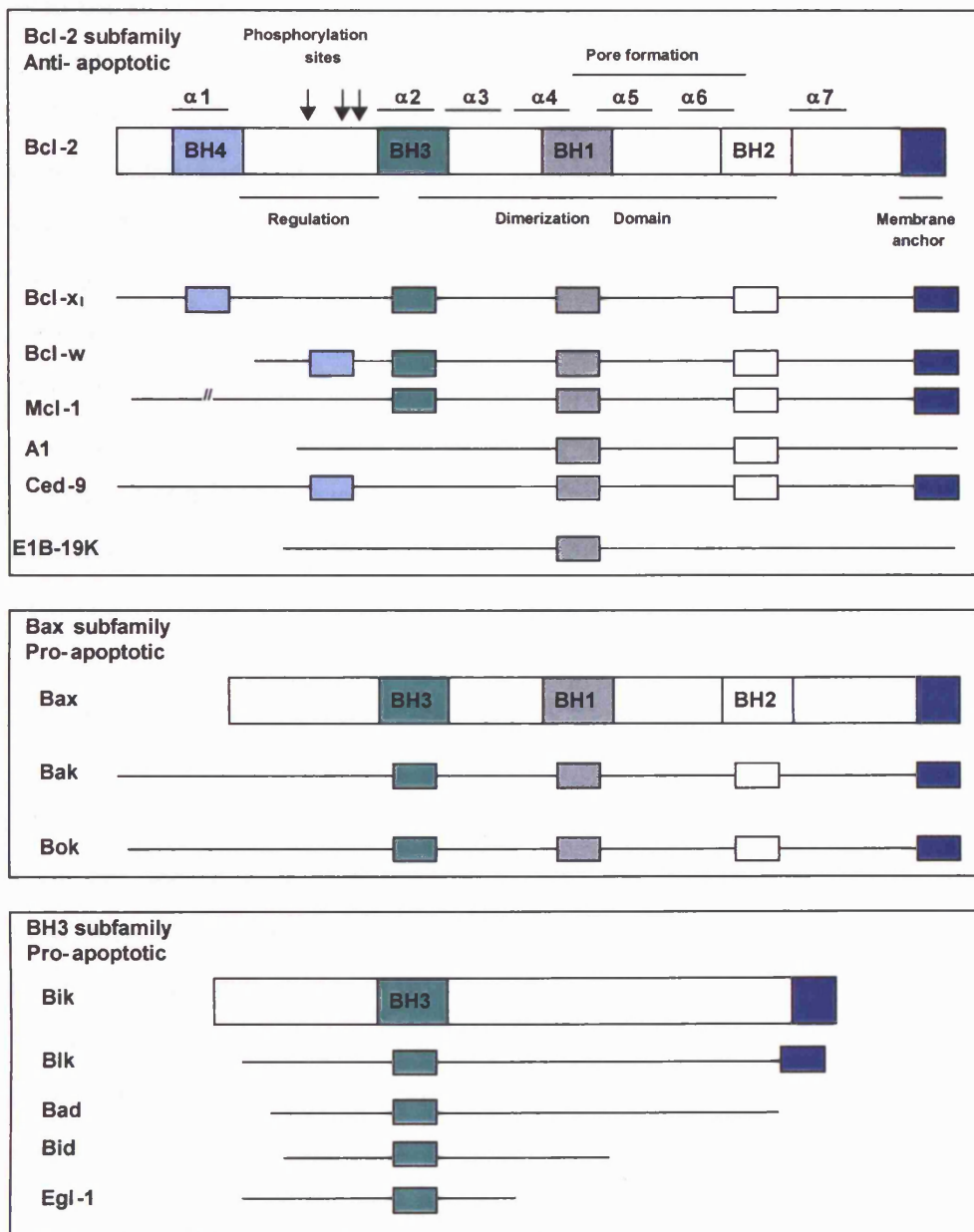


**Figure 1.5 Summary of anti-apoptotic and pro-apoptotic members of the Bcl-2 oncoprotein family showing the Bcl-2 homology domains BH1, BH2, BH3 and BH4.** Bcl-2 subfamily members contain the BH4 which is necessary for anti-apoptotic function. Members of the Bax subfamily resemble Bcl-2 but lack a BH4 domain; except for the BH3 domain, BH3 family members are unrelated. Mutagenesis of Bid and Bad indicate that the BH3 domain is essential for binding to Bcl-2 and Bcl-x and death agonist activity. The hydrophobic pore forming  $\alpha 5$  and  $\alpha 6$  helices are flanked by five amphipathic helices. The loop domain is situated between  $\alpha 1$  and  $\alpha 2$  helices. Adapted from Adams & Cory, (1998) and Chao & Korsmeyer, (1998).

Mutations in the BH1, BH2 and BH3 domains of death antagonists such as Bcl-2, disrupt heterodimerization with Bax but do not alter their anti-apoptotic activity (Yin et al., 1994; Cheng et al., 1996). The conserved N-terminal BH4 domain, present only in the anti-apoptotic Bcl-2 subfamily, has also been shown to play an important role in cell survival (Borner et al., 1994; Hanada et al., 1995; Hunter et al., 1996; Hirotsu et al., 1999). Recent evidence suggests the BH4 domain could mediate binding between the Bcl-2 subfamily of proteins and ced-4 and its homologues, thus inhibiting the pro-apoptotic activity of ced-4 (Huang et al., 1998). The BH4 domain may also mediate interactions with other proteins such as calcineurin (Shibasaki and McKeon, 1995) and Raf-1 (Wang et al., 1994). Cleavage of Bcl-2 at a DAGD motif by caspase-3 results in removal of the BH4 domain, and not only negates its anti-apoptotic function but also releases a pro-apoptotic c-terminal fragment (Cheng et al., 1997; Grandgirard et al., 1998).

### **1.7.2 Determination of cell fate by Bcl-2 family member ratios**

The extent to which a cell will respond to any apoptotic stimulus is partially determined by the ratio of pro-apoptotic to anti-apoptotic members and is mediated by equimolar dimerization between the two (Oltvai et al., 1993). An excess of Bax homodimers for example will instigate cell death whilst an excess of Bcl-2 or Bcl-xl homodimers will favour survival. The binding between Bcl-2 and Bax to form a heterodimer is thought to neutralize their respective activities (Figure 1.6). Although heterodimerization is necessary for pro-apoptotic BH3 subfamily function, it may not be an essential requirement for the function of either pro-survival Bcl-2 or pro-apoptotic Bax subfamily members (Chittenden et al., 1995; Cheng et al., 1996; Simonian et al., 1996; Adams and Cory, 1998; Gross et al., 1998; Minn et al., 1999).

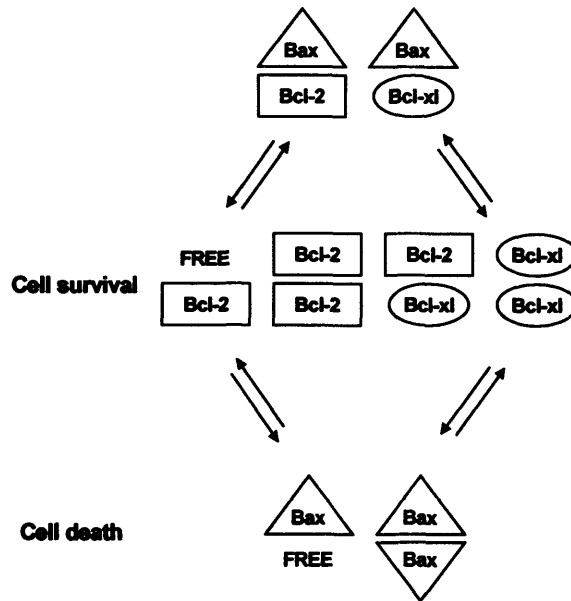


**Figure 1.6 Determination of cell fate and the importance of anti-apoptotic and pro-apoptotic Bcl-2 family ratios.** The equilibrium state between dimers is determined by the relative abundance and subcellular location of each binding partner. An excess of Bcl-2/anti-apoptotic proteins results in cell survival and such an excess of pro-apoptotic members, such as Bax, results in cell death. The relative levels of unbound or 'free' Bcl-2 or Bax can also inhibit or induce apoptosis independently of dimerization events. (Adapted from Reed et al., 1996).

The anti-apoptotic effects of Bcl-2 may also be dependent upon the level of endogenously expressed 'free' or unbound protein (Oltvai et al., 1993; Yin et al., 1994; Otter et al., 1998). Similarly, cytosolic Bax can induce apoptosis independently of dimerization (Xiang et al., 1996; Zha and Reed, 1997; McCarthy et al., 1997).

### 1.7.3 Localization of Bcl-2

Subcellularly, Bcl-2 and Bcl-x are found localized to the endoplasmic reticulum, nuclear envelope and outer mitochondrial membranes (Chen-Levy et al., 1989; Hockenberry et al., 1990; Krajewski et al., 1993; Akao et al., 1994). Bcl-2 is able to target interacting proteins such as Raf-1 and ced-4 to the mitochondria by virtue of a carboxy terminal membrane anchoring domain in the native protein (Hunter et al., 1996; Vance et al., 1996). In murine thymocytes, Bcl-2 is exclusively membrane bound whilst Bcl-xl is present in both soluble and bound forms. Bax is predominantly found in the cytosol as a monomer. Upon the

induction of apoptosis there is a rapid redistribution to mitochondrial membranes followed by homodimer formation (Gross et al., 1998; Goping et al., 1998). Formation of Bax homodimers is sufficient to induce mitochondrial dysfunction and apoptosis, which can be inhibited by Bcl-2 or Bcl-xl. The c-terminal hydrophobic segment serves as transmembrane (TM) anchor domain. Deletion of the TM domain either abrogates or diminishes the cell death inhibitory function of Bcl-2 whilst similar mutations in Bax prevent its targeting to mitochondria and inhibit its cytotoxic activity in yeast cells (Zha et al., 1996). In a study where Bcl-2 was targeted either to mitochondrial membranes or endoplasmic reticulum, the anti-apoptotic function of Bcl-2 was shown to be dependent on subcellular location (Zhu et al., 1996). In MDCK (Madin-Darby canine kidney) epithelial cells, Bcl-2 targeted to the mitochondria was as effective as wild type protein in protecting cells from apoptosis induced by serum starvation whilst the ER localized protein was ineffective. In contrast, localization to the ER and mitochondrial membranes resulted in inhibition of myc-induced apoptosis in rat fibroblasts. Thus, the localization of Bcl-2 may determine its effectiveness in inhibiting different pathways of apoptosis. In support of this view, Bcl-2 has been implicated in the maintenance of calcium homeostasis and reduce thapsigargin-induced  $\text{Ca}^{2+}$  effluxes and apoptosis by maintaining the ER calcium pool (Lam et al., 1994; He et al., 1997).

#### **1.7.4 Membrane channel function of Bcl-2**

The observation that many of the Bcl-2 protein family members localize to mitochondrial membranes suggested a potential mechanism for the inhibition of apoptosis (Krajewski et al., 1993). Certain members of the Bcl-2 family, such as Bcl-2, Bcl-xl, Bax, and Bak, show a propensity for channel formation within membranes (Schendel et al., 1997; Minn et al., 1997; Antonsson et al., 1997; Schlesinger et al., 1997). This is thought to be mediated by the  $\alpha 5$  and  $\alpha 6$  helices lying between the BH1 and BH2 domains, which resemble the insertion domains of bacterial toxins such as diphtheria toxin and colicins A and E1, and have the potential to form discriminating channels on intracellular membranes (Muchmore et al., 1996). Bcl-xl has been proposed to regulate apoptosis not only by heterodimerization-dependent mechanisms but also by a heterodimerization-independent mechanism, which is related to its ability to form ion channels within reconstituted lipid membranes (Matsuyama et al., 1998; Minn et al., 1999).

### 1.7.5 Further functions of Bcl-2

Bcl-2 has been shown to have additional functions which may contribute to its overall anti-apoptotic effects (Reed, 1997). Bcl-2 overexpressing T cells exhibit delayed entry into S-phase and reduced proliferative rates (O'Reilly et al., 1996; Vairo et al., 1996; Borner, 1996; Mazel et al., 1996). Interestingly some of these effects can be countered by pro-apoptotic members of the Bcl-2 family, such as Bax (Brady et al., 1996). Recent studies have suggested that Bcl-2 can also modulate the activity of the ribonucleoprotein, telomerase (Mandal et al., 1996). Telomerase activity is strongly associated with the acquisition of immortality in cancer (Broccoli et al., 1995). Therefore, Bcl-2 could potentially provide a link between the regulation of apoptosis, cell cycle progression and telomerase activity all of which are deregulated in cancer.

## 1.8 Induction of apoptosis

Cells can undergo apoptosis in response to a wide variety of stimuli including receptor stimulation, cytotoxic drugs and radiation (Williams et al., 1992). Despite the diversity in stimuli there is a convergence in signalling at the level of caspase activation and subsequent morphological and biochemical changes typical of apoptosis (Wyllie et al., 1980b). Recent evidence suggests that the signalling events which occur after apoptotic stimulation define two basic mechanisms for the induction of apoptosis (Green, 2000). The first is dependent on signalling via the mitochondria and the second is dependent upon signalling directly from death receptors on the cell surface.

### 1.8.1 Induction of apoptosis via the mitochondria

Treatment of cells with chemical stimuli has been shown to result in features associated with apoptosis and has been used as a model for dissecting the apoptotic pathway in many *in vitro* systems (Kaufmann, 1989; Bertrand et al., 1994; Martins et al., 1997). Chemical-induced apoptosis often signals via the mitochondria in a cytochrome c-dependent manner (Slee et al., 1999; Li et al., 2000). Upon the induction of apoptosis mitochondria are stimulated to release a number of caspase activating proteins such as cytochrome c and the

apoptosis inducing factor (AIF) (Oltvai et al., 1993; Susin et al., 1996; Liu et al., 1996; Bossy-Wetzell et al., 1998). Furthermore, mitochondria have also been shown to contain sub-pools of caspase-2, -3 and -9 which are released during apoptosis (Mancini et al., 1998; Susin et al., 1999; Samali et al., 1999). Cytochrome c release results in the activation of downstream caspases via an interaction with Apaf-1 and caspase-9, forming a functional 'apoptosome' (Zou et al., 1999). Apoptosome formation is thought to depend on Apaf-1 oligomerization in the presence of cytochrome c and ATP/dATP and subsequent recruitment and activation/autoactivation of procaspase-9 (Li et al., 1997; Srinivasula et al., 1998; Zou et al., 1999).

### **1.8.2 Mitochondria and the permeability transition (PT) pore**

One potential mechanism for the release of cytochrome c from mitochondria appears to be dependent on the alteration of mitochondrial membrane permeability which could either be due to rupture of the outer mitochondrial membrane or opening of mitochondrial PT pores in the outer membrane (Martinou et al., 2000) (Figure 1.7). Studies have shown that a decrease in mitochondrial membrane potential ( $\Delta\psi_m$ ) is a common early event during apoptosis induced by a variety of stimuli irrespective of cell type and occurring prior to DNA fragmentation (Zamzami et al., 1995; Mignotte and Vayssiere, 1998). The decrease in  $\Delta\psi_m$  and cytochrome c release can be mediated by the opening of a large conductance channel known as the mitochondrial permeability transition (PT) pore complex (Marchetti et al., 1996). The complex consists of a number of proteins including the adenine nucleotide translocator (ANT) (Marzo et al., 1998), the benzodiazepine receptor and porin/voltage dependent anion channel (VDAC) (Rostovtseva and Columbini, 1997; Compton, 1999). However, some studies have shown that cytochrome c release and caspase activation can occur before any detectable loss in  $\psi\Delta_m$ , (Kluck et al., 1997; Vander Heiden et al., 1997; Bossy-Wetzell et al., 1998). Furthermore, caspases can directly induce PT pore opening, also suggesting the presence of a feed back amplification loop (Green and Reed, 1998).

## 1.3.4 Bcl-2 and the mitochondria

One mechanism by which Bcl-2 related proteins are proposed to inhibit apoptosis is via the inhibition of cytochrome c release from the mitochondria (Kluck et al., 1997; Yang et al., 1997). Indeed, Bcl-2 has been shown to inhibit Bax-induced cytochrome c release and subsequent cell death (Fracumano et al., 1998). The exact mechanism by which anti-apoptotic Bcl-2 family members inhibit cytochrome c release and the decrease in mitochondrial membrane potential is still unclear (Van der Linden and Thompson, 1997).

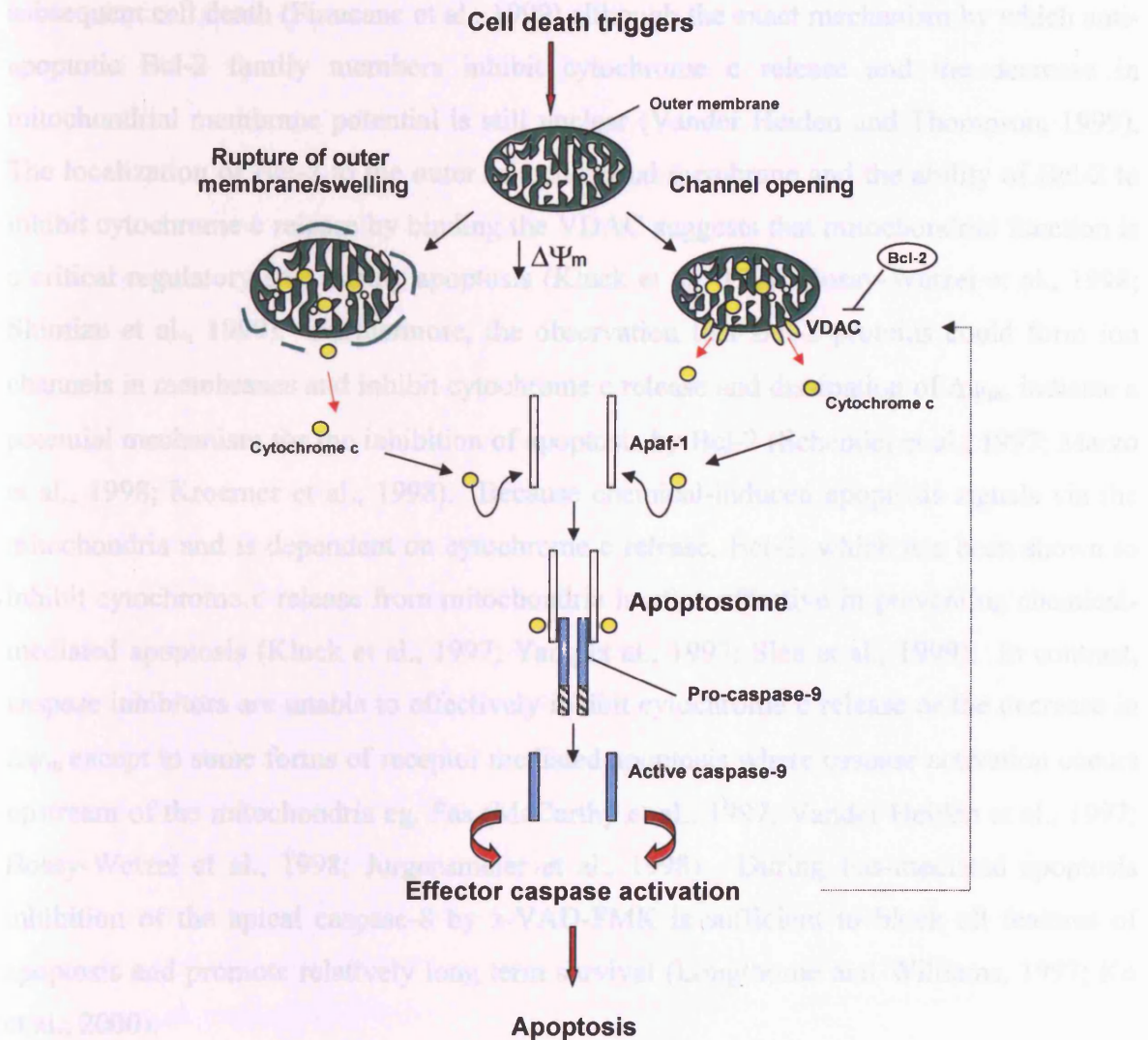


**Figure 1.7 Model for mitochondrial involvement in apoptosis.** Multiple stimuli such as Bax, oxidants,  $\text{Ca}^{2+}$ , staurosporine and other chemicals, cause cellular stress and induce the release of apoptosis-inducing proteins such as cytochrome c and AIF from the mitochondria. Release of these proteins can occur either via rupture of the outer mitochondrial membrane or through the opening of membrane channels such as VDAC. Cytochrome c then binds to Apaf-1 causing recruitment and activation of pro-caspase-9 and subsequent downstream effector caspases. A potential feedback loop occurs between caspase-3 and cytochrome c release by perturbing membrane integrity. Bcl-2 localizes to the outer mitochondrial membrane and blocks the release of cytochrome c and decrease in mitochondrial membrane potential ( $\Delta\Psi_m$ ) upstream of caspase activation. Adapted from (Green and Reed, 1998).

#### 1.8.4 Bcl-2 and the mitochondria

One mechanism by which Bcl-2 related proteins are proposed to inhibit apoptosis is via the inhibition of cytochrome c release from the mitochondria (Kluck et al., 1997; Yang et al., 1997). Indeed, Bcl-xl has been shown to inhibit Bax-induced cytochrome c release and subsequent cell death (Finucane et al., 1999) although the exact mechanism by which anti-apoptotic Bcl-2 family members inhibit cytochrome c release and the decrease in mitochondrial membrane potential is still unclear (Vander Heiden and Thompson, 1999). The localization of Bcl-2 to the outer mitochondrial membrane and the ability of Bcl-2 to inhibit cytochrome c release by binding the VDAC suggests that mitochondrial function is a critical regulatory step during apoptosis (Kluck et al., 1997; Bossy-Wetzell et al., 1998; Shimizu et al., 1999). Furthermore, the observation that Bcl-2 proteins could form ion channels in membranes and inhibit cytochrome c release and dissipation of  $\Delta\psi_m$ , indicate a potential mechanism for the inhibition of apoptosis by Bcl-2 (Schendel et al., 1997; Marzo et al., 1998; Kroemer et al., 1998). Because chemical-induced apoptosis signals via the mitochondria and is dependent on cytochrome c release, Bcl-2, which has been shown to inhibit cytochrome c release from mitochondria is often effective in preventing chemical-mediated apoptosis (Kluck et al., 1997; Yang et al., 1997; Slee et al., 1999). In contrast, caspase inhibitors are unable to effectively inhibit cytochrome c release or the decrease in  $\Delta\psi_m$  except in some forms of receptor mediated apoptosis where caspase activation occurs upstream of the mitochondria eg. Fas (McCarthy et al., 1997; Vander Heiden et al., 1997; Bossy-Wetzell et al., 1998; Jurgensmeier et al., 1998). During Fas-mediated apoptosis inhibition of the apical caspase-8 by z-VAD-FMK is sufficient to block all features of apoptosis and promote relatively long term survival (Longthorne and Williams, 1997; Ko et al., 2000).

### 1.8.5 Receptor-mediated apoptosis.

Apoptosis can occur after activation of cell surface 'death receptors' upon binding of the appropriate ligand (Nagata, 1997). Death signals are then transduced across the plasma membrane and initiate the caspase cascade culminating in the biochemical and morphological features typical of apoptosis (Hirata et al., 1998; Zheng et al., 1998). The importance of receptor-mediated apoptosis in normal cell turnover and disease is perhaps illustrated most effectively by study of the Fas system. Fas/APO-1/CD95 was identified due to its ability to induce apoptosis in certain cell lines. Two groups independently isolated monoclonal antibodies from EBV transformed B cells (Trauth et al., 1989) and FS-7 Fibroblasts (Yonehara et al., 1989) which were potent inducers of apoptosis and recognized the same cell surface antigen, Fas/APO-1/CD95. Fas is a 45kDa, 319-amino acid type I transmembrane protein and is a member of the Tumour necrosis factor (TNF) family of membrane receptors (Oehm et al., 1992) (Figure 1.8). The TNF superfamily are characterized by 3-6 homologous cysteine rich extracellular domains (Schulze-Osthoff et al., 1994b). In addition certain members of the family, namely TNF-R1 (Wallach et al., 1997), Fas/CD95/APO-1 (Itoh et al., 1991), DR-3 (Marsters et al., 1998), DR-4 (Pan et al., 1997) and DR-5 (Walczak et al., 1997) also share homology in an 80 amino acid stretch termed the death domain (DD), as it is essential for transmitting a cytotoxic signal across the membrane (Tartaglia et al., 1991; Itoh and Nagata, 1993; Yuan, 1997). Fas is expressed in a wide variety of tissues and organs including lymphoid tissues, thymus (Trauth et al., 1989; Yonehara et al., 1989; Itoh et al., 1991; Watanabe-Fukunaga et al., 1992), liver (hepatocytes) (Galle, 1997), heart (Fine et al., 1997), kidney (Leithauser et al., 1993), ovary (Guo et al., 1994) but not in brain, bone marrow and spleen (Watanabe-Fukunaga et al., 1992).

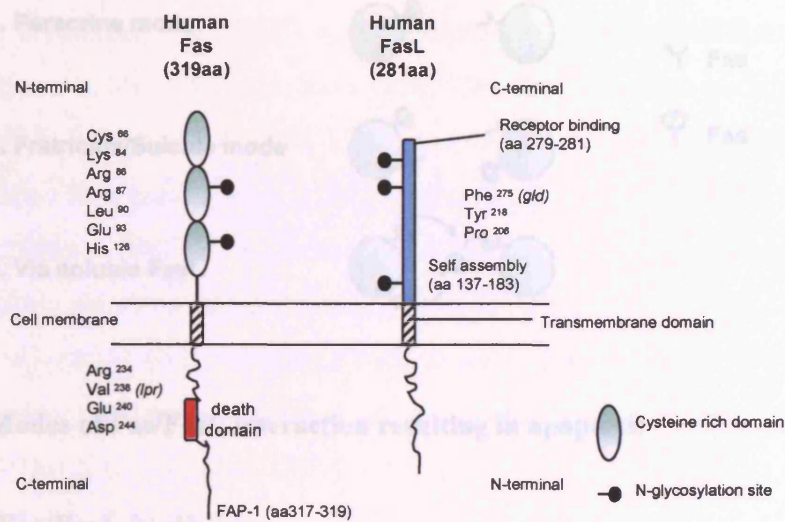


**Figure 1.8 Schematic representing structures of human Fas and FasL.** Fas is a type I glycoprotein and characterized by three cysteine rich extracellular domains important for Fas/FasL binding. C-terminal domain consists of the conserved death domain, mutation in Val<sup>238</sup> corresponds to the *lpr* mutation observed in lymphoproliferative disease. FAP-1 is a protein tyrosine phosphatase which negatively modulates Fas mediated apoptosis. FasL is a type II glycoprotein. The c-terminal contains domains important for self assembly and trimerization and high affinity receptor binding. Mutations at Phe<sup>275</sup> are analogous to the *gld* mutation. Adapted from Maggi 1998.

In order to induce apoptosis, the Fas receptor must be crosslinked by either agonistic antibodies, cells expressing Fas-ligand (FasL) or soluble FasL (sFasL) (Maggi, 1998). Upon binding of ligand or antibody, receptor crosslinking and trimerization of Fas occurs (Schneider et al., 1997). FasL was purified from cytotoxic T-cell line as a 281 amino acid (26kDa) type II transmembrane protein of the TNF superfamily (Suda et al., 1993). There are three potential mechanisms by which Fas/FasL interactions occur (Figure 1.9). The first is in a paracrine manner where FasL<sup>+</sup> cells induce apoptosis on Fas<sup>+</sup> cells. The second is a ‘fratricide/suicide’ mode where cells simultaneously express FasL and Fas; this mechanism is thought to be important in the activation-induced cell death (AICD) of T cells (Dhein et al., 1995; Ju et al., 1995; Brunner et al., 1995; Alderson et al., 1995). Finally, apoptosis can be induced by sFasL which is released from the cell surface via the action of a matrix metalloproteinase to induce apoptosis at distant sites (Mariani et al., 1995).

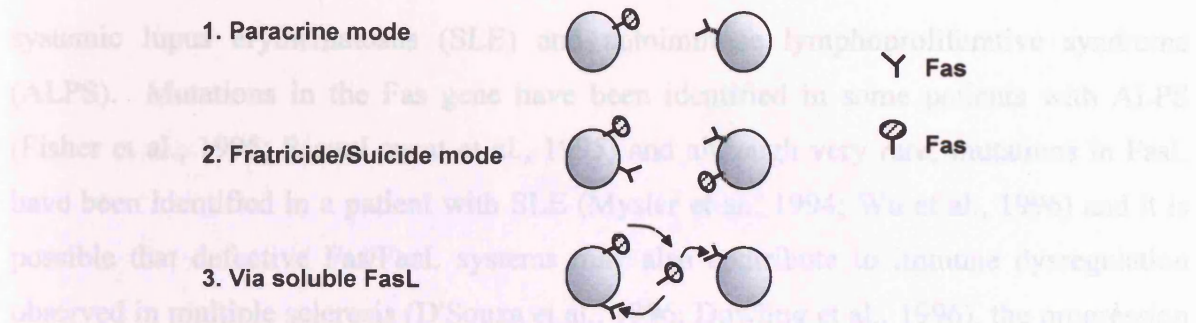


**Figure 1.9** Modes of Fas/FasL interaction resulting in apoptosis

### 1.8.6 Role of Fas/FasL in disease

#### 1.8.7 Apoptosis signalling through Fas

Studies in mice have helped further elucidate the role of Fas and FasL in the immune system (Watanabe-Fukunaga et al., 1992; Cohen and Eisenberg, 1992; Takahashi et al., 1994). Mice carrying mutation in the Lymphoproliferative (*lpr*) gene exhibit lymphoid enlargement due to accumulation of T cells and systemic autoimmunity (Cohen and Eisenberg, 1992). Mapping of the murine Fas and *lpr* genes to chromosome 19 indicated that *lpr* represents a defective form of the Fas encoding gene (Watanabe-Fukunaga et al., 1992a, Watanabe-Fukunaga et al., 1992b, Allen et al., 1990). The mutation is the result of insertion of a retroviral transposon into the second exon of the Fas gene causing premature transcription and reduced transcripts (Adachi et al., 1993; Wu et al., 1993; Chu et al., 1993). The importance of the death domain to proximal receptor signalling is underlined by studies in *lpr<sup>cg</sup>* mice which have a point mutation located within the death domain and manifest a similar phenotype to *lpr* mice (Watanabe-Fukunaga et al., 1992). In addition mice with generalized lymphoproliferative disease (*gld*) develop a condition which is indistinguishable from *lpr* (Takahashi et al., 1994). The gene encoding *gld* was found to colocalize with the FasL gene to chromosome 1 (Takahashi et al., 1994; Lynch, 1995). Mice with *gld* exhibited a point mutation (Phe<sup>275</sup>) proximal to the extracellular c-terminus of FasL preventing the required interaction with Fas receptor (Takahashi et al., 1994; Hahne et al., 1995). Thus *lpr* and *gld* mutations represent defects in a pair of interacting Fas and FasL genes, respectively (Allen et al., 1990; Schulze-Osthoff, 1994a; Reap et al., 1995). Although extrapolating from murine to human models is difficult, defects in human Fas and FasL may contribute to various diseases associated with autoimmunity (Le Deist et al., 1996). Manifestations of defects in *lpr* or *gld* in mice, show similarities to human

systemic lupus erythematosus (SLE) and autoimmune lymphoproliferative syndrome (ALPS). Mutations in the Fas gene have been identified in some patients with ALPS (Fisher et al., 1995; RieuxLaucat et al., 1995) and although very rare, mutations in FasL have been identified in a patient with SLE (Mysler et al., 1994; Wu et al., 1996) and it is possible that defective Fas/FasL systems may also contribute to immune dysregulation observed in multiple sclerosis (D'Souza et al., 1996; Dowling et al., 1996), the progression of cancer by co-operation with oncogenes such as cMyc (Hueber et al., 1997), evasion of tumour surveillance mechanisms (Hahne et al., 1996; Strand et al., 1996) and HIV (Debatin et al., 1994; Katsikis et al., 1995).

### **1.8.7 Apoptosis signalling through Fas**

Transduction of the apoptotic signal from the cell membrane is dependent on signalling from the death domain of Fas and other family members such as TNFR1. Upon receptor crosslinking and activation there follows clustering of the death domains (Huang et al., 1996) and subsequent recruitment of DD containing proteins to form a death inducing signalling complex (DISC) (Kischkel et al., 1995). Using the yeast two hybrid system three death domain containing proteins, TRADD (TNFR1 associated death domain), FADD (Fas-associating protein with a death domain) and RIP (Receptor interacting protein) (Boldin et al., 1995; Stanger et al., 1995; Chinnaiyan et al., 1995; Hsu et al., 1995) were found to interact with the death domains of Fas and TNFR1 and were also capable of interacting with each other (Varfolomeev et al., 1996; Hsu et al., 1996), suggesting a convergence of death inducing signalling pathways between members of the TNFR1 superfamily. FADD also contains a death effector domain (DED) or caspase recruitment domain (CARD) which when mutated blocks the recruitment of caspases to the DISC (Muzio et al., 1996). The involvement of caspases in the receptor-mediated signalling pathway was suggested by the use of specific peptide inhibitors such as Ac-YVAD.CHO and Ac-DEVD.CHO and the virally encoded serpin inhibitor Crm-A which inhibited Fas-mediated apoptosis (Los et al., 1995; Enari et al., 1995; Tewari and Dixit, 1995a; Enari et al., 1996).

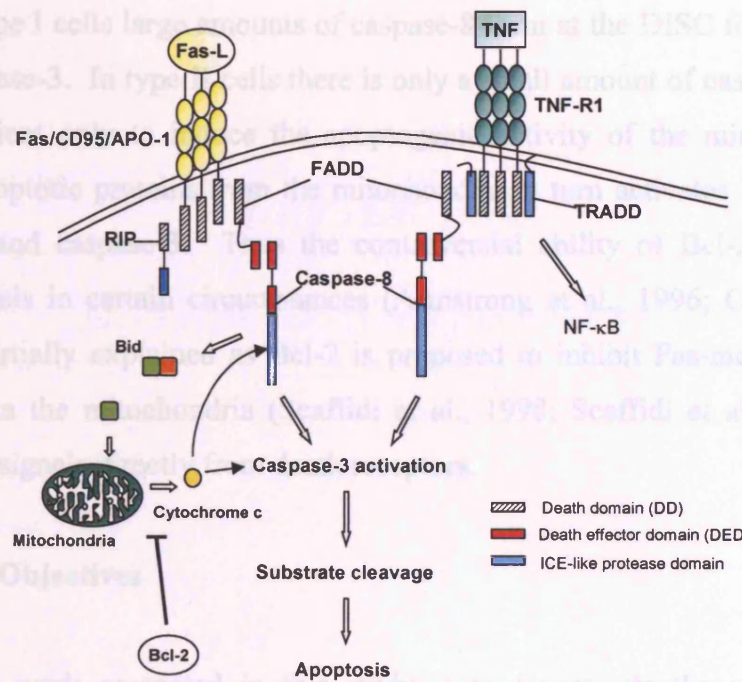


**Figure 1.10 Model for receptor-mediated apoptosis.** Receptor trimerization and ligation results in recruitment of caspase-8 and subsequent activation. Amplification of caspase-8 is mediated by cleavage of Bid and cytochrome c release from the mitochondria which can be inhibited by Bcl-2.

The identity of the ICE-like protease MACH/FLICE/Mch5/Caspase-8 as a FADD interacting protein at the apex of the Fas signalling cascade (Muzio et al., 1996; Boldin et al., 1996; Srinivasula et al., 1996a), conclusively linked signalling events from the Fas receptor to downstream events mediated by effector caspases (Figure 1.10) (Hasegawa et al., 1996, Griedinger et al., 1996; Whyte, 1996). Caspase-8 contains a death effector domain with homology to the death effector domain of FADD. FADD recruitment of caspase-8 via the DED results in caspase-8 autocatalytic cleavage (Muzio et al., 1998) and activation of downstream effector caspases such as caspase-3 (Stennicke et al., 1998). This identifies caspase-8 as the apical caspase in the receptor-mediated signalling cascade (Juo et al., 1998). Apoptosis induced by caspase-8 is amplified through the mitochondrial release of cytochrome c (Kuwana et al., 1998) via Bid, a BH3 domain-containing protein which interacts with Bcl-2 and Bax (Luo et al., 1998). Caspase-8 cleaves Bid and the carboxy terminal fragment translocates to the mitochondria whereupon cytochrome c release is triggered, amplifying caspase-8 and caspase-3 activation (Luo et al., 1998; Kuwana et al., 1998). Signalling from the Fas receptor has been proposed to occur via either mitochondrial dependent (Type II) or independent (Type I) mechanisms (Scaffidi et

al., 1998). In type I cells large amounts of caspase-8 form at the DISC followed by direct cleavage of caspase-3. In type II cells there is only a small amount of caspase-8 formed at the DISC sufficient only to induce the apoptogenic activity of the mitochondria. The release of proapoptotic proteins from the mitochondria in turn activates large amounts of both caspase-8 and caspase-3. Thus the controversial ability of Bcl-2 to inhibit Fas-mediated apoptosis in certain circumstances (Armstrong et al., 1996; Chinnaiyan et al., 1996) can be partially explained as Bcl-2 is proposed to inhibit Fas-mediated apoptosis which signals via the mitochondria (Scaffidi et al., 1998; Scaffidi et al., 1999) but not apoptosis which signals directly from death receptors.

### **1.9 Aims and Objectives**

The aim of the work presented in this study is to investigate the regulation of the biochemical and morphological features of receptor and chemical-induced apoptosis primarily by the Bcl-2 family of proteins and peptide-based caspase inhibitors, as both have been shown to act at distinct points during the apoptotic program in response to different stimuli. To dissect the effect of these inhibitors various biochemical features of apoptosis will be studied, in particular caspase activation, after treatment with either anti-Fas or staurosporine in Jurkat T cells.

**CHAPTER TWO**  
**MATERIALS AND METHODS**

## **2.1 CELL CULTURE TECHNIQUES**

### **2.1.1 Culture of Jurkat T cells**

Jurkat cells (Clone E6-1) derived from human leukaemic T-cell lymphoblasts (Schneider et al., 1977; Gillis and Watson, 1980) were obtained from ATTC (Rockville, MD, USA) and maintained with RPMI 1640 (Gibco BRL, Paisly, UK) supplemented with 10% foetal calf serum (FCS) (Sigma, UK) and 2mM L-Glutamine (complete medium). All cell cultures were kept in a humidified atmosphere at 37°C and 5% CO<sub>2</sub>. Bcl-2 and Bcl-xl transfected Jurkat cells were cultured in complete medium supplemented with 150units/ml Hygromycin B (Calbiochem, UK). All Jurkat cells were maintained in the active log phase by seeding at a density of approximately 0.5x10<sup>6</sup>/ml and subculturing every 2-3days.

### **2.1.2 Culture of MCF-7 cells**

The MCF-7 cells were generously provided by Marja Jäätelä (Danish Cancer Society, Copenhagen, Denmark), and maintained in complete medium. Cells were seeded at a density of 0.25x10<sup>6</sup>/ml and grown to confluent monolayers before subculturing. For routine passage of MCF-7 cells, the medium was poured off and the cells were washed twice with PBS to remove any excess FCS and calcium. Trypsin/EGTA (from a 10x stock) was diluted in sterile PBS and added to the cells. The cells were then incubated for 2min at 37°C. The trypsin/EDTA solution was then poured off and the cells were incubated for a further 10-15min. Cells were then dislodged in the presence of 5mls of PBS. The cell suspension was pipetted up and down to form a single cell suspension, which could be counted on a haemocytometer before plating out at an appropriate density.

### **2.1.3 Treatment of cells**

During the course of this study a number of stimuli were used to induce apoptosis. Agonistic Fas antibody (IgM, Clone CH-11) was obtained from MBL (USA) and was diluted accordingly in complete medium to give a final concentration of 100ng/ml. Staurosporine (Sigma, UK) was used at a final concentration of 0.5µM. N,N,N',N'-tetrakis (2-pyridylmethyl) ethylenediamine (TPEN) (Sigma, UK) was used at a final concentration of 5µM. Tetradecanoylphorbol-13-acetate (TPA) (Sigma, UK) was used at a final

concentration of 20ng/ml. Etoposide (Sigma, UK) was used at a final concentration of 5 $\mu$ M. Thapsigargin (Sigma, UK) was used at a final concentration of 50nm. Phytohaemagglutinin (PHA) (Sigma, UK) was made up in complete medium and used at a final concentration of 2 $\mu$ g/ml. Unless otherwise stated all chemicals were prepared using DMSO as the carrier solvent. In all cases, the final concentration of DMSO never exceeded 0.002%. Unless otherwise stated Jurkat cells were seeded at a density of 1x10<sup>6</sup> cells/ml/treatment but for larger experiments the volume and cell number were scaled up accordingly. MCF-7 cells were seeded at a density of 0.5x10<sup>6</sup> cells/2ml in 45mm diameter petri dishes or 6 well plates for 24h. Prior to treatment the medium was carefully removed and replaced with 1ml fresh medium before addition of the appropriate stimuli.

## **2.2 BIOCHEMICAL ASSAYS**

### **2.2.1 Electrophoretic analysis of protein**

#### **2.2.1.1 Background**

SDS polyacrylamide gel electrophoresis (SDS PAGE) is used to separate proteins on the basis of molecular weight. Proteins are denatured when heated in the presence of SDS and a reducing agent such as dithiothreitol (DTT) or  $\beta$ -Mercaptoethanol. SDS is an anionic detergent which binds to the polypeptide back bone of the protein conferring a net negative charge, which is proportional to the polypeptide length. As a result, all of the proteins in any complex mixture will have an identical charge density per unit length and can be separated electrophoretically based only on their molecular weight/size. Separation of complex protein mixtures and good resolution of protein bands is best achieved by using a discontinuous gel system. Such a system consists of an upper stacking gel and a lower resolving gel, which contain different amounts of polyacrylamide and have differing pH. Upon electrophoresis the mobility of the protein, which is dependent on charge, lies between that of the buffer ion of the stacking gel and the buffer ion of the running buffer in the upper reservoir. This results in the protein concentrating down in the stacking gel as a very thin band or 'zone' before entering the resolving gel therefore increasing the resolution. The amount of polyacrylamide used in the lower resolving gel is dependent upon the molecular weight of the protein to be analysed. In general the higher the molecular weight of the protein, the less polyacrylamide used in the gel. Gels containing a low percentage of polyacrylamide have a larger pore size and therefore allow high

molecular weight proteins to run further down the gel, making analysis easier. In contrast, low molecular weight proteins are analysed on gels containing a higher percentage of polyacrylamide resulting in a small pore size, which retains them at a higher position in the gel. For example, PARP (116kDa) is run on a 7% polyacrylamide gel, whereas cytochrome c (15kDa) is run on a 15% polyacrylamide gel. All the caspases were run on a 13% gel unless otherwise stated and the upper stacking gel contains 5% polyacrylamide for all protein analysis.

### **2.2.1.2 Preparation of gel buffers**

The pH of the lower and upper running buffers of the SDS gel is crucial to the successful separation of proteins and therefore the pH of all solutions was checked before use.

#### ***Lower gel resolving buffer pH8.8 (250ml)***

(1.5M Tris.Cl containing 0.4% SDS)

45.41g Tris base was dissolved in 100ml dH<sub>2</sub>O to which 10mls of a 10% SDS stock (w/v) was added. The solution was then adjusted to pH8.8 with concentrated HCl and made up to 250ml with dH<sub>2</sub>O.

#### ***Upper gel stacking buffer pH6.8 (100ml)***

(0.5M Tris.Cl containing 0.4% SDS)

6.06g Tris base was dissolved in 50ml dH<sub>2</sub>O to which 4mls of a 10% SDS stock (w/v) was added. The solution was then adjusted to pH6.8 with concentrated HCl and made up to 100ml with dH<sub>2</sub>O.

#### ***Running Buffer (1l)***

(25mM Tris, 192mM Glycine, 0.1% SDS)

3.03g Tris base and 14.4g Glycine were dissolved in 500ml dH<sub>2</sub>O to which 10mls of a 10% SDS stock (w/v) solution was added. The volume was then made up to 1l with dH<sub>2</sub>O.

### 2.2.1.3 Preparation of the lower resolving gel and upper stacking gel

All the gels were cast using the Miniprotean II Electrophoresis cell (Biorad). Glass plates were thoroughly washed and dried and the glass plate sandwich was made using a large and small glass plate separated by 1mm spacers (the thickness of spacer used is dependent on the thickness of gel required). The glass plates were assembled on the casting stand and tested for leakage with water. The appropriate volumes of lower gel buffer (pH8.8), polyacrylamide (National Diagnostics, USA), and water were gently mixed in a wide-bottomed flask (Table 2.1). TEMED (N,N,N',N'-tetramethylethylenediamine) and APS (ammonium persulphate) (0.1g/ml dH<sub>2</sub>O) were added just prior to casting the gel. APS acts as the initiator peroxide whilst TEMED acts as the catalyst in the polymerisation process by crosslinking bisacrylamide monomers. The solution was poured up to a mark 5cm from the base of the plates. A few mls of water was carefully pipetted over the gel to prevent the formation of a meniscus without disturbing the gel interface. The lower gel was allowed to set for about an hour, or until fully polymerised and the water layer removed using a syringe. The upper gel was prepared in a similar manner using upper stacking gel buffer (pH6.8) and poured over the polymerised lower gel. Combs were inserted into the upper gel, which was left to polymerise for a further hour. Once the upper gel had set, the combs were removed and the wells were rinsed out twice with running buffer using a syringe to remove any unpolymerised solution. The buffer chamber was then assembled and immersed into an electrophoresis cell containing 1l running buffer.

Table 2.1

	Lower Resolving Gel <sup>a</sup>					Upper Gel	
	Final polyacrylamide concentration in the gel (%)						
	15%	14%	13%	12%	10%	7%	5%
Gel Buffer <sup>b</sup> (ml)	6.3	6.3	6.3	6.3	6.3	6.3	5
Polyacrylamide <sup>c</sup> (ml)	12.4	11.6	10.8	10.0	8.4	5.8	2.6
dH <sub>2</sub> O (ml)	6.3	7.1	7.9	8.7	10.3	12.9	12.4
APS <sup>d</sup> (μl)	150	150	150	150	150	150	75
TEMED (μl)	20	20	20	20	20	20	10

<sup>a</sup> Columns represent volumes (ml/μl) of reagents required to make 25ml gel mixture

<sup>b</sup> Lower gel buffer pH8.8, Upper gel buffer pH6.8

<sup>c</sup> Polyacrylamide – 30% (w/v) acrylamide, 0.8% (w/v) bis-acrylamide (37.5:1)

<sup>d</sup> APS (Ammonium persulphate) 0.1g/ml dH<sub>2</sub>O prepared fresh

#### 2.2.1.4 Preparation of protein samples for SDS PAGE.

Cell pellets were resuspended in 30μl sample resuspension buffer (0.1M NaCl, 0.01M Tris.HCl (pH7.6), 0.001M EDTA and 1mM PMSF) and taken through three freeze thaw cycles to produce a crude cell lysate. The protein content of each lysate (μg/μl) was determined using the Biorad protein assay. To ensure equal concentrations of protein were loaded onto each lane, the volume of lysate needed to load 30μg total protein was calculated and diluted with resuspension buffer and the appropriate amount of 2x SDS sample buffer (4% SDS, 20% Glycerol, 1M Tris/HCl pH8.6, 0.2% bromophenol blue, 100mM DTT-added fresh and 1mM PMSF) was added to give a final volume of 20μl. For PARP analysis, 4M urea was included in the sample buffer and the samples were sonicated (using a probe) on 3x 5sec cycles to aid PARP solubilization and extraction. All samples were incubated in a boiling water bath for 8 min and spun down at 8000rpm for 10sec in a benchtop mini-centrifuge prior to loading. The time between adding the sample buffer to lysates and loading was kept to a minimum.

### **2.2.1.5 Determination of protein concentration using the Biorad protein assay**

The protein to be quantified (1 $\mu$ l/2 $\mu$ l aliquots) was added to semi-micro cuvettes containing 0.8ml water. 200 $\mu$ l of Biorad reagent was added to each cuvette to give a final volume of 1ml. The solution was mixed, by gently inverting 2-3 times and kept at room temperature for 5min-1h. The absorbance of the protein dye complex is relatively stable and therefore the assay does not require critical timing. Several dilutions of bovine serum albumin (BSA) at 2,4,8,16 and 20 $\mu$ g/ml for the standard curve, were prepared from a 2mg/ml stock. Absorbance at OD<sub>595</sub> versus reagent blank was measured using a spectrophotometer and plotted against the known protein concentration of the standards. The absorbance of unknown samples were read from the standard curve and the protein concentration ( $\mu$ g/ $\mu$ l) calculated for each sample.

### **2.2.1.6 SDS Polyacrylamide Gel Electrophoresis**

Prepared protein samples were loaded into the wells of an SDS polyacrylamide minigel in an electrophoresis cell (Biorad) containing running buffer (25mM Tris, 192mM Glycine, 0.1% SDS) and run at 120V for approximately 1hr or until the dye front had run off the bottom of the gel. Following the run the lower resolving gel was cut away from the upper stacking gel and was either stained with coomassie blue or transferred to nitrocellulose membrane for immunodetection procedures.

### **2.2.1.7 Coomassie blue staining of proteins in SDS polyacrylamide gels**

After electrophoresis the gel was stained in rapid coomassie blue stain (0.06% coomassie blue G-250, 10% acetic acid). The gel was placed in a covered container, immersed in staining solution and placed on a shaker for 30-60min. The staining solution was replaced with destain solution (5% methanol, 7% glacial acetic acid with dH<sub>2</sub>O) which was changed twice a day until the gel background was clear. To speed up the destain process, folded white tissue paper was placed in one corner of the container to help absorb coomassie blue from the gel without changing the destain solution.

### 2.2.2 Western Transfer and immunodetection procedures

For Western transfer, the gel, 4 sheets of Whatman paper and 2 scotchbrite sponges were equilibrated in transfer buffer (25mM Tris, 192mM Glycine, 20% methanol) for about 30min. Nitrocellulose membrane (Hybond C-extra, Amersham) was first activated in distilled water for 10min before soaking in transfer buffer. The transfer sandwich was then assembled in a transfer cassette as illustrated below.

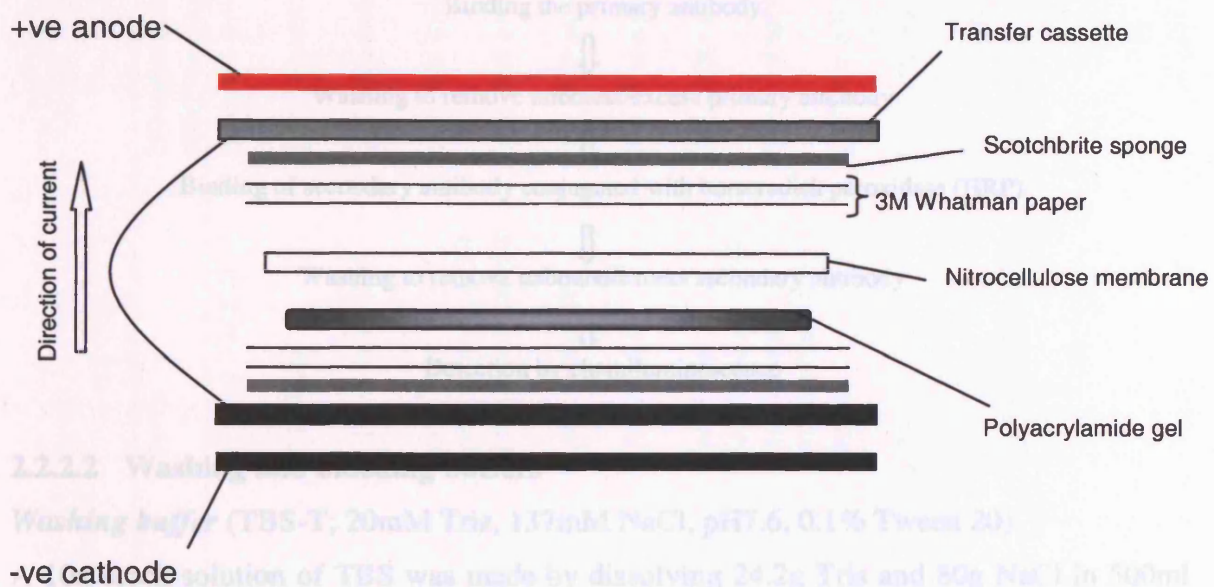
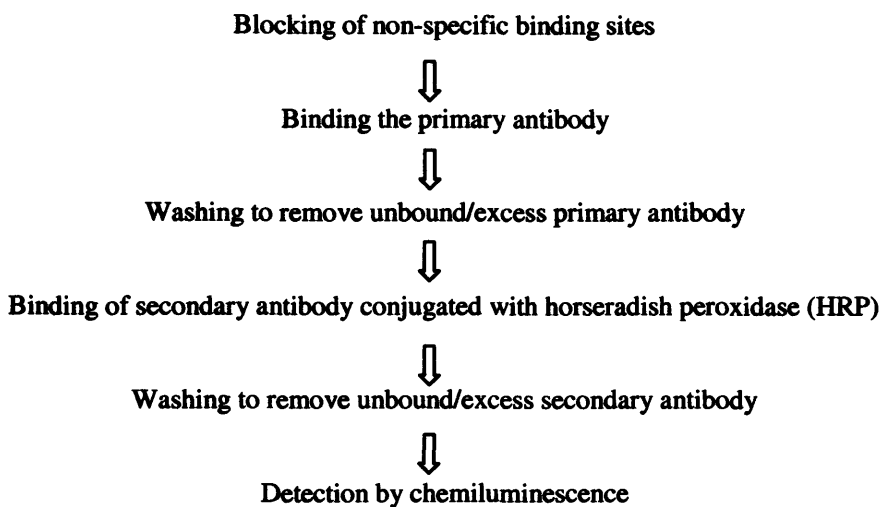


**Figure 2.1 Assembly of transfer sandwich for western blotting.**

The transfer cassette was then immersed into a transblot cell (Biorad), which was filled with transfer buffer. The proteins were transferred from negative to positive i.e. from the gel to the nitrocellulose membrane at 60V for 2h at 4°C or 30V in a cold room overnight. After the transfer the gel was stained with coomassie blue stain, as described above, to visualize residual protein and assess the efficacy of protein transfer. The membrane was stained with Ponceau S solution (0.1% (w/v) ponceau S, 5% acetic acid) for one minute and rinsed with water to visualise the transferred protein profiles. The membrane was then rinsed in water until all ponceau S stain had been removed and taken through immunodetection with the appropriate antibody.

### 2.2.2.1 Immuno-detection procedures

Following successful transfer to a nitrocellulose membrane, specific proteins can be detected by probing the membrane with the appropriate primary and secondary antibodies and visualized by chemiluminescence. An outline of the procedure is shown below:



### 2.2.2.2 Washing and blocking buffers

**Washing buffer** (TBS-T; 20mM Tris, 137mM NaCl, pH7.6, 0.1% Tween 20)

A 10x stock solution of TBS was made by dissolving 24.2g Tris and 80g NaCl in 500ml dH<sub>2</sub>O and adjusting the pH to 7.6 with 1N HCl before making the volume up to 1l with dH<sub>2</sub>O. A solution of 1x TBS-T was made by diluting the 10x stock and adding 1ml Tween-20 to give a final concentration of 0.1%. The pH of the TBS-T solution should be at pH7.6 as any major deviation from this may affect the efficacy of both primary and secondary antibody binding and could result in the absence of a detectable HRP-signal upon addition of chemiluminescence reagents.

**Blocking buffer** (TBS-T+5% non-fat dried milk)

To make the blocking solution, 25g of Marvel non-fat dried milk was dissolved in 500ml of 1x TBS-T solution (as described above). TBS-T + 5% non-fat dried milk was made up fresh and can be kept for 2-3 days at 4°C.

#### **Antibody solutions**

All primary and secondary antibodies were diluted to the appropriate concentration in 15ml TBS-T (Table 2.2). After use primary antibody solutions were retained and kept frozen in order to be used again.

**Table 2.2 Antibodies used for Immunodetection Procedures**

<b>Protein to be detected</b>	<b>Type of antibody (Clone-if known)</b>	<b>Dilution Used</b>	<b>Source</b>	<b>Secondary Antibody (HRP-conjugated)<sup>a</sup></b>	<b>Source</b>
PARP <sup>b</sup>	Mouse monoclonal (C2-10)	1:10,000	G.Poirier, Canada	IgG Goat anti-Mouse	DAKO Ltd.
Bcl-2 oncoprotein	Mouse monoclonal (C-2)	1:1000	DAKO Ltd.	IgG Goat anti-Mouse	DAKO Ltd.
Bcl-x <sub>l</sub>	Mouse monoclonal (2A1)	1:10,000	C. Thompson, USA	IgG Goat anti-Mouse	DAKO Ltd.
Caspase-2	Rabbit polyclonal	1:1000	Santa Cruz Biotechnology, USA	IgG Goat anti-Rabbit	DAKO Ltd.
Caspase-3	Rabbit polyclonal	1:10,000	Merck Frost, Canada	IgG Goat anti-Rabbit	DAKO Ltd.
Caspase-6	Mouse monoclonal	1:1000	Pharmingen, UK	IgG Goat anti-Mouse	DAKO Ltd.
Caspase-7	Rabbit polyclonal	1:2000	X.M.Sun, UK	IgG Goat anti-Rabbit	DAKO Ltd.
Caspase-8	Goat polyclonal	1:1000	Santa Cruz Biotechnology, USA	IgG Rabbit anti-Goat	DAKO Ltd.
Fas Ligand	Mouse monoclonal (E6-1)	1:1000	Transduction Laboratories, USA	IgG Goat anti-Mouse	DAKO Ltd.
Penta.His tag	Mouse monoclonal	1:1000	Qiagen,	IgG Goat anti-Mouse	DAKO Ltd.
DFF45 <sup>c</sup>	Rabbit polyclonal	1:5000	X.Wang, USA	IgG Goat anti-Rabbit	DAKO Ltd.
Cytochrome c	Rabbit polyclonal	1:1000	Santa Cruz Biotechnology, USA	IgG Goat anti-Rabbit	DAKO Ltd.

### 2.2.2.3 Immunodetection of transferred proteins

Following protein transfer and staining with ponceau S, the membrane was incubated in blocking buffer for 1h to block non-specific protein binding sites. The blocking buffer was poured off and the membrane was then washed twice for 5min in TBS-T to remove any residual blocking buffer. The membrane was then incubated for 1h with the appropriately diluted primary antibody directed against the protein of interest (Table 2.2). The primary antibody solution was poured off and the membrane was taken through one complete wash procedure. All incubations and washes were carried out at room temperature under continuous gentle agitation.

#### *Washing Procedure*

1. 15 minutes in blocking buffer (TBS-T + 5% non-fat dried milk)
2. Repeat 2x 5min washes (TBS-T + 5% non-fat dried milk)
3. 15 minutes in washing buffer (TBS-T)
4. Repeat 2x 5min washes (TBS-T)

Secondary antibodies (HRP conjugated) were diluted in TBS-T and incubated with the membrane for 1h. The membrane was again taken through one complete wash procedure before incubating with the chemiluminescence reagents (Supersignal, Luminol/Enhancer solutions, Pierce Ltd.) according to manufacturers specifications for 5min. The HRP acts as a catalyst oxidizing the luminol substrate and producing a luminescent signal, which can be detected on film. The membrane was then carefully enveloped in cling-film avoiding air bubbles, placed in a photographic cassette, and exposed to Hyperfilm ECL (Amersham) before being developed. Luminescent signals can be detected after 30sec and varying the length of exposure will result in more or less sensitivity.

The membrane can be reprobed with different antibodies after incubating with stripping buffer (62.5mM Tris Hcl pH6.8, 2% SDS, 100mM  $\beta$ -Mercaptoethanol) for 30min at 60-70°C. However, it must be noted that stripping of the nitrocellulose membrane can remove membrane bound protein as well as antibodies and may therefore result in weaker antibody binding and subsequent chemiluminescent signals.

#### **2.2.2.4 Double-immunodetection procedure**

As an alternative to stripping, the membrane was reprobbed with different antibodies following extensive washing in TBS-T. This procedure is especially effective if the second protein to be detected has a different molecular weight to the first, which could obscure new binding. The membrane was thoroughly washed in TBST, either overnight at 4°C or for 6x 5min washes before further analysis by Western blotting with different antibodies. This reprobing procedure was modified to enable 'double-immunodetections' to be carried out by consecutively using two different primary antibodies. The methodology is briefly outlined below.

1. Blocking of membrane in blocking buffer (1h)
2. Membrane washed in washing buffer (2x 5min)
3. Primary antibody (A1) incubation (1h)
4. Membrane is taken through one complete wash procedure
5. Secondary antibody (A2) incubation (1h)
6. Membrane is taken through one complete wash procedure
7. Primary antibody (B1) incubation (1h)
8. Membrane is taken through one complete wash procedure
9. Secondary antibody (B2) incubation (1h)
10. Membrane is taken through one complete wash procedure
11. Chemiluminescence detection

#### **2.2.2.5 Analysis of sFasL secretion by Dot Blotting**

After treatments the Jurkat cells were centrifuged at 5000rpm for 10min on a benchtop centrifuge. The supernatant was carefully removed and either analysed immediately or frozen at -20°C. The pellet was also frozen and retained for standard Western blot analysis. HyBond Nitrocellulose membrane was activated in water for 10min before placing in a Biorad dot-blot unit and applying a little suction. The supernatant (200µl) was loaded into each well. The nitrocellulose membrane was then allowed to dry for 20min, removed from the dot-blot unit and stained with Ponceau S to visualise protein. The membrane was then taken through the standard immunodetection procedure (section

2.2.1), using an antibody specific for FasL (Table 2.2). The relative levels of FasL secretion into the supernatant were quantified by scanning densitometry.

### **2.2.3 DNA fragmentation analysis**

#### **2.2.3.1 Analysis of DNA fragmentation into oligonucleosomal-length fragments by Conventional Agarose Gel Electrophoresis (CAGE)**

##### **2.2.3.2 Background**

The fragmentation of DNA into oligonucleosomal length fragments is a hallmark feature of apoptosis (Wyllie, 1980). Upon the induction of apoptosis, endogenous nuclease activities degrade DNA by targeting the linker regions between nucleosome structures generating single or multiple DNA fragments of 180-200bp in length. Upon conventional agarose gel electrophoresis, these oligonucleosomal fragments appear as a distinctive laddering pattern. In contrast, necrotic cells undergo random, unordered DNA cleavage resulting in a smear when electrophoresed under similar conditions.

##### **2.2.3.3 Preparation of agarose gel**

The casting tray and comb were thoroughly washed, dried and the two ends of the casting tray were sealed with tape. The comb was fixed in place approximately 1.5 cm from the top of the casting tray. A 1.8% agarose gel was then made up by adding 1.8g ultrapure agarose to 90ml dH<sub>2</sub>O and 10ml 5x TBE (TBE 5x stock =445mM Tris buffer, 445mM Boric acid, 12.5mM EDTA), mixing in a loosely capped duran bottle and carefully heated in a microwave oven. Once all agarose had dissolved the gel solution was cooled to 50°C in a water bath set at 50°C and poured into the casting tray and left to set. When the gel had set, the area directly above the comb was cut away leaving a trench for the digestion gel (0.8% agarose). The digestion gel was made up by dissolving 0.16g ultrapure agarose in 15.5ml ultrapure water, 2.5ml 20% SDS and and 2ml 5xTBE. The mixture was heated until all agarose had dissolved and left to cool to 50°C. 10ml of the gel solution was mixed with 500µl of 25µg/ml proteinase K, and then the gel was poured into the pre-cut trench above the wells and allowed to set. The tape sealing the ends of the gel was then removed and the comb removed. The complete gel was then immersed in a gel tank containing 1x TBE buffer.

### **2.2.3.4 Sample Preparation**

After treatments, samples of  $1 \times 10^6$  cells were spun at 6000rpm for 10min in a bench-top centrifuge. The supernatants were removed and the cell pellets were resuspended in 10 $\mu$ l water and 5 $\mu$ l of 50mg/ml RNase A and left to incubate at room temperature for 20min. Loading buffer (5 $\mu$ l) containing 0.2% bromophenol blue was then added, mixed and 15 $\mu$ l from each sample was loaded into the wells of the prepared agarose gel. The gel was run overnight at 20V. At the end of the run, the gel was rinsed in water and stained with ethidium bromide (0.1mg/ml) for 30min, washed in TE8 buffer (10mM Tris pH8.0, 1mM EDTA) and photographed.

### **2.2.3.5 Field Inversion Gel Electrophoresis (FIGE) for analysis of High Molecular Weight DNA fragments**

#### **2.2.3.6 Background**

Prior to the formation of the oligonucleosomal length DNA fragments, chromatin is first cleaved into high molecular weight fragments of 50-700kbp in length. These fragments, which cannot be resolved using CAGE can be separated using field inversion gel electrophoresis which can separate DNA molecules up to 2000kb in length (Carle and Olsen, 1986; Gel Electrophoresis of nucleic acids -A practical approach, Edited by D.Rickwood and B.D.Hames). Using this technique the DNA travels through an agarose gel under the influence of an homogenous electrical field in which the polarity is switched back and forth throughout the run. This results in the DNA making small backward and forward movements through the gel. A net forward movement is achieved by using either a greater part of the switching cycle or a higher voltage for movement in the forward direction. Increasing the length of a switching cycle increases the size of DNA that can be resolved and *vice versa*. By incorporating a ramp between the lower and upper switching cycle limits, DNA molecules with a relatively wide range of sizes can be resolved.

### 2.2.3.7 Preparation of cell samples in agarose plugs

A solution of 1% low melting point agarose was made up in PBS and cooled to 50°C in a heated waterbath. Plug insert moulds were cleaned and taped along the bottom surface with cellotape. After treatment cell samples ( $1 \times 10^6$  cells) were spun at 5000rpm for 10min in a benchtop centrifuge. The supernatants were removed and the cell pellets were resuspended in 40µl of pre-warmed PBS and incubated for 2-3min at 50°C in the waterbath. This was followed by the addition of 60µl 1% Low melting point agarose (in PBS) followed by gentle mixing and dispensed into the plug insert moulds. The moulds were placed on ice for 10min to allow the agarose plugs to set. Once set, the tape along the bottom of the moulds was carefully removed and each plug was gently pushed out into 1ml NDS buffer (0.5M EDTA, 1% lauryl sarcosine, 10mM Tris) containing 20mg/ml pronase, and incubated at 50°C. After 24h the NDS buffer was replaced, more pronase was added and the plugs were incubated for a further 24h. Following the incubations, the plugs were rinsed twice in NDS (without pronase) for 2h and stored at 4°C in NDS. Prior to electrophoresis the plugs were washed at least three times in TE8 buffer to remove the lauryl sarcosine.

### 2.2.3.8 Preparation of FIGE Agarose Gel

Two glass plates (one normal and one frosted) were cleaned thoroughly, separated by spacers down either side and assembled on the casting table. The plates were tested for leaks with water, and then completely dried. The comb was prepared and the plates were warmed to 50°C for 30min. A 1% agarose gel was made up with 1g ultrapure agarose dissolved in 100ml 0.5x TBE and heated carefully in a microwave until all agarose had melted. The gel solution was then cooled to 50°C and dispensed between the pre-warmed glass plates using a 25ml pipette. About 5ml of the molten agarose was retained and kept in the water bath for later use. The comb was immediately inserted at the top of the gel between the glass plates and the gel was left to set for 1h. Once the gel had set, the comb was carefully removed, taking care not to tear the gel. One third of each agarose plug containing sample was placed into each well using a glass slide and small spatula. The agarose plugs were cemented into place with the remaining molten agarose and allowed to set. Any excess agarose on top of the well was then sliced away with a sharp scalpel to

provide a flush surface between the gel and glass plates. The upper reservoir tank was fitted above the glass plates making sure there was an airtight seal between the plates and the tank to prevent leakage. The whole cassette was carefully lowered into a tank containing 4l of 0.5x TBE and the upper reservoir was filled with 500mls 0.5x TBE. The whole electrophoresis tank was kept cool to less than 10°C by a refrigerated cooling unit. Electrodes were connected directly to a Hoeffer pulse switcher which was itself connected to a constant power supply of 200 volts. The running time of the gel totalled 7hr and consisted of two pre-set programs running in tandem:

**PROGRAM 1**

Run in time: 15min

Run time: 2h

Pulse: 2.4 sec to 2.4 sec

**PROGRAM 2**

Run in time: 0min

Run time: 5h

Pulse: 2.4 sec to 24 sec

Following the run the gel was rinsed in water, stained with ethidium bromide in TE8 buffer (0.1mg/ml) and photographed. Molecular weight markers used were Pulse marker 0.1-200kbp standard (Sigma, Poole,UK) and *S.cerevisiae* chromosomes (243-2200 kbp) (Clontech, Cambridge, UK).

#### **2.2.4 Column purification of His6 tagged proteins using metal affinity resin**

Because the DFF40/45 form heterodimers, the tandemly expressed proteins could be purified together by the binding of the His6 tag of DFF40 to a Talon™ cobalt-based metal affinity resin (Clontech, USA) under non-denaturing conditions. The resin is supplied as a 50% (v/v) slurry in nonbuffered 20% ethanol. Prior to use, 1ml Talon resin was centrifuged at 700g for 2min at 4°C. The ethanol was removed and replaced with an equal volume of PBS. The IPTG induced bacterial cell pellet was resuspended in 4ml PBS (containing 1mM PMSF) and sonicated on ice for 10cycles (5s on/5s off) to reduce viscosity. The suspension was placed on ice for 15min and the sonication repeated before incubating on ice for a further 30min. The suspension was centrifuged at 14,000rpm for 15min at 4°C and the supernatant was carefully removed and added to the freshly prepared Talon affinity resin in a 15ml Falcon tube. The resin/lysate suspension was incubated with rotation at 4°C for 12-16h. The resin/lysate suspension was then packed onto a 2ml gravity flow column and unbound protein allowed to flow through. The column was then washed twice with 10 bed volumes of wash buffer (50mM NaH<sub>2</sub>PO<sub>4</sub>, pH8.0, 300mM NaCl and 10mM imidazole). The bound protein was eluted with 10 bed volumes of Elution

buffer (50mM NaH<sub>2</sub>PO<sub>4</sub>, pH8.0, 300mM NaCl, 100mM imidazole) and collected in 1ml fractions. The protein content of the eluted fractions was determined using the Biorad protein assay. 20-30µl of each fraction was analysed by SDS-PAGE and Western blotting. It was found that transfer of the proteins to nitrocellulose and subsequent immuno detection with the appropriate antibodies was a more sensitive method of detecting eluted DFF40/45 protein in comparison to direct staining of the gel with coomassie blue. Using this method, it was possible to select the eluted fractions and pool those which contained the desired protein. Pooled fraction proteins were concentrated using the centricon-10 concentrators according to manufacturers instructions.

### **2.2.5 *In Vitro* DFF nuclease assay**

In order to determine the nuclease activity of DFF40/45, an *in vitro* assay was set up using recombinant DFF fusion protein and recombinant caspase-3 based on that described previously by (Liu et al., 1999). pcDNA (Invitrogen) was incubated with 1µg of purified DFF40/45 fusion protein and 500ng recombinant caspase-3 (Gift from Dr. Don Nicholson, Merck Frost, Canada) in the absence or presence of 2.5µg histone H1 (Roche Molecular Biochemicals) and made up to a final volume of 100µl in Buffer A (20mM HEPES-KOH, pH7.5, 10mM KCl, 4mM MgCl<sub>2</sub>, 1mM sodium EDTA, 1mM EGTA, 1mM DTT, 0.1mM PMSF). The samples were mixed and incubated at 37°C for 2h. The reaction was stopped by adding EDTA to a final concentration of 5mM. The samples were mixed with DNA loading buffer and loaded onto a 2% agarose gel containing 0.1mg/ml ethidium bromide and visualized under UV light.

### **2.2.6 Analysis of cytochrome c release into cytosol during apoptosis.**

One of the consequences of apoptosis is the release of cytochrome c from the mitochondria. Thus the presence of cytochrome c in the cytosolic fraction of treated cells is an indication that the apoptotic process is being activated. In the majority of studies analysis of cytochrome c release is carried out by lysing the cells and obtaining a cytosolic and mitochondrial fraction. Briefly, the cells are resuspended in a hypotonic buffer which causes swelling and then lysed in a dounce-type homogenizer. In the course of this study, the homogenization technique was initially used. However, it was found that the use of the homogenizer did not result in consistent levels of cell lysis when the cell suspensions were

examined with trypan blue staining and light microscopy. In addition, the processing of more than two samples at any one time proved logistically impractical. Therefore, an alternative method was employed which was found to result in reproducible levels of cell lysis and processing of multiple samples at the same time, thus making comparisons between experiments more reliable. The method used is based on the ability of streptolysin O to permeabilize cellular membranes.

### **2.2.6.1 Optimisation of cell lysis using streptolysin O.**

A dose response study was carried out to determine the most appropriate concentration of streptolysin O required to achieve maximum cell lysis (Figure 2.2). Eight eppendorf tubes, each containing  $3 \times 10^6$  cells were centrifuged at 5000rpm for 10min at 4°C. The supernatants were removed and the pellets were washed once in ice cold PBS and centrifuged at 5000rpm for 10min at 4°C. The supernatants were discarded and the cell pellet was resuspended in 100µl of stabilization buffer (210mM mannitol, 70mM sucrose, 5mM HEPES (pH7.2), 1mM EGTA, 0.05% BSA, 5mM DTT, 0.02mM PMSF). The appropriate volume of streptolysin O (from a stock of 60units/µl) was added to each cell suspension to give final concentrations of 10, 20, 40, 50, 60, 80 and 100units/ $10^6$  cells. After mixing, the cell suspensions were incubated in a 37°C waterbath for 20min and the extent of cell lysis was assessed by counting the number of cells which take up trypan blue when viewed under light microscopy (Figure 2.2). As a result of this preliminary experiment, the optimum concentration of streptolysin O was found to be 60units/ $10^6$  cells. This method consistently resulted in 60-70% cell lysis without producing any potential secondary effects such as mitochondrial contamination of the cytosol.

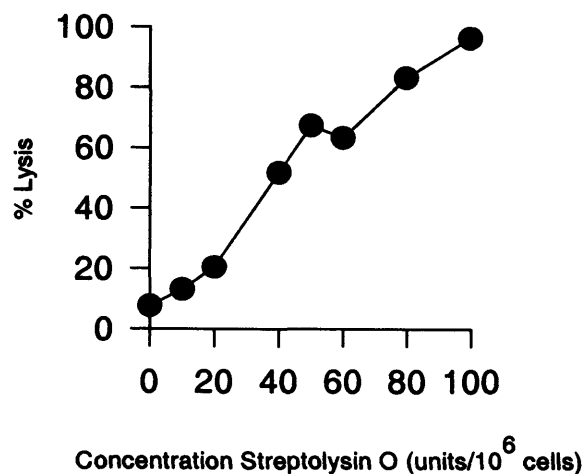


**Figure 2.2 Determination of cell lysis by Streptolysin O.** A concentration range of 0-100units/10<sup>6</sup> cells streptolysin O was used. From this preliminary study streptolysin O was used at a concentration of 60units/10<sup>6</sup> cells. 3x10<sup>6</sup> treated cells were centrifuged at 5000rpm for 10min at 4°C. The supernatant was removed and the pellet was washed once in ice cold PBS and centrifuged as above. The pellet was resuspended in 100µl of stabilization buffer (210mM mannitol, 70mM sucrose, 5mM HEPES (pH7.2), 1mM EGTA, 0.05% BSA, 5mM DTT, 0.02mM PMSF) and incubated at 37°C for 20min in the presence of streptolysin O. The percentage of cell lysis was determined by trypan blue uptake. Data represents the mean from two independent experiments.

Using the optimal concentration of streptolysin O, cytochrome c released from apoptotic cells was determined as follows. After treatments, 3x10<sup>6</sup> cells were centrifuged at 5000rpm for 10min at 4°C. The supernatants were removed and the cell pellets were washed once in ice cold PBS and centrifuged at 5000rpm for 10min at 4°C. The supernatants were discarded and the cell pellets were resuspended in 100µl of stabilization buffer. 3µl of streptolysin O (from a stock of 60units/µl) was added to each cell suspension giving a final concentration of 60units/10<sup>6</sup> cells. The cell suspensions were incubated in a 37°C waterbath for 20min. After incubation a small aliquot of each cell suspension was taken and the level of cell lysis was assessed with trypan blue. The cells were then spun at 15,000rpm for 30min at 4°C to separate cytosolic and mitochondrial fractions. The fractions were then analysed for the presence of cytochrome c using Western blot analysis.

### 2.2.7 Measurement of caspase enzymatic activity using fluorogenic substrates.

The measurement of caspase enzymatic activity is based on the ability of active caspases to cleave substrates specifically after aspartate residues. Caspase-3-like proteases cleave substrates specifically at DEVD motifs, whilst caspase-6 cleaves at VEID motifs. Synthetic tetrapeptides that mimic these specific caspase cleavage sites can be coupled to a fluorescent molecular marker such as 7-amino-4-methylcoumarin (AMC) or 7-amino-4-trifluoromethylcoumarin (AFC). Upon cleavage of the tetrapeptide by caspases, the fluorescent moiety is released and can be used as a measure of caspase activity. In the course of this study the fluorogenic substrates benzyloxycarbonyl-Asp-Glu-Val-Asp-7-amino-4-trifluoromethylcoumarin (Z-DEVD-AFC) and benzyloxycarbonyl-Val-Glu-Ile-Asp-7-amino-4-methylcoumarin (Z-VEID-AMC) were used to measure caspase-3 and caspase-6 like enzymatic activity.

#### 2.2.7.1 Preparation of cell lysates

Treated cells ( $1 \times 10^6$ ) were centrifuged down at 4°C, 5000rpm for 10min, and washed 1x in ice cold PBS. The supernatants was discarded and the cell pellets were resuspended in 50µl lysis buffer (10mM HEPES, 40mM β-glycerophosphate, 50mM NaCl, 2mM MgCl<sub>2</sub>, 5mM EGTA, pH7.0, 0.3% NP-40). The suspensions were vortexed and kept on ice for 10min. The lysed cell suspensions were then centrifuged at 15,000 rpm for 15 min at 4°C. The lysate was carefully removed and stored at 4°C. The protein concentration of each lysate was determined using the Biorad protein assay<sup>TM</sup> (Section 2.2.1. 5). To optimise the protein and substrate concentrations a series of preliminary experiments were carried out as illustrated in Figure 2. 3. Based on these experiments, throughout the rest of this study 30µg protein (lysate) and 40µM Z-DEVD-AFC/Z-VEID-AMC substrates were incubated for 0, 60 and 120min to assay caspase activity. The appropriate volume of lysate (30µg protein) was taken and made up to a volume of 100µl with buffer A (10mM HEPES, 40mM β-glycerophosphate, 50mM NaCl, 2mM MgCl<sub>2</sub>, 5mM EGTA, pH7.0) in a 96 well plate. The enzyme substrates (Z-DEVD-AFC/Z-VEID-AMC, Calbiochem, UK) were diluted to a concentration of 80µM in assay buffer (buffer A + 10mM DTT). 100µl of the substrate stock was added to the lysate/buffer A mixture to give a final concentration of

40 $\mu$ M substrate in each well. Alongside the samples to be analysed AFC/AMC standards (0.0, 0.2, 1.0, 2.0, 3.0 and 4.0nmols AFC/AMC) were also measured in order to calculate caspase activity. The plate was incubated at 37°C and fluorescence intensity was read at the appropriate wavelength on a Denley Fluoroplate reader.

The excitation and emission wavelengths used were:

Excitation 400nm and emission 505nm (AFC)

Excitation 380nm and emission 460nm (AMC),

the light intensity was set to 10 and photomultiplier gain set at 8.

The fluorescence units of the standards (free AFC/AMC) were plotted,

where x axis = nmole AFC/AMC and the y axis = Fluorescence units (FU).

From the slope of the calibration curve, the number of fluorescence units (FU) per nmoles AFC/AMC can be calculated.

Caspase activity = change in FU/hr x (calculated curve slope)<sup>-1</sup> x (nmole AFC/ $\mu$ g).

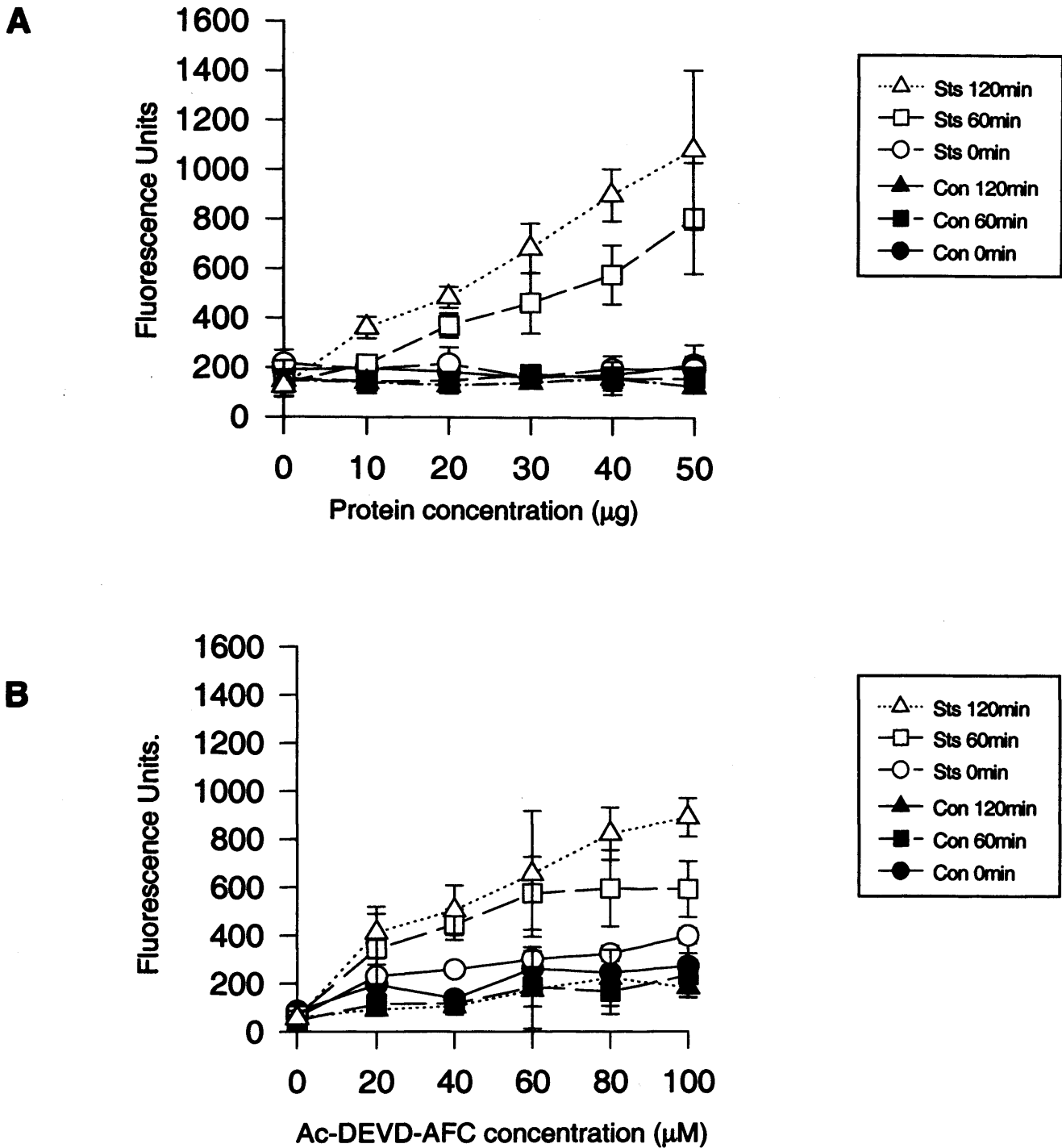


**Figure 2.3 Determination of optimal (A) protein concentration and (B) DEVD substrate concentration for caspase-3 fluorogenic enzyme assay.** Concentration ranges of 0-50 $\mu\text{g}$  protein and 0-100 $\mu\text{M}$  DEVD-AFC/VEID-AMC fluorogenic substrates were assayed for activity at 0, 60 and 120min. Each experiment was repeated three times for both the caspase-3 fluorogenic substrate, DEVD-AFC (above) and caspase-6 fluorogenic substrate, VEID-AMC (results not shown). Data shown represents three experiments  $\pm$  S.D. Using this data, the concentration of DEVD and VEID substrate used throughout the rest of the study was 40 $\mu\text{M}$ . The concentration of cell lysate used was 30 $\mu\text{g}$  and incubation time was 120min.

## 2.3 MOLECULAR BIOLOGY TECHNIQUES

The tandemly expressed DFF45 and His<sub>6</sub> tagged-DFF40 proteins were produced from the pET 15b-DFF vector (kindly provided by X.Wang, USA) transformed into *Escherichia coli* BL21(DE3) (Liu et al., 1998; Liu et al., 1999). For small scale preparation of plasmid DNA the pET-15b DFF plasmid was transformed into the more stable BH5 $\alpha$  cells.

### 2.3.1 Small scale sample preparation of plasmid DNA (mini-prep)

A single colony of transformed BH5 $\alpha$  *E.coli* cells was inoculated into 2ml of LB medium containing 100 $\mu$ g/ml Ampicillin in a loosely capped 15ml tube and incubated overnight in a 37°C shaking incubator. Approximately 1.5ml of the culture was poured into a microfuge tube and spun in a centrifuge at 15,000rpm for 30s at 4°C. The medium was then removed by aspiration leaving the bacterial pellet dry. Cell lysis and mini-prep analysis was carried out according to manufactures instructions (Qiagen, UK). The remainder of the bacterial culture was used to make glycerol stocks by diluting 0.5ml of culture with 0.5ml 30% sterile glycerol in 1.5ml sterile screwcap tubes and freezing at -80°C. To confirm the identity of plasmid DNA, restriction digests were carried out. The use of restriction enzymes is based on their ability to make sequence specific cuts in DNA. All DNA contains numerous restriction enzyme recognition sequences. When cleaved by the appropriate restriction enzyme they produce linear DNA fragments of specific sizes. When separated electrophoretically the fragment sizes can be used to determine the restriction enzyme map, which is highly specific for any one sequence of DNA. For example, digestion of plasmid DNA with a restriction enzyme that cuts at only one site, produces a linear fragment of specific size. Use of further restriction enzymes cutting at different sequences will produce more fragments of varying sizes whose sum total should equal the size of the plasmid.

### 2.3.2 Preparation of agarose gel and restriction enzyme digests.

The Casting tray and comb were cleaned, and cellotape was used to seal either end of the tray and hold the comb in place. A 1% agarose gel was made by dissolving 0.5g ultrapure agarose in 50ml 1x TBE. The solution was heated in a microwave oven and allowed to

cool to 50°C in a waterbath. Just before pouring the gel 3µl ethidium bromide (mg/ml) was added to the molten agarose. Once the gel had set, the tape and comb were carefully removed. The gel was then immersed in a horizontal gel tank containing 1x TBE running buffer.

Reaction mixture for typical restriction enzyme digestion:

Digested DNA		Undigested DNA (control)	
dH <sub>2</sub> O	3.5µl	dH <sub>2</sub> O	4µl
10x Buffer	1µl	10x Buffer	1µl
DNA	5µl	DNA	5µl
Enzyme	0.5µl	Enzyme	-
Total	10µl	Total	10µl

The DNA pellet was re-dissolved in 50µl of TE8 buffer and 25µg/ml DNase-free pancreatic RNase. 5µl Plasmid DNA was added to 10µl dH<sub>2</sub>O, 0.5µl of the required restriction enzyme and 1µl of its appropriate 10x restriction enzyme buffer in an eppendorf tube and vortexed. The samples were incubated with 0.5µl of 50mg/ml RNase for 30min-1hr in a 37°C waterbath. DNA loading buffer (5µl) was then added to each tube, mixed and the samples were loaded into the wells of the 1% agarose gel. The samples were separated at 100V for 45min-1h, stained with ethidium bromide (0.1mg/ml) and visualized under UV light. Restriction enzymes used included Xho I, BamHI and EcoR1 depending on the plasmid being studied and the standard DNA markers used were λHindIII (125-23130bp) and λBst E (117-8454bp).

### 2.3.3 Generation and purification of bacterially expressed DFF protein complexes.

#### 2.3.3.1 Transformation of competent E.coli with PET-15b-DFF vector

A single colony of competent Escherichia coli BL21(DE3) cells were inoculated into 20ml of Luria-Bertani (LB) broth and grown to midlog phase. (OD<sub>600</sub>=0.2-0.8). This was then poured into a 250ml flask containing 100ml LB and incubated under continuous agitation at 37°C for 6h or until cells had grown to OD<sub>600</sub>=0.5-0.9. When the cells had grown to OD<sub>600</sub>=0.6 the flask was put on ice to ensure rapid cooling. The required number of cells were transferred to a Falcon tube (on ice) and left for 10min. The cells were recovered by centrifuging at 4000rpm for 10min at 4°C. All supernatant was removed and

the pellet was resuspended in 20ml cold transforming buffer (10mM PIPES, 55mM MnCl<sub>2</sub>, 15mM CaCl<sub>2</sub>, 250mM KCl, pH6.7) by gentle shaking on ice. Using a chilled sterile pipette tip, 100µl of competent cell suspension was transferred to a sterile centrifuge tube into which 1µl pET-15b-DFF plasmid DNA was added. The contents were gently mixed and transferred to a 42°C waterbath for exactly 45sec. The tube was then placed on ice for 2 min to allow cells to recover. 900µl of SOC medium (2% tryptone, 0.5% yeast extract, 10mM NaCl, 2.5mM KCl, 10mM MgCl, 10mM MgSO<sub>4</sub>, 20mM glucose) was added to each tube, mixed and incubated in a 37°C waterbath for 1h. The tubes were spun down at 12000rpm for 10min. The supernatant was removed and the bacterial pellets were resuspended in 500µl LB broth. Working around a bunsen flame, 100µl and 200µl aliquots of the resuspended bacterial pellets were spread evenly on agar plates containing the appropriate antibiotic (Ampicillin 100µg/ml). The plates were left at room temperature until all of the liquid had been absorbed and then inverted and incubated at 37°C overnight. Colonies containing the plasmids, which harboured an antibiotic resistance gene, appeared in 12-16h.

### **2.3.3.2 Induction of DFF45 and His<sub>6</sub> tagged-DFF40 protein expression in E.coli**

A single colony of transformed *E.coli* was cultured overnight at 37°C in 20ml LB broth containing 100µg/ml ampicillin. The following morning, the 20ml culture was diluted in 400ml LB broth containing 100µg/ml ampicillin and incubated for a further 2h or until a density of 0.6-0.8 at OD<sub>600</sub> had been reached. Induction was carried out with 1mM isopropyl β-D-thiogalactoside (IPTG) at 37°C for 2h before recovering cells by centrifugation at 15,000rpm for 20min in a JA20 rotor (Beckman J2-MC centrifuge). The supernatant was removed and the resulting pellet stored at -20°C until used.

## **2.4 CELL BIOLOGY TECHNIQUES**

### **2.4.1 Generation of Jurkat E6.1 cell clones overexpressing Bcl-2/Bcl-x by electroporation.**

In order to generate stable Bcl-2/Bcl-x overexpressing cells wild type Jurkat cells were transfected with either Bcl-2 or Bcl-x cDNA by electroporation. The electroporation of Jurkat E6.1 cells was carried out using plasmids derived from the Epstein Barr Virus vector (EBV) and the expression cassette of the transient expression vector, pCDM8 (gifts from Märja Jäätela, Denmark). pEBS7-425 (Bcl-2) and pEBS7-623 (Bcl-x) plasmids contained full length human Bcl-2 and Bcl-x cDNA. The empty vector, pEBS7, was used as a control. 0.4ml of the Jurkat cell suspension ( $10 \times 10^6$  cells/ml) was pipetted into the electroporation cuvette and kept on ice. 2 $\mu$ l of the appropriate plasmid DNA was added, carefully mixed, and kept on ice for 5min. The electroporation cuvette was then placed in the Bio-Rad Gene Pulser II electroporator. Cells were electroporated at 300V, 960 $\mu$ F and immediately resuspended in 10ml of pre-warmed complete medium in a small 25ml tissue culture flask and allowed to recover at 37°C with 5% CO<sub>2</sub> in air for 24h. After that hygromycin B (300u/ml) was added to the flask to select out cells containing the plasmid which harbours a hygromycin resistance gene. Once cells were growing well, density gradient centrifugation using Lymphoprep (Nycomed Ltd.) was carried out to remove dead cells from the culture.

#### **2.4.1.2 Preparation of Conditioned Media**

Normal Jurkat cells were grown to log phase ( $0.5 \times 10^6$  cells/ml) and spun down at 1140rpm for 10 min at 4°C. The supernatants were collected and filtered through a 0.2 $\mu$ m filter. Hygromycin B (300units/ml) was added to the supernatants, which were then used as a conditioned media supplement in single cell cloning. Conditioned media was added to complete medium up to 30%.

### **2.4.1.3 Limiting dilution of transfected Jurkat cells**

After electroporation single cell clones were isolated from the pooled transfected cells using limiting dilution. 100µl of complete medium containing 150u/ml Hygromycin B was added to each well of a 96 well plate. Bcl-2 and Bcl-x1 transfected Jurkat cells were seeded at concentrations of 500 cells/ml and 100µl of this cell suspension (~50 cells) was added to well A1 of the 96 well plate and mixed the 100µl medium. Working across horizontally (Table 2.3), 100µl of the diluted cell suspension in well A1 was taken and mixed with the 100µl of medium in well A2. From well A2, 100µl of the diluted cell suspension was taken and mixed with the 100µl of medium in well A3, and so on, until the last well (A12) is reached. Effectively this results in a 1:2 dilution of cells across row A. Using a multi-channel pipette the procedure is repeated working vertically down the plate from row A to row H (Table 2.3). After the serial dilutions had been completed, 100µl of conditioned media containing hygromycin B was added to each well, giving a final volume of 200µl per well. The plates were incubated at 37°C with 5% CO<sub>2</sub> in air. Further plates were set up using cells seeded at concentrations of 100 and 50 cells/ml. Scoring was carried out by examination of plates under an inverted light microscope.

### **2.4.1.4 Expansion of clones derived from a single cell**

Only those cells that were found to be growing in wells statistically containing less than 0.3 cells according to the poisson distribution, were expanded in 24 well plates (Table 2.3). The clones were maintained in complete medium supplemented with 30% conditioned medium (containing 150units Hygromycin/ml). Cells were allowed to grow under these conditions until the cell density was high enough to be transferred into 50ml culture flasks. Once cells were growing well, aliquots were frozen down for later use.

**Table 2.3** Tables representing probability of obtaining a single cell clone**Plate 1 (500 cells/ml)**

Row	1	2	3	4	5	6	7	8	9	10	11	12
A	50	25	12.5	6.25	3.125	1.56	0.78	0.39	0.19	0.097	0.048	0.024
B	-	12.5	6.25	3.125	1.56	0.78	0.39	0.19	0.097	0.048	0.024	-
C	-	6.25	3.125	1.56	0.78	0.39	0.19	0.097	0.048	0.024	-	-
D	-	3.125	1.56	0.78	0.39	0.19	0.097	0.048	0.024	-	-	-
E	-	1.56	0.78	0.39	0.19	0.097	0.048	0.024	-	-	-	-
F	-	0.78	0.39	0.19	0.097	0.048	0.024	-	-	-	-	-
G	-	0.39	0.19	0.097	0.048	0.024	-	-	-	-	-	-
H	-	0.19	0.097	0.048	0.024	-	-	-	-	-	-	-

**Plate 2 (100 cells/ml)**

Row	1	2	3	4	5	6	7	8	9	10	11	12
A	10	5	2.5	1.25	0.625	0.312	0.15	0.08	0.04	0.020	0.01	0.005
B	-	2.5	1.25	0.625	0.312	0.15	0.08	0.04	0.02	0.01	-	-
C	-	1.25	0.625	0.312	0.15	0.08	0.04	0.02	0.01	-	-	-
D	-	0.625	0.312	0.15	0.08	0.04	0.02	0.01	-	-	-	-
E	-	0.312	0.15	0.08	0.04	0.02	0.01	-	-	-	-	-
F	-	0.15	0.08	0.04	0.02	0.01	-	-	-	-	-	-
G	-	0.08	0.04	0.02	0.01	-	-	-	-	-	-	-
H	-	0.04	0.02	0.01	-	-	-	-	-	-	-	-

**Plate 3 (50 cells/ml)**

Row	1	2	3	4	5	6	7	8	9	10	11	12
A	5	2.5	1.25	0.625	0.312	0.15	0.08	0.04	0.02	-	-	-
B	-	1.25	0.625	0.312	0.15	0.08	0.04	0.02	-	-	-	-
C	-	0.625	0.312	0.15	0.08	0.04	0.02	-	-	-	-	-
D	-	0.312	0.15	0.08	0.04	0.02	-	-	-	-	-	-
E	-	0.15	0.08	0.04	0.02	-	-	-	-	-	-	-
F	-	0.08	0.04	0.02	-	-	-	-	-	-	-	-
G	-	0.04	0.02	-	-	-	-	-	-	-	-	-
H	-	0.02	-	-	-	-	-	-	-	-	-	-

## **2.4.2 Techniques for cellular fluorescence staining**

### **2.4.2.1 Assessment of Apoptosis by Hoechst staining.**

Aliquots of treated cells were spun down at 5000rpm for 10min to form a pellet. The supernatants were discarded and the cell pellets were resuspended in 100 $\mu$ l 4% paraformaldehyde and incubated for 45min at room temperature. After fixing, 50 $\mu$ l Hoechst 33358 (8 $\mu$ g/ml) was added to the cells, mixed and incubated for 30min at room temperature. The stained cells were centrifuged down and the supernatants were removed. The cell pellets were resuspended in 20 $\mu$ l PBS/Glycerol (50:50v/v) and stored at 4°C protected from light. To visualise stained nuclei, 2-3 $\mu$ l of the cell suspensions were spread onto glass slides and covered with coverslips before viewing using a Zeiss Axioskop fluorescence microscope. Hoechst 33358 is a membrane permeable bisbenzamide dye which binds AT rich regions in the minor groove of DNA and fluoresces blue with UV excitation. Hoechst dyes are commonly used as a method to visualise or quantify apoptotic cells. Upon examination under UV light, normal cell nuclei appeared to be rounded, with homogenously stained, uncondensed chromatin and a low blue fluorescence. In contrast, apoptotic cell nuclei appeared smaller, were highly condensed or fragmented with the presence of smaller micronuclei and fluoresced brightly. However in the course of this study, a third distinctive phenotype was observed during chemical-induced apoptosis in the presence of the caspase inhibitors benzyloxycarbonyl-Val-Ala-Asp (OMe) fluoromethylketone, (z-VAD-FMK), *N*-acetyl Tyr-Val-Ala-Asp chloromethylketone, (YVAD-FMK) and benzyloxy-carbonyl-Asp-Glu-Val-Asp fluoromethylketone (DEVD-FMK). In these cells the nuclear morphology was neither normal nor apoptotic, as the chromatin was not homogenously stained, but instead staining was uneven and heterogenous in nature, appearing wrinkled or creased. The chromatin was only partially condensed and the nuclei were only slightly smaller than those nuclei of normal untreated cells. For the same reasons, this partially condensed nuclear morphology could not be classified as fully apoptotic. Therefore, in those experiments involving caspase inhibitors three phenotypes were scored, control/normal, partially condensed pre-apoptotic and apoptotic. For all experiments involving Hoechst staining at least 600 cells were counted per sample and all experiments were repeated at least three times.

### **2.4.2.2 Annexin V-FITC/Hoechst 33358 double staining**

During apoptosis, changes in the plasma membrane result in the externalization of phosphatidylserine (PS), a membrane phospholipid which is usually confined to the inner leaflet of the plasma membrane. The annexin family of proteins preferentially bind to PS in the presence of calcium ions (Tait et al., 1989; Raynal and Pollard, 1994) and can be used as an indicator of early plasma membrane changes in apoptotic cells (Martin et al., 1995). For detection of PS exposure and correlation of this apoptotic marker with nuclear morphological changes, the cells were double stained with Annexin-V FITC conjugate and the DNA binding dye Hoechst 33358. Treated cells were centrifuged down and washed twice in ice-cold Modified Annexin Buffer, (MAB) (PBS supplemented with 1mM CaCl<sub>2</sub>, pH7.2). The cell pellet was resuspended in 20µl MAB plus 1µl Annexin V and the sample incubated for 15min in the dark. The cells were then washed three times in ice-cold MAB before being incubated in 200µl 4% paraformaldehyde at room temperature for 30min. The fixed cells were centrifuged down, resuspended in 200µl Hoechst 33358 and incubated for 1hr in the dark at room temperature. The cells were centrifuged at 5000rpm for 5min and the supernatant was discarded. The cell pellets were resuspended in glycerol/PBS (50:50, v/v), and mounted on glass slides for examination using a Leica confocal scanning laser microscope equipped with a dual laser. Alternatively the cell pellets were resuspended in PBS and analysed using flow cytometry (FACscan: Becton & Dickinson, CA, USA) to determine the number of Annexin-V FITC positive cells.

### **2.4.2.3 Detection of mitochondrial membrane depolarization using tetramethylrhodamineethylester (TMRE).**

Accumulation of tetramethylrhodamineethylester (TMRE) in mitochondria has been shown to be driven by mitochondrial membrane potential. TMRE is a membrane permeable rhodamine based probe and is rapidly taken up by live cells and is used as an indicator of mitochondrial membrane depolarisation. Following the appropriate treatment,  $1 \times 10^6$  cells were incubated with 0.1µM TMRE for 15min at 37°C. Cells were washed twice in ice cold PBS and resuspended in 1ml of PBS before analysing by flow cytometry (FACscan: Becton & Dickinson, CA, USA). A decrease in the fluorescence intensity is an indication of mitochondrial membrane potential loss.

#### **2.4.2.4 Staining for cell surface antigen -FasL (non permeabilized cells)**

$1 \times 10^6$  cells were centrifuged down at 5000rpm for 10min at 4°C. The supernatant was removed and the pellet resuspended in 50 $\mu$ l ice-cold PBS/azide solution (PBS/0.02% NaN<sub>3</sub>) to which 1 $\mu$ l of anti-FasL monoclonal antibody was added. The cells were incubated on ice for 30min and then washed three times in PBS/azide solution. The cell pellet was resuspended in 20 $\mu$ l PBS/azide and incubated on ice for 30min in the dark with 1 $\mu$ l FITC conjugated goat anti-mouse secondary antibody. After incubation, the cells were washed three times in PBS/azide and resuspended in 1ml PBS for analysis by flow cytometry (FACscan: Becton & Dickinson, CA, USA).

#### **2.4.2.5 Intracellular staining for FasL (permeabilized cells)**

$1 \times 10^6$  cells were centrifuged down at 5000rpm for 5min at 4°C. The pellet was gently resuspended by adding 200 $\mu$ l methanol drop by drop to prevent aggregation of cells. The cell suspension was vortexed and incubated at room temperature for 10min. The cells were then centrifuged down and the supernatant discarded. The pellet was washed twice in PBS/azide and resuspended in 20 $\mu$ l PBS/azide + 3% BSA. 1 $\mu$ l of the FasL monoclonal antibody was added to the cell suspensions and incubated on ice for 30min. The cells were washed 3x in PBS/azide and resuspended in 20 $\mu$ l PBS/azide + 3% BSA. 1 $\mu$ l of the FITC conjugated goat anti-mouse secondary antibody was added to the cell suspensions and incubated on ice for 30min, in the dark. The cells were washed 3x in PBS/azide and then resuspended in 1ml PBS and analysed by flow cytometry (FACscan: Becton & Dickinson, CA, USA).

#### 2.4.2.6 Analysis of cell growth Kinetics

Cells were washed twice in complete medium and seeded at a density of  $0.25 \times 10^6$ /ml. The cell density was then determined at 24, 48 and 72h by trypan blue exclusion and counting using a haemocytometer. All cell counts were repeated in triplicate. As Bcl-2 cells were grown in the presence of Hygromycin B for selection, the experiment was repeated with and without hygromycin B to ensure that hygromycin B was not affecting cell growth *per se*.

#### 2.4.2.7 Cell cycle analysis

Cells were washed twice in complete medium and seeded at a density of  $0.25 \times 10^6$ /ml. Aliquots (1ml) were removed at 0, 24, 48 and 72h and centrifuged down at 5000rpm for 10 min. The supernatant was removed and the cells were resuspended in 0.5ml 70% ice cold ethanol, added drop by drop whilst vortexing to prevent aggregation. The cells were then stored at 4°C overnight. The suspension was centrifuged at 7000rpm for 10min and the ethanol was removed. The pellet was resuspended in 0.5ml Propidium Iodide (PI) (from a 50µg/ml stock solution) with RNase A (2mg/ml) and incubated at room temperature for 30min. The cells were then centrifuged down at 7000rpm for 10min and resuspended in 1ml PBS prior to analysis using Flow cytometry.

#### 2.4.2.8 Electron Microscopy

For ultrastructural analysis, cells were processed for electron microscopy as described previously (Eriksson et al., 1989; Weis et al., 1995). Briefly, control or treated cells ( $1 \times 10^6$  cells) were centrifuged down and the supernatants discarded. The cell pellets were resuspended in 1% low melting point agarose and dispensed into wells of a plug mould. The agarose plug was then fixed with 2.2% glutaraldehyde in PBS for 30min, post-fixed with 1% OsO<sub>4</sub> in PBS and then dehydrated in a graded series of ethanol and propylene oxide before embedded with Epon 812 resin. Thin sections were obtained and mounted onto uncoated grids and stained with uranyl acetate and lead nitrate, before viewing in a Jeol JSM transmission microscope.

### 2.4.2.9 Assessment of Cell Viability

Cell viability was assessed using the Cell Titer 96™ non-radioactive cell proliferation assay (Promega). The assay is based on the conversion of a tetrazolium salt compound, MTS (3-(4,5-dimethylthiazol-2-yl)-5-(3-carboxymethoxyphenyl)-2-(4-sulfophenyl)-2H-tetrazolium, inner salt) to a soluble formazan in the presence of an electron coupling reagent, PMS (phenazine methosulfate) by cellular dehydrogenases. The MTS is bioreduced by cells to produce a water soluble, brown coloured formazan, from which the absorbance can be measured at 490nm. The MTS bioreduction is thought to be mediated by dehydrogenase enzymes found in living cells and has also been shown to be mediated by DT-diaphorase (Tedeschi et al., 1995; Goodwin et al., 1996). The absorbance of the formazan product at 490nm is directly proportional to the number of living cells in culture. In the course of this study the cell viability assay was used as a method of quantifying cell viability and cell death in a given population of cells. The assay does not distinguish between apoptosis and necrosis. However, it can be used in conjunction with other apoptosis assays to determine the extent of cell death in response to a known apoptotic stimulus, or the level of protection that an inhibitor affords against this cell death.

After treatment with the appropriate stimuli aliquots of Jurkat cells (100µl) from each cell suspension was pipetted into wells of a 96well plate in triplicate. The MTS/PMS solution was prepared by mixing 1 part PMS (0.92mg/ml in PBS) to 5 parts MTS (2mg/ml in PBS) immediately before use. 20µl of the MTS/PMS solution was added to each well containing the cell suspensions in the 96 well plate. As a blank, 20µl MTS/PMS solution was added to 100µl complete medium. The plate was incubated for 2h at 37°C before reading absorbance at 490nm using an ELISA plate reader. Because MCF-7 cells grow as monolayers the set up of the MTS viability assay was modified slightly. MCF-7 cells (5000 cells/well) were added to each well of a 96 well plate and then incubated at 37°C for 24h, to allow population doubling, resulting in approximately 10,000 cells/well. The cells were then incubated with the appropriate treatments for the time indicated before adding 20µl MTS/PMS solution to each well, and the absorbance read at 490nm in an ELISA plate reader. The percentage of cell viability can be calculated as follows:

$\% \text{ Cell viability} = \text{absorbance of treated cells (-blank)} / \text{absorbance of control cells (-blank)} \times 100$

**CHAPTER THREE**

**EFFECT OF DIFFERENTIAL BCL-2 OVEREXPRESSION ON  
CHEMICAL- AND RECEPTOR-MEDIATED APOPTOSIS IN  
JURKAT T CELLS**

### 3.1 Introduction

It is now well established that Bcl-2 and its related family members play an important role in the regulation of apoptosis (Kroemer, 1997; Chao and Korsmeyer, 1998; Adams and Cory, 1998). Those members with the highest homology to Bcl-2, such as Bcl-x1 and Bcl-w, function as anti-apoptotic/pro-survival proteins and represent the mammalian counterparts of the *C.elegans* apoptotic agonist, ced-9 (Hengartner et al., 1992; Hengartner and Horvitz, 1994). Bcl-2 and Bcl-x1 are able to prevent apoptosis induced by a wide range of stimuli, including oxidative stress, UV radiation and chemical-induced apoptosis, in a variety of cell types (Memon et al., 1995; Jaattela et al., 1995; Chao et al., 1995; Mantal et al., 1996; Chen et al., 1996). Although the precise mechanism by which Bcl-2 blocks apoptosis is still unclear, evidence suggests that Bcl-2 may act at several control points to exert its anti-apoptotic effect (Oltvai and Korsmeyer, 1994; Hunter et al., 1996; Chinnaiyan et al., 1996; Adams and Cory, 1998). For instance, overexpression of Bcl-2 has been shown to act at the mitochondrial level (Susin et al., 1996), preventing cytochrome c release and therefore caspase activation (Kluck et al., 1997; Yang et al., 1997; Wu et al., 1997). Alternatively Bcl-2 has been shown to act directly on Apaf-1 thereby inhibiting Apaf-1-dependent caspase-9 activation *in vitro* (Zou et al., 1997; Hu et al., 1998; Pan et al., 1998), although this association is disputed *in vivo* (Moriishi et al., 1999). Bcl-2 also has the ability to form homo- and hetero-dimers with itself and other members of the Bcl-2 superfamily, notably Bcl-x and the pro-apoptotic Bax (Zhang et al., 1995; Chang et al., 1997). An increase in the ratio of Bax to Bcl-2 is thought to result in the acceleration of apoptosis (Oltvai et al., 1993), whereas increased levels of Bcl-2 or Bcl-x often result in a repressed cell death in response to a number of apoptotic stimuli including staurosporine (Estoppey et al., 1997b) and Fas (Jaattela et al., 1995; Armstrong et al., 1996; Mantal et al., 1996; Perry et al., 1997).

The overexpression of Bcl-2 can block the activation of caspase-3 and therefore PARP cleavage in Fas-mediated (Armstrong et al., 1996) and staurosporine-induced apoptosis (Estoppey et al., 1997b); suggesting that Bcl-2 functions at or upstream of the caspase-3 activation step in these pathways (Mantal et al., 1996). In contrast, other groups have found that Bcl-2 overexpression, whilst able to consistently block staurosporine induced apoptosis as assessed by PARP cleavage, caspase-3 processing and DNA laddering, has a

partial (Itoh et al., 1993) or total inability to block Fas induced apoptosis (Memon et al., 1995; Chiu et al., 1995; Strasser et al., 1995; Chinnaiyan et al., 1996).

One possible explanation for this apparent contradiction could be that the expression level of Bcl-2 protein in the cells examined is different (Chinnaiyan et al., 1996). More recently, it has been proposed that the ability of Bcl-2 to block Fas-mediated apoptosis is dependent on whether or not a particular cell type utilizes one of two Fas signalling pathways which are either mitochondria dependent (Type I) or independent (Type II) (Scaffidi et al., 1998; Scaffidi et al., 1999). In type I cells, Fas ligation results in the activation of large amounts of caspase-8 at the DISC followed by direct activation of caspase-3 (Stennicke et al., 1998). However, in type II cells there is only a small amount of caspase-8 activated at the DISC. This is sufficient to induce the release of apoptogenic factors from the mitochondria, possibly via the cleavage and translocation of Bid (Luo et al., 1998; Kuwana et al., 1998; Li et al., 1998; Gross et al., 1999). The release of apoptogenic factors such as cytochrome c and AIF from the mitochondria, then activate caspase-9 which in turn activates large amounts of both caspase-8 and caspase-3 via an amplification loop (Kuwana et al., 1998). Because Bcl-2 blocks the release of such apoptogenic factors from the mitochondria (Susin et al., 1996; Kluck et al., 1997; Yang et al., 1997; Susin et al., 1999), it is able to inhibit Fas-mediated apoptosis in type II cells. However, in type I cells, Bcl-2 is unable to block Fas mediated apoptosis which is largely dependent on caspase activation alone. Thus Bcl-2 acts to inhibit apoptosis at different points depending upon the apoptosis inducing stimuli.

More recently, the overexpression of Bcl-2 has been shown to delay cell cycle entry and proliferation (O'Reilly et al., 1996; Huang et al., 1997). This aspect of its multi-faceted character is receiving much interest, especially as this particular function appears to be unrelated to its anti-apoptotic activity (Vairo et al., 1996; Huang et al., 1997). The exact mechanism by which Bcl-2 prevents cell cycle entry and diminishes cellular proliferation is still unclear. However, the overexpression of Bax reverts the anti-apoptotic function and anti-proliferative effects of Bcl-2 (Borner, 1996). Furthermore, *in vivo* studies have shown that Bax $\alpha$ , a pro-apoptotic member of the Bcl-2 family, can increase the number of cycling thymocytes in Bax $\alpha$  transgenic mice (Brady et al., 1996), thus acting in an opposing manner to Bcl-2 in both cell proliferation and apoptosis (Oltvai et al., 1993; Antonsson et

al., 1997).

In this chapter the relationship between the constitutive differential overexpression of Bcl-2 and Bcl-xl in Jurkat T cells and its effect on Fas- and staurosporine-induced apoptosis was examined in order to address the question as to whether the differing effects of Bcl-2 observed in the literature, could be the result of differential expression levels of the protein. In addition the effects of Bcl-2 overexpression on Jurkat T cell proliferation was also examined. In order to achieve this, Jurkat T cells were transfected with Bcl-2 cDNA by electroporation and single cell clones expressing Bcl-2 to varying levels were isolated. Using these clones, the effect of differential overexpression of Bcl-2 on susceptibility to apoptosis induced by anti-Fas and the PKC inhibitor, staurosporine was examined.

## 3.2 RESULTS

### 3.2.1 Generation of stable Jurkat T cell clones overexpressing Bcl-2 and Bcl-x.

The aim of the work described in this chapter was to generate stable Jurkat T cell clones overexpressing various levels of Bcl-2/Bcl-x and determine the effect of this differential overexpression on the induction of apoptosis by staurosporine and anti-Fas. The plasmids, pEBS7-425 (Bcl-2), pEBS7-623 (Bcl-xl) and pEBS7 (control vector) were kindly provided by Märja Jäätela (Denmark). The vectors replicate episomally and therefore do not require linearization to generate stable transfection. Following transfection by electroporation (see materials and methods), the cells containing the Bcl-2 or Bcl-xl plasmids were placed under selection with hygromycin B for 24h. Before proceeding with single cell cloning, the level of Bcl-2/Bcl-xl overexpression in the pool population was assessed by SDS-PAGE and western blotting. In comparison to the pEBS7 pool population (J-pEBS7), both the Bcl-2 (J-Bcl-2) and Bcl-xl (J-Bcl-xl) pool populations showed an increase in Bcl-2 or Bcl-xl protein expression (Figure 3.1A). Therefore, the effect of staurosporine and anti-Fas on the pool populations of Bcl-2 and Bcl-xl transfected cells was assessed using the MTS viability assay (Figure 3.1B and C, respectively). An increase in viability was observed at 0.1 $\mu$ M staurosporine with J-Bcl-2 and J-Bcl-xl relative to J-pEBS7 pool populations (Figure 3.1B). J-Bcl-2 and J-Bcl-xl maintained viability at 100% and 60-70%, respectively. After treatment with anti-Fas, J-Bcl-2 and J-Bcl-xl maintained viability between approximately 70% and 80% in relation to J-pEBS7 in which viability was reduced to about 30% (Figure 3.1C). From this preliminary experiment, it was apparent that the Bcl-2 and Bcl-xl overexpressing pool populations of Jurkat T cells were able to protect against cell death induced by staurosporine and anti-Fas. Due to the random nature of DNA integration during electroporation, it is likely that not all cells in a given population will contain an equal copy number of the plasmid DNA. Therefore, cells in such a population will express varying amounts of protein, masking the effects of specifically high or low protein expression levels. Thus, the most effective way to study protein overexpression is to generate single cell clones, where the expression level of the protein will be homogenous within the cell population. In order to study the effect of staurosporine and anti-Fas on cells expressing Bcl-2 to varying levels, a series of limiting dilutions were set up in order to generate single cell clones overexpressing different levels of Bcl-2 or Bcl-xl as described in materials and methods. Once the cells were growing in

wells which statistically contained less than 0.3 cells/well, they were expanded and screened for the overexpression of Bcl-2/Bcl-xl by western blotting and scanning densitometry as described in materials and methods. Using this approach, a number of Bcl-2 overexpressing clones were isolated from the original pool population and four (J-Bcl-2/C6.1, J-Bcl-2/C4.1, J-Bcl-2/C5.2 and J-Bcl-2/A8) were selected for further study as they were found to overexpress Bcl-2 to varying levels above control vector transfected cells (Figure 3.2A). Wild type Jurkat cells (E6.1) were found to have quite a high level of endogenous Bcl-2, which was equivalent to that seen in J-pEBS7. Of the clones selected, J-Bcl2/C6.1 was found to express about a 2.9-fold increase in Bcl-2 compared to J-pEBS7. Clone J-Bcl-2/C4.1 and J-Bcl-2/C5.2 expressed 3.5- and 4.6-fold increases, respectively, and J-Bcl-2/A8 expressed the highest level, a 6.8-fold increase in Bcl-2 in comparison to pEBS7 control cells (Figure 3.2B). Thus, the four clones expressed an increase in Bcl-2 between 3- and 7-fold of that expressed in the control pEBS7 cells.

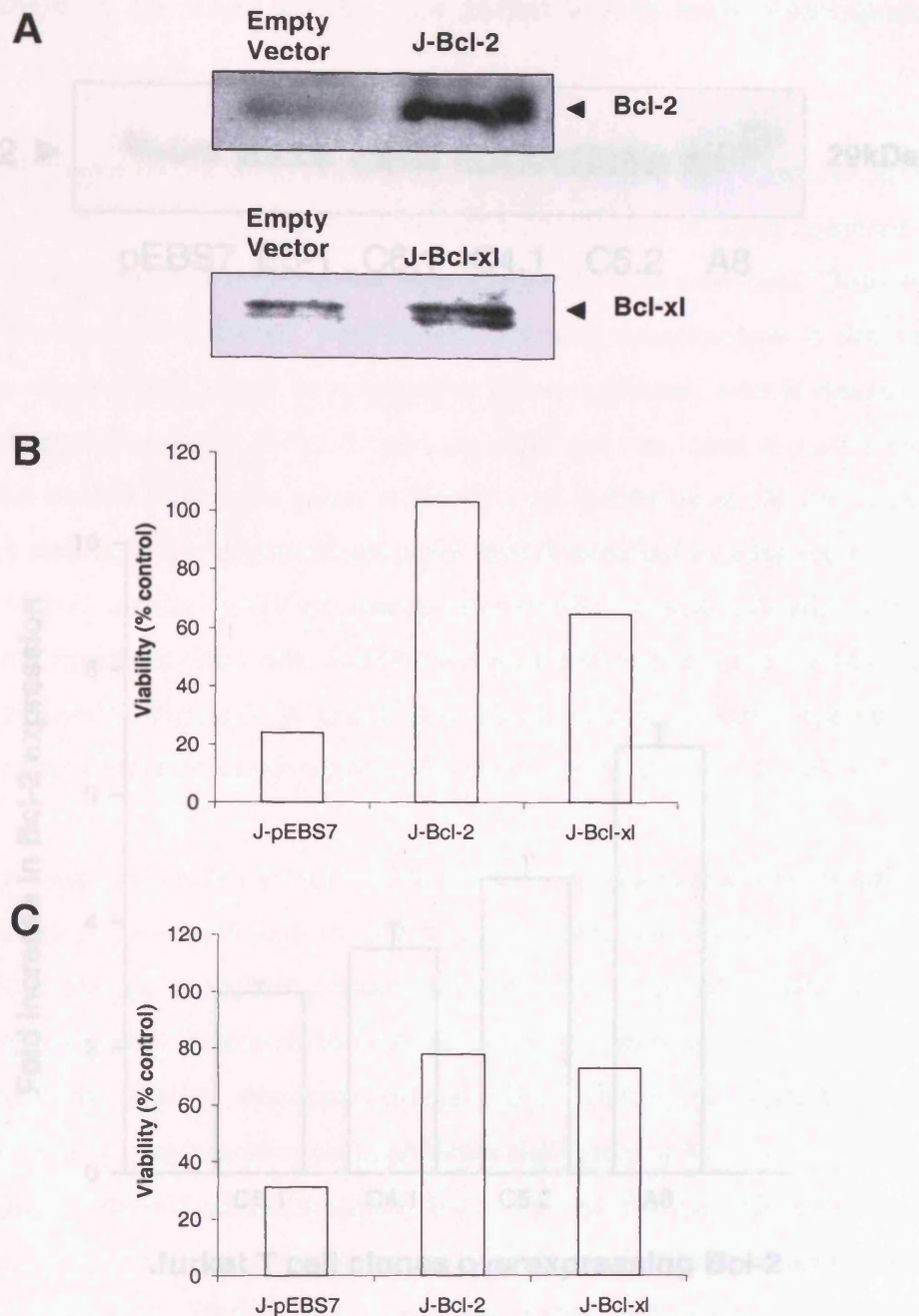
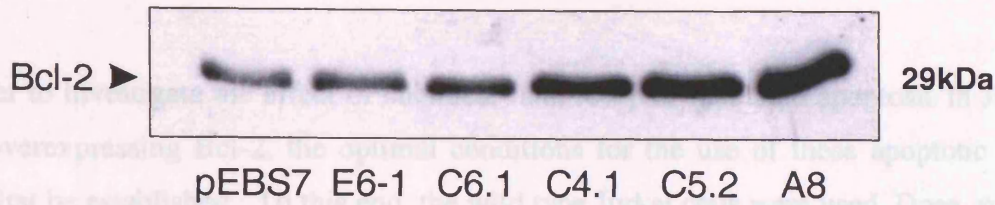


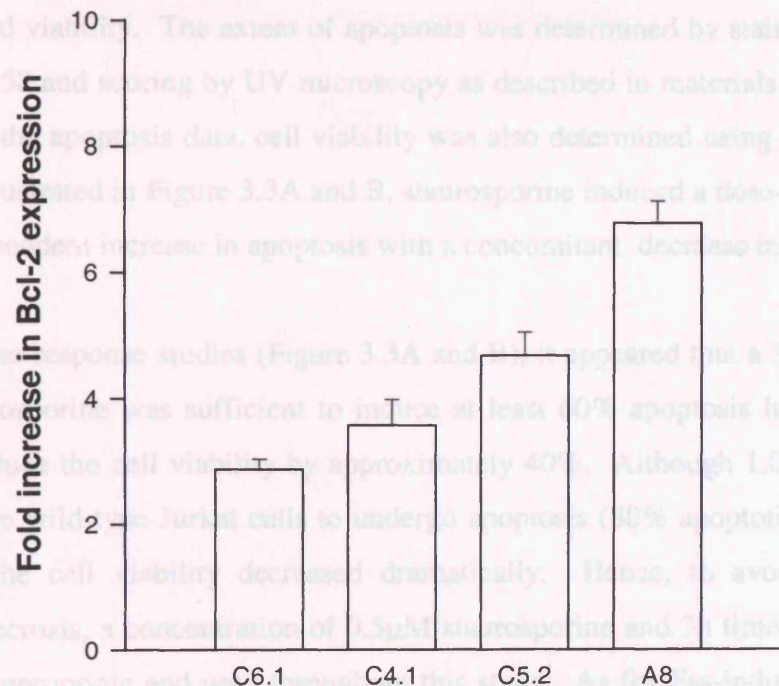
**Figure 3.1 Effect of overexpression of Bcl-2 and Bcl-xl on cell viability in wild type Jurkat T cells after treatment with staurosporine and anti-Fas.** A) Overexpression of Bcl-2 (J-Bcl-2) and Bcl-xl (J-Bcl-xl) in transfected pool populations of Jurkat T cells. Those cells transfected with an empty vector (J-pEBS7) were used as a control. B) Effect of staurosporine on cell viability in Bcl-2 and Bcl-xl transfected Jurkat cell pool populations. Cells ( $1 \times 10^6$ /ml) were treated with staurosporine ( $0.1 \mu\text{M}$ ) for 6h and viability was assessed using the MTS viability assay as described in materials and methods C) Effect of anti-Fas on cell viability in Bcl-2 and Bcl-xl transfected Jurkat cells. Cells ( $1 \times 10^6$ /ml) were treated with anti-Fas ( $100 \text{ng/ml}$ ) for 6h and viability was assessed using the MTS viability assay. Viability data represents the mean of two independent experiments carried out in duplicate.

### 3.2.2 Induction of apoptosis in wild type Jurkat T cells using staurosporine and anti-Fas

**A**



**B**



**Jurkat T cell clones overexpressing Bcl-2**

**Figure 3.2 Expression of Bcl-2 protein levels in Bcl-2 transfected Jurkat T cell clones.** The four clones selected for further study were J-Bcl-2/C6.1 (C6.1), J-Bcl-2/C4.1 (C4.1), J-Bcl-2/C5.2 (C5.2) and J-Bcl-2/A8 (A8). The expression level of Bcl-2 protein in each individual Bcl-2 transfected clone was assessed by A) Western blotting and B) densitometry analysis. An equivalent amount of protein (20 $\mu$ g) from each clone was analysed by SDS-PAGE and immunoblotting with a monoclonal antibody directed against Bcl-2. Wild type Jurkat T cells (E6.1) and the vector control pEBS7 were used as controls for densitometry analysis. The results are one representative of three for western blots and the mean of three experiments for densitometry analysis  $\pm$  SD.

### **3.2.2 Induction of apoptosis in wild type Jurkat T cells using staurosporine and anti-Fas**

In order to investigate the effect of chemical- and receptor-mediated apoptosis in Jurkat T cells overexpressing Bcl-2, the optimal conditions for the use of these apoptotic stimuli must first be established. To this end, the wild type Jurkat cells were used. Dose- response as well as time-dependent studies, were carried out with staurosporine to determine the optimal concentration that would be required to induce apoptosis over a reasonable time frame. A concentration range of 0.1-1.0 $\mu$ M staurosporine was used and after treatment, aliquots of the treated cells were taken at hourly time points up to 6h and assessed for apoptosis and viability. The extent of apoptosis was determined by staining the cells with Hoechst 33358 and scoring by UV microscopy as described in materials and methods. To compliment the apoptosis data, cell viability was also determined using the MTS viability assay. As illustrated in Figure 3.3A and B, staurosporine induced a dose-dependent as well as a time dependent increase in apoptosis with a concomitant decrease in cell viability.

From the dose-response studies (Figure 3.3A and B), it appeared that a 3h incubation with 0.5 $\mu$ M staurosporine was sufficient to induce at least 60% apoptosis in wild type Jurkat cells and reduce the cell viability by approximately 40%. Although 1.0 $\mu$ M staurosporine induced more wild type Jurkat cells to undergo apoptosis (80% apoptotic cells) compared to 0.5 $\mu$ M, the cell viability decreased dramatically. Hence, to avoid an increase in secondary necrosis, a concentration of 0.5 $\mu$ M staurosporine and 3h time point was chosen to be most appropriate and used throughout this study. As for Fas-induced apoptosis, the optimal concentrations and incubation times were established from previous studies (Chow et al., 1995; Chow et al., 1999). Based on these studies, wild type Jurkat T cells were incubated for 6h with 100ng/ml anti-Fas which routinely resulted in between 70-80% apoptosis and a 30-40% decrease in cell viability.

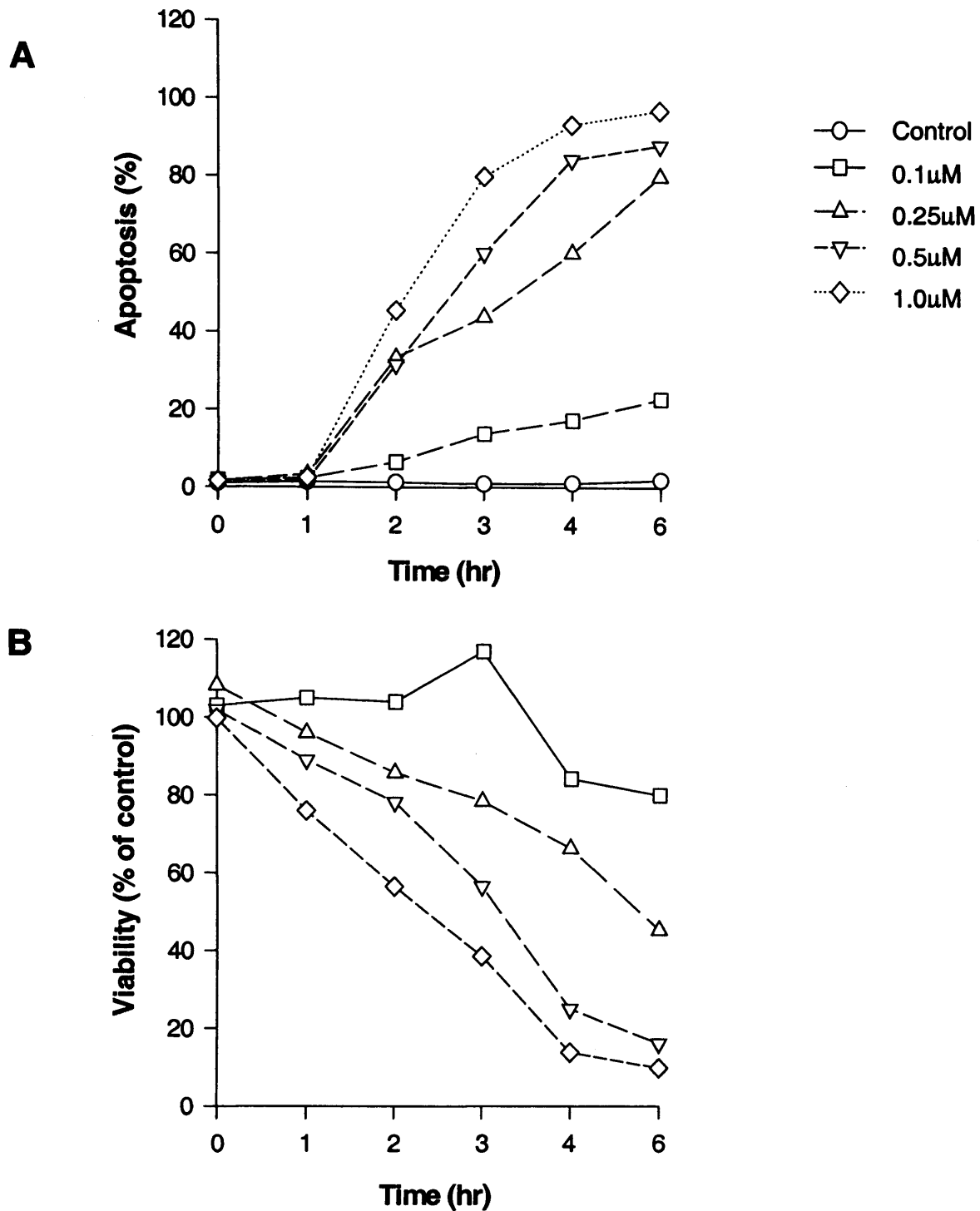


**Figure 3.3** Dose-response and time-course showing effects of staurosporine on A) apoptosis and B) viability in wild type Jurkat T cells. To determine the optimal conditions for induction of apoptosis in wild type Jurkat T cells, a staurosporine dose-response and time-course was carried out at concentrations between 0.1-1μM staurosporine over 6h. The percentage of apoptosis was assessed by staining cells with Hoechst 33358 and examining by UV microscopy. Viability was determined using the MTS assay and calculated as a percentage of untreated controls. The data represents the mean of three independent experiments.

### **3.2.3 Time dependent activation of caspases in wild type Jurkat T cells after treatment with staurosporine or anti-Fas.**

It is well established that the caspases play a pivotal role in the execution of the apoptotic process in virtually all cell types undergoing apoptosis (Cohen, 1997). Caspase processing and activation is an important indicator of apoptosis as well as being a useful means for dissecting the apoptotic pathway. Using the previously determined optimal conditions for induction of apoptosis with either staurosporine or anti-Fas (Figure 3.3 and results not shown), the time dependent activation of caspases was investigated in the wild type Jurkat T cell line. Wild type Jurkat cells were either treated with 0.5 $\mu$ M staurosporine or 100ng/ml anti-Fas for 3 or 6h, respectively. At hourly time points, aliquots of the treated cells were removed and centrifuged. Cell lysates were prepared for SDS PAGE and the processing of caspase-2, -3, -7 and -8 was investigated using immunoblotting as outlined in materials and methods. As illustrated in Figure 3.4, there was a time dependent activation of all the caspases examined in staurosporine-treated cells. Caspase-2 activation is denoted by the formation of the p12 active subunit (MacFarlane et al., 1997). The level of caspase-3 activation is indicated by the loss of the 32kDa pro-form and the subsequent appearance of lower molecular weight bands representing the p20 and active p17 subunits (MacFarlane et al., 1997; Han et al., 1997). Similarly, caspase-7 activation results in the appearance of a band representing the active p19 fragment. Caspase-8a and b (55.4 and 53.7kDa) were processed to the intermediate fragments of 42/43kDa within 1h, which is seen as a doublet band on the membrane. However, due to the limitations of the caspase-8 antibody used in this study the subsequent cleavage to an active p18 fragment was rarely detected. Therefore, the processing of caspase-8 to the intermediate p42/43 fragment was used as an indicator for caspase-8 activation. Upon treatment with staurosporine, cleavage fragments of caspase-2 and -7 were visible after 2h. Processing of caspase-3 and -8 appeared to precede the processing of caspase-2 and -7. There was a small amount of the intermediate p42/43 fragment of caspase-8 observed at the 1h timepoint and caspase-3 was partially processed to the p20 at 1h.

However, when wild type Jurkat cells were stimulated with anti-Fas the time-dependent processing of the caspases was different. As illustrated in Figure 3.5, after treatment with anti-Fas the cleaved fragments of caspase-8a and b, were visible between 1-2h. Caspase-3

processing appeared to occur after caspase-8 activation with the p20 and p17 fragments appearing after 2h treatment with anti-Fas. Similarly there was a small amount of caspase-2 and caspase-7 activation at 2h indicated by their cleaved fragments, p12 and p19 respectively, although it was more pronounced at 3h. The p12 fragment of caspase-2 appeared to decrease after 6h, suggesting it may be rapidly degraded. The results suggest that caspase-8 is the apical caspase activated after anti-Fas treatment in wild type Jurkat cells. This is in accordance with the model for receptor-mediated apoptosis where receptor activation leads to the activation of the apical initiator caspase-8 and this in turn results in downstream effector caspase processing (Los et al., 1995; Enari et al., 1996; Medema et al., 1997; Takahashi et al., 1997a; Juo et al., 1998).

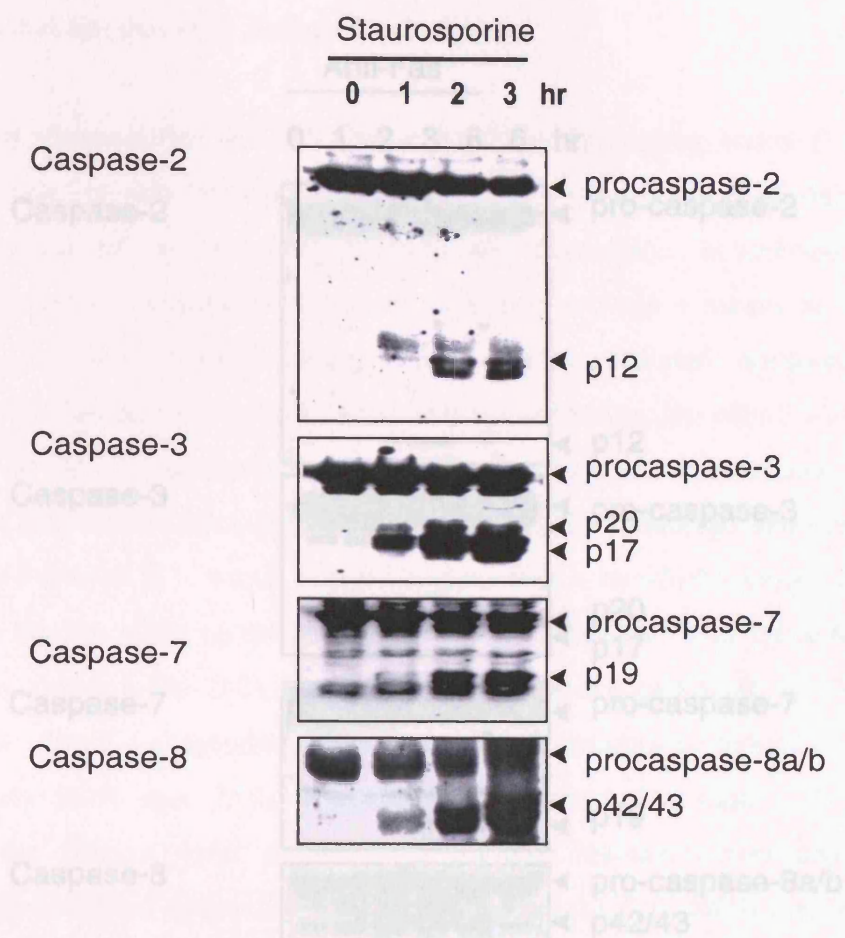


**Figure 3.4** Time dependent processing of caspase-2, -3, -7 and -8 in wild type Jurkat T cells (clone E6.1) in response to staurosporine. Wild type Jurkat T cells were incubated with  $0.5\mu\text{M}$  staurosporine and at the time points where indicated aliquots of cells ( $1 \times 10^6$ ) were removed and prepared for SDS PAGE. Processing of caspases reflected the induction of apoptosis. The experiments were repeated at least twice with similar findings.

### 3.2.4 Effect of differential overexpression of Bcl-2 on staurosporine- and anti-Fas-induced apoptosis in Jurkat T cell clones.

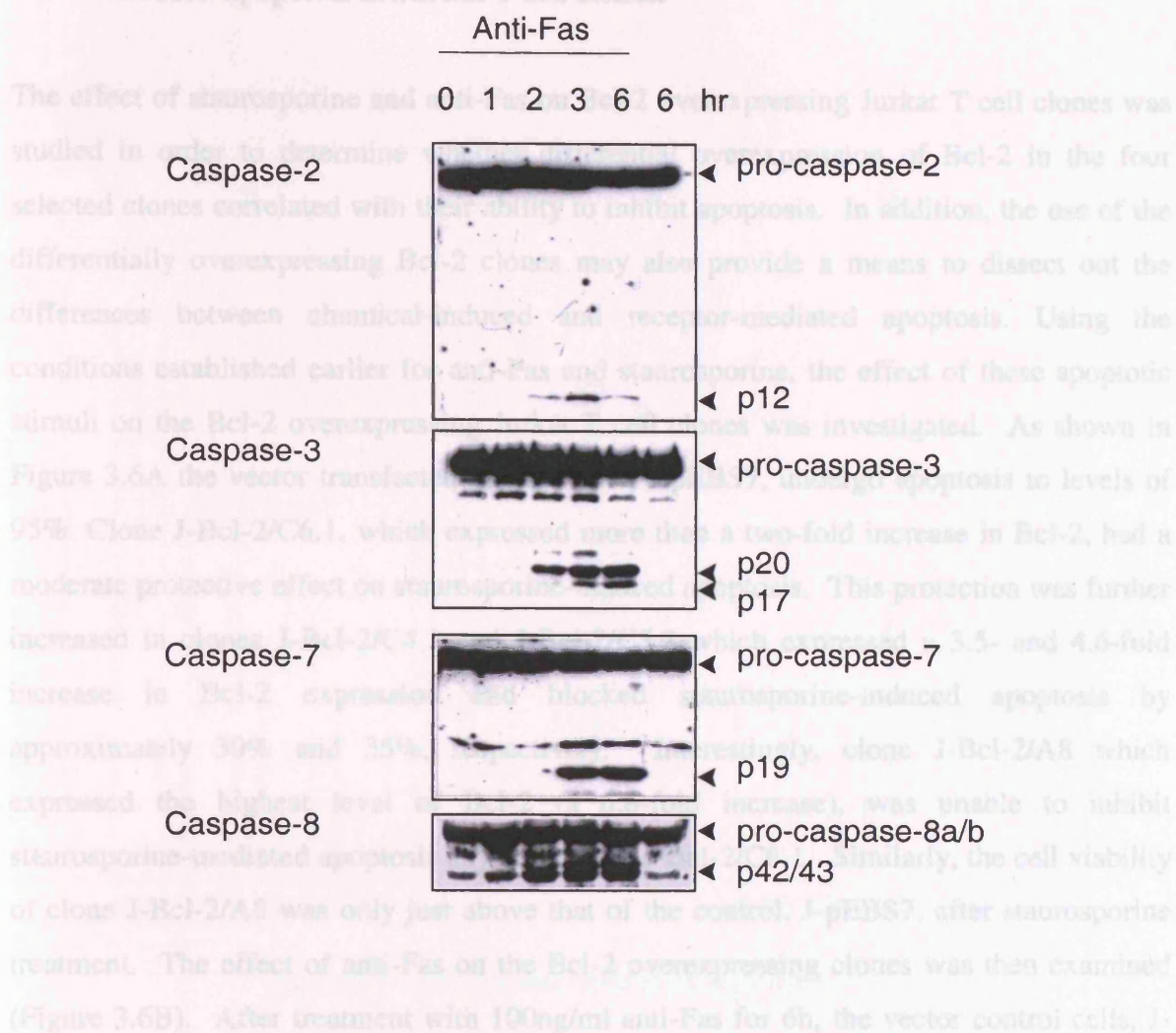


**Figure 3.5 Time-dependent processing of caspase-2, -3, -7 and -8 in wild type Jurkat T cells in response to anti-Fas.** Wild type Jurkat cells were incubated with 100ng/ml anti-Fas and at the timepoint where indicated aliquots of cells ( $1 \times 10^6$  cells/ml) were removed, washed and lysed prior to SDS PAGE and western blotting with the appropriate antibodies. The experiments were repeated at least twice with similar findings.

### **3.2.4 Effect of differential overexpression of Bcl-2 on staurosporine- and anti-Fas-induced apoptosis in Jurkat T cell clones.**

The effect of staurosporine and anti-Fas on Bcl-2 overexpressing Jurkat T cell clones was studied in order to determine whether differential overexpression of Bcl-2 in the four selected clones correlated with their ability to inhibit apoptosis. In addition, the use of the differentially overexpressing Bcl-2 clones may also provide a means to dissect out the differences between chemical-induced and receptor-mediated apoptosis. Using the conditions established earlier for anti-Fas and staurosporine, the effect of these apoptotic stimuli on the Bcl-2 overexpressing Jurkat T cell clones was investigated. As shown in Figure 3.6A the vector transfected control cells, J-pEBS7, undergo apoptosis to levels of 95%. Clone J-Bcl-2/C6.1, which expressed more than a two-fold increase in Bcl-2, had a moderate protective effect on staurosporine-induced apoptosis. This protection was further increased in clones J-Bcl-2/C4.1 and J-Bcl-2/C5.2 which expressed a 3.5- and 4.6-fold increase in Bcl-2 expression and blocked staurosporine-induced apoptosis by approximately 30% and 35%, respectively. Interestingly, clone J-Bcl-2/A8 which expressed the highest level of Bcl-2 (a 6.8-fold increase), was unable to inhibit staurosporine-mediated apoptosis any better than J-Bcl-2/C6.1. Similarly, the cell viability of clone J-Bcl-2/A8 was only just above that of the control, J-pEBS7, after staurosporine treatment. The effect of anti-Fas on the Bcl-2 overexpressing clones was then examined (Figure 3.6B). After treatment with 100ng/ml anti-Fas for 6h, the vector control cells, J-pEBS7, readily undergo apoptosis (82%) to levels reflecting those achieved with the wild type Jurkat T cells (results not shown). Clone J-Bcl-2/C6.1 inhibited Fas-induced apoptosis and increased cell viability moderately (74% and 33%, respectively). With clones J-Bcl-2/C4.1 and J-Bcl-2/C5.2, there was a marked inhibition of apoptosis (62% and 38%, respectively). Similarly, the decrease in cell viability was markedly inhibited in these clones. However, clone J-Bcl-2/A8, again gave little protection against Fas-mediated apoptosis in comparison to clones J-Bcl-2/C4.1 and J-Bcl-2/C5.2. Interestingly, clone J-Bcl-2/A8, although unable to inhibit Fas-induced apoptosis, consistently maintained cell viability in a manner comparable to clone J-Bcl-2/C4.1. This is in contrast to staurosporine treatment where J-Bcl-2/A8 had little protective effect on cell viability. Unfortunately, it was not possible to continue with the characterization of the Bcl-xl overexpressing clones generated during this study due to bacterial contamination.

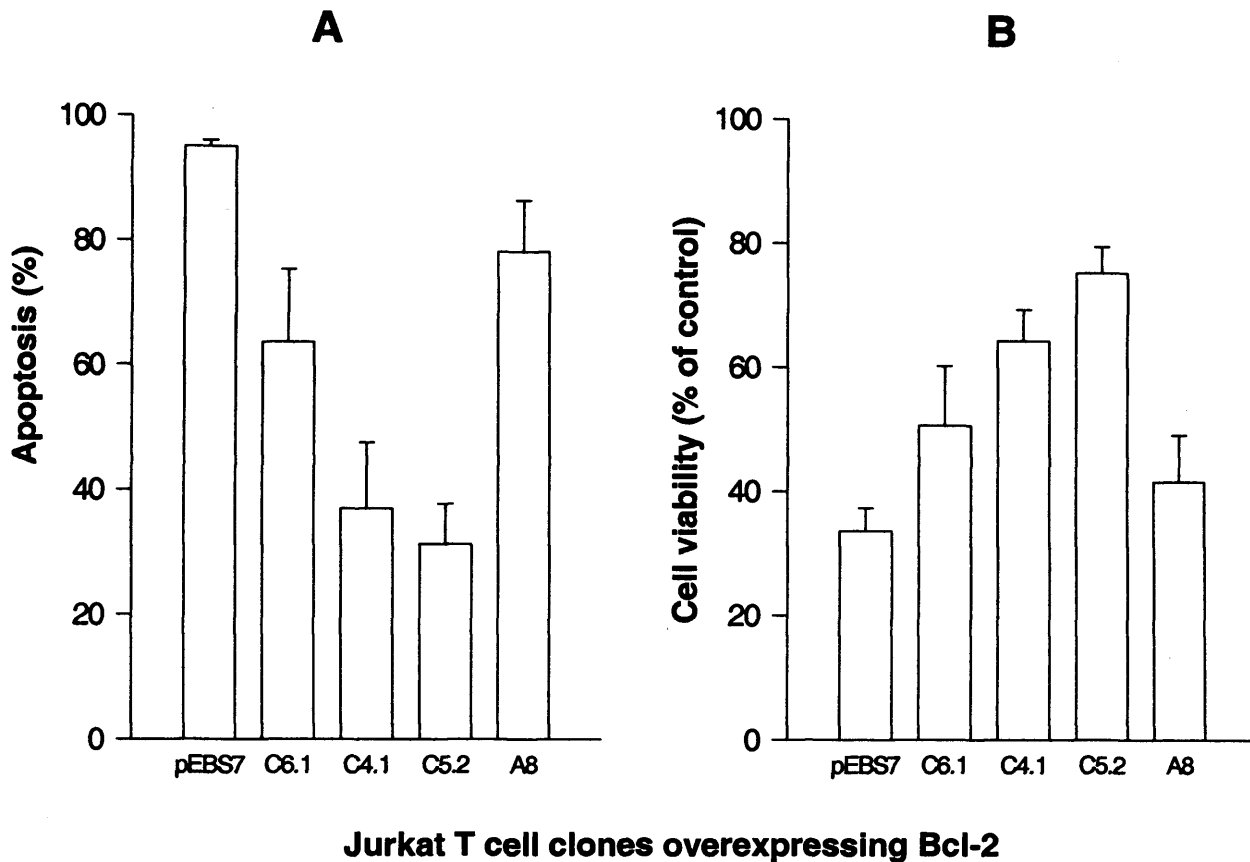


**Figure 3.6A Effect of differential overexpression of Bcl-2 in Jurkat T cells on staurosporine-induced apoptosis.** The various Jurkat T cell clones overexpressing different levels of Bcl-2 were incubated with 0.5 $\mu$ M staurosporine for 3h followed by determination of (A) apoptosis and (B) cell viability as described in material and methods. The clones used were J-pEBS7 (pEBS7), J-Bcl-2/C6.1 (C6.1), J-Bcl-2/C4.1 (C4.1), J-Bcl-2/C5.2 (C5.2) and J-Bcl-2/A8 (A8). The results are the means  $\pm$  SEM from three independent experiments.

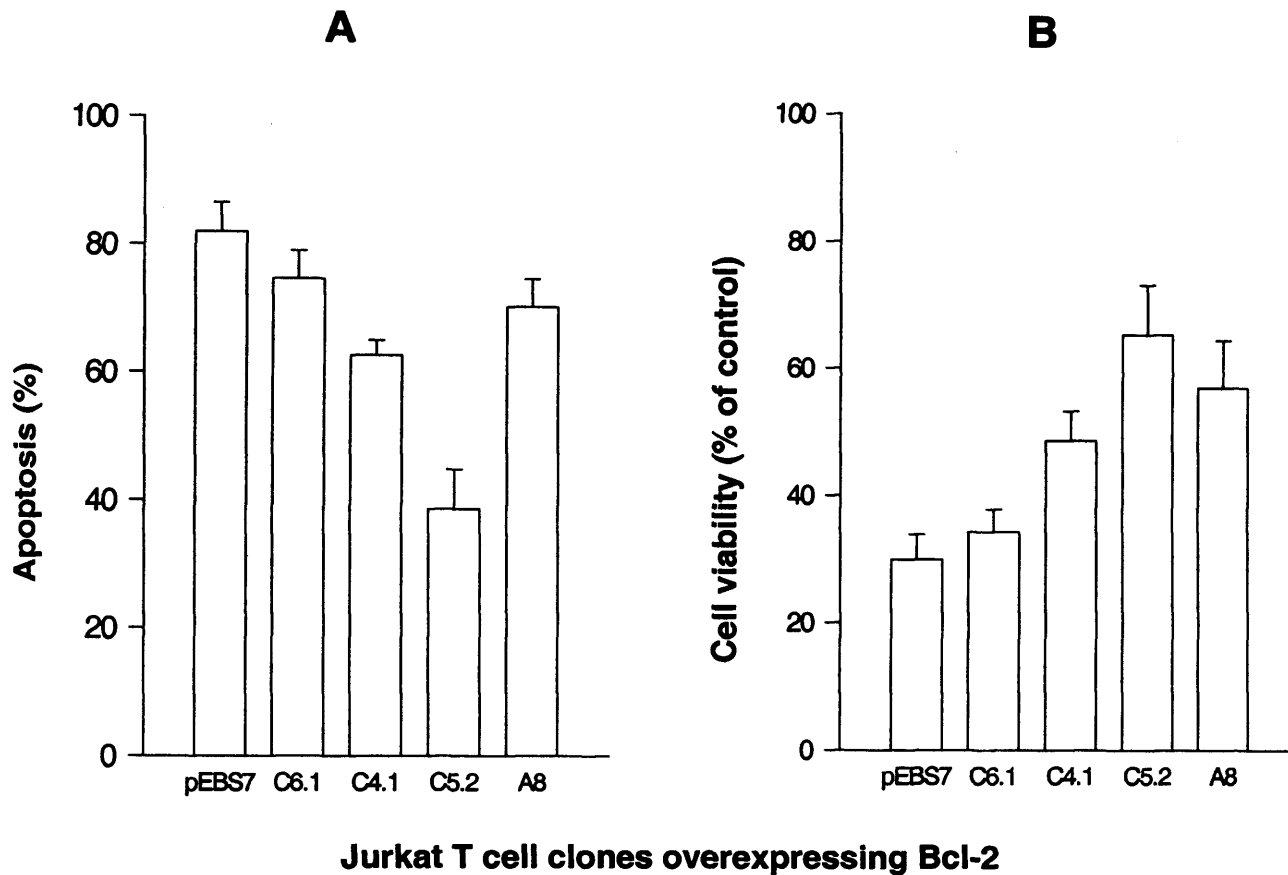


**Figure 3.6B Effect of differential overexpression of Bcl-2 in Jurkat T cells on anti-Fas-induced apoptosis.** The various Jurkat T cell clones overexpressing different levels of Bcl-2 were incubated with 100ng/ml anti-Fas for 6h followed by determination of (A) apoptosis and (B) cell viability as described in materials and methods. The clones used were J-pEBS7 (pEBS7), J-Bcl-2/C6.1 (C6.1), J-Bcl-2/C4.1 (C4.1), J-Bcl-2/C5.2 (C5.2) and J-Bcl-2/A8 (A8). The results are the means  $\pm$  SEM from three independent experiments.

### **3.2.5 Effect of differential overexpression of Bcl-2 on caspase processing during staurosporine- and Fas-mediated apoptosis.**

As shown in Figure 3.6A and B, the differential overexpression of Bcl-2 appeared to have different protective effects on staurosporine- and Fas-mediated apoptosis. The processing of caspase-2, -3, -7 and -8 was therefore examined in the Bcl-2 overexpressing clones to determine whether there was any correlation with the induction of apoptosis. Upon treatment with staurosporine, clones J-Bcl-2/C6.1, J-Bcl-2/C4.1 and J-Bcl-2/C5.2 showed a reduction in the activation of the pro-form of caspase -2, -3, -7 and -8 in comparison to pEBS7 control. Similarly, clone J-Bcl-2/A8, which was less effective in protecting against staurosporine-induced apoptosis, was unable to prevent the processing of the caspases examined. The pattern of caspase processing in response to anti-Fas was slightly different to that observed with staurosporine. The processing of caspase-2 mediated by anti-Fas was inhibited in all the clones and correlated well with the level of overexpression of Bcl-2 in each of the clones tested. Interestingly, after anti-Fas stimulation clone J-Bcl-2/A8, which expressed the highest level of Bcl-2, completely inhibited the processing of caspase-2 despite over 70% of the cells being apoptotic. This is in contrast to caspase-2 processing in the same clone after treatment with staurosporine suggesting that caspase-2 may be dispensable during Fas-mediated apoptosis. Processing of caspase-3 and caspase-7 reflected the propensity of the clones to undergo anti-Fas-induced apoptosis. Clone J-Bcl-2/C6.1 showed caspase-3 and caspase-7 processing, whilst J-Bcl-2/C4.1 and J-Bcl-2/C5.2 showed a partial inhibition of this processing. Caspase-8 was activated to a similar extent in all of the clones tested irrespective of the resistance of these clones to Fas mediated apoptosis.



### **3.2.6 Effect of Bcl-2 overexpression on the time-dependent processing of caspase-8 and caspase-3 during staurosporine- and anti-Fas-mediated apoptosis.**

Recent studies have suggested that caspase-8 can mediate apoptosis by mitochondria-dependent (Type II) or -independent (Type I) pathways (Scaffidi et al., 1998). Since the processing of caspase-8 after anti-Fas treatment was unaffected by the overexpression of Bcl-2, the results presented in Figure 3.7, suggest that the Jurkat cells used in this study may behave like Type I, as oppose to Type II cells. To further determine whether these Jurkat cells behave as type I or II cells the effect of Bcl-2 on the kinetics of caspase-8 and caspase-3 processing after staurosporine and anti-Fas treatments was examined. The clone J-Bcl-2/C5.2 which has been previously shown to be effective in inhibiting both staurosporine- and Fas-mediated apoptosis (Figure 3.8) was used in this study. A timecourse experiment was carried out to determine the effect of Bcl-2 on the kinetics of caspase-8 and caspase-3 activation in comparison to the control clone J-pEBS7. After treatment with staurosporine the processing of caspase-8 and -3 in the vector control J-pEBS7 was observed after 1h correlating with the results in Fig 3.5A. The overexpression of Bcl-2 caused a marked inhibition of caspase-8 and caspase-3 processing in clone J-Bcl-2/C5.2 after treatment with staurosporine for 3h. In addition, the overexpression of Bcl-2 in this clone delayed caspase-8 and caspase-3 processing by approximately 1hr, reflected by the slower appearance of the p42/43 fragment of caspase-8 and the p17 fragment of caspase-3 in comparison to J-pEBS7. However, when J-Bcl-2/C5.2 was treated with anti-Fas, there appeared to be only a slight delay in the kinetics of caspase-8 activation and after 6h there was no significant difference between the extent of caspase-8 processing in J-Bcl-2/C5.2 and the vector control, pEBS7. Similarly the processing of caspase-3 in J-Bcl-2/C5.2 was also slightly delayed as evidenced by the appearance of the intermediate p20 fragment. The results suggest that Bcl-2 overexpression delays rather than completely blocks, staurosporine- and anti-Fas-mediated apoptosis although in agreement with the results in Figure 3.7. This data is slightly at odds with studies by Scaffidi et al. (1998), which propose that Bcl-2 completely blocks Fas-induced apoptosis by blocking the caspase-8 mediated release of apoptogenic mitochondrial factors. To examine the possibility that Fas is signalling directly from the receptor to initiate caspase activation in the Jurkat cells used in this study, the general caspase inhibitor z-VAD-FMK was used. Unlike Bcl-2, z-VAD-FMK has been shown to be ineffective in the inhibition of

cytochrome c release from the mitochondria (Finucane et al., 1999) and therefore, if Fas was signalling via the mitochondria in these cells, z-VAD-FMK would be expected to have little effect on Fas-induced cell death. As shown in Figure 3.9, z-VAD-FMK inhibits the processing of caspase-2, -3, and -7. In the presence of z-VAD-FMK, treatment of Jurkat cells with anti-Fas results in a small amount of caspase-8 processing, seen as a faint 42/43kDa band. This correlates to the mode of action of such inhibitors which block the active site of caspases by acting as substrates and therefore prevent downstream caspase activation events ( Thornberry et al., 1994; Garcia-Calvo et al., 1998). Thus z-VAD-FMK appears to be preventing downstream effector caspase activation by directly blocking caspase-8 activation.



**Figure 3.8 Effect of Bcl-2 on staurosporine- and Fas-mediated caspase-3 and caspase-8 processing.** Both pEBS7 and clone J-Bcl-2/C5.2 were treated with 0.5 $\mu$ M staurosporine and 100ng/ml anti-Fas for 3h or 6h respectively. Aliquots of cells were removed at the appropriate time points and subjected to SDS-PAGE analysis followed by western blotting analysis as outlined in materials and methods.

## 3.2.7 Effect of Bcl-2 overexpression on cell proliferation

In addition to its anti-apoptotic activity, Bcl-2 has also been found to have negative effects on cell proliferation (O'Reilly et al., 1996; D'Amico et al., 1997). Therefore using the Bcl-2 overexpressing clones, the effect of Bcl-2 overexpression on cell proliferation was examined. Figure 3.10 shows the effect of Bcl-2 overexpression on cell proliferation at 72h in clones J-Bcl-2/C6.1, J-Bcl-2/C2/C5.2 and J-Bcl-2/C4.1. The effect of Bcl-2 overexpression on cell proliferation was examined. After 24h there was a noticeable increase in cell proliferation in J-Bcl-2/C6.1, but the effect was more pronounced at 48 and 72h. After 72h the density of the vector control cells and wild type Jurkat cells had reached  $0.25 \times 10^6$  cells/ml. Interestingly, clone J-Bcl-2/C6.1, which expressed the highest level of Bcl-2, reached a density of less than  $0.25 \times 10^6$  cells/ml. This suggests that Bcl-2 overexpression is ineffective in preventing apoptosis induced by Fas in Jurkat cells. Clones J-Bcl-2/C5.2 and J-Bcl-2/C4.1 also had decreased proliferative capacity by 72h. A direct correlation ( $r=0.74$ ) was observed between the doubling time of each clone and the level of Bcl-2 protein expression within each clone. In addition, the effect of Bcl-2 protein expression on the cell cycle was also examined by FACS analysis as described in materials and methods. The results are shown in Figure 3.11. The cells had a delayed cell cycle with prolonged S-phase and G2/M phase. This is indicative of tetraploidy (Graham et al., 1997).

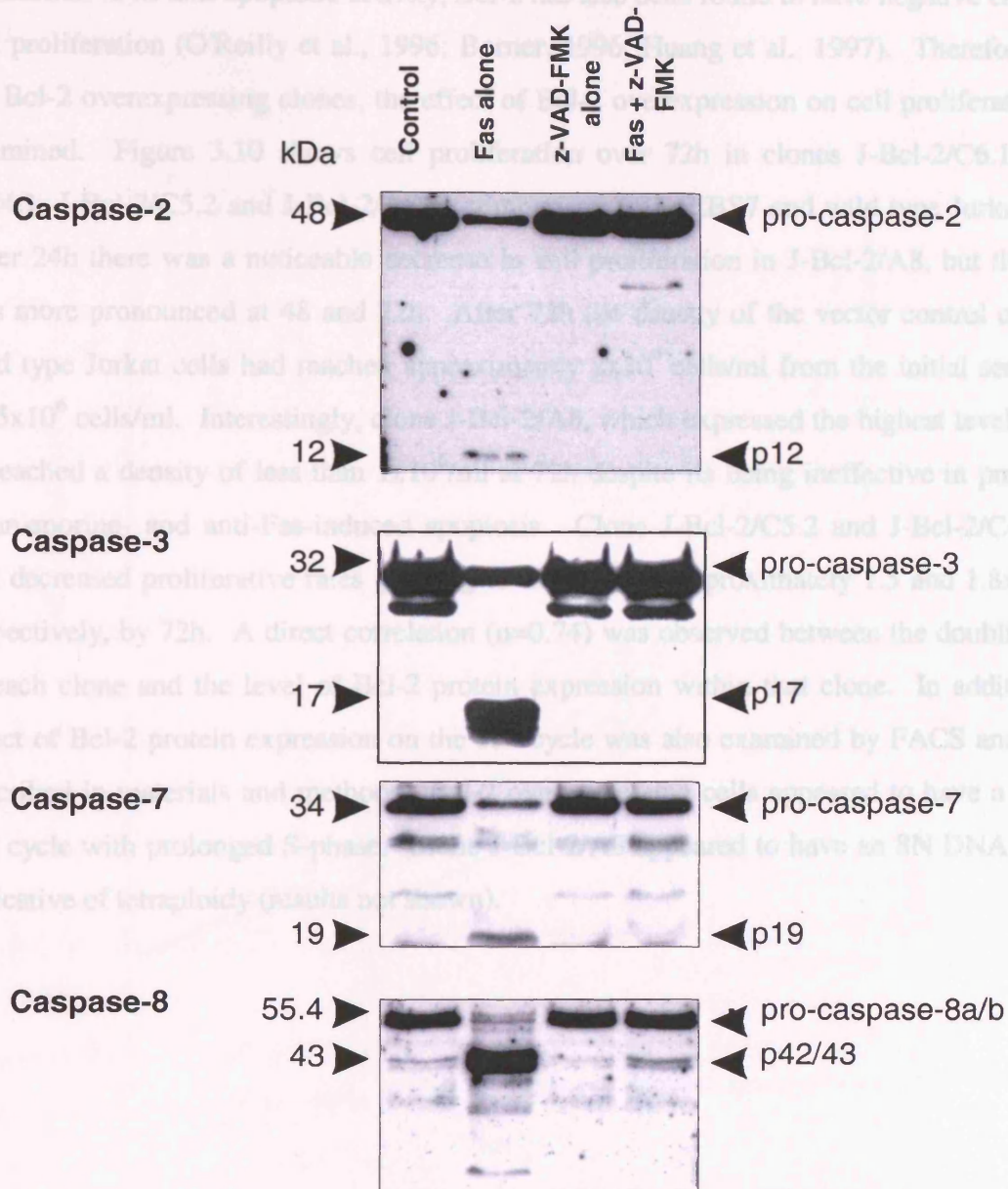


**Figure 3.9 Inhibition of anti-Fas induced caspase-2, -3, -7 and -8 processing in wild type Jurkat T cells by z-VAD-FMK.** Jurkat cells ( $1 \times 10^6$  cells/ml) were treated with anti-Fas (50ng/ml) in the presence or absence of  $10 \mu\text{M}$  z-VAD-FMK for 24h. The cells were centrifuged down, washed and lysed prior to SDS PAGE analysis. The proteins were transferred onto nitrocellulose membrane and probed with antibodies to caspase-2, -3, -7 and -8 as described in materials and methods.  $30 \mu\text{g}$  protein was loaded onto each lane. The results are one representative of at least three independent experiments.

### 3.2.7 Effect of Bcl-2 overexpression on cell proliferation

In addition to its anti-apoptotic activity, Bcl-2 has also been found to have negative effects on cell proliferation (O'Reilly et al., 1996; Borner, 1996; Huang et al., 1997). Therefore using the Bcl-2 overexpressing clones, the effect of Bcl-2 overexpression on cell proliferation was examined. Figure 3.10 shows cell proliferation over 72h in clones J-Bcl-2/C6.1, J-Bcl-2/C4.1, J-Bcl-2/C5.2 and J-Bcl-2/A8 in comparison to J-pEBS7 and wild type Jurkat cells. After 24h there was a noticeable decrease in cell proliferation in J-Bcl-2/A8, but the effect was more pronounced at 48 and 72h. After 72h the density of the vector control cells and wild type Jurkat cells had reached approximately  $2 \times 10^6$  cells/ml from the initial seeding of  $0.25 \times 10^6$  cells/ml. Interestingly, clone J-Bcl-2/A8, which expressed the highest level of Bcl-2, reached a density of less than  $1 \times 10^6$ /ml at 72h despite its being ineffective in preventing staurosporine- and anti-Fas-induced apoptosis. Clone J-Bcl-2/C5.2 and J-Bcl-2/C4.1 also had decreased proliferative rates growing to densities of approximately 1.5 and  $1.8 \times 10^6$ /ml, respectively, by 72h. A direct correlation ( $r=0.74$ ) was observed between the doubling time of each clone and the level of Bcl-2 protein expression within that clone. In addition, the effect of Bcl-2 protein expression on the cell cycle was also examined by FACS analysis as described in materials and methods. Bcl-2 overexpressing cells appeared to have a delayed cell cycle with prolonged S-phase. Clone J-Bcl-2/A8 appeared to have an 8N DNA content indicative of tetraploidy (results not shown).

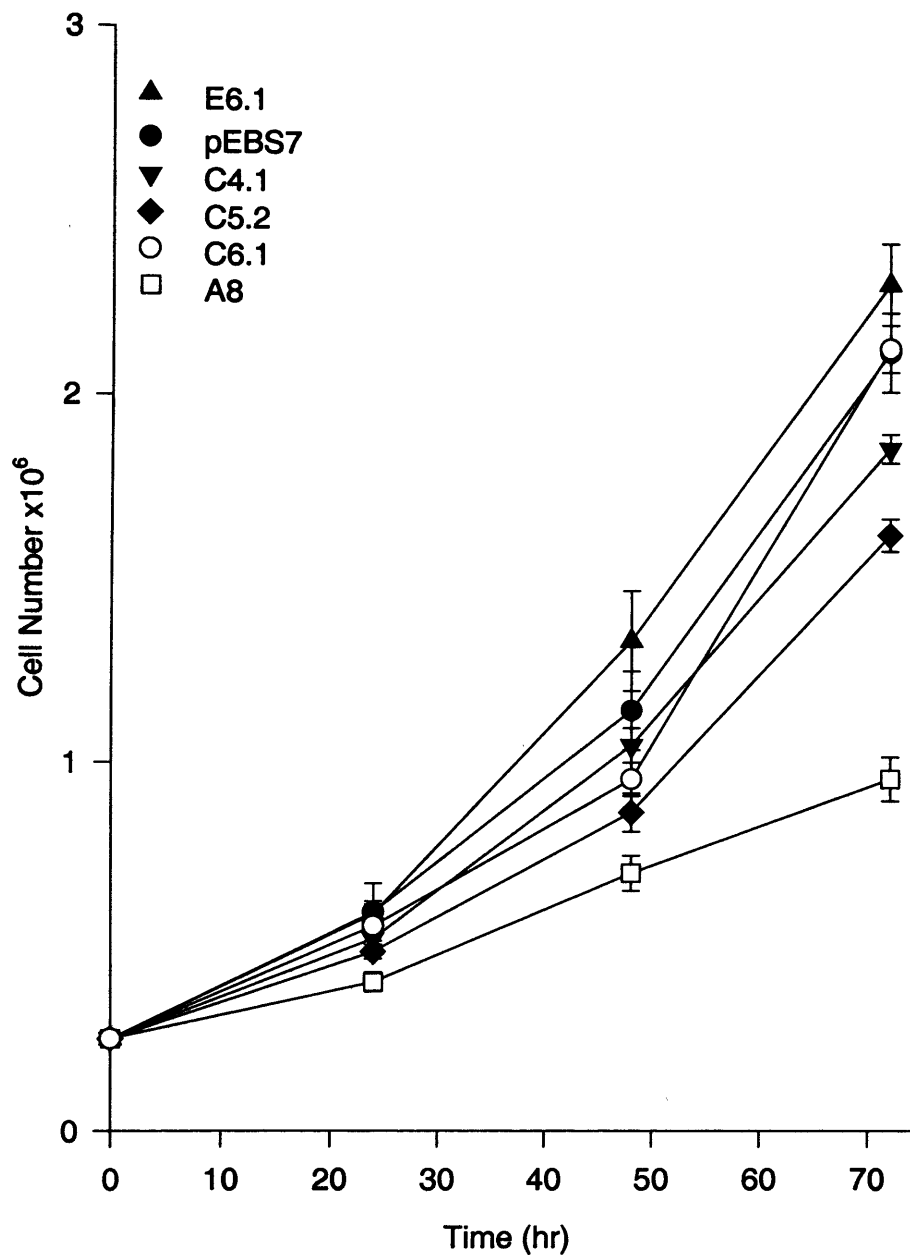


**Figure 3.10 Decreased cell proliferation in Jurkat T cell clones overexpressing Bcl-2.** Proliferation of each clone was assessed by seeding the cells at an initial density of  $0.25 \times 10^6$  cells/ml. The cell density and viability were assessed every 24h over a 72h period using the trypan blue exclusion assay as described in materials and methods. The experiment was repeated three times both in the absence (above) and presence (results not shown) of hygromycin B giving similar results. The clones used were J-pEBS7 (pEBS7), J-Bcl-2/C6.1 (C6.1), J-Bcl-2/C4.1 (C4.1), J-Bcl-2/C5.2 (C5.2) and J-Bcl-2/A8 (A8). Data represents the mean  $\pm$  SEM from three independent experiments.

### 3.3 Discussion

It is well established that Bcl-2 overexpression is able to prevent the onset of apoptosis in many cell types induced by a variety of stimuli (Itoh et al., 1993; Armstrong et al., 1996; Estoppey et al., 1997a) but the ability of Bcl-2 to consistently block Fas-mediated apoptosis remains controversial (Itoh et al., 1993; Armstrong et al., 1996; Chinnaiyan et al., 1996). One possible explanation for this controversy could be a difference in the relative expression levels of Bcl-2 in the cells used. Therefore in order to study the effect of differential overexpression of Bcl-2 on staurosporine- and Fas-mediated apoptosis, a number of stable Bcl-2 clones which overexpressed Bcl-2 protein to various levels above wild type Jurkat cells, were established. In accordance with previous studies, Bcl-2 was found to have a protective effect on staurosporine-induced apoptosis (Chinnaiyan et al., 1996; Perry et al., 1997; Estoppey et al., 1997a). The protective effect was related to the level of Bcl-2 expression as clones J-Bcl-2/C6.1, J-Bcl-2/C4.1 and J-Bcl-2/C5.2 all inhibited apoptosis in a manner which correlated to increased levels of protein expression in each clone. However, clone J-Bcl-2/A8 which expressed about a 6.8-fold increase in Bcl-2 as compared to controls, was unable to inhibit apoptosis induced by staurosporine. Consistent with these results, the processing of caspase-2, -3, -7 and -8, reflected the propensity of each clone to inhibit staurosporine-induced apoptosis. Because chemical-induced apoptosis results in efflux of cytochrome c from the mitochondria and subsequent caspase activation, which can be inhibited by Bcl-2, the results presented here are consistent with the ability of Bcl-2 to act on the mitochondria to exert its anti-apoptotic effect (Kluck et al., 1997; Yang et al., 1997). After treatment with anti-Fas, a similar pattern of inhibition was observed but to a slightly lesser extent. Bcl-2 overexpression correlated to the extent of protection from Fas-mediated apoptosis in clones J-Bcl-2/C6.1, J-Bcl-2/C4.1 and J-Bcl-2/C5.2. However, clone J-Bcl-2/A8 showed little resistance to Fas-mediated apoptosis, in a similar manner to the effect seen upon treatment with staurosporine. These results suggest that the level of Bcl-2 expression is not always effective in the inhibition of apoptosis and an excess of Bcl-2 may result in the negation of any anti-apoptotic activity. Recent work has shown that deletions causing increased expression of Bcl-2 mRNA and protein result in increased cell death via the caspase cascade in 293 cells (Uhlmann.E.J. et al., 1998). There is also some evidence that Bcl-2 overexpression can cause apoptosis in photoreceptor cells (Chen et al., 1996). Thus, high

levels of Bcl-2 expression, are not always predictive of anti-apoptotic activity.

During Fas-induced apoptosis the pattern of caspase processing in the Bcl-2 overexpressing clones was different to that observed during staurosporine-induced cell death. The processing of caspase-3 and -7 reflected the ability of the clones to inhibit apoptosis induced by anti-Fas. Interestingly, the extent of caspase-2 processing was directly correlated to the level of Bcl-2 expression, even though, in the case of clone J-Bcl-2/A8, over 70% of the cells displayed an apoptotic morphology after anti-Fas treatment. This observation suggests that caspase-2 may be redundant during Fas-mediated apoptosis and implies a divergence in signalling pathways between staurosporine and Fas-induced apoptosis (Sun et al., 1999). After Fas ligation, caspase-8 was completely processed in all of the clones examined, irrespective of their ability to inhibit apoptosis suggesting that caspase-8 activation is an early event during Fas-mediated apoptosis. This is consistent with previous findings where caspase-8 has been shown to be the apical caspase in Fas-mediated apoptosis (Enari et al., 1996; Srinivasula et al., 1996; Takahashi et al., 1997b; Stennicke et al., 1998; Juo et al., 1998). After Fas antigen ligation, the Fas receptor trimerizes resulting in the formation of the DISC (Kischkel et al., 1995; Peter et al., 1996; Medema et al., 1997). This involves the recruitment of FADD/MORT-1 to the intracellular death domain of the Fas receptor which in turn allows caspase-8 to bind to the DED of FADD and become activated (Chinnaiyan et al., 1995; Muzio et al., 1996; Boldin et al., 1996; Muzio et al., 1997; Vincenz and Dixit, 1997; Thome et al., 1997). Recent studies have shown that caspase-8 can mediate Fas-induced apoptosis by mitochondria-dependent and independent pathways (Scaffidi et al., 1999). Work by Scaffidi et al., (1999) suggests that mitochondrial dependent and independent Fas signalling is cell type specific (Type II and Type I) which may explain the controversy surrounding the effect of Bcl-2 on Fas-mediated apoptosis. Type I cells are characterized by a large amount of caspase-8 activation at the DISC following ligation of the Fas antigen, which directly activates caspase-3. In contrast, only a small amount of caspase-8 is activated in type II cells, and this is sufficient to stimulate the release of mitochondrial apoptogenic factors such as cytochrome c and AIF. Only in type II cells, could caspase-8 and caspase-3 processing and therefore subsequent apoptosis be blocked by Bcl-2 overexpression, because these cells are dependent on the mitochondria. Based on these studies, Jurkat T cells are proposed to be type II cells utilizing the mitochondrial pathway during Fas-induced apoptosis. However, two lines of evidence

from the results presented in this chapter suggest that the Jurkat cells used in this study do not behave as type II cells. Firstly, all caspase-8 is processed in the Bcl-2 overexpressing clones and secondly Bcl-2 delays, rather than blocks, Fas-induced apoptosis. These results are very much at odds with previous findings (Scaffidi et al., 1998) defining Jurkat cells as being type II.

Recently Bcl-2 has been shown to delay the cell cycle and cell proliferation in a manner which is independent of its anti-apoptotic activity (O'Reilly et al., 1996; Vairo et al., 1996; Borner, 1996; Huang et al., 1997). Therefore the effect of differential Bcl-2 overexpression on cell proliferation was examined in the four clones. In agreement with previous studies (Borner, 1996), the increased overexpression of Bcl-2 in the clones used in the present study, directly correlated with the decrease in cell proliferation. Most notable was the decreased proliferative rate in clone J-Bcl-2/A8 which expressed the highest level of Bcl-2. This suggests that the anti-proliferative effect of Bcl-2 can be dissociated from its anti-apoptotic effects which is in agreement with previous studies (Borner, 1996; Huang et al., 1997). The mechanisms by which Bcl-2 inhibits the cell cycle and impedes proliferation are at present unclear, although potential mechanisms may include regulation of CDK2 activation (Gil-Gomez et al., 1998), and sequestration of calcineurin, which prevents the interaction with NF-AT and subsequent cell proliferation (Shibasaki and McKeon, 1995; Linette et al., 1996). Furthermore, Bcl-2 has been shown to be phosphorylated during M-phase of the cell cycle in a manner which is unrelated to its anti-apoptotic activity, further illustrating potential functions for Bcl-2 in the cell cycle as well as apoptosis (Ling et al., 1998).

Taken together the work described in this chapter shows that the Bcl-2 overexpressing Jurkat cells inhibited staurosporine-induced and to a lesser extent Fas-mediated apoptosis in a manner which was related to the level of Bcl-2 overexpression. However, high levels of Bcl-2 expression appeared to negate this anti-apoptotic effect. The ability of Bcl-2 to more effectively inhibit staurosporine-induced apoptosis, suggests that Bcl-2 could be acting on either the mitochondrial pathway or disrupting Apaf-1/caspase-9 association (Pan et al., 1998; Moriishi et al., 1999). In contrast during Fas-mediated apoptosis, Bcl-2 appears to be acting at a point downstream of caspase-8 activation and potentially downstream of the mitochondria suggesting that the Jurkat cell line used in this study behaves in some ways as a type I, rather than a type II cell. In addition the anti-apoptotic

function of Bcl-2 has been shown to be distinct from the anti-proliferative effects of Bcl-2. These results lend weight to the idea that the expression level of Bcl-2 in *in vitro* systems is important in determining the function of the protein at any one time. So, whilst Bcl-2 anti-apoptotic activity may be reduced when the protein is highly overexpressed, the anti-proliferative effects may be enhanced; thus establishing a number of distinct cellular roles for the Bcl-2 protein, which, when in combination could contribute to oncogenesis (King and Cidlowski, 1995; Reed, 1997; Chao and Korsmeyer, 1998).

**Note**

Some of the results presented in this chapter have been published in the following:

Johnson, V.L., Cooper, I.R., Jenkins, J.R., and Chow, S.C. (1999). Effects of differential overexpression of Bcl-2 on apoptosis, proliferation, and telomerase activity in Jurkat T cells. *Experimental Cell Research*, 252, 175-184.

Ko, S.C.W., Johnson, V.L., and Chow, S.C. (2000). Functional characterization of Jurkat T cells rescued from CD95/Fas-induced apoptosis through the inhibition of caspases. *Biochemical and Biophysical Research Communications*, 270, 1009-1015.

**CHAPTER FOUR**

**EFFECT OF BCL-2 OVEREXPRESSION ON ACTIVATION-  
INDUCED CELL DEATH IN JURKAT T CELLS**

## 4.1 Introduction

Activation-induced cell death (AICD) is a process by which a T lymphocyte dies by any signal resulting in continuous lymphocyte activation particularly through stimulation of the T cell receptor (TCR)/CD3 with antigens associated with the MHC complex or antibodies to the TCR (Green and Scott, 1994). AICD plays an important role in the deletion of immature T cells in the thymus which are reactive to self antigens, peripheral deletion of autoreactive T cells, and down regulation of activated T cells after an immune response (Strasser, 1995). Resting T cells express low levels of Fas and do not express FasL. However, after T cell activation there is an up regulation of Fas and FasL (Hanabuchi et al., 1994; Nagata, 1994; Suda et al., 1995). Thus the interaction between activated T cells which express Fas receptor and/or FasL will induce apoptosis in a fratricide/suicide manner (Singer and Abbas, 1994; Dhein et al., 1995; Ju et al., 1995; Brunner et al., 1995). The importance of the Fas/FasL system in AICD is underscored by the development of lymphoproliferation disorder and generalized lupus like autoimmune disease in the *lpr* (lacking Fas) and *gld* (non-functional Fas-ligand) mice (Watanabe-Fukunaga et al., 1992; Takahashi et al., 1994; Russell, 1995).

The signalling mechanism of the TCR by anti-TCR/CD3 antibody crosslinking (Smith et al., 1989; Shi et al., 1991) or stimulation with phytohaemagglutinin (PHA) (Peter et al., 1997) involves the rapid activation of tyrosine kinases (p56<sup>lck</sup> and ZAP-70), Ras and phospholipase c (PLC) intermediates (Weiss and Littman, 1994). PLC subsequently hydrolyses phosphatidylinositol-4,5-bisphosphate (PIP<sub>2</sub>) yielding the two second messengers, inositol triphosphate (IP<sub>3</sub>) and diacylglycerol (DAG) (Berridge, 1987; Nishizuka, 1988; Berridge and Irvine, 1989). IP<sub>3</sub> induces the release of calcium from intracellular stores such as the endoplasmic reticulum (ER), which in turn activates the influx of calcium from the extracellular milieu (Berridge and Irvine, 1989). This increase in cytosolic free calcium then activates the calcium-dependent serine phosphatase, calcineurin which in turn dephosphorylates cytosolic NF-AT allowing its translocation to the nucleus (Liu et al., 1991; Jain et al., 1993; Weiss and Littman, 1994; Garcia-Cozar et al., 1998). DAG, on the other hand activates protein kinase c (PKC), which then modulates the function of various proteins by phosphorylation and activation of NFκB

(Cantrell, 1996). The calcium signalling pathway following T cell activation can be mimicked experimentally by the use of  $\text{Ca}^{2+}$  ionophores such as ionomycin or inhibitors of the endoplasmic reticular  $\text{Ca}^{2+}$ -ATPase, such as thapsigargin (Thastrup et al., 1990; Jiang et al., 1994). Similarly, PKC activation can be induced *in vitro* by use of phorbol esters such as 12-O-tetradecanoylphorbol 13-acetate (TPA).

Studies have shown that  $\text{CD4}^+$   $\text{CD8}^+$  T cells which overexpress Bcl-2 are resistant to lymphotoxic agents such as phorbol esters, ionomycin and glucocorticoids (Strasser et al., 1991; Sentman et al., 1991). Furthermore, overexpression of Bcl-2 has been shown to reduce the transient increase in cytosolic calcium induced by thapsigargin (Lam et al., 1994; Marin et al., 1996) and maintain calcium homeostasis in the ER, thereby inhibiting thapsigargin induced apoptosis (He et al., 1997). These data suggest that Bcl-2 may have additional anti-apoptotic roles which are complimentary to its involvement in the inhibition of caspase activation during receptor- and chemical-induced apoptosis (Reed, 1994; Memon et al., 1995). Therefore using the Bcl-2 overexpressing clones J-Bcl-2/C4.1, J-Bcl-2/C5.2 and J-Bcl-2/A8, the effect of Bcl-2 overexpression on AICD was examined.

## 4.2 Results

### 4.2.1 Effect of Bcl-2 overexpression on activation-induced cell death in Jurkat T cells.

Previous studies (Ko et al., 2000) have shown that wild type Jurkat cells are susceptible to AICD and readily undergo apoptosis when stimulated with the mitogen, PHA (Peter et al., 1997). In addition to this approach, a combination of TPA and TG, which mimics mitogenic signals during TCR signalling, was also used. In order to determine the optimal concentration of PHA, dose response studies were carried out and 2 $\mu$ g/ml was found to be optimal in causing AICD in wild type Jurkat cells (results not shown). This concentration was used throughout this chapter. TPA and thapsigargin were used at concentrations of 20ng/ml and 50nM, respectively. In order to investigate the effect of Bcl-2 overexpression on AICD, Bcl-2 overexpressing Jurkat T cell clones (J-Bcl-2/C4.1, J-Bcl-2/C5.2 and J-Bcl-2/A8) were incubated with either PHA (2 $\mu$ g/ml), or with a combination of TPA (20ng/ml) and thapsigargin (50nM) for 24h. After treatments the cells were harvested and the extent of apoptosis was assessed by staining with Hoechst 33358 and analysed using UV microscopy. Cell viability was determined using the MTS viability assay. As shown in Figure 4.1A and B, PHA and the combined TPA/TG induced ~25% and ~50% apoptosis respectively in the vector transfected control, J-pEBS7 (Figure 4.1A). Incidentally, both TPA and thapsigargin alone, also induced considerable apoptosis in J-pEBS7. In contrast, the overexpression of Bcl-2 markedly inhibited all of these effects in the three clones. Surprisingly, J-Bcl-2/A8 which gave little protection against Fas-mediated apoptosis (Section 3.2.5) was very effective in preventing AICD. Furthermore, cell viability was also increased most notably in the Bcl-2 overexpressing clones which were treated with a combination of TPA and thapsigargin (Figure 4.1B). These data suggest that Bcl-2 is able to effectively inhibit AICD in response to a number of mitogenic stimuli.

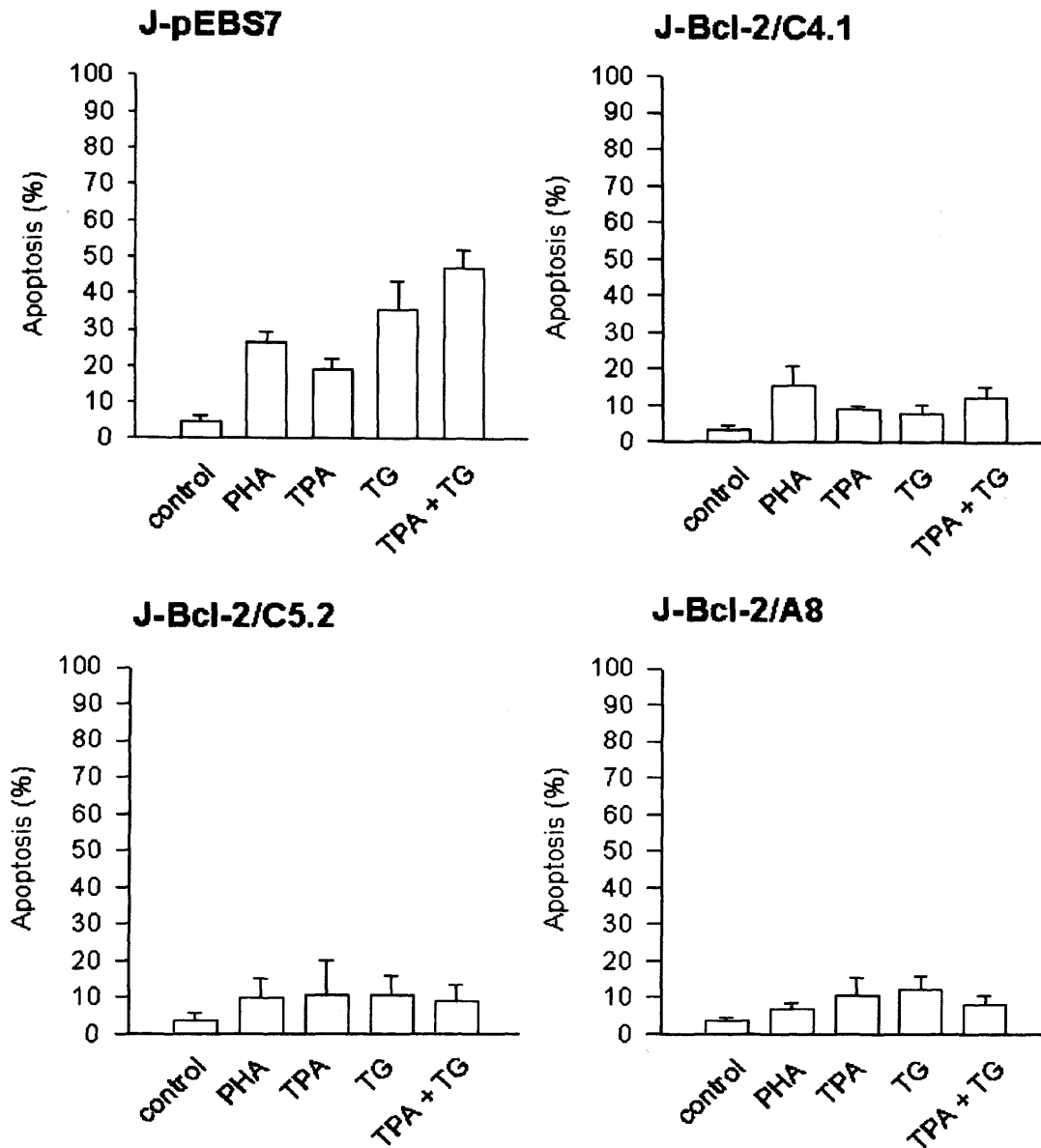


**Figure 4.1A** Effect of Bcl-2 overexpression on AICD in Jurkat T cells. AICD was induced with either PHA ( $2\mu\text{g/ml}$ ), TPA or thapsigargin (TG) or a combination of TPA ( $20\text{ng/ml}$ ) and thapsigargin (TG) ( $50\text{nm}$ ). Cells were incubated for 24h and then assessed for apoptotic morphology by staining with Hoechst 33358 and viewing under UV microscopy. The results represent the mean of four independent experiments  $\pm$  SEM.

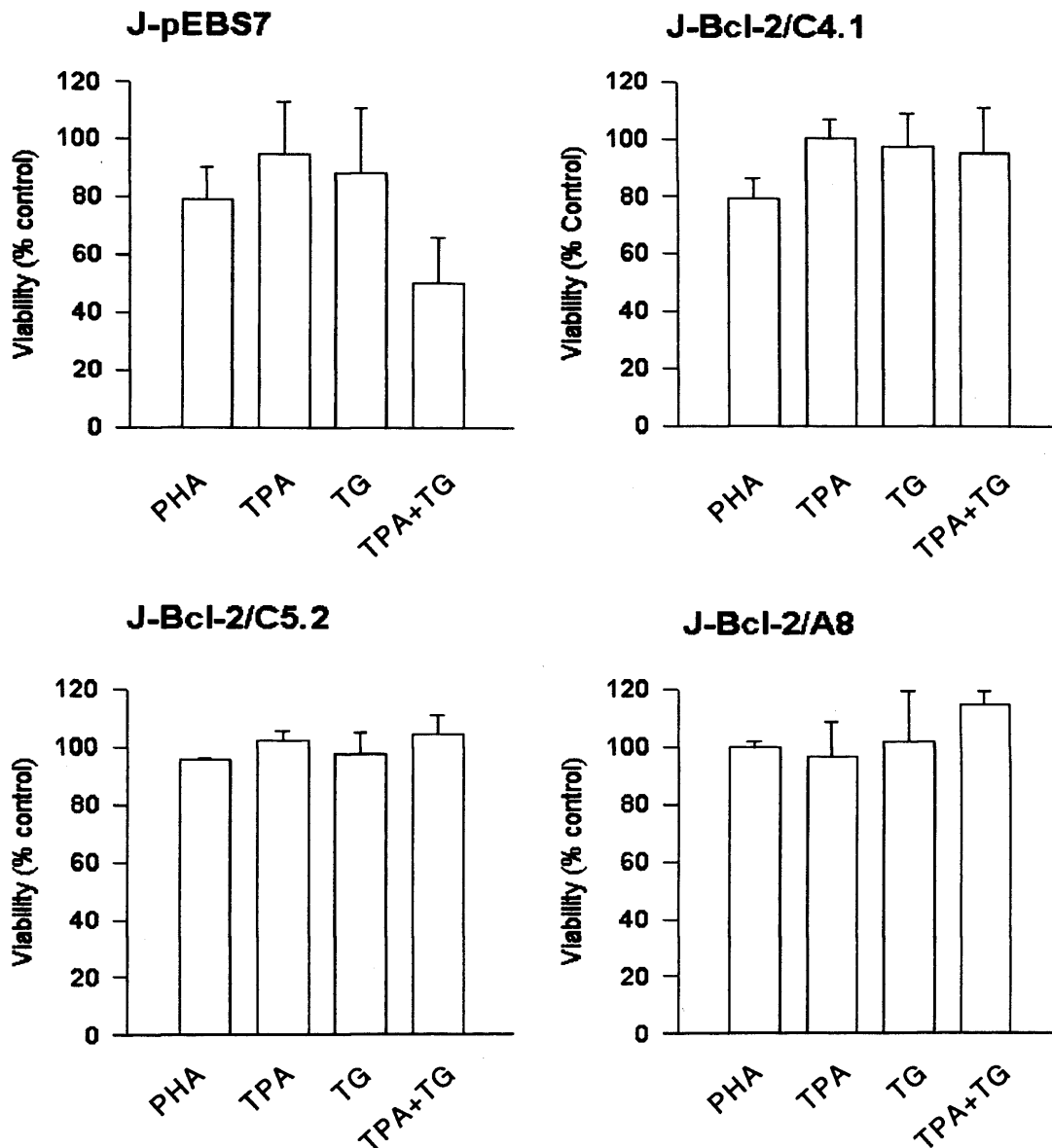


**Figure 4.1B Effect of Bcl-2 overexpression on Jurkat T cell viability during AICD.** AICD was induced with either PHA (2 $\mu$ g/ml), TPA (20ng/ml), thapsigargin (TG) (50nm) or a combination of TPA and thapsigargin. Cells were incubated for 24h and then assessed for viability using the MTS viability assay, as described in materials and methods. The results represent the mean of four independent experiments  $\pm$  SEM.

#### **4.2.2 Processing of caspase-8 and -3 during AICD in Bcl-2 overexpressing Jurkat T cells**

There is compelling evidence that the Fas antigen and FasL expressed on the surface of T cells after activation is the main cause of apoptosis during AICD (Medema et al., 1997). Interaction between the Fas receptor and Fas ligand results in the trimerization of the Fas receptor complex. This is followed by recruitment of FADD/MORT-1 to the intracellular domain of the Fas receptor (Chinnaiyan et al., 1995) which provides a docking platform for caspase-8 and subsequent activation of this pro-enzyme (Muzio et al., 1996; Boldin et al., 1996). Being the apical caspase in the Fas signalling pathway, caspase-8 activates downstream effector caspases and the subsequent proteolysis of cellular substrates (Srinivasula et al., 1996). Therefore to confirm that AICD involves the signalling of caspase-8 to effect an apoptotic outcome and to determine the level at which Bcl-2 was inhibiting AICD, the processing of caspase-8 and -3 was examined in the treated cells. As illustrated in Figure 4.2, there was no substantial processing of either caspase-8 or -3 after treatment with either PHA or TPA (lane 2 and 3, respectively) in the control J-pEBS7. However, after treatment with thapsigargin or a combination of thapsigargin and TPA (lane 4 and 5 respectively) there was marked increase in the amount of caspase-8 and -3 processing, as evidenced by the appearance of p42/43 fragment of caspase-8 and the p20 and p17 fragments of caspase-3. This increased caspase processing correlated to the increased levels of apoptosis observed by UV microscopy (Figure 4.1A). In clone J-Bcl-2/C4.1 caspase-8 and -3 processing was markedly inhibited after treatments, which correlated well to the ability of this clone to inhibit apoptosis. With J-Bcl-2/C5.2, caspase-8 and -3 processing was markedly inhibited after treatment with thapsigargin but after treatment with thapsigargin and TPA only a small amount of caspase-8 and -3 processing was observed despite a low level of apoptosis and cell death in this clone. Interestingly, clone J-Bcl-2/A8, which was previously shown to be sensitive to Fas and unable to block caspase-8 and -3 processing (Section 3.2.5), was very effective in blocking caspase-8 and -3 processing and AICD after treatment with PHA, TPA and thapsigargin. These results suggest that although clone J-Bcl-2/A8 is not able to directly block Fas-induced apoptosis, it may be acting at a point prior to Fas/FasL interaction during AICD.

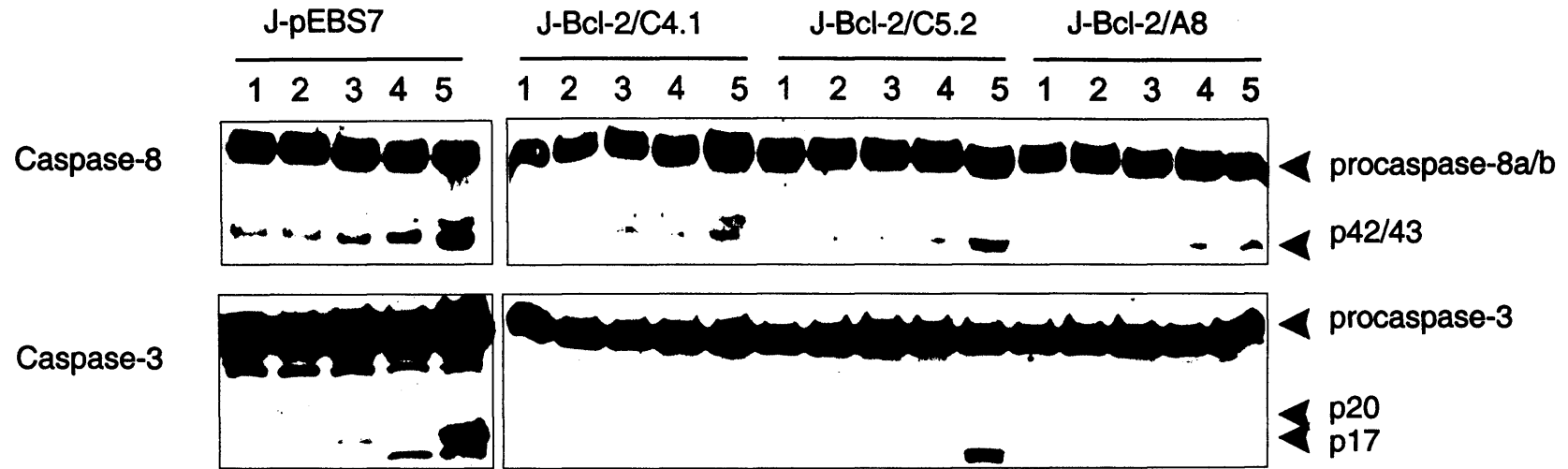


**Figure 4.2. Effect of Bcl-2 overexpression on caspase-8 and -3 processing during AICD in Jurkat T cells.** Cell clones were used at a density of  $1 \times 10^6$ /ml and treated with PHA, TPA or TG. Lanes represent 1, Untreated (control); 2, PHA ( $2 \mu\text{g}/\text{ml}$ ) 3, TPA ( $20 \text{ng}/\text{ml}$ ); 4, thapsigargin (TG) ( $50 \text{nm}$ ); 5, TPA ( $20 \text{ng}/\text{ml}$ ) + thapsigargin ( $50 \text{nm}$ ). Following treatment cell lysates were analysed by SDS PAGE and western blotting for caspase-8 (top panel) and -3 (bottom panel). The results are one representative of three independent experiments.

### 4.2.3 Effect of Bcl-2 on FasL expression

The findings that J-Bcl-2/A8 blocks AICD suggest that Bcl-2 may be blocking the expression or secretion of FasL, since this clone readily undergoes apoptosis when directly stimulated with anti-Fas. To this end the expression of FasL was first examined in the Bcl-2 clones as previous studies have shown that Jurkat T cells constitutively express FasL in the cytoplasm (Martinez-Lorenzo et al., 1996). As illustrated in Figure 4.3, there was no difference in the level of FasL expression in the different Bcl-2 clones compared to both vector control, pEBS7 or wild type Jurkat cells. To confirm that FasL is constitutively expressed in the cytoplasm and to determine whether Bcl-2 overexpression affects the localization of FasL, a more subtle approach was taken using flow cytometry analysis. Cell surface staining was carried out using non-permeabilized cells, as described in materials and methods. As illustrated in Figure 4.4A, there was no significant increase in fluorescence above the FITC control suggesting that FasL is indeed localized intracellularly. This was confirmed by indirect staining of permeabilized cells with anti-FasL. As shown in Figure 4.4B, there was a significant increase in fluorescence in all the clones suggesting a high level of intracellular FasL expression. Furthermore, the level of intracellular FasL expression was similar in all the clones, suggesting that the intracellular expression of FasL was not affected by Bcl-2 overexpression and is therefore unlikely to be the cause of the inhibition of AICD. From this experiment it was clear that the inhibition of AICD by Bcl-2 was not due to a decrease in constitutive FasL expression.

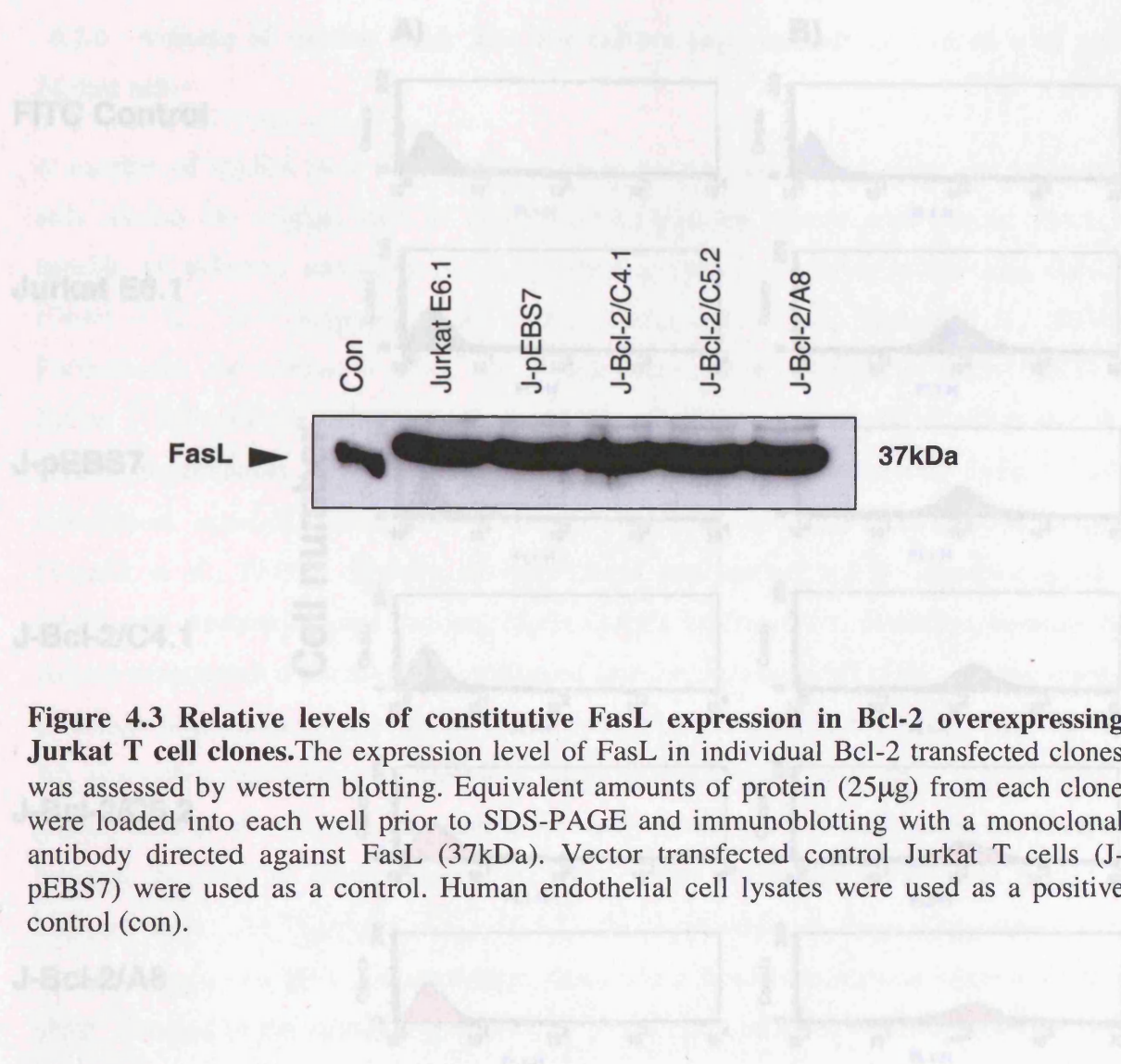


**Figure 4.3 Relative levels of constitutive FasL expression in Bcl-2 overexpressing Jurkat T cell clones.** The expression level of FasL in individual Bcl-2 transfected clones was assessed by western blotting. Equivalent amounts of protein (25 $\mu$ g) from each clone were loaded into each well prior to SDS-PAGE and immunoblotting with a monoclonal antibody directed against FasL (37kDa). Vector transfected control Jurkat T cells (J-pEBS7) were used as a control. Human endothelial cell lysates were used as a positive control (con).

Figure 4.4 Localization of FasL, constitutively expressed in Bcl-2 overexpressing Jurkat T cell clones. A) Cells ( $\times 10^6$ ) were taken and stained directly for cell surface expression of FasL with an anti-FasL monoclonal antibody followed by FITC-conjugated goat anti-mouse antibody. B) For intracellular staining of FasL, cells were permeabilized with methanol and then stained with anti-FasL monoclonal antibody followed by FITC-conjugated goat anti-mouse antibody. All procedures are as described in materials and methods. As a control, cells were incubated with the FITC-conjugated goat anti-mouse antibody alone. The results are representative of three independent experiments.



#### **4.2.4 Release of soluble FasL into the culture supernatants of treated wild type Jurkat cells**

A number of studies have shown that upon activation, some T cell lines and leukaemic cells release the soluble form of FasL (sFasL) into the culture supernatant which is capable of inducing apoptosis in Fas expressing cells in a paracrine/autocrine fashion (Dhein et al., 1995; Kayagaki et al., 1995; Tanaka et al., 1995; Mariani et al., 1995b). Furthermore, the release of sFasL has been shown to be a major factor during AICD in Jurkat T cells (Martinez-Lorenzo et al., 1996). Therefore, the release of sFasL into the culture supernatants of activated wild type Jurkat cells was examined using a FasL monoclonal antibody which was directed against the c-terminal extracellular domain (Tanaka et al., 1995). Initially, the experiment was carried out by conventional SDS PAGE and western blotting analysis of the culture supernatants. However, because the culture supernatant of treated cells contained low concentrations of sFasL, a large volume of culture supernatant was required for analysis which is not practical using SDS PAGE. An alternative approach was therefore taken, using dot blot analysis. This allowed a greater volume of culture supernatant to be analysed and a direct comparison can be made between the level of sFasL secreted into the culture supernatants from cells treated in different ways. As illustrated in Figure 4.5, after treatment with PHA, TPA, thapsigargin or thapsigargin and TPA in combination, there was a significant increase in the amount of sFasL detected in the culture supernatant of Jurkat E6.1 cells. In contrast, untreated cells have little or no detectable sFasL in the culture supernatant. From the dot-blot analysis, it appears that combined treatment with TPA and thapsigargin was the most effective way of inducing the release of sFasL into the culture supernatants of wild type Jurkat T cells (Figure 4.5). In addition the finding that thapsigargin and TPA can also induce the release of sFasL on their own is consistent with their ability to induce AICD in Jurkat cells (Figure 4.1A and B).

#### 4.3.5 Release of sFasL into the culture supernatants of treated Bcl-2 overexpressing clones

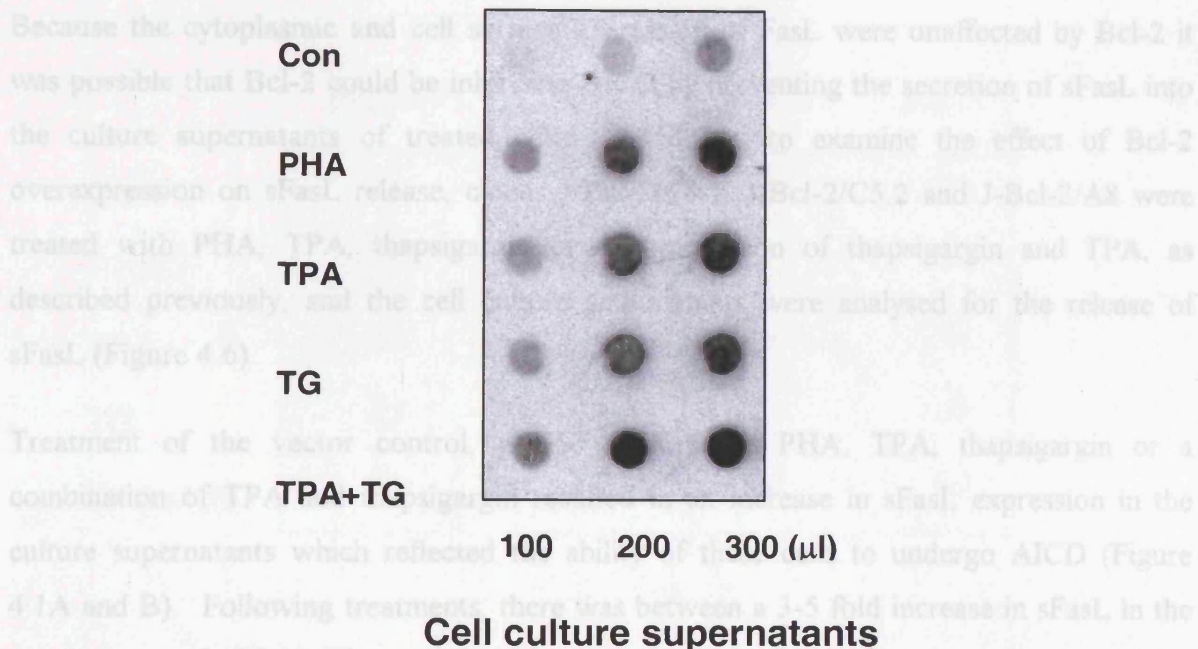


**Figure 4.5 Preliminary Dot-Blot analysis to determine the optimum volume ( $\mu\text{l}$ ) of cell culture supernatant required for sFasL detection.** Wild type Jurkat T-cells were treated with PHA ( $2\mu\text{g/ml}$ ), TPA ( $20\text{ng/ml}$ ) and TG ( $50\text{nM}$ ) for 24h. Following treatments, 100, 200 and  $300\mu\text{l}$  culture supernatants were added to the wells of a Biorad-dot blot apparatus and filtered onto the blotting membrane via suction. The membrane was then incubated with FasL antibody before ECL detection as outlined in materials and methods. In all subsequent experiments,  $200\mu\text{l}$  cell culture supernatant was used for detection of sFasL by dot blot analysis.

#### **4.2.5 Release of sFasL into the culture supernatants of treated Bcl-2 overexpressing Jurkat T cell clones.**

Because the cytoplasmic and cell surface expression of FasL were unaffected by Bcl-2 it was possible that Bcl-2 could be inhibiting AICD by preventing the secretion of sFasL into the culture supernatants of treated cells. Therefore, to examine the effect of Bcl-2 overexpression on sFasL release, clones J-Bcl-2/C4.1, J-Bcl-2/C5.2 and J-Bcl-2/A8 were treated with PHA, TPA, thapsigargin or a combination of thapsigargin and TPA, as described previously, and the cell culture supernatants were analysed for the release of sFasL (Figure 4.6).

Treatment of the vector control, pEBS7 with either PHA, TPA, thapsigargin or a combination of TPA and thapsigargin resulted in an increase in sFasL expression in the culture supernatants which reflected the ability of these cells to undergo AICD (Figure 4.1A and B). Following treatments, there was between a 3-5 fold increase in sFasL in the supernatants of pEBS7 (Figure 4.7). After treatment with PHA, TPA, thapsigargin or TPA and thapsigargin, the Bcl-2 overexpressing clones J-Bcl-2/C4.1, J-Bcl-2/C5.2 and J-Bcl-2/A8 had reduced levels of sFasL in the culture supernatants. The most dramatic effect was seen after treatment with thapsigargin and combined treatment with thapsigargin and TPA. After treatment with TG, there was more than a 5-fold increase in the level of sFasL in the culture supernatants of J-pEBS7. In contrast, there was only a 1.5-fold increase in clone J-Bcl-2/C4.1. In clones J-Bcl-2/C5.2 and J-Bcl-2/A8 the secretion of sFasL into the culture supernatants was reduced to ~0.5-fold in comparison to untreated culture supernatants. After treatment with TPA and thapsigargin, there was more than a 3-fold increase in sFasL secretion in J-pEBS7, whereas in clones J-Bcl-2/C4.1, J-Bcl-2/C5.2 and J-Bcl-2/A8, this was reduced to between 1-1.5-fold. The overall reduction in sFasL secretion in the Bcl-2 overexpressing clones correlated with the ability of each clone to inhibit AICD (Figure 4.1A and Figure 4.7). These results suggest that Bcl-2 may inhibit AICD by preventing the release of sFasL from the activated cells.

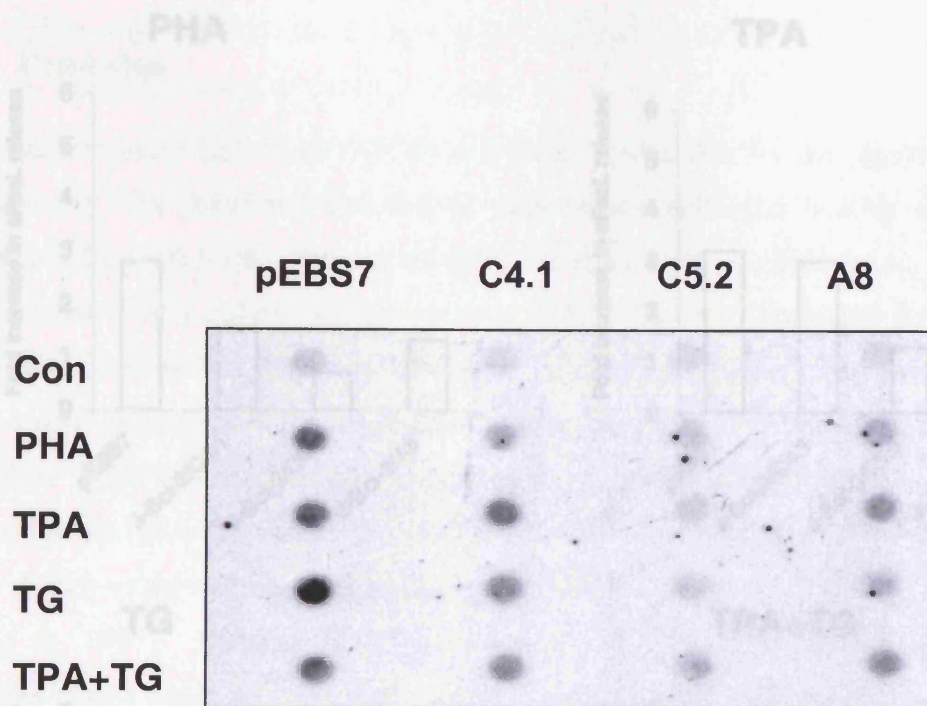


**Figure 4.6** Dot blot analysis showing the secretion of sFasL in cell culture supernatants of treated Jurkat T cell clones overexpressing Bcl-2. Cells were incubated with either PHA (2 $\mu$ g/ml), TPA (20ng) and/or TG (50nM) for 24h. The cell suspension was centrifuged down and 200 $\mu$ l of each culture supernatant was loaded onto a nitrocellulose membrane using dot blot apparatus as described in materials and methods. The membrane was then probed with a monoclonal antibody to FasL. The experiment was repeated three times with similar findings.

Figure 4.7 Analysis of sFasL secretion into the culture supernatants during AICD in Jurkat T cell clones overexpressing Bcl-2. Bcl-2 overexpressing clones ( $1 \times 10^6$  cells/ml) were incubated for 24h in the presence of either PHA (2 $\mu$ g/ml), TPA (20ng/ml), theophylline (TG) (50nM) or a combination of TPA + TG. Quantitation of sFasL release into the culture supernatant was examined by dot blot analysis and quantified using densitometry. The relative level of sFasL release into the culture supernatant of each clone is shown relative to the control level of sFasL in the culture supernatant of the untreated vector control (pEBS7) and was arbitrarily assigned a value of 1. The data shown represent the mean of three independent experiments.

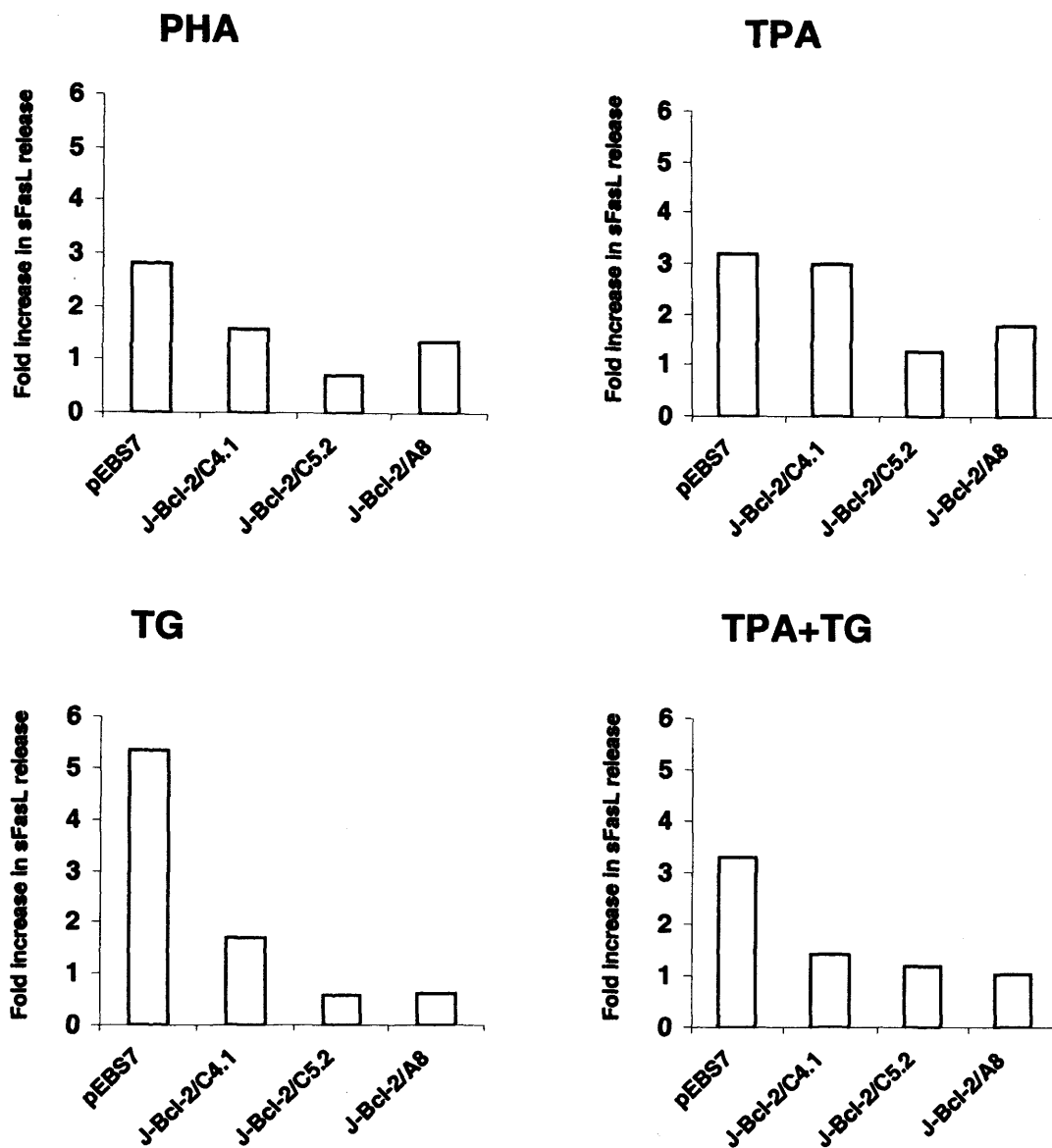


**Figure 4.7 Analysis of sFasL secretion into the culture supernatants during AICD in Jurkat T cell clones overexpressing Bcl-2.** Bcl-2 overexpressing clones ( $1 \times 10^6$  cells/ml) were incubated for 24h in the presence of either PHA ( $2 \mu\text{g/ml}$ ), TPA ( $20 \text{ng/ml}$ ), thapsigargin (TG) ( $50 \text{nm}$ ) or a combination of TPA + TG. Quantitation of sFasL release into the culture supernatant was examined by dot blot analysis and quantified using densitometry. The relative level of sFasL release into the culture supernatant of each clone is shown relative to the control level of sFasL in the culture supernatant of the untreated vector control (J-pEBS7) and was arbitrarily assigned a value of 1. The data shown represents the mean of three independent experiments.

### 4.3 Discussion

Activation induced cell death (AICD) is a major mechanism for the regulation of immune homeostasis, the peripheral deletion of autoimmune cells and limiting cellular immune responses after infection (Dhein et al., 1995; Ju et al., 1995; Brunner et al., 1995). After T cell activation there follows an upregulation of Fas and FasL expression on the cell surface and secretion of sFasL. Interaction between Fas and FasL results in receptor trimerization, recruitment of caspase-8 and subsequent apoptosis. Bcl-2 overexpression has been shown to inhibit T cell death and confer resistance to lymphotoxic agents such as phorbol esters, ionomycin and glucocorticoids (Strasser et al., 1991; Sentman et al., 1991). Bcl-2 has also been shown to inhibit thapsigargin-mediated AICD (Lam et al., 1994; Marin et al., 1996; He et al., 1997). Because Bcl-2 has a number of independent anti-apoptotic roles it is possible that it could be regulating multiple control points during AICD and apoptosis in general (Reed, 1997). The controversy surrounding the ability of Bcl-2 to inhibit Fas-mediated apoptosis coupled with its effectiveness against AICD suggests that it may be acting at sites other than the mitochondria to exert its anti-apoptotic effects in response to certain stimuli which result in AICD (Shibasaki and McKeon, 1995). Therefore in the light of the results presented in the previous chapter, the effect of Bcl-2 overexpression on AICD was examined.

In chapter three, Fas-mediated apoptosis was partially inhibited by clones J-Bcl-2/C4.1 and J-Bcl-2/C5.2, suggesting that Bcl-2 acts at a point downstream of caspase-8 activation. Interestingly, clone J-Bcl-2/A8, which expressed a high level of Bcl-2 had no effect on Fas-mediated apoptosis. However, all three clones had a significant anti-apoptotic effect in response to AICD and markedly inhibited caspase-8 and -3 activation. These results suggest that Bcl-2 may function at a point upstream of caspase-8 activation, ie. prior to receptor engagement during AICD. Upon stimulation by PHA, functional sFasL is released into the culture supernatants and acts as the major factor for AICD in Jurkat T cells by binding to Fas which is constitutively expressed on the cell surface (Dhein et al., 1995; Martinez-Lorenzo et al., 1996). The decrease in sFasL in the culture supernatants of the treated clones J-Bcl-2/C4.1, J-Bcl-2/C5.2 and J-Bcl-2/A8 suggests that Bcl-2 may be preventing the secretion of sFasL from the cells during AICD. It is well established that the secretion of sFasL into the supernatant of activated T cell during AICD is mediated by

a metalloproteinase (Mariani et al., 1995). Inhibition of sFasL release can be achieved by use of metalloproteinase inhibitors such as the  $Zn^{2+}$  chelator 1,10 phenanthroline (Kayagaki et al., 1995; Mariani et al., 1995). Although Bcl-2 has been shown to possess multiple anti-apoptotic functions there is no direct evidence that it is involved in the regulation of this pathway. A more likely explanation for the decrease in sFasL secretion in the clones tested, is that the Bcl-2 may be preventing the *de novo* synthesis of FasL after the initial Bcl-2-independent release of preformed sFasL. Release of preformed FasL from within the cell is proposed to occur 1-2h after activation, followed by *de novo* FasL synthesis (Dhein et al., 1995; Martinez-Lorenzo et al., 1996). Therefore after the initial early release of sFasL into the supernatant and induction of low levels of apoptosis, any further FasL production could be prevented by Bcl-2, and sFasL release would be inhibited. Indeed, Bcl-2 has been shown to regulate transcription during calcium-mediated AICD by the sequestration of the calcium activated protein phosphatase, calcineurin (Linette et al., 1996; Shibasaki et al., 1997). Calcineurin is under the control of calcium/calmodulin and plays an important role in the coupling of calcium signals to cellular responses (Fruman et al., 1992; Shibasaki and McKeon, 1995). Calcineurin dephosphorylates NF-AT (Nuclear Factor of Activated T cells) which is an essential requirement for its translocation to the nucleus (McCaffrey et al., 1993; Garcia-Cozar et al., 1998). NF-AT is one of a family of transcription factors regulating the expression of inducible genes such as IL-2 upon T cell activation (Northrop et al., 1994; Rao et al., 1997). Furthermore, NF-AT binding sites in the FasL promoter have been shown to be important in FasL expression during T cell activation (Latinis et al., 1997; Li-Weber et al., 1998). Bcl-2 has been shown to prevent NF-AT dependent IL-2 transcription in transgenic mice (Linette et al., 1996) and block apoptosis induced by calcineurin overexpression (Shibasaki and McKeon, 1995). Thus, Bcl-2 could be acting to directly down regulate FasL transcription by sequestering calcineurin. If Bcl-2 were affecting the activation and translocation of NF-AT from the cytosol to the nucleus, the subsequent expression of FasL might also be down regulated in consequence (Latinis et al., 1997). Therefore the observed anti-apoptotic effects of Bcl-2 overexpression during AICD presented in this chapter could be due to the sequestration of calcineurin and inhibition of NF-AT activity leading to subsequent down regulation of sFasL expression. Bcl-2 has also been shown to inhibit calcium-mediated cell death by sequestering calcineurin to the ER or mitochondrial membranes, thereby preventing its interaction with, and dephosphorylation of, NF-AT

(Shibasaki et al., 1997). Bcl-2 could also prevent  $\text{Ca}^{2+}$  efflux from the ER resulting in reduced calcineurin activation, affecting NF-AT translocation and hence sFasL expression (Lam et al., 1994). This might explain why Bcl-2 appears to be more effective in the inhibition of AICD by thapsigargin or a combination of thapsigargin and TPA.

Interestingly, caspase-12 has recently been found to localize to the ER and mediate ER-specific apoptosis induced by thapsigargin (Nakagawa et al., 2000). Furthermore, caspase-12 was activated in response to ER stress, such as that caused by disruption of calcium homeostasis, but not by membrane or mitochondrial mediated signals by Fas or staurosporine (Nakagawa et al., 2000). Because Bcl-2 can functionally interact with members of the caspase family of proteases to inhibit their function, it could also be blocking AICD at the level of caspase-12 activation. Bcl-2 has also been shown to localize to the ER and therefore could be preventing caspase-12 release from the ER in a manner which could be analogous to its effect on cytochrome c release from the mitochondria. Because of the multifunctional nature of the Bcl-2 protein is it possible that it could be mediating AICD via a number of pathways including sequestration of calcineurin and inhibition of NF-AT signalling, membrane channel function in the ER regulating calcium efflux and inhibition of caspase processing, particularly caspase-12. The results presented in this chapter suggest that Bcl-2 overexpression in Jurkat T cells results in a decrease in AICD in response to PHA, TPA and TG by affecting the secretion of sFasL, although the exact mechanism by which Bcl-2 inhibits this secretion remains to be determined.

## **CHAPTER FIVE**

# **EFFECTOR CASPASE INDEPENDENT NUCLEAR MORPHOLOGICAL CHANGE DURING CHEMICAL- INDUCED APOPTOSIS IN JURKAT T CELLS**

## 5.1 Introduction

During apoptosis, a dying cell progresses through a series of well defined biochemical and morphological changes occurring in the cytoplasm and the nucleus (Kerr et al., 1972; Arends and Wyllie, 1991). Many of these changes are mediated by the caspases, a family of cysteine proteases which are key mediators of the apoptotic program in virtually all cell types undergoing apoptosis (Cohen, 1997; Thornberry and Lazebnik, 1998). Caspases exist as inactive proenzymes and require specific cleavage at aspartate residues for activation, releasing the prodomain and the large and small subunits. They are divided into functional sub-families based on prodomain length and substrate sequence preferences (Cohen, 1997; Nicholson and Thornberry, 1997; Thornberry et al., 1997). Effector caspases such as caspase-3, -6 and -7 have short prodomains and generally act during the execution phase of apoptosis cleaving cellular substrates specifically after aspartate residues (MacFarlane et al., 1997; Cohen, 1997).

A number of these substrates appear to have a direct physiological significance in the morphological and biochemical changes that are hallmarks of apoptosis (Cryns and Yuan, 1998; Wolf et al., 1999). These include structural proteins of the cytoskeleton and nucleus, such as Gas2 (Brancolini et al., 1995), fodrin (Janicke et al., 1998a), gelsolin (Kothakota et al., 1997) and nuclear lamins (Lazebnik et al., 1995; Takahashi et al., 1996; Rao et al., 1996). In addition the cleavage of DFF by caspase-3 plays a critical role in the activation of chromatin cleavage into oligonucleosomal length DNA fragments (Liu et al., 1997; Enari et al., 1998). Other biochemical changes induced by effector caspases include the externalisation of PS to the outer leaflet of the plasma membrane which acts as a marker for identifying apoptotic cells for engulfment by macrophages (Fadok et al., 1992; Savill et al., 1993; Fadok et al., 2000) and the cleavage of the DNA repair enzyme PARP (Lazebnik et al., 1994).

The effector caspases are themselves activated by upstream initiator caspases which possess long prodomains such as caspase-8 and -10 in receptor-mediated apoptosis and caspase-9 in chemical-induced apoptosis (Boldin et al., 1996; Srinivasula et al., 1996; Li et al., 1997; Muzio et al., 1998; Hirata et al., 1998; Stennicke and Salvesen, 1998b). The different signalling pathways for caspase-activation during receptor- and chemical-induced

apoptosis converge at the level of caspase-3 activation which, in the majority of systems results in the characteristic proteolysis of various cellular substrates contributing to the apoptotic phenotype (Liu et al., 1997; Woo et al., 1998; Janicke et al., 1998b; Porter and Janicke, 1999; Wolf et al., 1999; Sun et al., 1999).

In many systems the use of peptide-based caspase inhibitors has proved an essential tool for dissecting out the various biochemical and morphological features of apoptosis (Chow et al., 1995; Nicholson et al., 1995; Slee et al., 1996; Garcia-Calvo et al., 1998). Such inhibitors act by mimicking the preferred substrate sequence cleavage sites of caspases, thereby blocking caspase activity and in some cases, apoptosis (Thornberry et al., 1994; Longthorne and Williams, 1997; Thornberry et al., 1997). The use of such inhibitors, amongst others, has been integral in defining caspase function and enzymatic activity in *in vitro* and *in vivo* systems (Talanian et al., 1997; Thornberry and Lazebnik, 1998; Garcia-Calvo et al., 1998). Although the effector caspases play a major role in the execution of apoptosis, not all the morphological and biochemical changes associated with apoptosis are caspase-dependent (Kass et al., 1996; Samejima et al., 1998; Hughes et al., 1998b). In this chapter, the aim is to investigate in greater detail the role of effector caspases in mediating nuclear morphological changes during apoptosis. Using chemical-induced apoptosis as a model, the effect of blocking caspase activity on biochemical and nuclear morphological changes was investigated using several peptide based caspase inhibitors.

## 5.2 Results

### 5.2.1 Observation of a novel nuclear morphological change in staurosporine-treated Jurkat cells in the presence of caspase inhibitors.

Routinely, when Jurkat T cells are treated with 0.5 $\mu$ M staurosporine for 3h more than 85% of the cells have the appearance of typically apoptotic nuclei with condensed nuclear morphology when stained with Hoechst 33358 (Figure 5.1). However, in the presence of 50 $\mu$ M of the irreversible caspase inhibitor, z-VAD-FMK, the nuclei of staurosporine-treated Jurkat cells were not condensed but a distinctive nuclear morphological change was observed which neither resembled control nuclei nor fully condensed apoptotic nuclei. The nuclei of these cells appeared to be heterogenous in texture, with uneven chromatin staining representing areas of partial chromatin condensation (Figure 5.1). This nuclear morphological change was characterized by the heavily convoluted nuclei with numerous cavitations indicating that a change in chromatin structure had occurred. When observed under light microscopy the shape of some cells treated with staurosporine and z-VAD-FMK appeared slightly elongated but there was no evidence of blebbing (results not shown). Jurkat cells which were treated with z-VAD-FMK alone had a normal nuclear morphology similar to untreated control cells (results not shown and Figure 5.1). This indicated that the distinct nuclear morphological change observed in staurosporine-treated cells in the presence of z-VAD-FMK was not due to non-specific effects of the inhibitor, nor a result of the fixation and staining process.

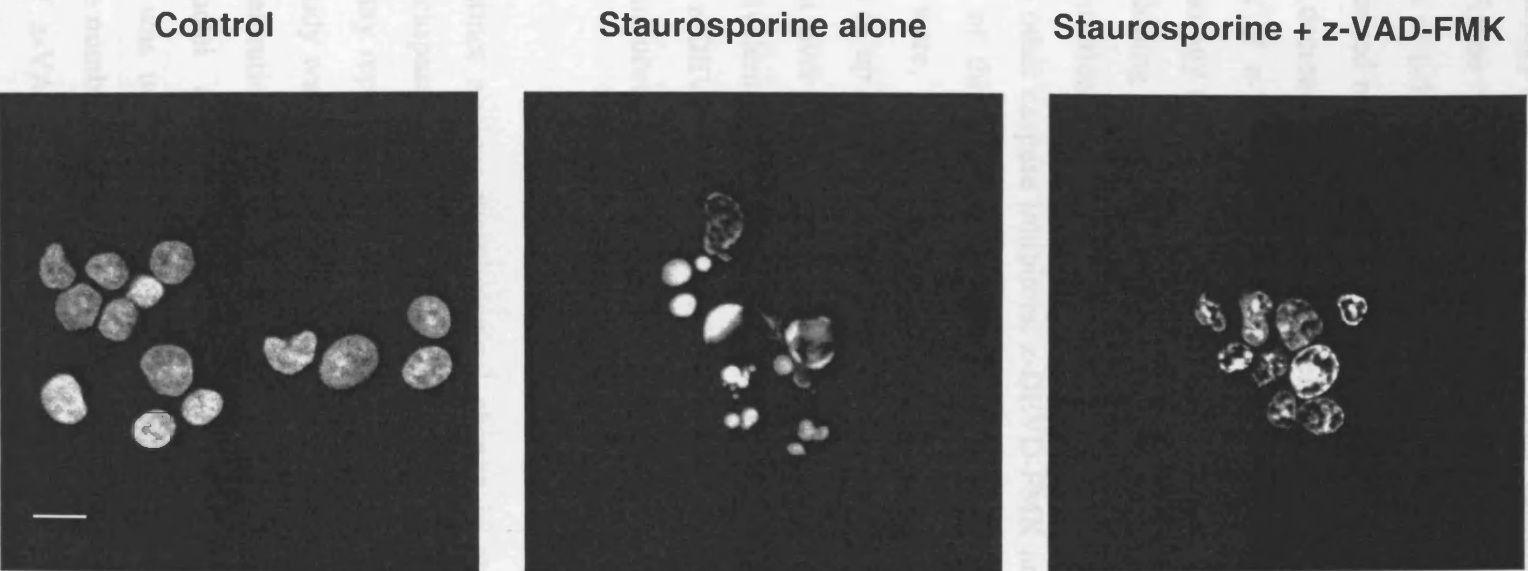


**Figure 5.1** Distinct nuclear morphological changes in Jurkat T cells treated with staurosporine in the absence or presence of z-VAD-FMK. Jurkat T cells were incubated with  $0.5\mu\text{M}$  staurosporine for 3h in the absence or presence of  $50\mu\text{M}$  z-VAD-FMK. The cells were fixed with 4% paraformaldehyde and stained with Hoechst 33358 as described in materials and methods. Cells were viewed using confocal laser microscopy. Scale bar represents  $5\mu\text{m}$ .

To examine further the effect of z-VAD-FMK on the formation of the partially condensed nuclear morphology in staurosporine-treated cells, various concentrations of z-VAD-FMK were used (Figure 5.2). In the presence of 0.5 $\mu$ M staurosporine, z-VAD-FMK at concentrations of 1-50 $\mu$ M caused a dose-dependent increase in the number of cells with a partially condensed nuclear morphology, which paralleled an increase in cell viability and a concomitant decrease in the number of cells with apoptotic nuclei (Figure 5.2). At higher concentrations of z-VAD-FMK (50-100 $\mu$ M) the formation of this partially condensed nuclear morphology decreased from 80% to ~25% in staurosporine-treated cells and there was a corresponding increase in the appearance of normal nuclei from 20% to ~75%. At higher concentrations of z-VAD-FMK (50-100 $\mu$ M) cell viability was above 95%. Similarly, two other caspase inhibitors, z-DEVD-FMK and Ac-YVAD-CMK also caused the formation of this partially condensed nuclear morphology in staurosporine-treated cells. They were, however, less effective compared to z-VAD-FMK and required concentrations of up to 100 $\mu$ M to induce the formation of the partially condensed nuclear morphology in over 80% of cells. In contrast, 10 $\mu$ M z-VAD-FMK was sufficient to induce an equivalent amount of cells (>80%) displaying the partially condensed nuclear morphology. z-DEVD-FMK and Ac-YVAD-CMK were also less effective in blocking staurosporine-induced cell death and at concentrations of 50-100 $\mu$ M resulted in only 60-70% viability.

Since this distinct nuclear morphological change in staurosporine-treated cells in the presence of caspase inhibitors appeared partially condensed, it suggests that the morphology may represent an early stage of the apoptotic process. To determine this, a time course study was carried out. Because 50 $\mu$ M z-VAD-FMK appeared to be the most effective concentration in the dose-response studies in inducing the formation of partially condensed nuclei and preventing cell death in staurosporine-treated cells, this concentration was used throughout this study. As shown in Figure 5.3, there was a decrease in the number of normal nuclei in cells treated with staurosporine in the presence or absence of z-VAD-FMK, from about 100% to below 10%. In cells treated with staurosporine alone, there was an increase in the number of apoptotic nuclei from below 5% to about 95% over the 4h time course. However, in staurosporine-treated cells in the presence of z-VAD-FMK, there was a parallel increase in the number of partially

condensed nuclei whilst the number of apoptotic nuclei never reached more than 20%. Interestingly, upon treatment with staurosporine alone, there appeared to be an early transient increase (~25%) in cells exhibiting the partially condensed nuclear morphology at 1h. This suggested that the formation of the partially condensed nuclear morphology was an early event in staurosporine-mediated apoptosis.

The results from the time course studies suggest that the partially condensed nuclear morphology is an early event and precedes chromatin condensation. In order to confirm this, an experiment was carried out to determine whether cells exhibiting this nuclear morphological change can proceed to become apoptotic, ie. with fully condensed nuclei, after the removal of the caspase inhibitor z-VAD-FMK. To this end cells were treated with staurosporine in the presence of 50 $\mu$ M z-VAD-FMK for 3h which routinely resulted in ~80% of the nuclei appearing partially condensed. After treatment the cells were washed twice with cold medium and resuspended in complete medium warmed to 37°C. The nuclear morphology and cell viability was followed over 3h as illustrated in Figure 5.4A. Following the removal of z-VAD-FMK the nuclei progressed to the full apoptotic morphology with characteristic condensation of chromatin. After 3hr the number of partially condensed nuclei in the staurosporine-treated cells had decreased from ~80% to ~10% and the number of apoptotic nuclei had increased from 5% to ~80% (Figure 5.4B). Cell viability also decreased over time as the number of apoptotic cells increased (results not shown). These results confirmed that the partially condensed nuclear morphology represented an early morphological change during staurosporine-induced apoptosis which preceded full apoptotic morphology.

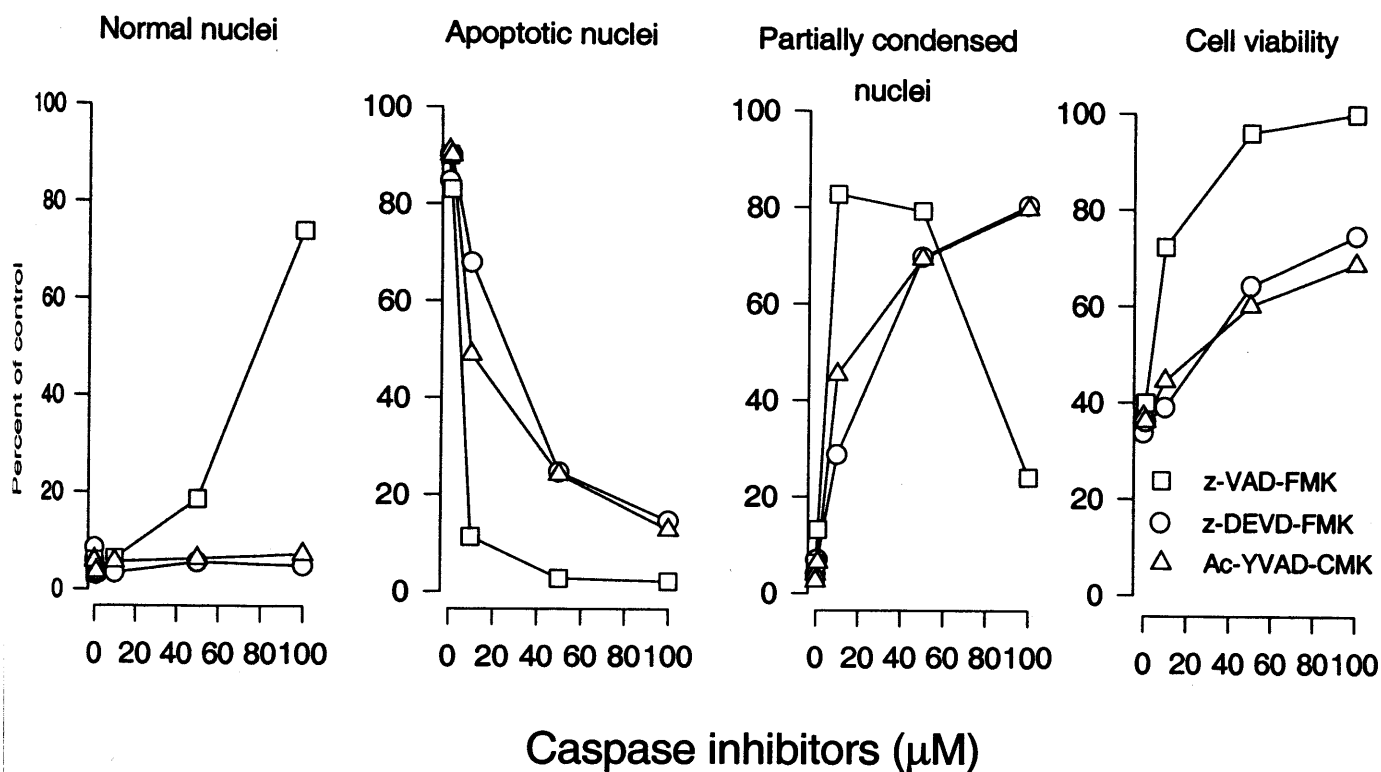


**Figure 5.2** Effect of various concentrations of caspase inhibitors on staurosporine-treated Jurkat cells. Jurkat cells were incubated with  $0.5\mu\text{M}$  staurosporine in the absence or presence of various concentrations of caspase inhibitors. Changes in nuclear morphology were determined using UV microscopy and cell viability was assessed using the MTS assay as described in materials and methods. The data represents the mean of 4-7 separate experiments with SEM values below 5%.

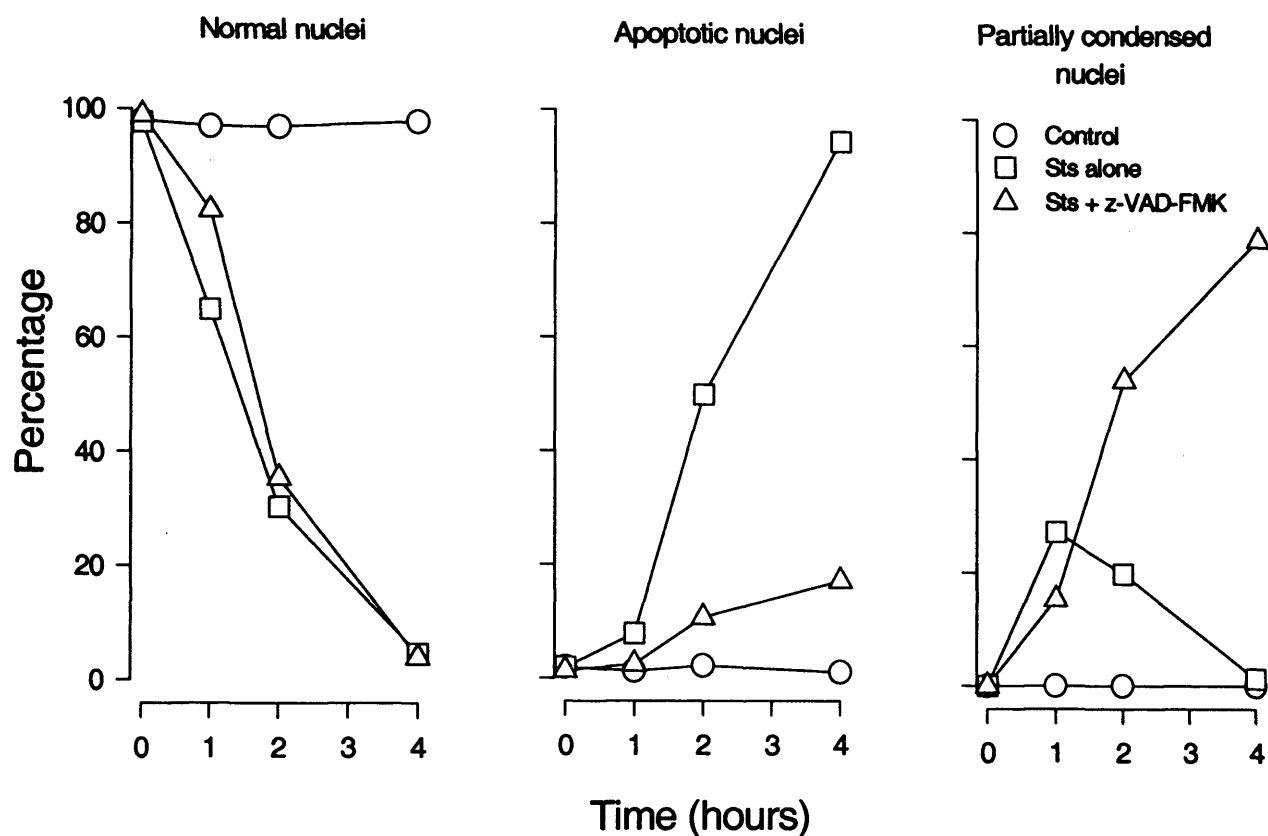


**Figure 5.3 Partially condensed nuclear morphology represents an early event during staurosporine induced apoptosis.** A time course showing the appearance of a partially condensed nuclear morphology in Jurkat cells over 4h. Cells were treated with staurosporine (Sts) in the presence or absence of 50 $\mu$ M z-VAD-FMK. At the times indicated cells were taken and processed for UV microscopy. The data represents the means from three separate experiments with SD less than 15%.

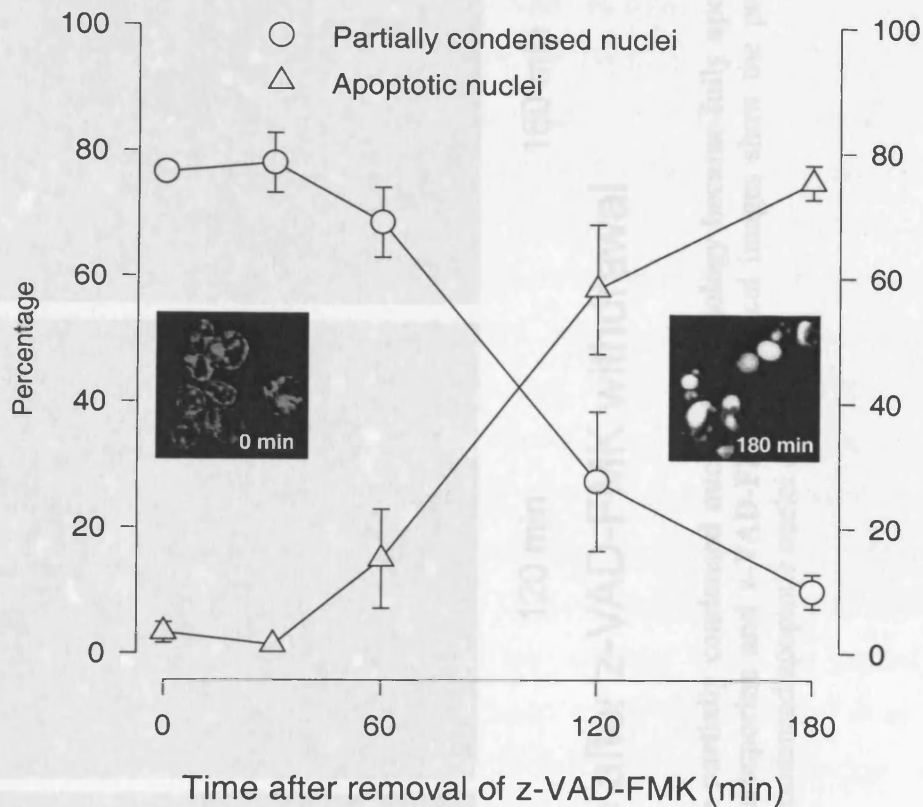
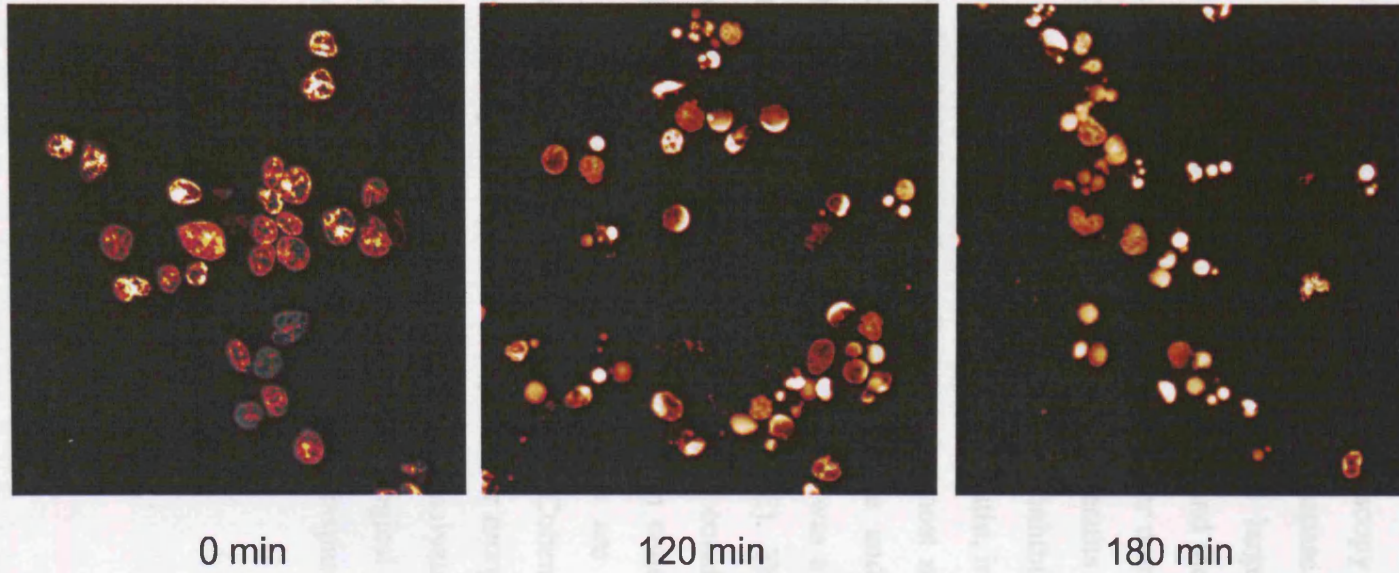


**Figure 5.4A** Jurkat T cells with a partially condensed nuclear morphology became fully apoptotic after removal of z-VAD-FMK. Cells were incubated with  $0.5\mu\text{M}$  staurosporine for 3h in the presence of  $50\mu\text{M}$  z-VAD-FMK. The cells were then washed twice with cold complete medium to remove excess staurosporine and z-VAD-FMK from the incubation medium before resuspending in complete medium at  $37^\circ\text{C}$ . Changes in nuclear morphology were followed over the next 3hr as described under materials and methods. Only the apoptotic and partially condensed nuclear morphology are shown. Control untreated cells and z-VAD-FMK control cells exhibited a normal uncondensed nuclear morphology and viability in these cells was maintained between 95-100%. Results are the mean  $\pm$  SEM from 4 independent experiments.



0 min

120 min

180 min

### Time after z-VAD-FMK withdrawal

**Figure 5.4B** Jurkat T cells with a partially condensed nuclear morphology became fully apoptotic after the removal of extracellular staurosporine and z-VAD-FMK. Confocal images show the progression of partially condensed nuclei to fully condensed apoptotic nuclei over time.

### 5.2.2 Ultrastructural characterization of partially condensed nuclear morphology.

In order to characterize the partially condensed nuclear morphology in more detail ultrastructural analysis using electron microscopy was carried out on cells treated with staurosporine in the presence or absence of caspase inhibitors. As illustrated in Figure 5.5, normal Jurkat cells are characterized by a large nucleolus and upon treatment with staurosporine the nuclear volume decreases and the chromatin becomes highly condensed and accumulates as crescents against the inner membrane of the nuclear envelope (Figure 5.5B) or fragments into many micronuclei (results not shown). In contrast, staurosporine treated cells in the presence of caspase inhibitors showed a different morphology characterized by a partially condensed chromatin, in agreement with the observations made with Hoechst 33358 staining. Perhaps the most striking difference was the dilatation of both the cisternae of the nuclear envelope and the endoplasmic reticulum and the convoluted appearance of the nucleus which was a feature observed in the presence of all three caspase inhibitors (Figure 5.5C, D and E). The latter could be due to contractions in the nuclear envelope as there appeared to be considerable clustering of nuclear pores, an event which has been previously reported in cells undergoing apoptosis (Reipert et al., 1998). The characteristics described here are different from the partial chromatin condensation described in previous reports (Cohen et al., 1992; Walker et al., 1994) and may therefore represent a novel early nuclear morphological change during staurosporine induced apoptosis. Thus, the ultrastructural analysis confirmed the observations made with the Hoechst 33358 staining that a morphological change had occurred in the nuclei of staurosporine-treated cells in the presence of caspase inhibitors.

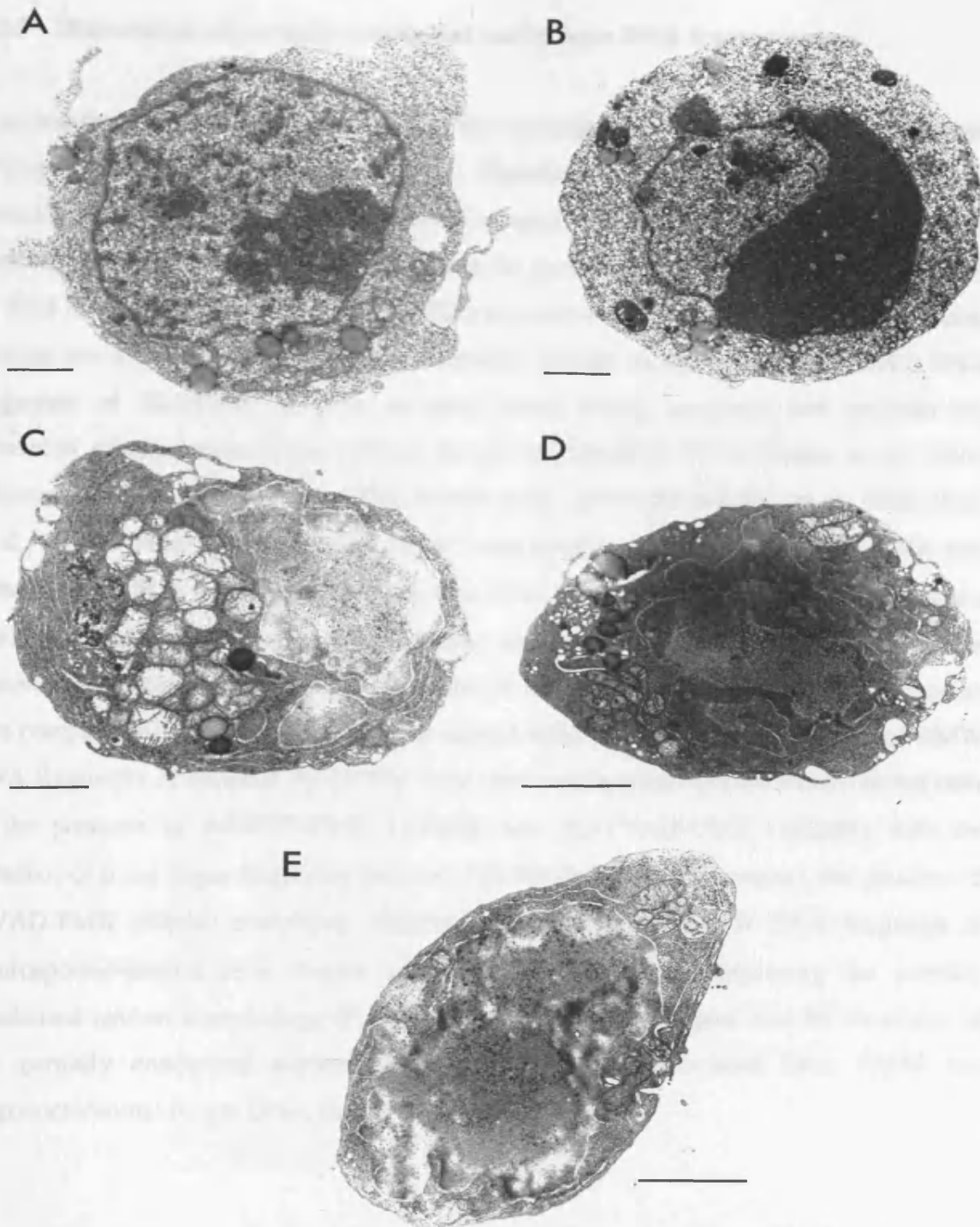


**Figure 5.5 Ultra-structural analysis of Jurkat cells with partially condensed nuclear morphology.** Jurkat cells were treated with staurosporine ( $0.5\mu\text{M}$ ) in the absence or presence of z-VAD-FMK ( $50\mu\text{M}$ ), z-DEVD-FMK ( $100\mu\text{M}$ ) and Ac-YVAD-CMK ( $100\mu\text{M}$ ) for 3h. The cells were processed for electron microscopy as outlined in materials and methods. The electron micrographs represent Jurkat cells without any treatment (A), treated with staurosporine alone (B) treated with staurosporine in the presence of z-VAD-FMK (C), z-DEVD-FMK (D) or Ac-YVAD-CMK (E). Scale bars represent  $5\mu\text{m}$ .

### 5.2.3 Dissociation of partially condensed nuclei from DNA fragmentation

It is clear from the UV and EM results that the chromatin structure had been altered in cells having this nuclear morphological change. Therefore, in order to further characterize the partially condensed nuclear morphological change, the integrity of the chromatin was assessed in cells treated with staurosporine in the presence or absence of caspase inhibitors by field inversion gel electrophoresis (FIGE) and conventional agarose gel electrophoresis. Besides the activation of caspases, the formation of high molecular weight (HMW) DNA fragments of 50-200kbp is quite an early event during apoptosis and precedes the formation of oligonucleosomal (200bp) length fragments of DNA (Cohen et al., 1992; Brown et al., 1993; Cohen et al., 1994; Walker et al., 1994; Oberhammer et al., 1994; Weis et al., 1995). After treatment with 0.5 $\mu$ M staurosporine Jurkat T-cell nuclear DNA was cleaved into HMW fragments <50kbp in size when analysed by FIGE (Figure 5.6A) and a typical laddering pattern was observed upon analysis by CAGE (Figure 5.6B). In the presence of caspase inhibitors, the formation of oligonucleosomal length DNA fragments was completely blocked in staurosporine-treated cells. However, the formation of HMW DNA fragments of between 50-250kbp were observed in staurosporine-treated Jurkat cells in the presence of z-DEVD-FMK (100 $\mu$ M) and Ac-YVAD-CMK (100 $\mu$ M), with the presence of some larger fragments between 250-700kbp in size. In contrast, the presence of z-VAD-FMK (50 $\mu$ M) completely inhibited the formation of HMW DNA fragments in staurosporine-treated cells despite over 70% of these cells displaying the partially condensed nuclear morphology (Figure 5.2). These results suggest that the formation of the partially condensed nuclear morphology can be dissociated from HMW and oligonucleosomal length DNA fragmentation.

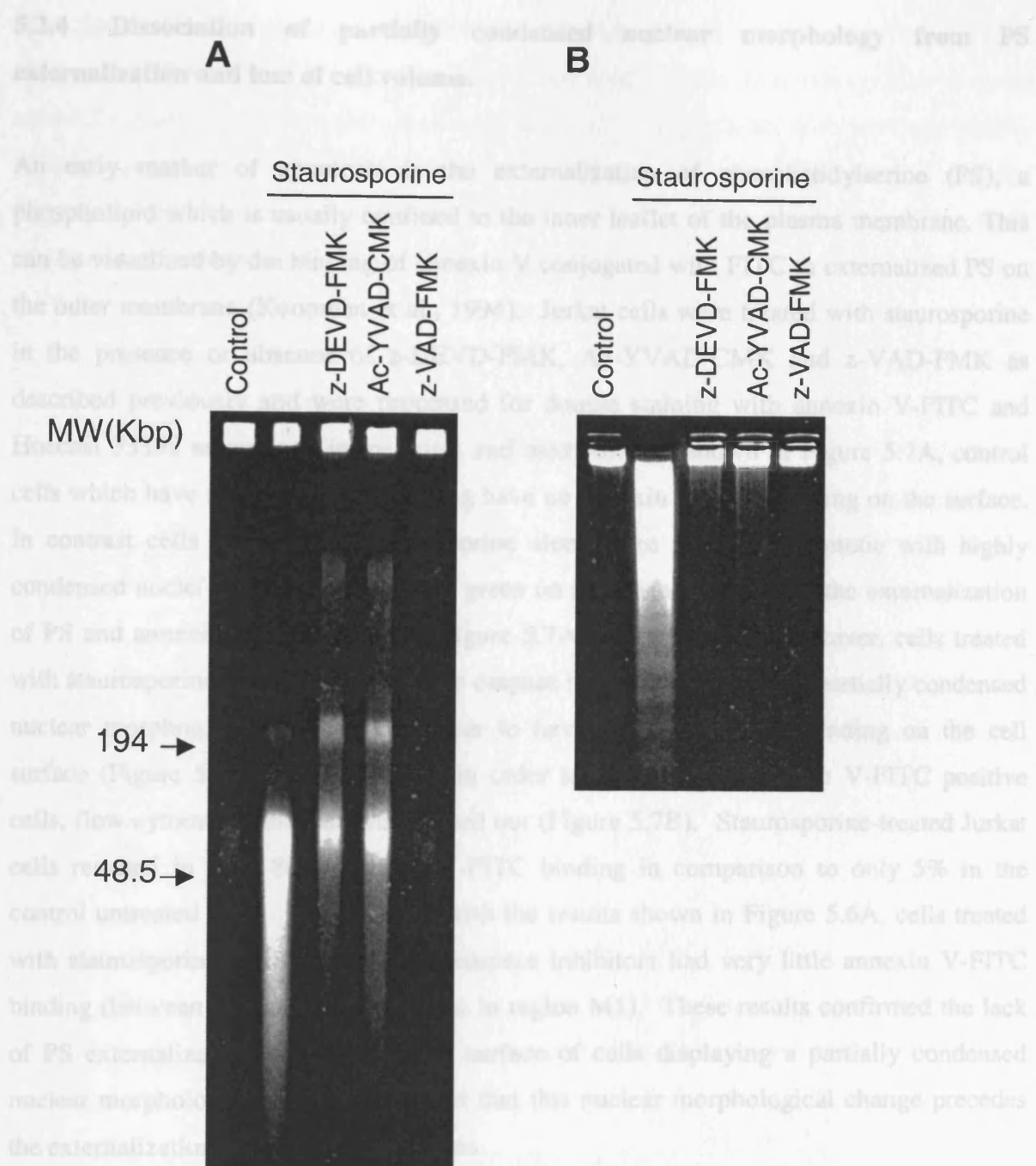


**Figure 5.6 Effect of caspase inhibitors on chromatin cleavage in staurosporine-treated Jurkat T cells.** Jurkat T cells were incubated with 0.5  $\mu$ M staurosporine in the absence or presence of z-VAD-FMK (50  $\mu$ M), z-DEVD-FMK (100  $\mu$ M) or Ac-YVAD-CMK (100  $\mu$ M) for 3h. The cells were collected and assessed for A) High Molecular Weight (HMW) and B) oligonucleosomal length DNA fragments by either FIGE or CAGE as described in materials and methods. The results are representative of at least two independent experiments.

affected the loss in cell volume caused by staurosporine although z-VAD-FMK did afford some protection. These results suggest that some, but not all, cells treated with

#### **5.2.4 Dissociation of partially condensed nuclear morphology from PS externalization and loss of cell volume.**

An early marker of apoptosis is the externalization of phosphatidylserine (PS), a phospholipid which is usually confined to the inner leaflet of the plasma membrane. This can be visualized by the binding of annexin V conjugated with FITC to externalized PS on the outer membrane (Koopman et al., 1994). Jurkat cells were treated with staurosporine in the presence or absence of z-DEVD-FMK, Ac-YVAD-CMK and z-VAD-FMK as described previously and were processed for double staining with annexin V-FITC and Hoechst 33358 as outlined in materials and methods. As shown in Figure 5.7A, control cells which have normal nuclear staining have no annexin V-FITC binding on the surface. In contrast cells treated with staurosporine alone were typically apoptotic with highly condensed nuclei and fluoresced bright green on the surface indicating the externalization of PS and annexin V-FITC binding (Figure 5.7A, upper panels). However, cells treated with staurosporine in the presence of the caspase inhibitors displayed a partially condensed nuclear morphology, but did not appear to have annexin V-FITC binding on the cell surface (Figure 5.7A, lower panels). In order to quantify the annexin V-FITC positive cells, flow cytometry analysis was carried out (Figure 5.7B). Staurosporine-treated Jurkat cells resulted in over 80% annexin V-FITC binding in comparison to only 5% in the control untreated cells. In agreement with the results shown in Figure 5.6A, cells treated with staurosporine in the presence of caspase inhibitors had very little annexin V-FITC binding (between 9.1 and 10.8%, shown in region M1). These results confirmed the lack of PS externalization observed on the surface of cells displaying a partially condensed nuclear morphology and further suggest that this nuclear morphological change precedes the externalization of PS during apoptosis.

The effect of caspase inhibitors on cell volume was also examined in relation to the appearance of the partially condensed nuclei, since cell shrinkage is a commonly observed early event during apoptosis (Arends and Wyllie, 1991). Upon treatment with staurosporine there was a marked decrease in cell volume in the treated cell as compared to control cells (Figure 5.8). The presence of z-DEVD-FMK and Ac-YVAD-CMK did not affect the loss in cell volume caused by staurosporine although z-VAD-FMK did afford some protection. These results suggest that some but not all cells treated with

staurosporine in the presence of z-VAD-FMK undergo cell shrinkage. These results suggest that the formation of the partially condensed nuclear morphology can to some extent be dissociated from cell shrinkage. This is in accordance with previous studies which, suggest that volume loss and cell shrinkage can be independent of cellular fragmentation (Benson et al., 1996) and largely independent of caspases depending upon the apoptotic stimulus (Bortner and Cidlowski, 1999).

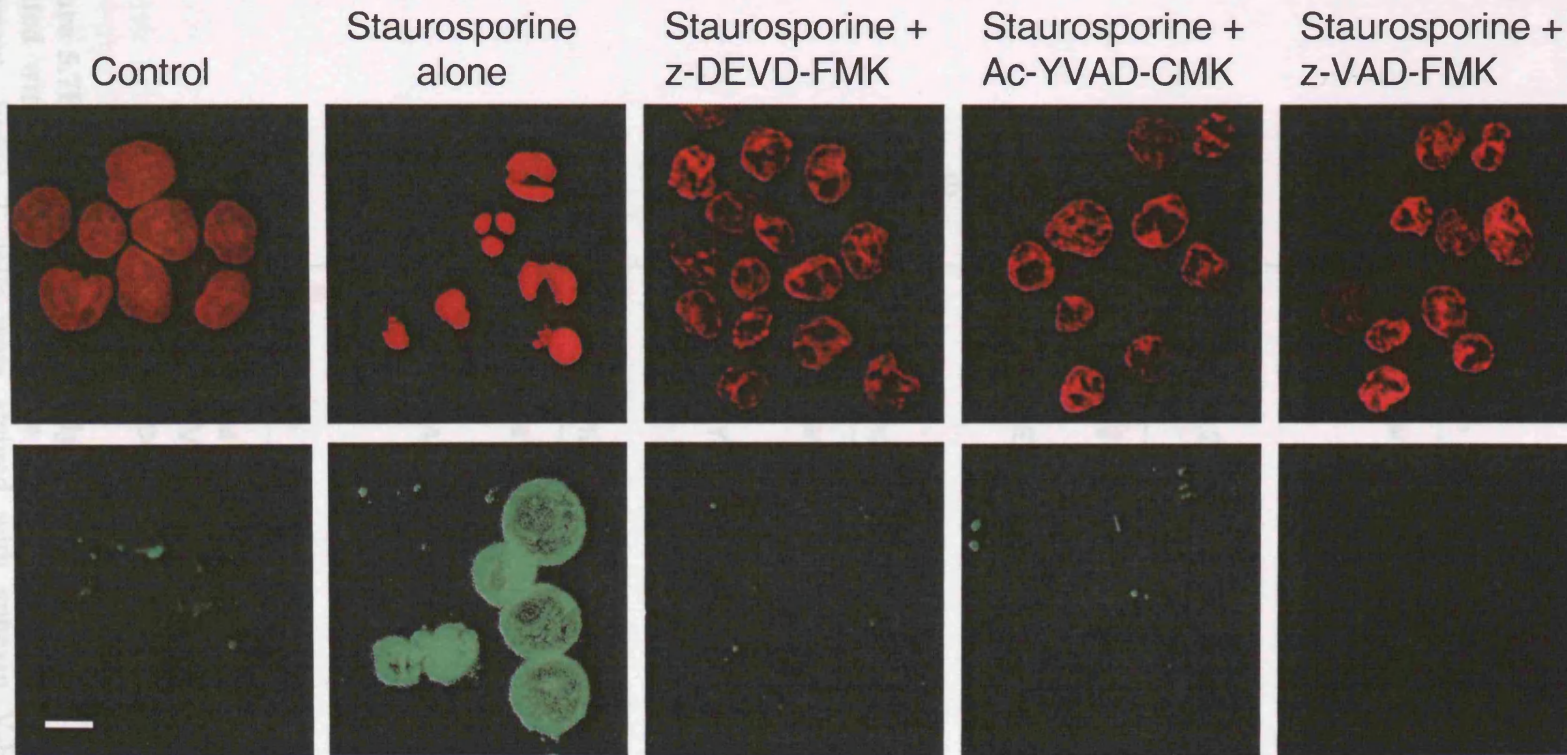


**Figure 5.7A Effect of caspase inhibitors on the binding of annexin V-FITC in Jurkat T cells treated with staurosporine.** After treatments, the cells were incubated with annexin V-FITC and then fixed, followed by DNA staining using Hoechst 33358 as described in materials and methods. Top panel (Hoechst 33358 staining) illustrates the nuclear morphology of Jurkat T cells treated with staurosporine for 3h in the presence or absence of caspase inhibitors using confocal microscopy. The same cells, as illustrated in the top panel, were also examined for annexin V-FITC binding (lower panel). The concentrations of caspase inhibitors were 50 $\mu$ M z-VAD-FMK and 100 $\mu$ M of z-DEVD-FMK and Ac-YVAD-CMK. The images are maximum projections of superimposed confocal laser scanned images for both Hoechst 33358 (in red) and FITC (in green). Scale bar represents 5 $\mu$ m.

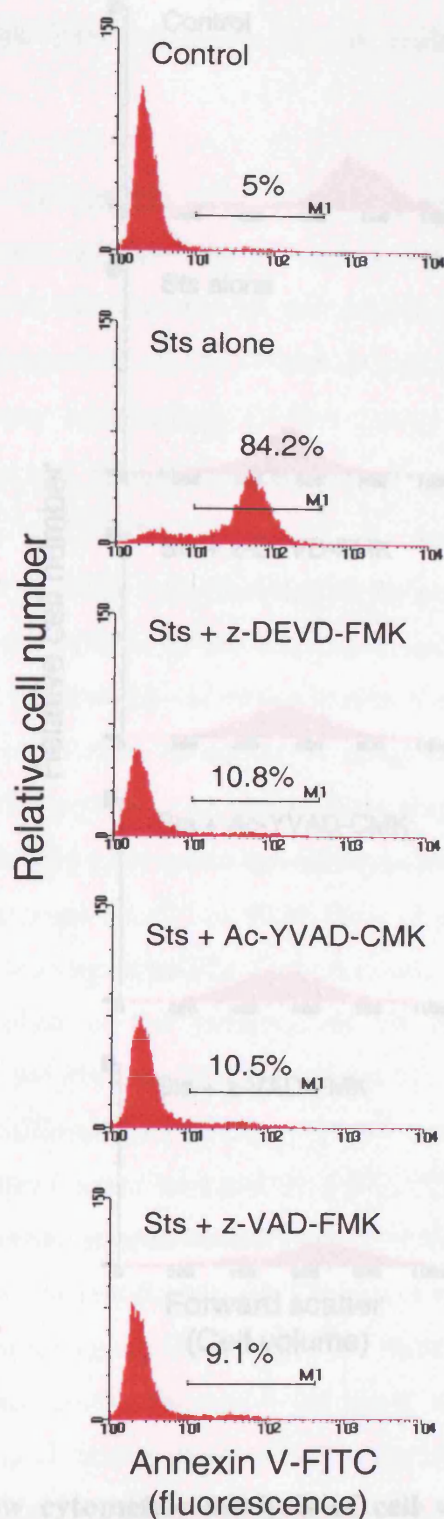


**Figure 5.7B** Flow cytometric analysis of annexin V-FITC binding in Jurkat T cells treated with staurosporine in the absence or presence of caspase inhibitors. After treatment, Jurkat T cells were stained with annexin V-FITC and analysed by flow cytometry as described in materials and methods. The percentage of annexin V-FITC positive cells are shown within region M1. Concentrations of caspase inhibitors used were 50 $\mu$ M z-VAD-FMK, and 100 $\mu$ M of z-DEVD-FMK and Ac-YVAD-CMK.

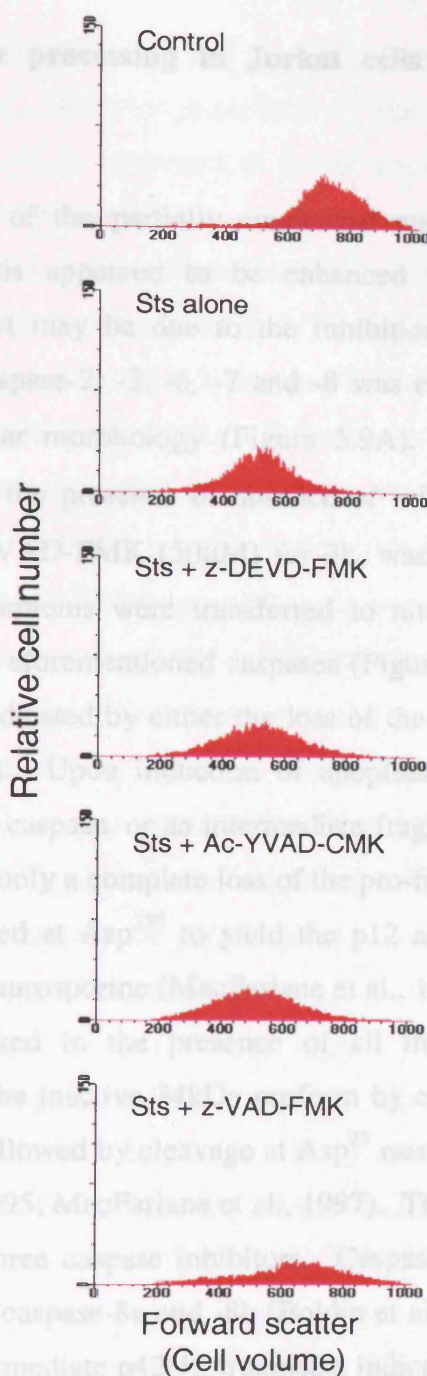


**Figure 5.8** Flow cytometric analysis of cell volume in Jurkat T cells treated with staurosporine in the absence or presence of caspase inhibitors. Concentrations of caspase inhibitors used were 50 $\mu$ M z-VAD-FMK, and 100 $\mu$ M of z-DEVD-FMK and Ac-YVAD-CMK. Forward scatter parameter (cell volume) was plotted as histograms using the FACSCAN software.

### 5.2.5 Caspase processing in Jurkat cells with a partially condensed nuclear morphology.

The appearance of the partially condensed nuclear morphology during staurosporine-induced apoptosis appeared to be enhanced in the presence of caspase inhibitors, suggesting that it may be due to the inhibition of caspase processing. Therefore, the processing of caspase-2, -3, -6, -7 and -8 was examined in cells displaying the partially condensed nuclear morphology (Figure 5.9A). Jurkat cells were treated with 0.5 $\mu$ M staurosporine in the presence or absence of z-DEVD-FMK (100 $\mu$ M), Ac-YVAD-FMK (100 $\mu$ M) and z-VAD-FMK (50 $\mu$ M) for 3h, washed and then lysed prior to SDS PAGE analysis. The proteins were transferred to nitrocellulose membrane and probed with antibodies to the aforementioned caspases (Figure 5.9A). The activation of the caspases examined was indicated by either the loss of the pro-form or the appearance of an active subunit fragment. Upon induction of apoptosis the appearance of the active subunit fragment of each caspase, or an intermediate fragment, was observed except in the case of caspase-6 where only a complete loss of the pro-form was observed. The 48kDa caspase-2 proform is cleaved at Asp<sup>330</sup> to yield the p12 active subunit which was observed upon treatment with staurosporine (MacFarlane et al., 1997; Cohen, 1997). This processing was completely blocked in the presence of all three caspase inhibitors. Caspase-7 was processed from the inactive 34kDa proform by cleavage at Asp<sup>198</sup> between the large and small subunits followed by cleavage at Asp<sup>23</sup> resulting in the 19kDa fragment (Fernandes-Alnemri et al., 1995; MacFarlane et al., 1997). This processing was again prevented in the presence of all three caspase inhibitors. Caspase-8 was observed as a 55.3kDa doublet corresponding to caspase-8a and -8b (Boldin et al., 1996; Scaffidi et al., 1997) which was processed to intermediate p42/43 fragments indicative of activation of both isoforms. Due to the limitations of the caspase-8 antibody, the expected p18 fragment produced by proteolytic removal of the death effector domains of p42/43 (Srinivasula et al., 1996; Scaffidi et al., 1997), was not detected. Similar to caspase-2 and -7, the processing of caspase-8 was blocked by the caspase inhibitors. Because the caspase-6 antibody used detects only the pro-form of the enzyme, caspase-6 activity was denoted by the loss of the 34kDa fragment. To further confirm that caspase-6 was activated the enzyme activity was examined directly by using the caspase-6 substrate, Ac-VEID-AMC. When Ac-VEID-AMC is cleaved by caspase-6 the AMC moiety is released and fluorescence can be

measured using a fluorimeter and directly related to enzyme activity (Thornberry et al., 1997; Gurtu et al., 1997) (Figure 5.9B). In the presence of staurosporine, the caspase-6 activity in Jurkat cells increased to 6-fold above that observed in untreated cells. The presence of the caspase inhibitors completely abrogated this activity. This data confirms that caspase-6 was indeed activated in staurosporine-treated Jurkat cells and that caspase-6 processing was not observed in cells displaying a partially condensed nuclear morphology. Like all the caspases examined, caspase-3 was processed to the active p17 subunit in staurosporine-treated Jurkat cells. However, in the presence of the caspase inhibitors, caspase-3 processing was partially blocked. The presence of z-DEVD-FMK (100 $\mu$ M) and Ac-YVAD-CMK (100 $\mu$ M) in staurosporine-treated cells resulted in the appearance of a small amount of the p17 fragment but there was also an accumulation of the p20 subunit. In cells treated with staurosporine in the presence of z-VAD-FMK (50 $\mu$ M), caspase-3 was only processed to the p20 subunit and there was no evidence of any p17 fragment. Caspase-3 activation is dependent on cleavage at two sites. The first cleavage occurs at an IETD↓S sequence (amino acids 172-176) producing a p12 subunit, and a p20 subunit which consists of the p17 subunit and the prodomain. The second cleavage event involves autocatalytic cleavage of the p20 fragment at an ESMD↓S site (amino acids 25-29) to release the prodomain and the mature p17 subunit (Nicholson et al., 1995; Han et al., 1997). The results presented here suggest that z-VAD-FMK may be blocking the autocatalytic cleavage of the p20 subunit of caspase-3. Both the p17 and the p20 subunit of caspase-3 have similar enzymatic activity *in vitro* (Stennicke et al., 1998a), suggesting that caspase-3 may be responsible for the nuclear morphological change. To determine this, cleavage of the caspase-3 substrate, PARP was used as an intracellular marker for caspase-3 activity. During apoptosis PARP is specifically cleaved from a 116kDa protein to an 85kDa fragment at a DEVD motif (Lazebnik et al., 1994; Tewari et al., 1995; Nicholson et al., 1995). As illustrated in Figure 5.9C, Jurkat cells treated with staurosporine resulted in complete cleavage of PARP. Both z-DEVD-FMK and Ac-YVAD-CMK dramatically reduced this cleavage and z-VAD-FMK completely inhibited PARP cleavage. These findings were further confirmed when the enzymatic activity of caspase-3 was determined using the substrate z-DEVD-AFC. As shown in Figure 5.10, z-VAD-FMK effectively blocked the cleavage of z-DEVD-AFC even though caspase-3 was processed to the p20. The present findings suggest that either the p20 fragment is more sensitive to z-VAD-FMK or may have a different substrate preference *in vivo*. Because

PARP is not cleaved in staurosporine-treated Jurkat cells in the presence of z-VAD-FMK, these results suggest that caspase-3 is not responsible for the early nuclear morphological change in these cells.

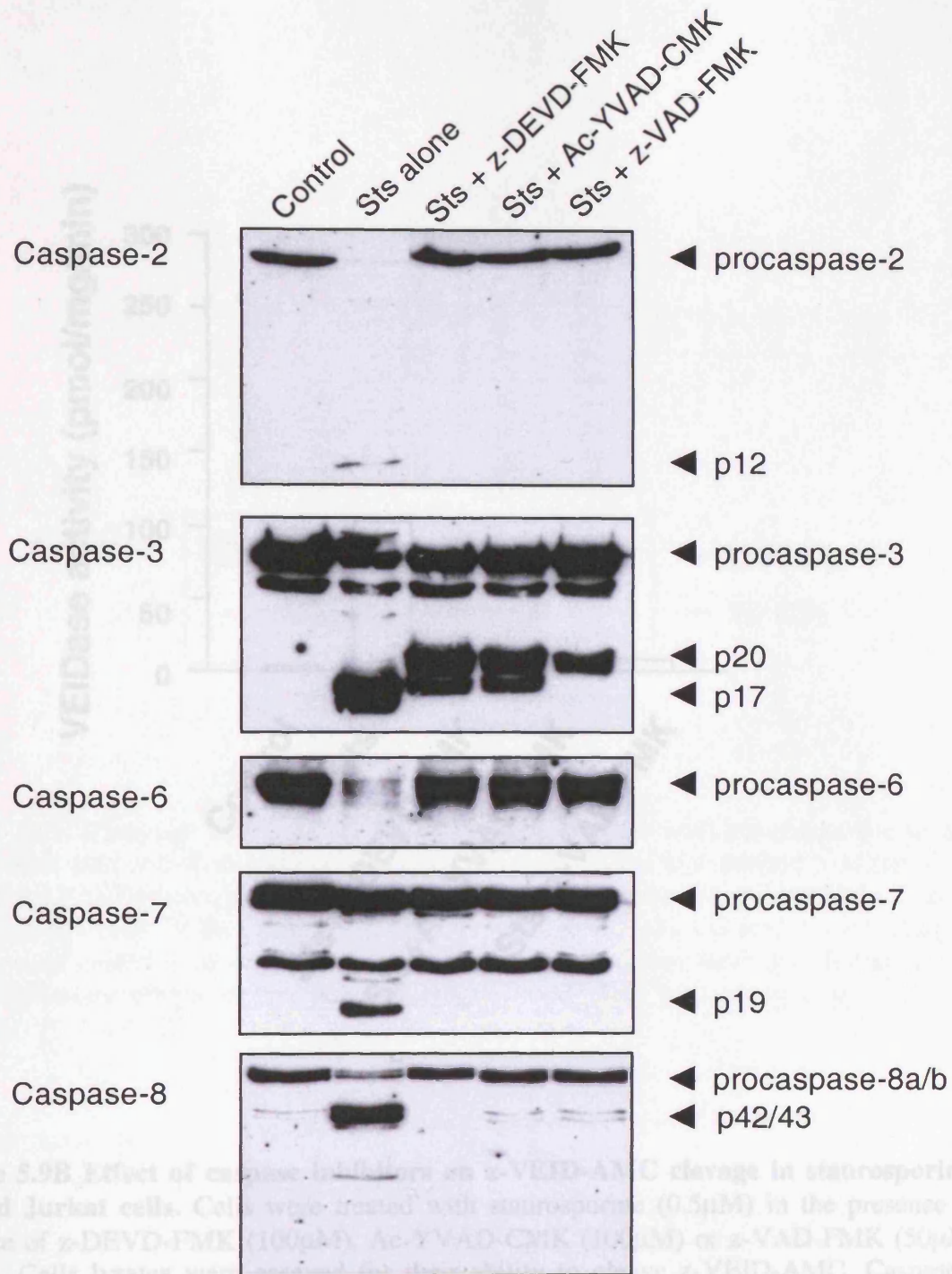
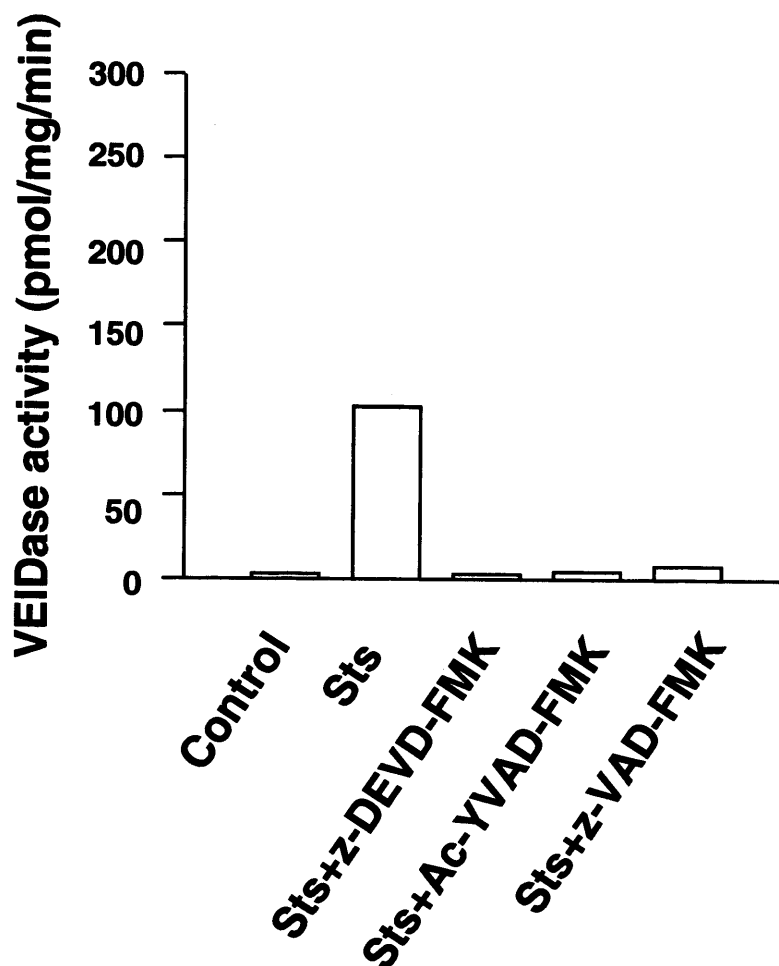
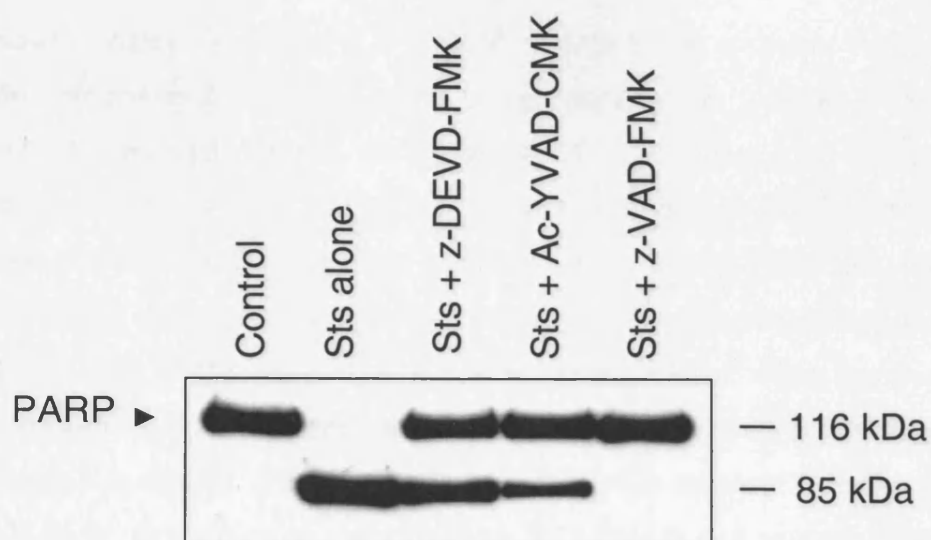


Figure 5.9B Effect of caspase inhibitors on z-VEID-AMC cleavage in staurosporine-treated Jurkat cells. Cells were treated with staurosporine (0.5 $\mu$ M) in the presence or absence of z-DEVD-FMK (100 $\mu$ M), Ac-YVAD-CMK (100 $\mu$ M) or z-VAD-FMK (50 $\mu$ M) for 3h. Cells lysates were assayed for z-VEID-AMC. Caspase-6 activity is represented by liberation of free AMC (pmol/mg/min). The data above

**Figure 5.9A Caspase processing in Jurkat T cells with a partially condensed nuclear morphology.** Jurkat T cells were treated with staurosporine (0.5 $\mu$ M) in the presence or absence of the caspase inhibitors z-DEVD-FMK (100 $\mu$ M), Ac-YVAD-CMK (100 $\mu$ M) and z-VAD-FMK (50 $\mu$ M). Following treatment the cells were centrifuged down, washed and lysed prior to SDS PAGE analysis. The proteins were transferred onto nitrocellulose membrane and then probed with antibodies to caspase-2, -3, -6, -7 and -8. Equivalent amounts of protein (30 $\mu$ g) were loaded into each well of all gels. The data is representative of at least two independent experiments.



**Figure 5.9B** Effect of caspase inhibitors on z-VEID-AMC cleavage in staurosporine-treated Jurkat cells. Cells were treated with staurosporine ( $0.5\mu\text{M}$ ) in the presence or absence of z-DEVD-FMK ( $100\mu\text{M}$ ), Ac-YVAD-CMK ( $100\mu\text{M}$ ) or z-VAD-FMK ( $50\mu\text{M}$ ) for 3h. Cells lysates were assayed for their ability to cleave z-VEID-AMC. Caspase-6 activity is represented by liberation of free AMC (pmol/mg/min). The data above represents the means of triplicate samples in one representative experiment out of three.



**Figure 5.9C Cleavage of PARP in Jurkat T cells treated with staurosporine in the presence or absence of caspase inhibitors.** Cells were treated as described in the previous legend and PARP cleavage was examined as described in materials and methods. Treated cells were sonicated in the presence of 4M urea prior to SDS PAGE analysis and 30 $\mu$ g of protein was loaded onto each well of a 7% gel. The proteins were transferred onto a nitrocellulose membrane and probed with a monoclonal PARP antibody (C2-10).

### 5.2.6 Processing of caspase-3 correlated with the formation of the partially condensed nuclear morphology.

As previously shown in Figure 5.2, 100 nM staurosporine (Sts) caused a dose-dependent increase in the number of nuclei which appeared normal or partially condensed. To examine the effect of higher concentrations of z-VAD-FMK on the formation of partially condensed nuclei and caspase 3 processing, Jurkat cells were treated with Sts (100 nM) in the presence of z-VAD-FMK (50-100 μM) for 24 hours. The cells were then harvested and analyzed by SDS-PAGE and western blotting (Figure 5.11B). In agreement with previous data (Figure 5.9A), 50 μM z-VAD-FMK resulted in the partial processing of caspase-3 to the p20 subunit. With increasing concentrations of z-VAD-FMK, there was a dose-dependent inhibition of the p20 subunit formation, which

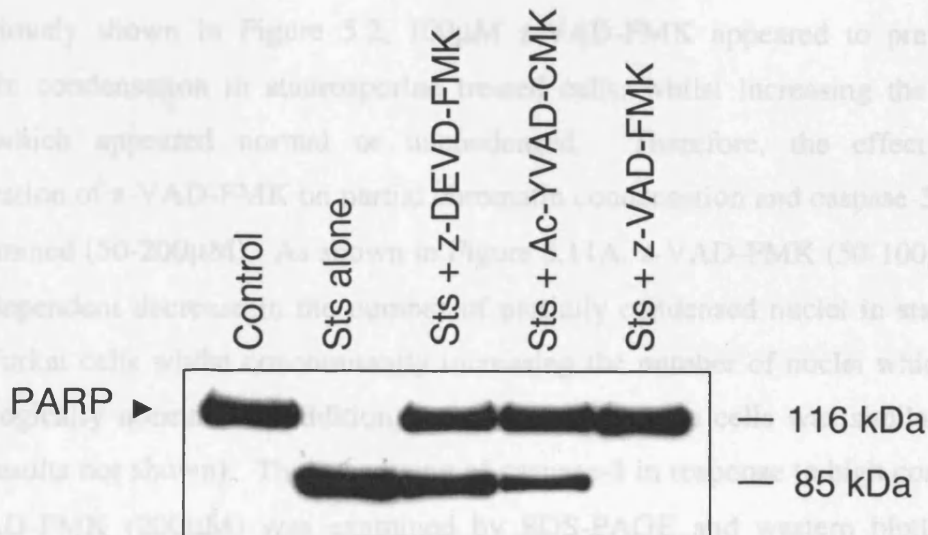


**Figure 5.9C Cleavage of PARP in Jurkat T cells treated with staurosporine in the presence or absence of caspase inhibitors.** Cells were treated as described in the previous legend and PARP cleavage was examined as described in materials and methods. Treated cells were sonicated in the presence of 4M urea prior to SDS PAGE analysis and 30 μg of protein was loaded onto each well of a 7% gel. The proteins were transferred onto a nitrocellulose membrane and probed with a monoclonal PARP antibody (C2-10).

The p20 fragment and decrease in pre-apoptotic nuclear morphology, strongly suggests that an upstream caspase that cleaves caspase-3 may be involved in this novel nuclear morphological change.

### **5.2.6 Processing of caspase-3 correlates with the formation of the partially condensed nuclear morphology.**

As previously shown in Figure 5.2, 100 $\mu$ M z-VAD-FMK appeared to prevent partial chromatin condensation in staurosporine treated cells, whilst increasing the number of nuclei which appeared normal or uncondensed. Therefore, the effect of higher concentration of z-VAD-FMK on partial chromatin condensation and caspase-3 processing was examined (50-200 $\mu$ M). As shown in Figure 5.11A, z-VAD-FMK (50-100 $\mu$ M) caused a dose-dependent decrease in the number of partially condensed nuclei in staurosporine-treated Jurkat cells whilst concomitantly increasing the number of nuclei which appeared morphologically normal. In addition, cell viability in these cells was similar to control levels (results not shown). The processing of caspase-3 in response to high concentrations of z-VAD-FMK (200 $\mu$ M) was examined by SDS-PAGE and western blotting (Figure 5.11B). In agreement with previous data (Figure 5.9A), 50 $\mu$ M z-VAD-FMK resulted in the partial processing of caspase-3 to the p20 subunit. With increasing concentrations of z-VAD-FMK, there was a dose-dependent inhibition of the p20 subunit formation, which correlated to the inhibition of the partially condensed nuclear morphology. Although the appearance of the p20 fragment correlates with the formation of the partially condensed nuclear morphology, it is unable to cleave PARP and lacks caspase-3-like activity (Figure 5.10A and B). The close correlation between the inhibition of caspase-3 processing to the p20 fragment and decrease in pre-apoptotic nuclear morphology, strongly suggests that an upstream caspase that cleaves caspase-3 may be involved in this novel nuclear morphological change.

A

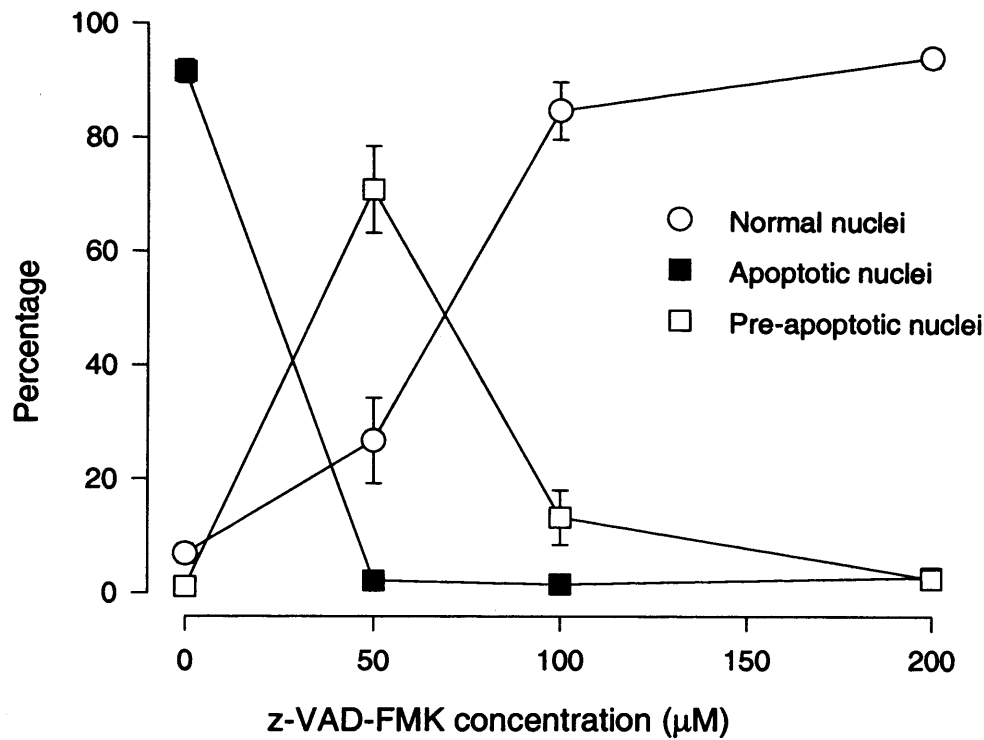
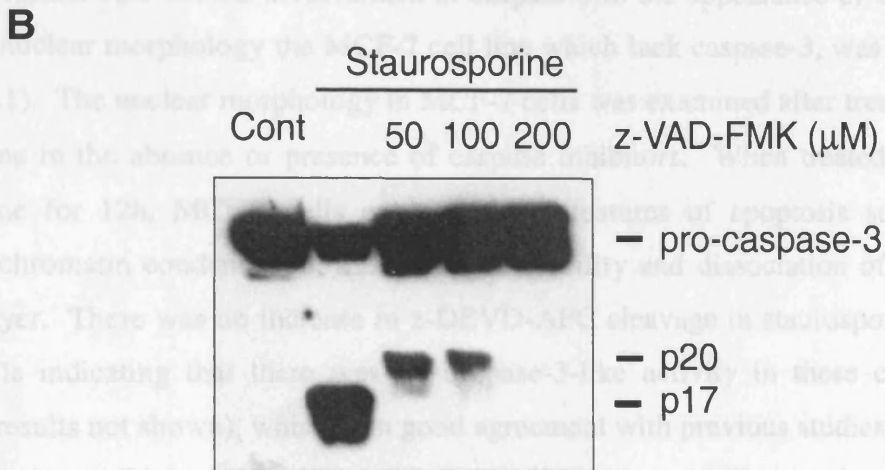


**Figure 5.11A Effect of high concentrations of z-VAD-FMK on staurosporine-treated Jurkat cells.** Jurkat cells were treated with 0.5 μM staurosporine in the presence or absence of various concentrations of z-VAD-FMK (50-200 μM) for 3h. The cells were then fixed and analysed under UV microscopy. Control (untreated) cells have 98% normal nuclei and ~2% apoptotic nuclei. Results represent the mean  $\pm$  SEM from 3-4 separate experiments.

### 5.2.7 Caspase-3 is dispensable for the formation of the partially condensed nuclear morphology.

In order to further evaluate the involvement of caspase-3 in the appearance of the partially condensed nuclear morphology the Jurkat T cells which lack caspase-3, was used (refer to Figure 6.1). The nuclear morphology was examined after treatment with staurosporine in the absence or presence of z-VAD-FMK. Jurkat T cells were treated with 2 $\mu$ M staurosporine for 12h. Morphological changes such as cell shrinkage, chromatin condensation and nuclear fragmentation were observed in staurosporine-treated Jurkat T cells. There was no increase in z-DEVD-AFK cleavage in staurosporine-treated Jurkat T cells indicating that the increase in caspase-3 activity during apoptosis (results not shown) was in good agreement with previous studies (Janicke et al., 1996a). In addition, partially condensed nuclear morphology were observed when treated with staurosporine alone. However, in the presence of z-VAD-FMK (5 $\mu$ M) or Ac-YVAD-CMK (5 $\mu$ M), over 80% of the cells displayed the partially condensed nuclear morphology which was similar to that observed

**Figure 5.11B Effect of high concentrations of z-VAD-FMK on caspase-3 processing in staurosporine-treated Jurkat T cells.** Jurkat T cells treated with 0.5 $\mu$ M staurosporine were incubated in the presence or absence of various concentrations of z-VAD-FMK (50-200 $\mu$ M) for 3h. The cells were collected and processed for SDS PAGE, followed by western blot analysis for caspase-3. The western blot data is representative of at least 4 independent experiments showing similar results.



### **5.2.7 Caspase-3 is dispensable for the formation of the partially condensed nuclear morphology.**

In order to further rule out the involvement of caspase-3 in the appearance of the partially condensed nuclear morphology the MCF-7 cell line which lack caspase-3, was used (refer to Figure 6.1). The nuclear morphology in MCF-7 cells was examined after treatment with staurosporine in the absence or presence of caspase inhibitors. When treated with 2 $\mu$ M staurosporine for 12h, MCF-7 cells exhibit typical features of apoptosis such as cell shrinkage, chromatin condensation, a decrease in viability and dissociation of cells from the monolayer. There was no increase in z-DEVD-AFC cleavage in staurosporine-treated MCF-7 cells indicating that there was no caspase-3-like activity in these cells during apoptosis (results not shown), which is in good agreement with previous studies (Janicke et al., 1998a). In addition, a small number of cells with partially condensed nuclear morphology were observed when treated with staurosporine alone. However, in the presence of z-VAD-FMK (5 $\mu$ M) or Ac-YVAD-CMK (5 $\mu$ M), over 80% of the cells displayed the partially condensed nuclear morphology which was similar to that observed in Jurkat cells (Figure 5.12). In agreement with the results observed in Jurkat cells, Ac-YVAD-CMK was less effective in preventing MCF-7 cell death as determined by the MTS viability assay. These results further confirmed that caspase-3 is not involved in the formation of the pre-apoptotic morphology in cells undergoing chemical-induced apoptosis.

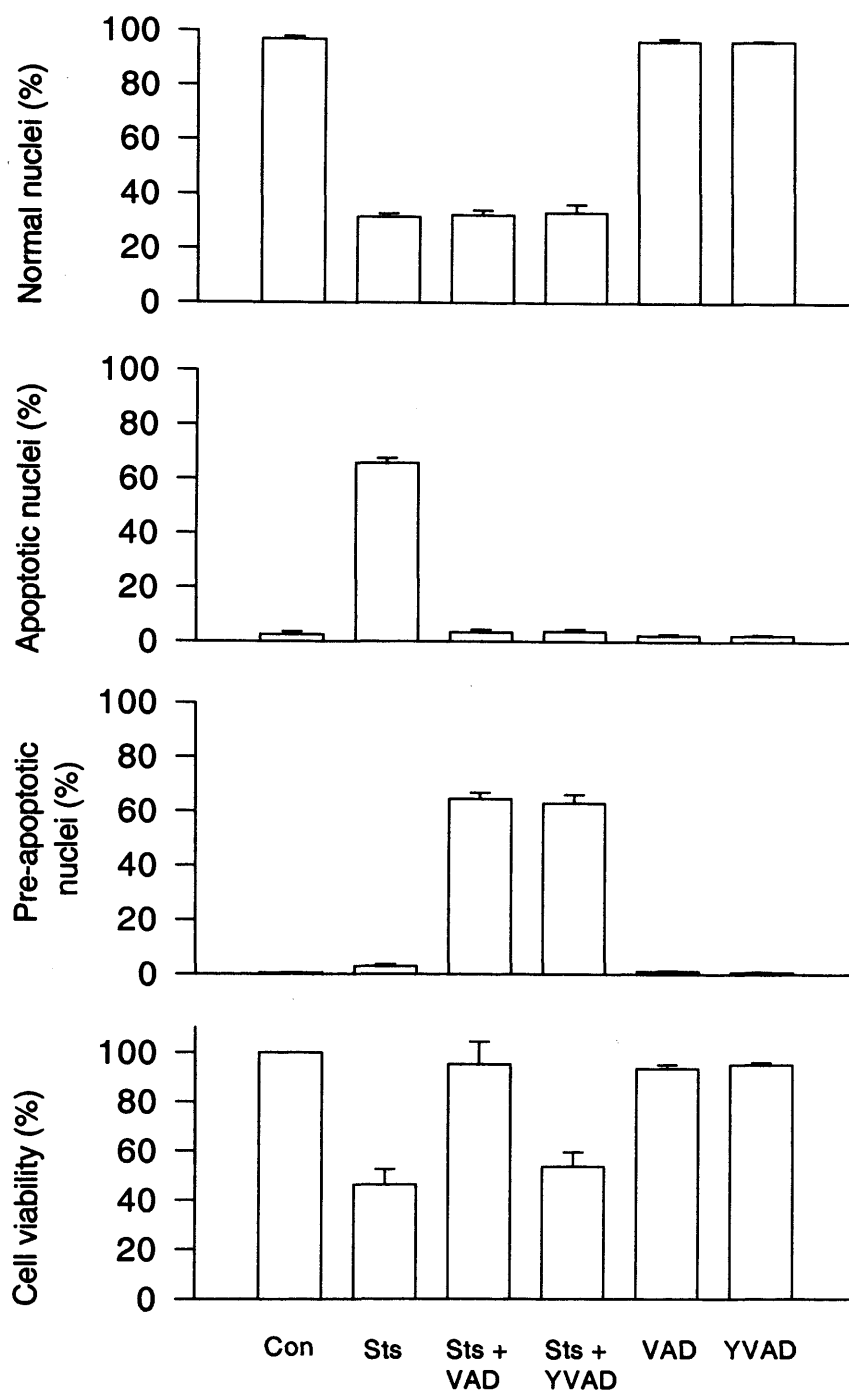


**Figure 5.12 Partially condensed nuclear morphology in MCF-7 cells treated with staurosporine.** MCF-7 cells were plated onto petri-dishes overnight prior to treatment with  $2\mu\text{M}$  staurosporine (Sts) for 12h in the presence of either  $5\mu\text{M}$  z-VAD-FMK (VAD) or  $5\mu\text{M}$  Ac-YVAD-CMK (YVAD). Control cells (Con) were left untreated. After treatment the cells were detached, fixed and stained with Hoechst 33358 before UV microscopy analysis. Cell viability was determined using the MTS assay as described in materials and methods. Results represent the mean  $\pm$  SEM from 3-4 independent experiments.

### **5.2.8 The partially condensed nuclear morphology occurs downstream of the mitochondrial release of cytochrome c.**

Induction of apoptosis by chemical stimuli often signals via the mitochondria resulting in the release of apoptogenic factors such as AIF (apoptosis inducing factor) and cytochrome c (Bossy-Wetzel et al., 1998; Susin et al., 1999; Slee et al., 1999; Sun et al., 1999). The release of cytochrome c plays an important role in the formation of the Apaf-1/caspase-9 functional apoptosome (Zou et al., 1997; Li et al., 1997) which results in the activation of caspase-9 and subsequent activation of downstream caspases (Zou et al., 1997). The finding that caspase-3 is processed in Jurkat cells having the pre-apoptotic nuclear morphology (Figure 5.9A) suggests that cytochrome c release may have occurred. Therefore the release of cytochrome c from the mitochondria of cells treated with staurosporine was examined. Initially, Jurkat cells were treated with 0.5 $\mu$ M staurosporine for 3hr and the cytosolic fractions were prepared as described in materials and methods. The concentration of cytosolic protein required to allow cytochrome c detection, was determined by using various concentrations of protein from the cytosolic fraction of staurosporine-treated Jurkat cells and analysing by immunodetection procedures. As illustrated in Figure 5.13A, 150 $\mu$ g of cytosolic protein was adequate for detection and this concentration of protein was used for subsequent experiments. A time course study was first carried out to examine the release of cytochrome c in staurosporine-treated Jurkat cells over the 3h. To ensure that the pellet contained the mitochondrial fraction equivalent amounts of the cell pellet were analysed alongside for cytochrome c levels (Figure 5.13B). Cytochrome c was detected in the cytosolic fraction after 1h and increased substantially by 3h. In parallel, the cytochrome c present in the cell pellet, which contained the mitochondrial fraction, decreased over time. The decrease in cytochrome c from the cell pellet correlates well with the increase in cytochrome c in the cytosolic fraction. Therefore the effect of caspase inhibitors on cytochrome c release in staurosporine-treated Jurkat cells was examined. The presence of the caspase inhibitors z-DEVD-FMK, Ac-YVAD-FMK and z-VAD-FMK did not prevent cytochrome c release from the mitochondria in staurosporine-treated Jurkat cells. However, the amount of cytochrome c release in the staurosporine treated cells was markedly reduced (Figure 5.14). These results suggest that the caspase inhibitors may not block the initial release of cytochrome c during chemical-induced apoptosis but may prevent the proposed downstream feedback loop involving

caspase-3 (Kuwana et al., 1998; Slee et al., 1999). Thus, the appearance of the partially condensed nuclear morphology occurs downstream of mitochondrial cytochrome c release during staurosporine-mediated apoptosis.

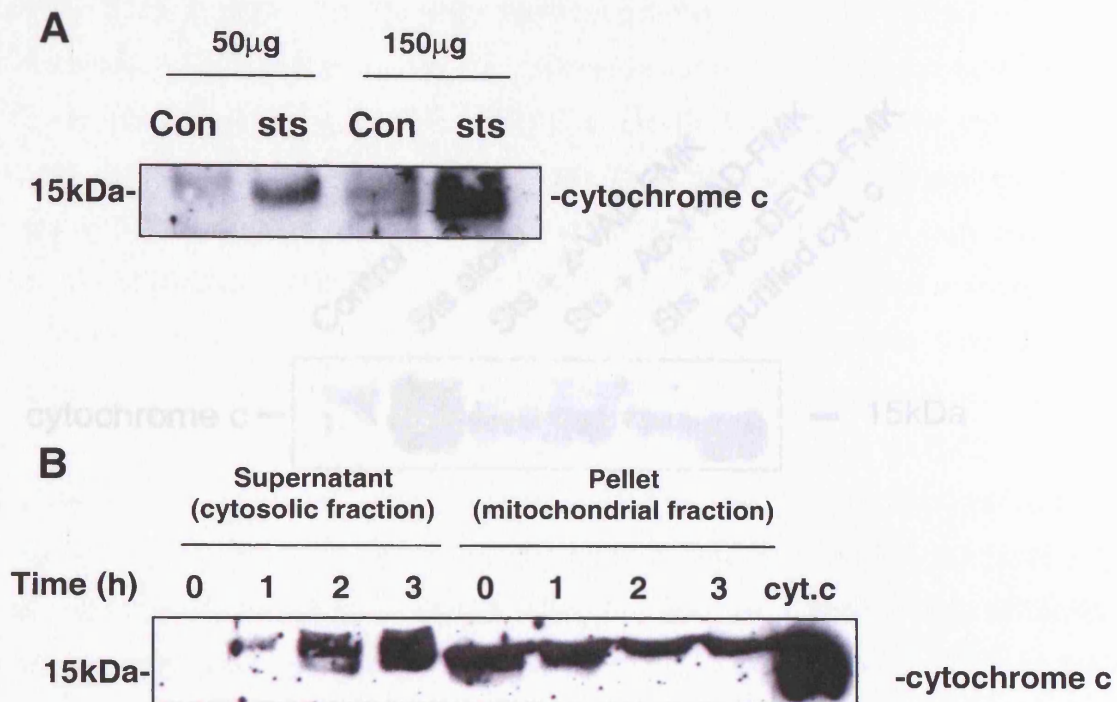


Figure 5.14 Effect of caspase inhibitors on staurosporine-induced cytochrome c release in cells with partially condensed nuclear morphology. Jurkat cells were treated with staurosporine (0.5µM) in the presence or absence of z-VAD-FMK (50µM), Ac-YVAD-FMK (100µM) and Ac-DEVD-FMK (100µM) and lysed with streptolysin O for analysis of cytochrome c release as described in materials and methods. Purified horse heart cytochrome c was used as a positive control.

**Figure 5.13 Cytochrome c release during staurosporine-induced apoptosis.** Jurkat T cells were treated with 0.5µM staurosporine for 3h and the cytosolic fraction was obtained as described in materials and methods. Briefly, treated cells were lysed with streptolysin O for 20min at 37°C and centrifuged at 15,000rpm for 30min at 4°C. The supernatant contained the cytosolic fraction and the pellet represented the mitochondrial fraction. A. Detection of cytochrome c in treated Jurkat cell lysates showing comparison between 50 and 150µg protein loading. B. Time course showing the release of cytochrome c into the cytosol during staurosporine induced apoptosis. Purified horse heart cytochrome c was used as a positive control.

### 5.2.9. The partially condensed nuclear morphology occurs downstream of mitochondrial membrane depolarization and is inhibited by Bcl-2.

Apoptosis 2004, 2(1): 1-10

The release of cytochrome c from staurosporine-treated Jurkat cells in the presence of caspase inhibitors suggests that the mitochondrial membrane potential ( $\Delta\Psi_m$ ) may have been disrupted. To investigate this, the membrane-permeable rhodamine-based probe TMRE was used (Lalini et al., 1999). TMRE is specific for mitochondria and is commonly used to monitor changes in the mitochondrial membrane potential. After treatment with staurosporine the cells were stained with TMRE and analyzed by flow cytometry analysis. As illustrated in Figure 5.13, the percentage of cells with a low mitochondrial potential after staurosporine treatment, the

percentage of cells having a low mitochondrial potential was increased to 48.9%. The presence of z-VAD-FMK (50  $\mu$ M), Ac-YVAD-FMK (100  $\mu$ M) and Ac-DEVD-FMK (100  $\mu$ M) inhibited the loss in mitochondrial membrane potential by between 70-85%. These results suggest that the appearance of the partially condensed nuclear morphology in staurosporine-treated Jurkat cells occurs after the loss in mitochondrial membrane potential. Since high concentrations of z-VAD-FMK blocked the formation of the partially

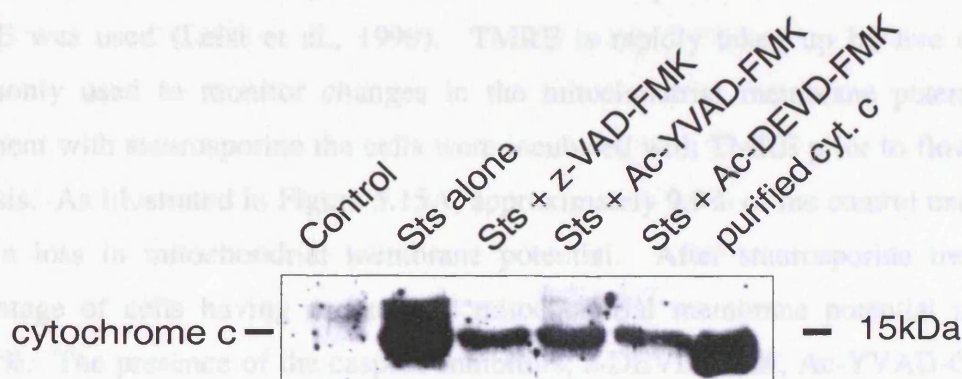


**Figure 5.14 Effect of caspase inhibitors on staurosporine-induced cytochrome c release in cells with partially condensed nuclear morphology.** Jurkat cells were treated with staurosporine (0.5  $\mu$ M) in the presence or absence of z-VAD-FMK (50  $\mu$ M), Ac-YVAD-FMK (100  $\mu$ M) and Ac-DEVD-FMK (100  $\mu$ M) and lysed with streptolysin O for analysis of cytochrome c release as described in materials and methods. Purified horse heart cytochrome c was used as a positive control.

together with those in Figures 5.11 and 5.14 suggest that the partially condensed nuclear morphology occurs downstream of mitochondrial membrane depolarization and cytochrome c release but upstream of caspase 3 processing. The results so far suggest that the partially condensed nuclear morphological change occurs at a point downstream of ( $\Delta\Psi_m$ ) during apoptosis.

Since Bcl-2 stabilizes mitochondrial membranes and blocks cytochrome c efflux (Yang et al., 1997; Kluck et al., 1997a), the effect of Bcl-2 overexpression on the formation of this early nuclear morphological change was investigated. To this end, two Bcl-2 overexpressing clones (J-Bcl-2/C4.1 and J-Bcl-2/C5.2, see chapter 3 and 4) were used. The cells were treated with staurosporine in the presence or absence of 10  $\mu$ M z-VAD-

### **5.2.9 The partially condensed nuclear morphology occurs downstream of mitochondrial membrane depolarisation and is inhibited by Bcl-2.**

The release of cytochrome c from staurosporine-treated Jurkat cells in the presence of caspase inhibitors suggests that the mitochondrial membrane potential ( $\Delta\Psi_m$ ) may have been disrupted. To investigate this, the membrane-permeable rhodamine-based probe TMRE was used (Leist et al., 1999). TMRE is rapidly taken up by live cells and is commonly used to monitor changes in the mitochondrial membrane potential. After treatment with staurosporine the cells were incubated with TMRE prior to flow cytometry analysis. As illustrated in Figure 5.15A, approximately 9.9% of the control untreated cells have a loss in mitochondrial membrane potential. After staurosporine treatment, the percentage of cells having a disrupted mitochondrial membrane potential increased to ~48.9%. The presence of the caspase inhibitors, z-DEVD-FMK, Ac-YVAD-CMK and z-VAD-FMK inhibited the loss in mitochondrial membrane potential by between 10-15%. These results suggest that the appearance of the partially condensed nuclear morphology in staurosporine-treated Jurkat cells occurs after the loss in mitochondrial membrane potential. Since high concentrations of z-VAD-FMK blocked the formation of the partially condensed nuclear morphology in staurosporine-treated Jurkat cells (Figure 5.2A), the loss of membrane potential in cells under similar conditions was also examined. As illustrated in Figure 5.15B, at high concentrations of z-VAD-FMK (200 $\mu$ M) where the nuclei appeared morphologically normal and caspase-3 processing was inhibited (Figure 5.11A and 5.11B), the mitochondrial membrane potential was still disrupted. These results taken together with those in Figures 5.11 and 5.14 suggest that the partially condensed nuclear morphology occurs downstream of mitochondrial membrane depolarisation and cytochrome c release but upstream of caspase-3 processing. The results so far suggest that the partially condensed nuclear morphological change occurs at a point downstream of ( $\Delta\Psi_m$ ) during apoptosis.

Since Bcl-2 stabilizes mitochondrial membranes and blocks cytochrome c efflux (Yang et al., 1997; Kluck et al., 1997a), the effect of Bcl-2 overexpression on the formation of this early nuclear morphological change was investigated. To this end, two Bcl-2 overexpressing clones (J-Bcl-2/C4.1 and J-Bcl-2/C5.2, see chapter 3 and 4) were used. The cells were treated with staurosporine in the presence or absence of 10 $\mu$ M z-VAD-

FMK, the minimum concentration of the inhibitor found to result in partially condensed nuclear morphology (Figure 5.2A). Treatment with staurosporine alone for 3h resulted in approximately 90% apoptosis in control cells (J-pEBS7) and 20-30% in the Bcl-2 overexpressing clones (Figure 5.16). In addition the cell viability was also maintained in the Bcl-2 overexpressing cells. However, after 6h treatments the percentage of apoptosis in the Bcl-2 clones increased to 50-60% and the cell viability decreased, suggesting a delay in the onset of apoptosis. Upon treatment with staurosporine in the presence of z-VAD-FMK, the appearance of the partially condensed nuclear morphology in the Bcl-2 clones reached levels of only ~20% in comparison to levels of 80-90% in J-pEBS7 and wild type Jurkat cells (E6.1), at the 3h timepoint. There was also an increase in the number of cells with a partially condensed nuclear morphology which reflected the levels of apoptosis observed in cells treated with staurosporine alone in both the control and Bcl-2 overexpressing clones. After 6h, the number of Bcl-2 overexpressing cells with partially condensed nuclear morphology increased markedly, suggesting that Bcl-2 is delaying the formation of the partially condensed nuclear morphological change. This is in agreement with the results obtained in Figures 5.14 and 5.15 suggesting that the nuclear morphological change occurs downstream of mitochondrial membrane depolarisation and cytochrome c release, both of which can be inhibited by Bcl-2 (Yang et al., 1997; Kluck et al., 1997a; Luo et al., 1998). The results suggest that overexpression of Bcl-2 in Jurkat cells delays rather than blocks apoptosis and in the presence of caspase inhibitors, is held back at the partially condensed stage at a point downstream of Bcl-2.

Cell number

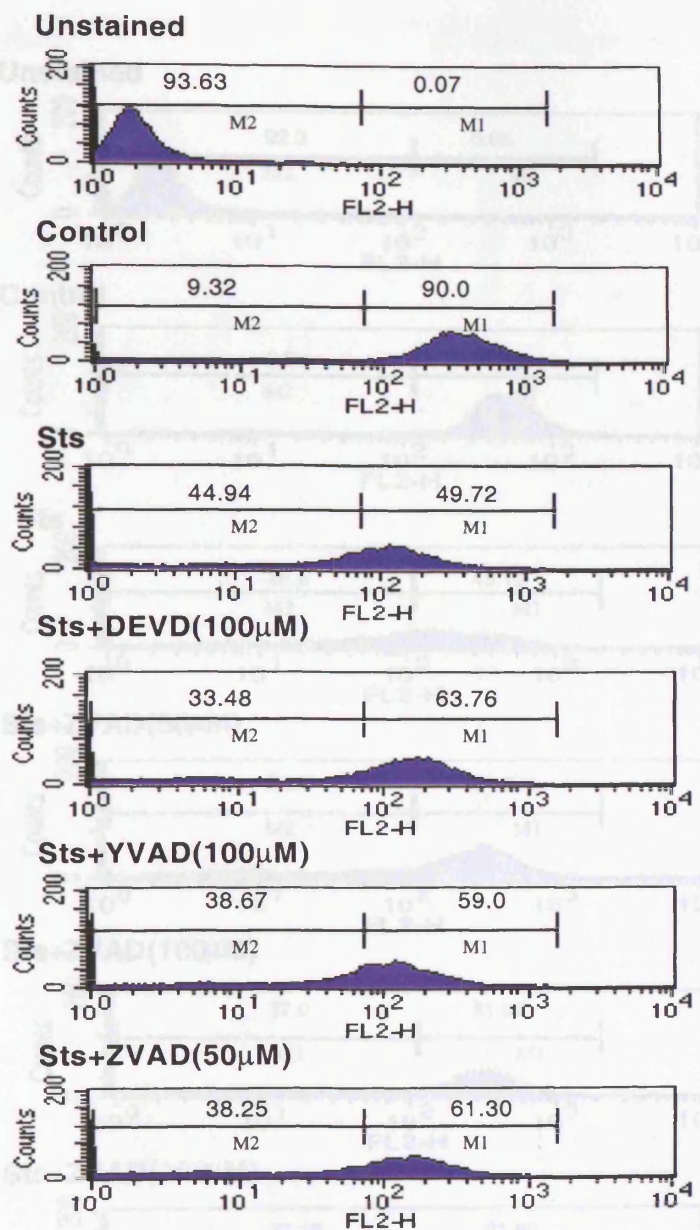


**Figure 5.15A Effect of caspase inhibitors on mitochondrial membrane potential in cells with partially condensed nuclear morphology.** Treated cells were incubated with TMRE as described in materials and methods and analysed by flow cytometry. Control cell mitochondrial membrane potential is represented in region M1. Region M2 represents cells with a reduced or disrupted mitochondrial membrane potential. The results are one representative of three independent experiments.

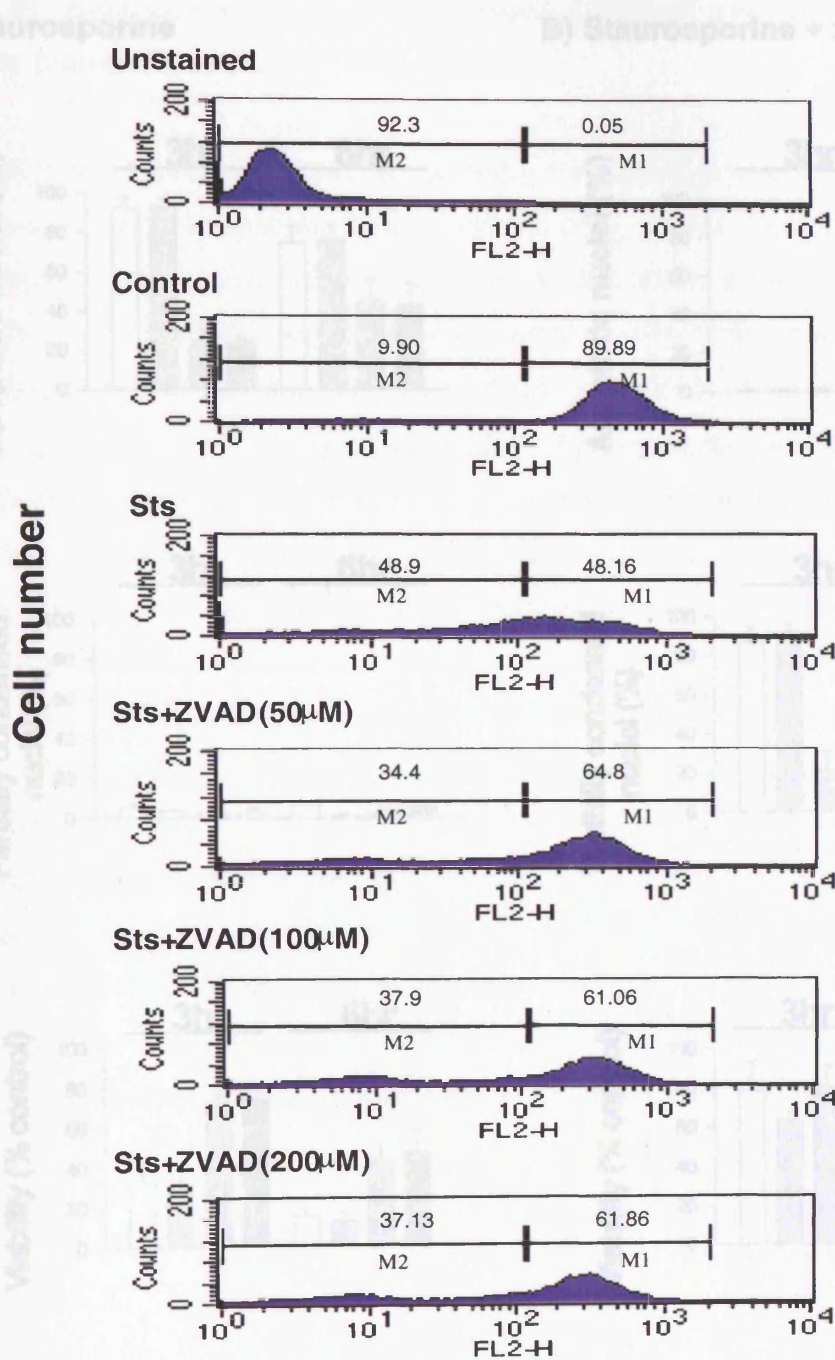


**Figure 5.15B Effect of high concentrations of z-VAD-FMK on mitochondrial membrane potential.** Treated cells were incubated with TMRE as described in materials and methods and analysed by flow cytometry. Mitochondrial membrane potential of control cells is represented in region M1. Region M2 represents cells with a reduced or disrupted mitochondrial membrane potential indicative of apoptosis. The results are one representative of three independent experiments.

## A) Staurosporine

## B) Staurosporine + z-VAD-FMK

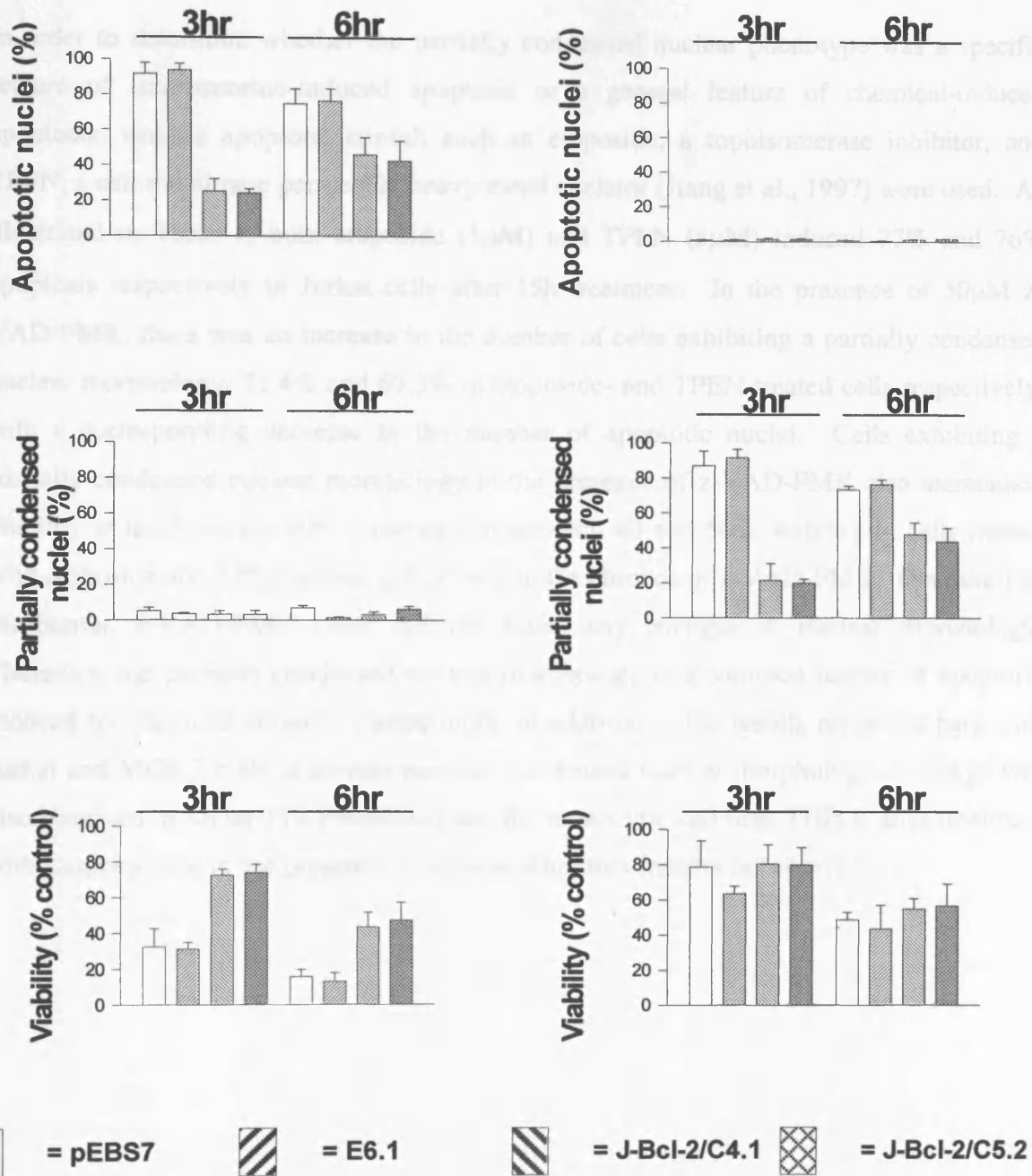


**Figure 5.16** Effect of Bcl-2 on the formation of a partially condensed nuclear morphology. Bcl-2 transfected Jurkat T cells (J-Bcl-2/C4.1 and J-Bcl-2/C5.2) were treated with staurosporine in the presence or absence of z-VAD-FMK (10 $\mu$ M) for 3 or 6h and processed for UV microscopy or the MTS viability assay. The experiments represent the mean of at least three independent experiments  $\pm$  SEM.

### **5.2.10 Induction of the partially condensed nuclear morphology in Jurkat cells by other chemical stimuli.**

In order to determine whether the partially condensed nuclear phenotype was a specific feature of staurosporine-induced apoptosis or a general feature of chemical-induced apoptosis, various apoptotic stimuli such as etoposide, a topoisomerase inhibitor, and TPEN, a cell membrane permeable heavy metal chelator (Jiang et al., 1997) were used. As illustrated in Table 1, both etoposide (5 $\mu$ M) and TPEN (5 $\mu$ M) induced 77% and 76% apoptosis respectively in Jurkat cells after 15h treatment. In the presence of 50 $\mu$ M z-VAD-FMK, there was an increase in the number of cells exhibiting a partially condensed nuclear morphology, 71.4% and 67.5% in etoposide- and TPEN-treated cells respectively, with a corresponding decrease in the number of apoptotic nuclei. Cells exhibiting a partially condensed nuclear morphology in the presence of z-VAD-FMK also maintained viability at levels above 80% compared to between 40 and 50% viability in cells treated with etoposide and TPEN alone respectively in the absence of z-VAD-FMK. Over the 15h incubation, z-VAD-FMK itself did not cause any changes in nuclear morphology. Therefore, the partially condensed nuclear morphology is a common feature of apoptosis induced by chemical stimuli. Furthermore, in addition to the results presented here with Jurkat and MCF-7 cells, a similar partially condensed nuclear morphological change was also observed in Swiss 3T3 Fibroblasts and the monocytic cell line, THP-1, after treatment with staurosporine in the presence of caspase inhibitors (results not shown).

**Table 5.1 Induction of pre-apoptotic nuclei in Jurkat cells treated with etoposide or TPEN in the presence of z-VAD-FMK.**

Treatments	Normal nuclei	Apoptotic nuclei	Pre-apoptotic nuclei	Cell viability
Control	97.8 + 0.77	2.2 + 0.77	ND	100
Etoposide alone	22.4 + 4.5	77.1 + 4.4	0.3 + 0.17	42.3 + 2.7
TPEN alone	22.9 + 6.7	76.0 + 6.2	1.0 + 0.77	49.0 + 1.95
Etoposide + z-VAD-FMK	30.7 + 3.7	1.0 + 0.5	71.4 + 2.2	89.0 + 8.07
TPEN + z-VAD-FMK	24.4 + 2.9	2.5 + 0.78	67.6 + 3.2	82.0 + 6.38
z-VAD-FMK alone	98.9 + 0.5	0.4 + 0.02	0.7 + 0.45	103 + 6.1

Jurkat cells ( $1 \times 10^6$  cells/ml) were incubated with either etoposide (5  $\mu$ M) or TPEN (5  $\mu$ M) in the presence or absence of z-VAD-FMK (50  $\mu$ M) for 15h. The cells were collected and processed for UV microscopy analysis and cell viability was determined using the MTS assay as described in Materials and Methods. Results are the means  $\pm$  SEM from three independent experiments. ND - not detected.

### 5.3 Discussion

The caspases are a family of cysteine proteases which represent the effector arm of the apoptotic pathway, orchestrating the structured and highly specific breakdown of the cell via cleavage and inactivation of intracellular substrates (Kaufmann et al., 1993; Lazebnik et al., 1994; Brancolini et al., 1995; Rao et al., 1996). Although effector caspases have been implicated as having a major role in the morphological changes during apoptosis there is evidence to suggest that not all of these processes are caspase-dependent (Kass et al., 1996; Samejima et al., 1998; Hughes et al., 1998a). To examine this possibility in greater detail, several peptide based caspase inhibitors were used to block the activation of caspases and their activity in cells undergoing apoptosis mediated by staurosporine. In this chapter, the effect of the caspase inhibitors z-VAD-FMK, z-DEVD-FMK and Ac-YVAD-FMK, on caspase activity and their activation was studied in relation to the morphological and biochemical features of apoptosis in staurosporine-treated Jurkat cells. As a result, a distinct early nuclear morphological change was identified during chemical-induced apoptosis in Jurkat T cells in the presence of caspase inhibitors. The nuclear morphological change, which preceded many of the hallmark biochemical features of apoptosis, was characterized by a partially condensed nuclear morphology with heavily convoluted nuclei and a dilated nuclear envelope and ER. This distinct nuclear morphology was also observed as a transient event in cells treated with staurosporine in the absence of caspase inhibitors. In addition, Jurkat cells exhibiting this partially condensed nuclear morphology went on to become fully apoptotic upon the removal of z-VAD-FMK further confirming that it represented an early apoptotic event. Although no oligonucleosomal length DNA fragmentation was observed in staurosporine-treated cells in the presence of caspase inhibitors, HMW DNA fragment formation was detected in the presence of Ac-YVAD-FMK and z-DEVD-FMK, whereas none was detected in the presence of Ac-Z-VAD-FMK. These observations suggest that the partially condensed nuclear morphological change was unlike previously described early morphological changes (Cohen et al., 1993; Walker et al., 1994) as it could be dissociated from the formation of HMW DNA fragments.

A further early event during apoptosis is the externalization of PS to the outer leaflet of the plasma membrane which acts as a marker for phagocytic clearance of apoptotic cells

(Fadok et al., 1992; Savill et al., 1993). PS exposure is proposed to be dependent on caspase activation (Verhoven et al., 1995; Martin et al., 1995; Martin et al., 1996). However, in the presence of caspase inhibitors, staurosporine-treated cells with the distinct nuclear morphology did not externalise PS to the outer leaflet of the plasma membrane, as indicated by the lack of annexin V-FITC binding. The results also suggest that PS exposure may occur independently of caspase-3 activation, as cells treated with staurosporine in the presence of z-DEVD-FMK and Ac-YVAD-FMK, show caspase-3 processing and PARP cleavage but lack annexin V-FITC binding. This suggests that PS exposure can be dissociated from other biochemical features of apoptosis, which is in agreement with previous studies proposing that events governing phagocytic recognition may occur independently of other biochemical features of apoptosis (Zhuang et al., 1998). Taken together, these results suggest that the partially condensed nuclear morphology may occur in parallel, or prior to HMW DNA fragmentation, cell shrinkage and externalization of PS.

The use of caspase inhibitors to block biochemical and morphological features of apoptosis is well documented (Slee et al., 1996; Talanian et al., 1997; Longthorne and Williams, 1997; Thornberry et al., 1997; MacFarlane et al., 1997; Garcia-Calvo et al., 1998). The caspase inhibitors used in this study consistently arrested staurosporine treated Jurkat T cells at the partially condensed nuclear morphological stage suggesting that the phenomenon was due to an inhibition of caspase activity. It is unlikely that the Group I subfamily of caspases (caspase-1, -4 and -5) are responsible for the observed phenotype since Jurkat and MCF-7 cells do not express caspase-1 (Janicke et al., 1998b; Chow et al., 1999). Furthermore, there is little evidence supporting a role for caspase-4 in apoptosis and caspase-5 has been shown to be important mainly during inflammation (Nicholson and Thornberry, 1997; Cryns and Yuan, 1998). Key morphological and biochemical changes during apoptosis have been shown to be mediated mainly by members of the group II subfamily of effector caspases (caspase-2, -3 and -7), particularly caspase-3, a prototypical effector caspase (Fernandez-Alnemri et al., 1994; Tewari et al., 1995; Nicholson et al., 1995; Casciola-Rosen et al., 1996). Caspase-3 has been shown to be involved in the formation of the typical apoptotic phenotype by virtue of its ability to cleave structural proteins of both the cytoskeleton and nucleus, including as actins, gelsolin and fodrin (Kothakota et al., 1997; Zheng et al., 1998; Janicke et al., 1998a; Janicke et al., 1998b). In

addition caspase-3 has also been shown to have a direct involvement in the regulation of DNA fragmentation by cleaving DNA fragmentation factor (DFF) (Liu et al., 1997; Janicke et al., 1998b; Wolf et al., 1999) and has been proposed to play an integral role in the mediation of nuclear apoptosis (Woo et al., 1998; Hirata et al., 1998). However, in staurosporine-treated cells in the presence of z-VAD-FMK, PARP was not cleaved and no DEVD-AFC cleavage was detected even though >70% of the cells displayed a partially condensed nuclear morphology indicating that caspase-3 is unlikely to be the caspase responsible for the partially condensed nuclear morphology. The role of caspase-3 in causing this partially condensed nuclear morphology was further ruled out by using MCF-7 cells which lack caspase-3 (Janicke et al., 1998a). These cells also exhibited a partially condensed nuclear morphological change upon treatment with staurosporine in the presence or absence of caspase inhibitors. Together with the lack of caspase-2 and -7 activation these results suggest that the group II family of effector caspases are not responsible for this pre-apoptotic nuclear morphological change.

The processing of caspase-3 in staurosporine-treated Jurkat cells parallels the appearance of the preapoptotic nuclear morphology, suggesting that an upstream caspase may be still active in the presence of caspase inhibitors. Using high concentrations of z-VAD-FMK, the appearance of this morphology was completely blocked in staurosporine-treated Jurkat cells and a concomitant inhibition of caspase-3 processing. These results suggest that the pre-apoptotic nuclear morphology is likely to be mediated by the group III caspases (caspase-6, -8, -9 and 10). However, both caspase-6 and -8 were not activated suggesting they were not involved. In addition caspase-10, is more likely to be involved in receptor-mediated cell death and therefore does not play a significant role in chemical-induced apoptosis.

During chemical-induced apoptosis, apoptogenic factors such as cytochrome c and AIF are released from the mitochondria (Liu et al., 1996; Kluck et al., 1997a; Kluck et al., 1997b; Bossy-Wetzel et al., 1998; Susin et al., 1999). The released cytochrome c then complexes with cytosolic APAF-1 and dATP to form a functional 'apoptosome' which subsequently recruits and transactivates caspase-9 (Zou et al., 1997; Li et al., 1997; Hu et al., 1999). Being the apical caspase activated during chemically-induced apoptosis, caspase-9 also processes caspase-3 (Zou et al., 1997; Li et al., 1997; Kluck et al., 1997b; Pan et al., 1998;

Slee et al., 1999), suggesting that caspase-9 may be responsible for the nuclear morphological change. This was further corroborated by the efflux of cytochrome c, and loss of mitochondrial membrane potential in cells displaying the partially condensed nuclear morphology. However, in the presence of caspase inhibitors there was a slight inhibition of the mitochondrial membrane potential disruption, which paralleled the partially abrogated cytochrome c efflux. This observation could be explained by the potential 'feed-forward' amplification loop that exists between caspases and cytochrome c release. Caspases have been shown to induce PT pore opening and cytochrome c release further amplifying caspase activation (Marzo et al., 1998; Green and Reed, 1998). Thus the caspase inhibitors used in this study could be preventing the caspase-dependent PT pore opening and cytochrome c release which amplifies the original apoptosis-inducing signal. This would explain the partial inhibition of cytochrome c release and mitochondrial membrane potential in staurosporine-treated Jurkat cells in the presence of caspase inhibitors. Although, caspase inhibitors are unable to directly block the release of cytochrome c from the mitochondria (Yang et al., 1997; Kluck et al., 1997a; Bossy-Wetzel et al., 1998; Zhuang et al., 1998) they can inhibit cytochrome c-induced apoptosis (Zhivotovsky et al., 1998; Brustugun et al., 1998). This is entirely compatible with the idea that inhibition of downstream caspases indirectly abrogates or blocks the feed-back amplification mechanisms which result in PT pore opening, cytochrome c release, and caspase-9 activation (Kuwana et al., 1998; Slee et al., 1999). The results also suggest that cytochrome c release and decrease in mitochondrial membrane potential occur upstream of any morphological changes in staurosporine-treated cells in the presence of z-VAD-FMK, as the appearance of the partially condensed nuclear morphology can be completely inhibited under conditions where a decrease in mitochondrial membrane potential has occurred.

Previous studies have shown that Bcl-2 and Bcl-xl are able to inhibit both the release of cytochrome c, loss in mitochondrial membrane potential (Yang et al., 1997; Kharbanda et al., 1997; Kluck et al., 1997a; Bossy-Wetzel et al., 1998; Vander Heiden and Thompson, 1999) and subsequent caspase activation observed during apoptosis (Chinnaiyan et al., 1996; Perry et al., 1997; Estoppey et al., 1997). Using Bcl-2 overexpressing clones the appearance of the partially condensed nuclear morphology after staurosporine treatment was inhibited, further suggesting that this nuclear morphological change occurs

downstream of cytochrome c release and the loss of mitochondrial membrane potential. The morphological changes described in this chapter were also observed after treatment of Jurkat cells with other chemicals known to induce apoptosis in the presence of caspase inhibitors. Both TPEN and etoposide caused this morphological change, suggesting that the partially condensed nuclear morphology is not an event induced specifically by staurosporine, but may be a common early apoptotic feature during chemical-induced apoptosis. Furthermore, the partially condensed nuclear morphology was not only observed in Jurkat cells but also MCF-7, Swiss 3T3 fibroblasts and THP-1 cells, suggesting that early effector caspase-independent nuclear morphological changes may be common to a number of cell types.

Taken together the results presented in this chapter describe a novel nuclear morphological change in cells, which occurs early in the apoptotic process during chemical-induced apoptosis. This process is an early event and precedes chromatin condensation, externalization of PS, DNA fragmentation and is independent of caspase-2, -3, -6, -7 and -8. It appears to be dependent upon an apical caspase activity following the efflux of cytochrome c and loss in mitochondrial membrane potential.

#### Note

Some of the results presented in this chapter have been published in the following:

Johnson, V.L., Ko, C.W.S., Holmstrom, T.H., Eriksson, J.E., and Chow, S.C. (2000). Effector caspases are dispensable for the early nuclear morphological changes during chemical-induced apoptosis. *Journal of Cell Science* 113, 2941-2953.

## **CHAPTER SIX**

# **ROLE OF CASPASE-3 AND DFF40/45 IN HIGH MOLECULAR WEIGHT AND OLIGONUCLEOSOMAL LENGTH DNA FRAGMENTATION DURING APOPTOSIS**

## 6.1 Introduction

One of the most definitive biochemical features of apoptosis is the ordered degradation of nuclear DNA (Wyllie, 1980a). Chromatin is first cleaved into large, high molecular weight (HMW) fragments >700 Kbp followed by further degradation to fragments of 50-200Kbp (Cohen et al., 1992; Brown et al., 1993; Oberhammer et al., 1994). These fragments are then cleaved further into oligonucleosomal-length fragments of 200bp or multiples thereof, giving the characteristic laddering pattern when analysed by conventional agarose gel electrophoresis (Wyllie, 1980a; Arends et al., 1990). The two stages of DNA fragmentation have been shown to be mediated by endonucleases with differing requirements for  $\text{Ca}^{2+}$  and  $\text{Mg}^{2+}$  (Sun and Cohen, 1994; Walker et al., 1994; Hughes et al., 1998b). Possible candidates for the endonuclease(s) responsible for oligonucleosomal-length DNA fragmentation include NUC18/cyclophilin (Montague et al., 1997), DNase I (Peitsch et al., 1994), DNase II (Barry and Eastman, 1993) and most recently a caspase-activated DNase (CAD) which is homologous to human DNA fragmentation factor (DFF) (Liu et al., 1997b; Sakahira et al., 1998; Enari et al., 1998). The discovery of a caspase-activated nuclease activity has provided an attractive model for DNA fragmentation by linking the activation of caspases and the subsequent cleavage of chromatin into characteristic oligonucleosomal length fragments (Liu et al., 1997b). However the influence of DFF and caspase activation on HMW DNA fragmentation has yet to be determined.

DNA Fragmentation Factor exists as a complex consisting of a 40kDa and a 45kDa subunit with homology to murine CAD and ICAD (Liu et al., 1997b; Enari et al., 1998). The 45kDa subunit acts as a chaperone localizing DFF40 to the cytoplasm whilst inhibiting its activity (Inohara et al., 1999). Upon activation by caspase-3 at conserved DXXD motifs, DFF45 is cleaved at Asp<sup>224</sup> and Asp<sup>117</sup> to yield 31kDa and 11kDa fragments. Cleavage at Asp<sup>117</sup> is both essential and sufficient for the release of DFF40 and its activation and translocation to the nucleus (Sakahira et al., 1998; Wolf et al., 1999). DFF40 contains intrinsic nuclease activity (Liu et al., 1998) which is enhanced by the presence of chromatin associated proteins such as Histone H1 and HMG2 (Toh et al., 1998; Liu et al., 1999). DFF40 consequently cleaves nuclear DNA resulting in the hallmark apoptotic feature of oligonucleosomal-length DNA fragmentation (Liu et al., 1997b). However, the involvement of DFF40 in the initial formation of HMW DNA fragments is unclear, as is the contribution of caspase-3. It is

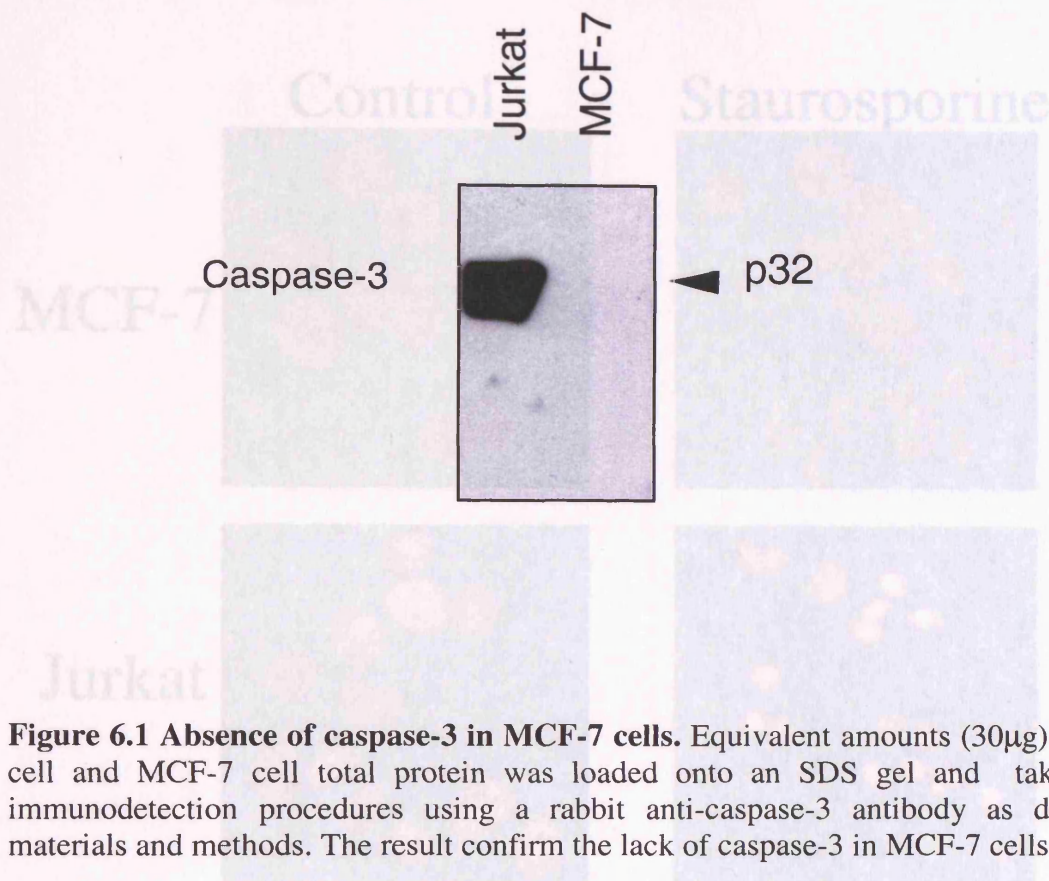
possible that further caspase-dependent/independent nuclease activity(s) may be acting upstream of DFF to induce this early event (Hughes et al., 1998a). Therefore the aim of this chapter was to examine the contribution of caspase-3 and DFF to both HMW and oligonucleosomal-length DNA fragmentation. This was achieved in the first instance, by use of the MCF-7 cell line which lacks caspase-3, and secondly by using the serine protease inhibitor, N-tosyl-phenylalanine chloromethyl ketone (TPCK) which has previously been used effectively to dissect the processes of HMW and oligonucleosomal-length DNA fragmentation (Chow et al., 1995; Weis et al., 1995).

## 6.2 Results

### 6.2.1 Caspase-3 is not required for HMW DNA fragmentation during staurosporine-induced apoptosis.

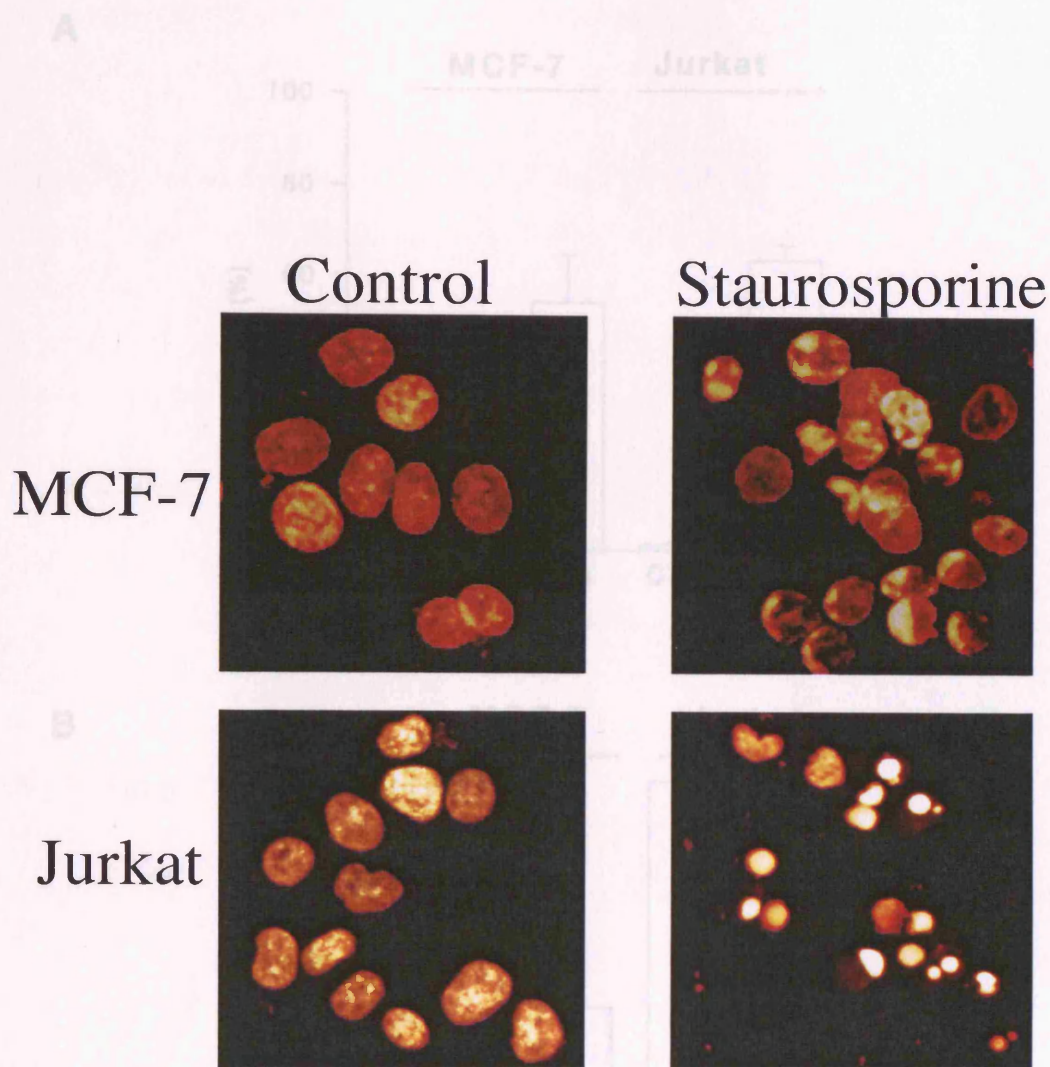
In order to study the contribution of caspase-3 to HMW and oligonucleosomal-length DNA fragmentation, the MCF-7 cell line, which lack caspase-3, was utilised. MCF-7 cells have been shown to lack caspase-3 due to a functional deletion of the caspase-3 gene (Janicke et al., 1998b). To confirm the absence of caspase-3 in MCF-7 cells, 30 $\mu$ g of MCF-7 and Jurkat T cell lysates were analysed by western blotting and immunodetection with caspase-3 antibody. As shown in Figure 6.1, there was no detectable caspase-3 protein in MCF-7 cell lysates, whereas the enzyme is highly expressed in Jurkat T cells. MCF-7 cells can be induced to undergo apoptosis by a number of diverse stimuli but they do not exhibit all the features typical of apoptosis, most notably the absence of oligonucleosomal length DNA fragmentation (Janicke et al., 1998b). When MCF-7 cells were treated with staurosporine, a difference was observed between chromatin structure in the normal and treated MCF-7 cells (Figure 6.2). Although chromatin condensation was not as distinctive as that observed in Jurkat T cells, the chromatin was clearly condensed and abutted towards the nuclear membrane and was clearly distinguishable from that of non-apoptotic cells. The changes described here are similar to previously reported morphological changes which were associated with HMW DNA fragmentation (Cohen et al., 1992; Walker et al., 1994). Using this nuclear morphological change as a criteria for apoptosis, treatment of MCF-7 cells with 2 $\mu$ M staurosporine for 12h resulted in between 50-60% apoptosis (Figure 6.3A). Similarly, cell viability was also significantly reduced in MCF-7 cells treated with staurosporine in comparison to untreated cells (Figure 6.3B). For direct comparison, Jurkat T cells were treated with 0.5 $\mu$ M staurosporine for 3hr to induce equivalent amounts of apoptosis. The integrity of nuclear chromatin in staurosporine treated MCF-7 and Jurkat T cells was examined by FIGE and CAGE. As shown in Figure 6.4A, the chromatin of staurosporine treated MCF-7 cells was cleaved into HMW fragments of between 50-200kbp fragments. However, further degradation of the HMW fragments into smaller pieces was not observed. In contrast, staurosporine treated Jurkat cells show further degradation of chromatin to fragments of less than 50kbp in size. As illustrated in Figure 6.4B, the chromatin of staurosporine-treated MCF-7 cells was not cleaved into oligonucleosomal-length fragments since no laddering pattern was observed by CAGE, despite showing condensed chromatin

and exhibiting over 50% apoptosis. This is in agreement with previous studies which show that MCF-7 cells do not undergo oligonucleosomal-length DNA fragmentation (Tang and Kidd, 1998; Janicke et al., 1998b; Wolf et al., 1999). However, in staurosporine-treated Jurkat cells the DNA was cleaved into the distinctive laddering pattern (Figure 6.4B). The further degradation of DNA into oligonucleosomal-length fragments in the Jurkat cell line is likely to be due to the release of DFF40/CAD from DFF45/ICAD by caspase-3.



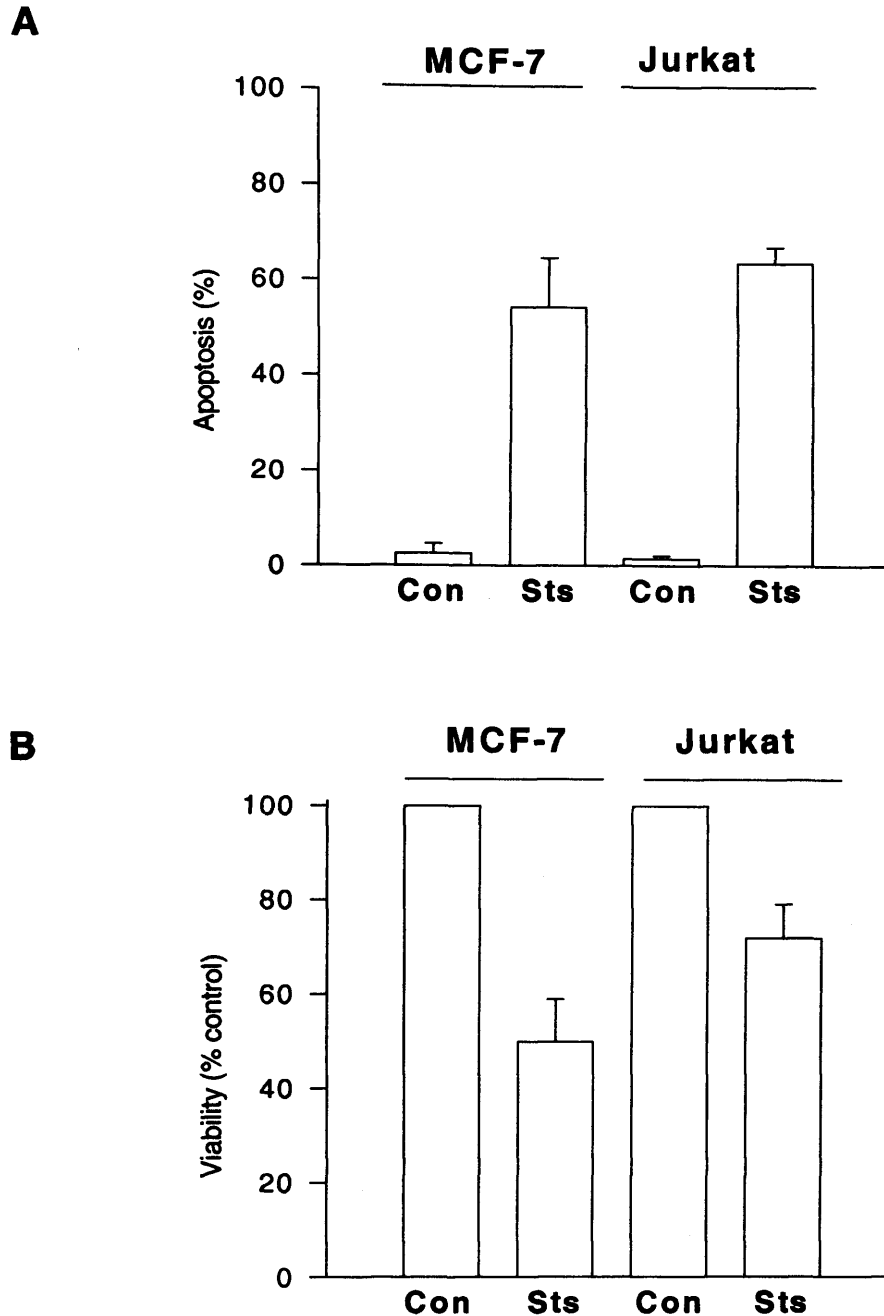
**Figure 6.1 Absence of caspase-3 in MCF-7 cells.** Equivalent amounts (30 $\mu$ g) of Jurkat T cell and MCF-7 cell total protein was loaded onto an SDS gel and taken through immunodetection procedures using a rabbit anti-caspase-3 antibody as described in materials and methods. The result confirm the lack of caspase-3 in MCF-7 cells.

Figure 6.2 Comparison of staurosporine-induced apoptotic morphology in MCF-7 and Jurkat T cells. To examine the relationship between caspase-3 mediated chromatin condensation and DNA fragmentation, the MCF-7 cell line, which lacks caspase-3 was utilized. MCF-7 cells were treated with staurosporine (2 $\mu$ M) for 12h and assessed for apoptotic morphology. For comparison, Jurkat T cells were treated with staurosporine (0.5 $\mu$ M) for 3h. Apoptotic morphology was examined by fixing and staining with Hoechst 33358 and scoring under UV light. Typically condensed chromatin is observed in MCF-7 and Jurkat T-cells. The above images were viewed by confocal laser scanning microscopy.



**Figure 6.2 Comparison of staurosporine-induced apoptotic morphology in MCF-7 and Jurkat T cells.** To examine the relationship between caspase-3 mediated chromatin condensation and DNA fragmentation, the MCF-7 cell line, which lacks caspase-3 was utilized. MCF-7 cells were treated with staurosporine ( $2\mu\text{M}$ ) for 12h and assessed for apoptotic morphology. For comparison, Jurkat T cells were treated with staurosporine ( $0.5\mu\text{M}$ ) for 3h. Apoptotic morphology was examined by fixing and staining with Hoechst 33358 and scoring under UV light. Typically condensed chromatin is observed in MCF-7 and Jurkat T-cells. The above images were viewed by confocal laser scanning microscopy.

treated with staurosporine ( $2\mu\text{M}$ ) for 12h and Jurkat cells were treated with staurosporine ( $0.5\mu\text{M}$ ) for 3h. Cells were assessed for A) apoptosis and B) viability. Apoptotic morphology was examined by fixing and staining with Hoechst 33358 and scoring under UV light as described in materials and methods. Typically condensed chromatin was observed in both MCF-7 and Jurkat T-cells. The results shown represent the mean  $\pm$ SEM from at least four independent experiments.



**Figure 6.3 Comparison of staurosporine induced apoptosis and cell viability in MCF-7 and Jurkat T-cells.** To induce equivalent amounts of apoptosis MCF-7 cells were treated with staurosporine ( $2\mu\text{M}$ ) for 12h and Jurkat cells were treated with staurosporine ( $0.5\mu\text{M}$ ) for 3h. Cells were assessed for A) apoptosis and B) viability. Apoptotic morphology was examined by fixing and staining with Hoechst 33358 and scoring under UV light as described in materials and methods. Typically condensed chromatin was observed in both MCF-7 and Jurkat T-cells. The results shown represent the mean  $\pm$ SEM from at least four independent experiments.

### 6.2.3 Partial cleavage of DFF40/45 correlates to lack of oligonucleosomal-length DNA fragmentation

Because caspase-3 has been shown to be the primary activator of DFF40 (Woff et al., 1999) the activation state of DFF40 in MCF-7 cells was examined in order to determine if DFF40 was activated. DFF40 activation can be directly correlated to the appearance of the 11 kDa fragment of DFF40 (Woff et al., 1999; Tang and Kidd, 1998; Wolf et al., 1998). The appearance of this fragment is an absolute requirement for DFF40 activation and activation of DFF40. As shown in Figure 6.5A, in staurosporine treated MCF-7 cells, DFF45 was cleaved into a 11 kDa fragment. This cleavage was observed in 50% of the cells, indicating that DFF45 was activated in 50% of the cells. This cleavage correlates well with the appearance of oligonucleosomal-length DNA fragments in MCF-7 cells. It has been proposed that caspase-3 cleaves DFF40 (Tang and Kidd, 1998) and this is illustrated in Figure 6.5B. In Jurkat T cells after treatment with staurosporine, DFF40 was cleaved into a 11 kDa fragment. This cleavage correlates with the appearance of oligonucleosomal-length DNA fragments in Jurkat T cells. The cleavage of DFF40 during oligonucleosomal-length DNA fragmentation (Tang and Kidd, 1998; Woff et al., 1998). However, caspase-3 appears to be dispensable for the formation of HMW DNA fragments. Studies have shown that non-caspase dependent proteases may also be involved in DNA fragmentation during apoptosis (Chow et al., 1995; Hughes et al., 1995a). In fact,

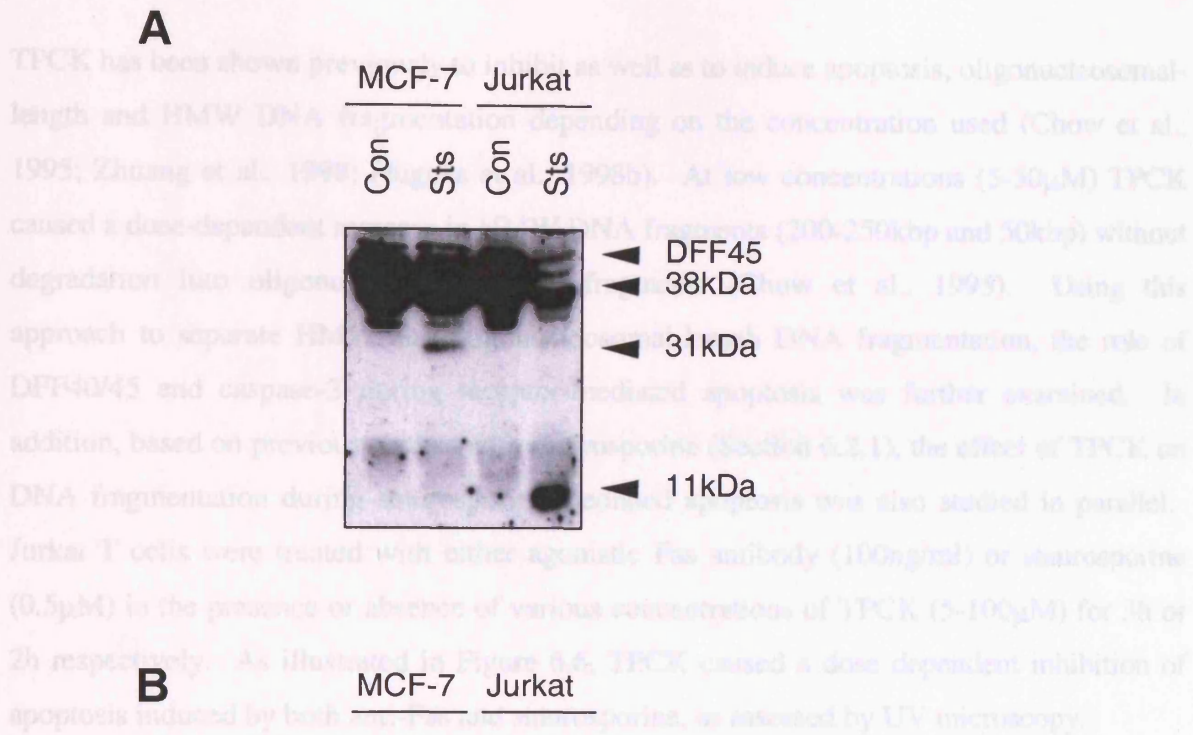
**Figure 6.4 Comparison of A) HMW and B) oligonucleosomal-length DNA cleavage in MCF-7 and Jurkat cells.** MCF-7 and Jurkat T cells were treated with staurosporine and oligonucleosomal-length and HMW DNA fragmentation was assessed by FIGE and CAGE, respectively, as described in materials and methods.

whilst inhibiting oligonucleosomal-length DNA fragment formation (Chow et al., 1995). However, the exact mechanism by which TPCK influences HMW and oligonucleosomal-length DNA fragmentation remains unresolved. Because DFF40/45 activity and caspase-3 appear to be essential for oligonucleosomal-length DNA fragment formation, but not a requirement for HMW DNA fragment formation in MCF-7 cells, one potential mechanism for the observed effects of TPCK in the Jurkat T cell system could be the modulation/regulation of either caspase-3 or DFF40/45 activity.

## 6.2.2 Partial cleavage of DFF40/45 correlates to lack of oligonucleosomal-length DNA fragmentation

Because, caspase-3 has been shown to be the primary activator of DFF40 (Wolf et al., 1999) the activation state of DFF40 in MCF-7 cells was examined in order to determine if DFF40 was activated. DFF40 activation can be directly correlated to the appearance of the 11kDa fragment of DFF45 (Liu et al., 1997b; Tang and Kidd, 1998; Sakahira et al., 1998). The appearance of this 11kDa fragment is an absolute requirement for the release and activation of DFF40. As shown in Figure 6.5A, in staurosporine treated MCF-7 cells, DFF45 was cleaved to a 31kDa fragment despite over 50% of the cells displaying an apoptotic morphology and viability being decreased by 50% (Figure 6.2). In contrast, DFF45 was substantially cleaved to the 11kDa fragment in staurosporine treated Jurkat T cells, indicative of the activation of DFF40. This correlates well with the appearance of oligonucleosomal length DNA fragments in the Jurkat cells. It has been proposed that DFF can be cleaved by caspases other than caspase-3 (Tang and Kidd, 1998) especially caspase-7 (Janicke et al., 1998a; Liu et al., 1999). Indeed, as illustrated in Figure 6.5B caspase-7 was processed to the active p19 fragment in MCF-7 cells after treatment with staurosporine. This correlates with the ability of caspase-7 to cleave DFF45 to yield the 31kDa intermediate fragment but suggests that caspase-3 may be required for complete cleavage of DFF45 and activation of DFF40 during oligonucleosomal-length DNA fragmentation (Tang and Kidd, 1998; Wolf et al., 1999). However, caspase-3 appears to be dispensable for the formation of HMW DNA fragments. Studies have shown that non-caspase dependent proteases may also be involved in DNA fragmentation during apoptosis (Chow et al., 1995; Hughes et al., 1998a). Infact, HMW and oligonucleosomal-length DNA fragmentation can also be effectively dissociated in Jurkat T cells using the serine protease inhibitor, TPCK (Chow et al., 1995; Weis et al., 1995; Hughes et al., 1998b). TPCK has been shown to induce HMW DNA fragmentation whilst inhibiting oligonucleosomal-length DNA fragment formation (Chow et al., 1995). However, the exact mechanism by which TPCK influences HMW and oligonucleosomal-length DNA fragmentation remains unresolved. Because DFF40/45 activity and caspase-3 appear to be essential for oligonucleosomal-length DNA fragment formation, but not a requirement for HMW DNA fragment formation in MCF-7 cells, one potential mechanism for the observed effects of TPCK in the Jurkat T cell system could be the modulation/regulation of either caspase-3 or DFF40/45 activity.

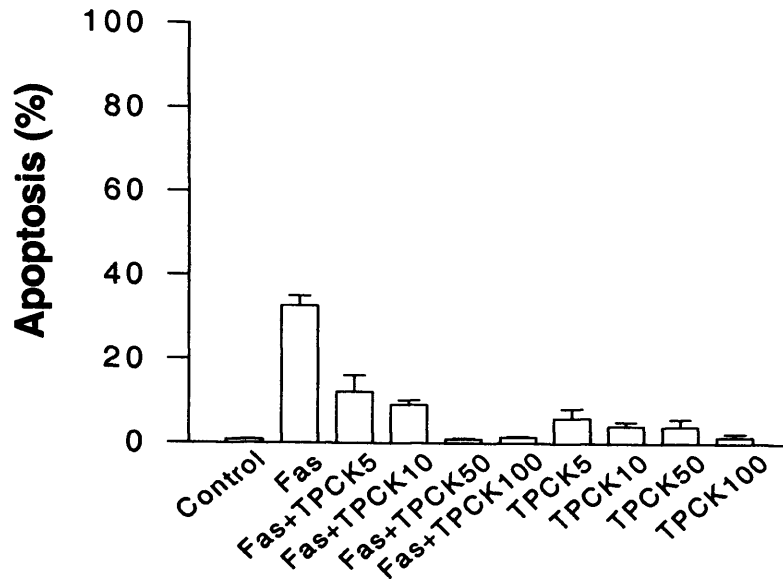
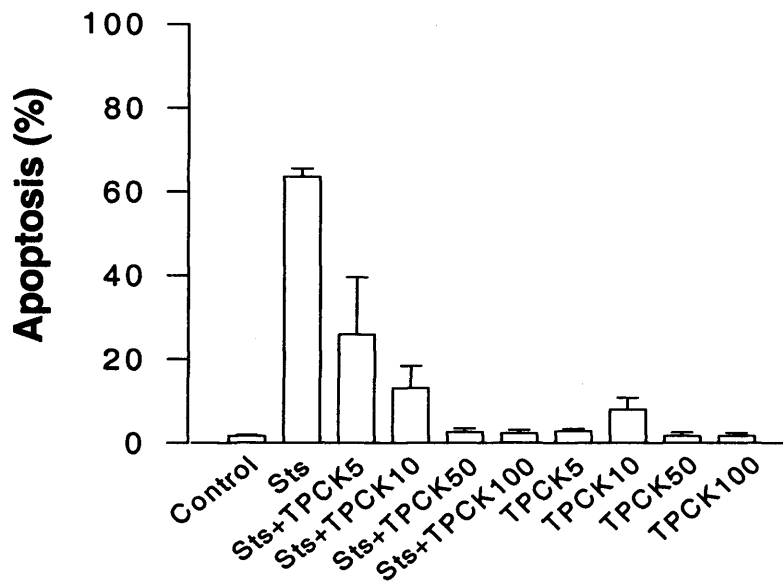
## 6.2.3 Effect of TPCK on apoptosis in Jurkat T cells



**Figure 6.5 Effect of staurosporine on A) DFF45 and B) caspase-7 processing in MCF-7 and Jurkat T cells.** MCF-7 cells were treated with  $2\mu\text{M}$  staurosporine for 12h and Jurkat T cells were treated with  $0.5\mu\text{M}$  staurosporine for 3h. Cell lysates were analysed by immunodetection procedures as described in materials and methods.

### 6.2.3 Effect of TPCK on apoptosis in Jurkat T cells

TPCK has been shown previously to inhibit as well as to induce apoptosis, oligonucleosomal-length and HMW DNA fragmentation depending on the concentration used (Chow et al., 1995; Zhuang et al., 1998; Hughes et al., 1998b). At low concentrations (5-50 $\mu$ M) TPCK caused a dose-dependent increase in HMW DNA fragments (200-250kbp and 50kbp) without degradation into oligonucleosomal-length fragments (Chow et al., 1995). Using this approach to separate HMW and oligonucleosomal-length DNA fragmentation, the role of DFF40/45 and caspase-3 during receptor-mediated apoptosis was further examined. In addition, based on previous studies with staurosporine (Section 6.2.1), the effect of TPCK on DNA fragmentation during staurosporine-mediated apoptosis was also studied in parallel. Jurkat T cells were treated with either agonistic Fas antibody (100ng/ml) or staurosporine (0.5 $\mu$ M) in the presence or absence of various concentrations of TPCK (5-100 $\mu$ M) for 3h or 2h respectively. As illustrated in Figure 6.6, TPCK caused a dose dependent inhibition of apoptosis induced by both anti-Fas and staurosporine, as assessed by UV microscopy.

**A****B**

**Figure 6.6 Effect of TPCK on receptor mediated and chemically induced apoptosis in Jurkat T cells.** Jurkat T cells were treated with either A) anti-Fas (100ng/ml) or B) staurosporine (0.5μM) for 3 or 2h respectively, in the presence of various concentrations of TPCK (5-100μM) and assessed for apoptosis by Hoechst 33358 staining and UV microscopy. The results represent the mean  $\pm$  S.E.M of four independent experiments.

#### **6.2.4 Effect of TPCK on HMW and oligonucleosomal-length DNA fragmentation in Fas-treated Jurkat cells**

After treatment with anti-Fas the effect of TPCK on HMW DNA fragmentation was examined. As illustrated in Figure 6.7A, TPCK (5-50 $\mu$ M) potentiated the formation of HMW DNA fragments (>50kbp) during Fas-mediated apoptosis but inhibited this process at high concentrations (100 $\mu$ M). In addition, TPCK alone (5-50 $\mu$ M) also potentiated the formation of HMW DNA fragments. Thus, TPCK appeared to be blocking HMW DNA fragment formation at the 50-200kbp stage. To confirm that TPCK was blocking the further degradation of DNA into smaller fragments, the formation of oligonucleosomal-length DNA fragments during Fas-mediated apoptosis was examined by CAGE. TPCK caused a dose-dependent inhibition of Fas-mediated oligonucleosomal-length DNA fragment formation (Figure 6.7B). This data is in agreement with previous studies where the formation of HMW DNA fragments has been shown to occur in the absence of oligonucleosomal length fragment formation during some forms of apoptosis (Oberhammer et al., 1993; Weis et al., 1995) (Brown et al., 1993; Beere et al., 1995).

#### **6.2.5 Effect of TPCK on HMW and oligonucleosomal-length DNA fragmentation in staurosporine-treated Jurkat cells**

For comparison, the effect of TPCK on chromatin cleavage during staurosporine-mediated apoptosis in Jurkat cells was also carried out to determine if the signalling pathways leading to DNA fragmentation were similar in receptor- and chemical-induced apoptosis. Jurkat cells were treated with staurosporine (0.5 $\mu$ M) for 2h and the cells were assessed for HMW DNA and oligonucleosomal length DNA fragmentation in the absence or presence of TPCK (5-100 $\mu$ M). As illustrated in Figure 6.8A, TPCK at concentrations of 5-50 $\mu$ M potentiated the formation HMW DNA fragments in staurosporine-treated cells in manner similar to that observed upon treatment with anti-Fas. There was an increase in HMW DNA fragments between 50-200kbp at intermediate concentrations (5-50 $\mu$ M), but at high concentrations of TPCK (100 $\mu$ M), the formation of HMW DNA fragments was inhibited as previously observed in the Fas system. When the chromatin was analysed by CAGE, TPCK dose-dependently inhibited staurosporine induced oligonucleosomal-length DNA fragmentation in a similar manner to that observed upon treatment with anti-Fas (Figure 6.8B). The results

presented in Figure 6.7 and 6.8 confirmed the results previously described by Weis et al., (1995) suggesting that HMW and oligonucleosomal length DNA fragmentation can be separated using TPCK. The formation of oligonucleosomal length DNA fragments appears to be highly sensitive to TPCK whereas HMW DNA fragment formation is less sensitive to TPCK and requires higher concentrations ( $100\mu\text{M}$ ) for inhibition. TPCK at low to intermediate concentrations ( $5\text{-}50\mu\text{M}$ ) appears to induce or potentiate the formation of HMW DNA fragments. These results imply that two distinct protease activities may be involved in DNA fragmentation and that they have differing sensitivities to TPCK.

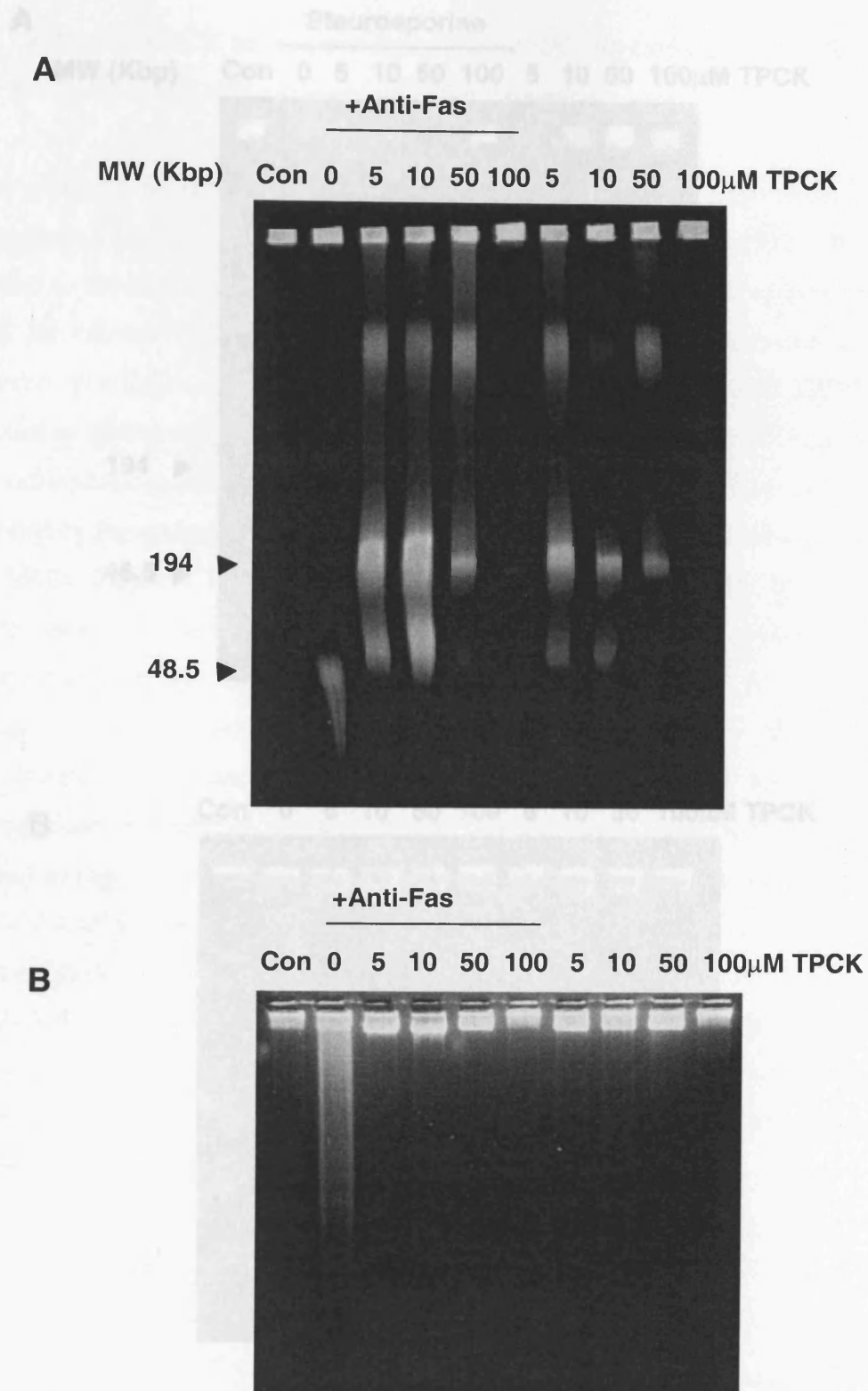
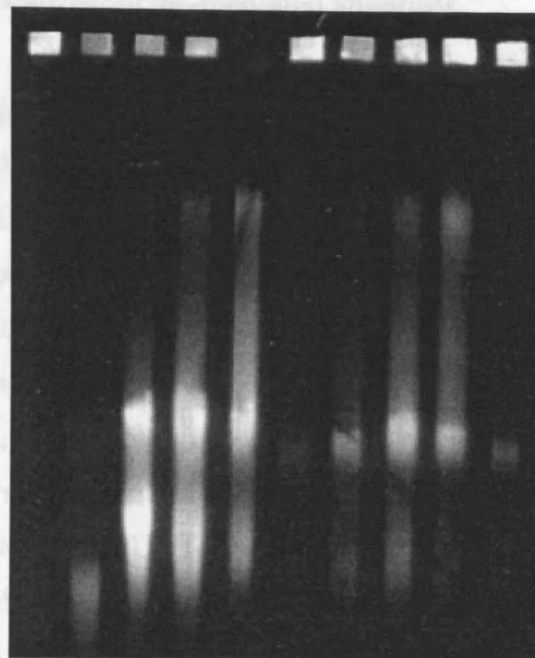
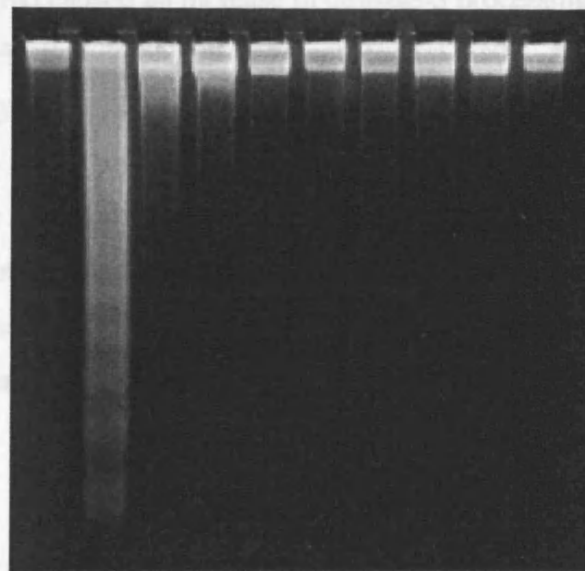


Figure 6.7 Effect of TPCK on formation of A) HMW and B) oligonucleosomal-length DNA fragments in staurosporine treated Jurkat T cells. Jurkat cells ( $1 \times 10^6$  cells/ml) were treated with 0.5  $\mu$ M staurosporine for 2h in the presence of various concentrations of TPCK as indicated. The cells were then treated with anti-Fas antibody (1  $\mu$ g/ml) for 2h. The gels shown are represent one typical experiment of three.

**A** **Staurosporine**  
MW (Kbp) Con 0 5 10 50 100 5 10 50 100  $\mu$ M TPCK



**B** **Staurosporine**  
Con 0 5 10 50 100 5 10 50 100  $\mu$ M TPCK



**Figure 6.8** Effect of TPCK on formation of A) HMW and B) oligonucleosomal-length DNA fragments in staurosporine treated Jurkat T cells. Jurkat cells ( $1 \times 10^6$  cells/ml) were treated with  $0.5 \mu$ M staurosporine for 2h in the presence of various concentrations of TPCK. The gels shown is one representative of at least three independent experiments.

### **6.2.6 Effect of TPCK on caspase-3 processing and the cleavage of PARP and DEVD-AFC during Fas- and staurosporine-mediated apoptosis.**

Recent evidence has suggested that oligonucleosomal-length DNA fragmentation is the result of a caspase-3 mediated nuclease, DFF (Liu et al., 1997b; Liu et al., 1998). Because TPCK appeared to block the formation of oligonucleosomal-length DNA fragments, the effect of TPCK on caspase-3 processing during Fas- and staurosporine-mediated apoptosis was examined. In addition, cleavage of the caspase-3 substrates, PARP and z-DEVD-AFC were also used as additional indicators of caspase-3 activity. As illustrated in Figure 6.9A, during Fas-mediated apoptosis, TPCK (5-50 $\mu$ M) causes the potentiation of caspase-3 processing as illustrated by the appearance of the mature p17 subunit and similarly PARP was cleaved from the 116kDa fragment to an 85kDa fragment (Figure 6.9B). TPCK at concentrations of 100 $\mu$ M partially inhibited caspase-3 processing and PARP cleavage whereas at concentrations between 50-100 $\mu$ M, TPCK alone caused caspase-3 processing and PARP cleavage. A similar pattern of was also observed in Jurkat cells after treatment with staurosporine. In staurosporine-induced apoptosis, TPCK at low to intermediate concentrations (5-50 $\mu$ M) caused an increase in caspase-3 processing to the active p17 subunit and the cleavage of PARP to an 85kDa fragment (Figure 6.10). As an additional indicator of caspase-3-like activity the effect of TPCK on the cleavage of z-DEVD-AFC was also examined during Fas- and staurosporine-mediated apoptosis (Figure 6.11). The extent of z-DEVD-AFC cleavage reflected the degree of caspase-3 processing as determined by western blotting during Fas- and staurosporine-induced apoptosis. Therefore, caspase-3 appeared to be active in the presence of TPCK during Fas- and staurosporine mediated apoptosis, as determined by PARP and z-DEVD-AFC cleavage.

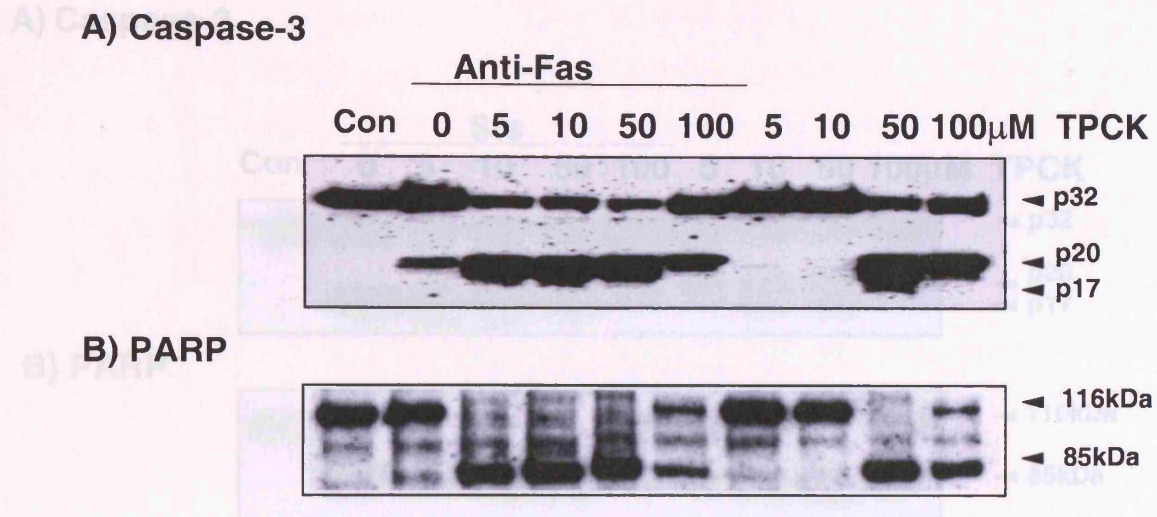
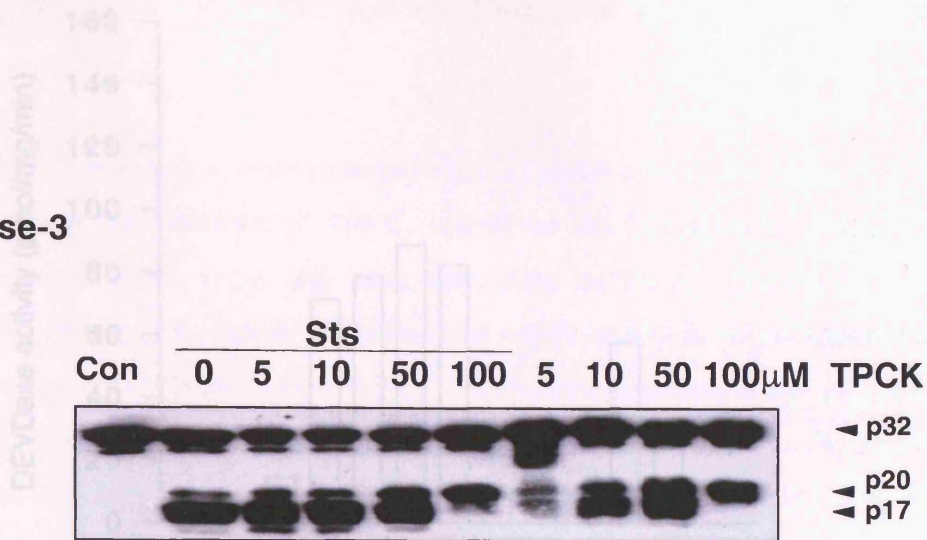
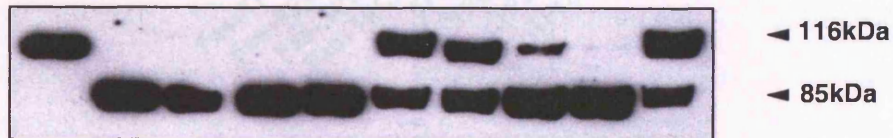


**Figure 6.9** Effect of TPCK on A) caspase-3 and B) PARP processing in Fas-treated Jurkat T cells. Cells were treated with anti-Fas (100ng/ml) for 3h in the presence of various concentrations of TPCK. After treatment cells were prepared for SDS PAGE and immunodetection procedures. Data shown represents one of at least two independent experiments with similar findings.

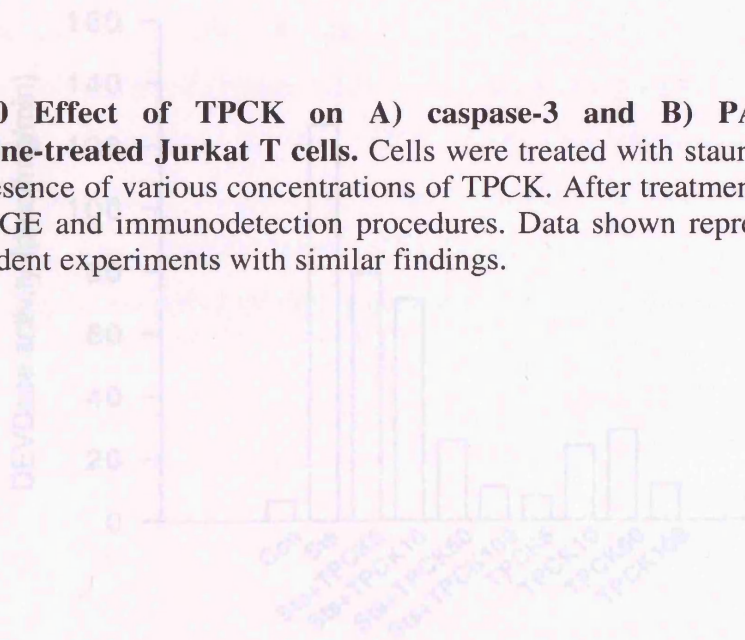
**A) Caspase-3**



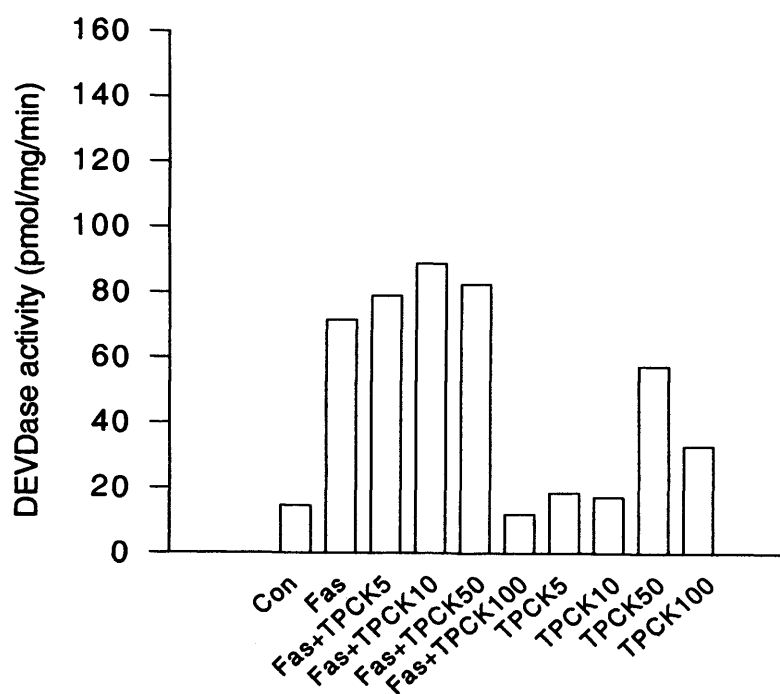
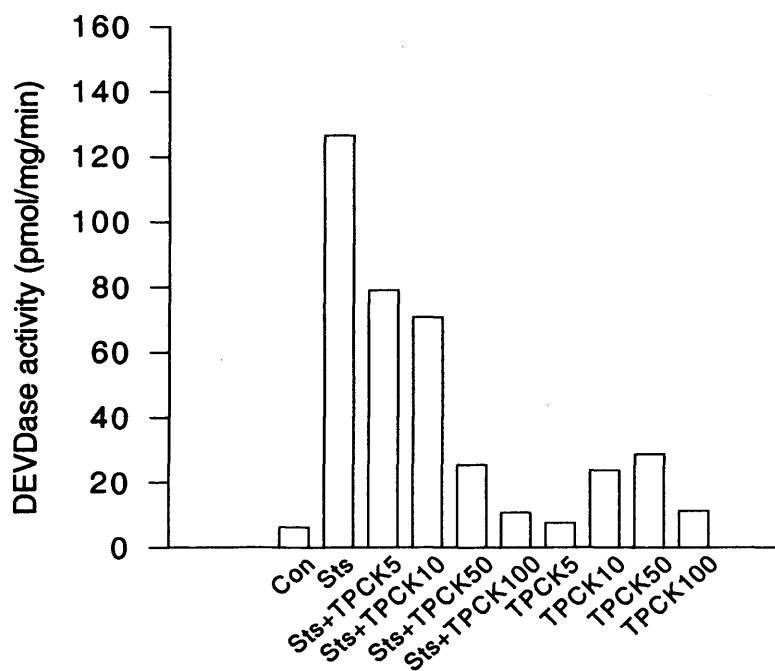
**B) PARP**



**Figure 6.10 Effect of TPCK on A) caspase-3 and B) PARP processing in Staurosporine-treated Jurkat T cells.** Cells were treated with staurosporine (0.5 $\mu$ M) for 2h in the presence of various concentrations of TPCK. After treatment cells were prepared for SDS PAGE and immunodetection procedures. Data shown represents one of at least two independent experiments with similar findings.



**Figure 6.11 Effect of TPCK on DEVDase activity in Fas- and staurosporine-treated cells.** Jurkat Cells were treated with either anti-Fas (100ng/ml) or staurosporine (0.5 $\mu$ M) in the presence of TPCK (0-100 $\mu$ M) for 3 or 2h respectively. Cell lysates were then assayed for DEVDase activity by measuring liberation of fluorescent AFC as described in materials and methods. The results show the mean of one typical experiment carried out in triplicate.

**A****B**

**Figure 6.11 Effect of TPCK on DEVDase activity in Fas- and staurosporine-treated cells.** Jurkat Cells were treated with either anti-Fas (100ng/ml) or staurosporine (0.5 $\mu$ M) in the presence of TPCK (0-100 $\mu$ M) for 3 or 2h respectively. Cell lysates were then assayed for DEVDase activity by measuring liberation of fluorogenic AFC as described in materials and methods. The results show the mean of one typical experiment carried out in triplicate.

### 6.2.7 Effect of TPCK on DFF45 cleavage during Fas and Staurosporine-mediated apoptosis

As shown earlier, caspase-3 appears to be activated in Jurkat cells treated with either anti-Fas or staurosporine in the presence of TPCK. However the formation of oligonucleosomal length DNA fragments in these cells was completely inhibited. Caspase-3 also cleaves DFF45 thereby releasing the active DFF40 subunit which results in oligonucleosomal length DNA fragmentation. Therefore the effect of TPCK on the cleavage of DFF45 was investigated in Jurkat cells treated with Fas or staurosporine. As shown in Figure 6.12, after treatment with Fas, DFF45 was cleaved to the intermediate 31kDa fragment (Tang and Kidd, 1998; Enari et al., 1998) and this is further cleaved to the 11kDa form denoting DFF40 activation (Liu et al., 1997b). When less protein was loaded on the gel, the 11kDa fragment of DFF was sometimes observed as a doublet corresponding to caspase-3 cleavage sites between Asp<sup>137</sup> and Ser<sup>13</sup>, and Asp<sup>244</sup> and Thr<sup>245</sup>. The cleavage of DFF45 to the 11kDa form was potentiated by TPCK concentrations of between 5-50 $\mu$ M, and inhibited by TPCK at high concentrations (100 $\mu$ M). After treatment with staurosporine a similar pattern of DFF45 cleavage was also observed (Figure 6.13). The results in Figure 6.12 and 6.13, suggest that despite DFF45 processing to the 11kDa form, no oligonucleosomal-length DNA fragmentation occurred. Because DFF45 was completely cleaved to the 11kDa fragment in the absence of oligonucleosomal-length DNA fragmentation, it is possible that TPCK could be acting directly on the active DFF40 to prevent DNA fragmentation.

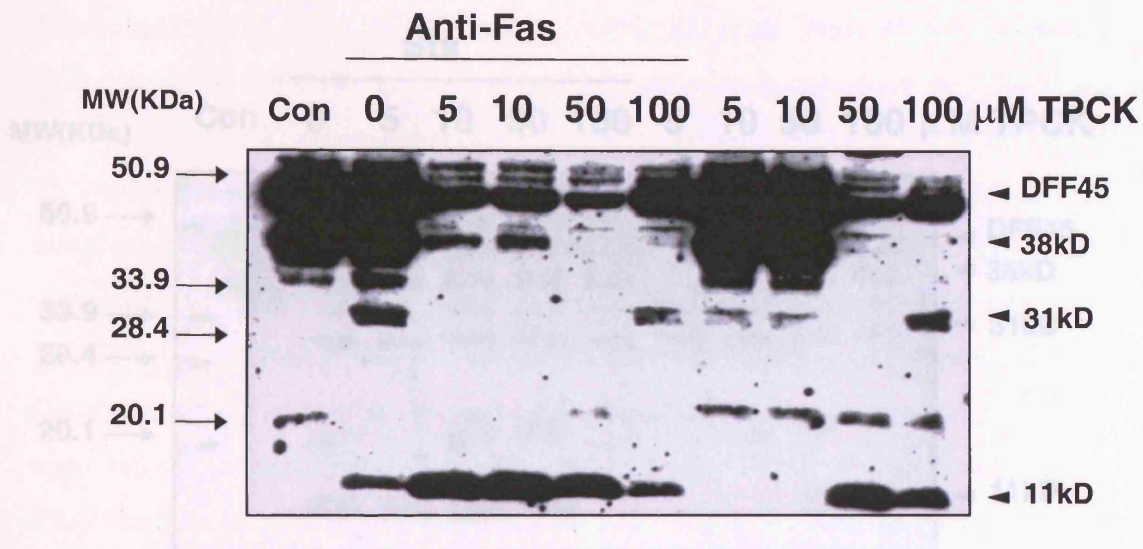


**Figure 6.12 Effect of TPCK on DFF45 processing during Fas-mediated apoptosis.** Cells were treated with anti-Fas (100ng/ml) for 3h in the presence of various concentrations of TPCK and analysed by SDS PAGE and immunodetection procedures as described in materials and methods. The results represent one of two independent experiments with similar findings.

### 6.2.8 *In vitro* assay to determine whether TPCK blocks DFF40 activity

To determine whether TPCK was interfering with either the activation of DFF40 by caspase-3 or directly acting on the DFF40 protein itself, an *in vitro* assay was designed using a recombinant DFF40/45 fusion protein. Using such an assay it would be possible to determine the precise effect of TPCK on the activity of DFF40 and oligonucleosomal-length DNA fragmentation (Liu et al., 1997a; Liu et al., 1998; Liu et al., 1999; Wöhrl and Häcker, 1999).

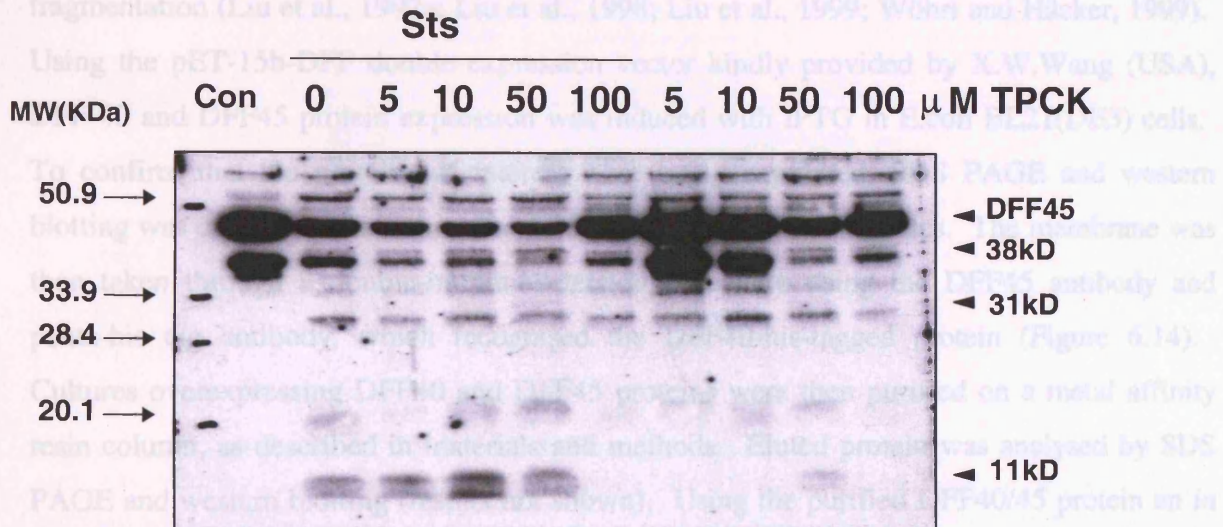


**Figure 6.13 Effect of TPCK on DFF45 processing during staurosporine-mediated apoptosis.** Cells were treated with staurosporine (0.5µM) for 3h in the presence of various concentrations of TPCK and analysed by SDS PAGE and immunodetection procedures as described in materials and methods. The results represent one of two independent experiments with similar findings.

activity (Figure 6.13A). Previous studies have shown that DFF activity *in vitro* is enhanced by the presence of histone H1 protein (Liu et al., 1997b). Therefore the *in vitro* nuclease assay was carried out in the presence of histone H1 (300ng). In a similar manner to the previous experiment, the presence of histone H1 had little effect on the extent of DNA fragmentation (Figure 6.15B). A fluorogenic DEVD-APC enzyme assay, as described in materials and methods, was carried out to confirm that the recombinant caspase-3 was used in the assay was indeed active. As shown in Figure 6.16, the recombinant caspase-3 used in the assay was active as indicated by the processing of the fluorogenic substrate r-DEVD-APC. Therefore it seemed likely that the purified DFF protein was inactive and this approach was not taken further due to time limitations. Therefore it was not possible to determine whether TPCK was directly or indirectly altering DFF40 activity.

### 6.2.8 *In vitro* assay to determine whether TPCK blocks DFF40 activity

To determine whether TPCK was interfering with either the activation of DFF40 by caspase-3 or directly acting on the DFF40 protein itself, an *in vitro* assay was designed using a recombinant DFF40/45 fusion protein. Using such an assay it would be possible to determine the precise effect of TPCK on the activity of DFF40 and oligonucleosomal-length DNA fragmentation (Liu et al., 1997a; Liu et al., 1998; Liu et al., 1999; Wöhrl and Häcker, 1999). Using the pET-15b-DFF double expression vector kindly provided by X.W.Wang (USA), DFF 40 and DFF45 protein expression was induced with IPTG in E.coli BL21(DE3) cells. To confirm that the proteins of interest were being expressed, SDS PAGE and western blotting was carried out on induced and uninduced bacterial cell lysates. The membrane was then taken through a double-immunodetection procedure using the DFF45 antibody and penta-his tag antibody, which recognised the DFF40-his-tagged protein (Figure 6.14). Cultures overexpressing DFF40 and DFF45 proteins were then purified on a metal affinity resin column, as described in materials and methods. Eluted protein was analysed by SDS PAGE and western blotting (results not shown). Using the purified DFF40/45 protein an *in vitro* assay was used to determine whether the DFF40/45 was active and retained its nuclease activity. pcDNA3 (3µg) was used as a substrate and mixed with either purified DFF40/45 (1µg) and/or recombinant caspase-3 (500ng) in buffer A and incubated for 2h at 37°C, as described in materials and methods. The DFF40 nuclease activity was determined using CAGE to analyse the DNA fragmentation of pcDNA3 (Figure 6.15). However, the extent of DNA fragmentation was minimal and it appeared that there was no significant nuclease activity (Figure 6.15A). Previous studies have shown that DFF activity *in vitro* is enhanced by the presence of histone H1 protein (Liu et al., 1997b). Therefore the *in vitro* nuclease assay was carried out in the presence of histone H1 (300ng). In a similar manner to the previous experiment, the presence of histone H1 had little effect on the extent of DNA fragmentation (Figure 6.15B). A fluorogenic DEVD-AFC enzyme assay, as described in materials and methods, was carried out to confirm that the recombinant caspase-3 used in the assay was indeed active. As shown in Figure 6.16, the recombinant caspase-3 used in the assay was active as indicated by the processing of the fluorogenic substrate z-DEVD-AFC. Therefore it seemed likely that the purified DFF protein was inactive and this approach was not taken further due to time limitations. Therefore it was not possible to determine whether TPCK was directly or indirectly altering DFF40 activity.

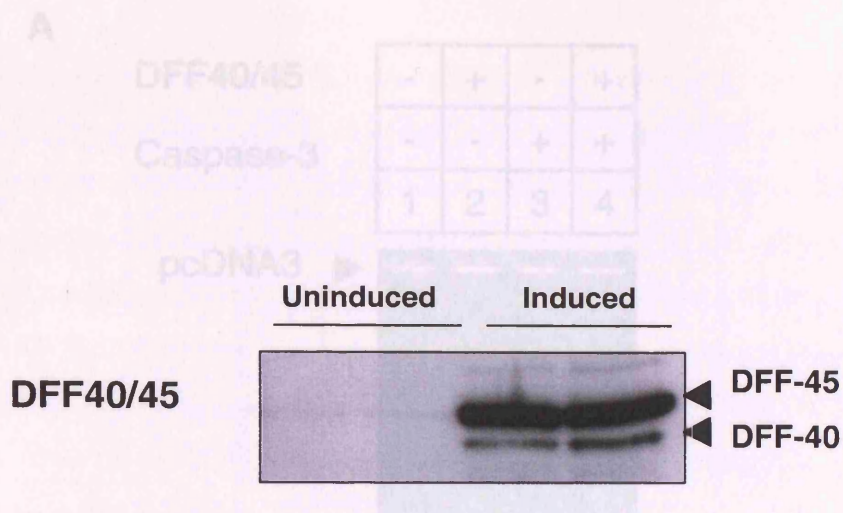


**Figure 6.14 Induction of DFF40/DFF45 expression from bacterial cultures.** Using the pET-15b-DFF40/45 double expression vector, DFF40 and DFF45 protein expression was induced with IPTG in *E. coli* BL21(DE3) cells. The bacterial cells were centrifuged down and resuspended in SDS PAGE sample buffer. Equal amounts of protein were loaded onto a 12% SDS PAGE gel and taken through double immunodetection procedures, as described in materials and methods, with DFF45 and penta-his antibodies which recognised DFF45 and DFF40-his tagged protein, respectively.

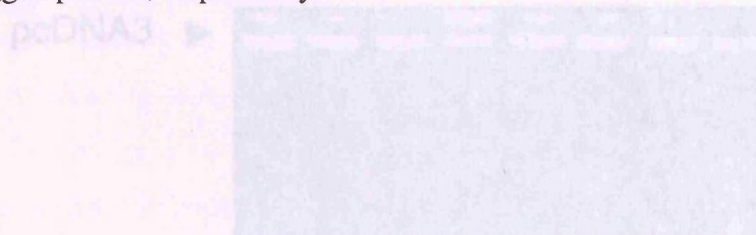
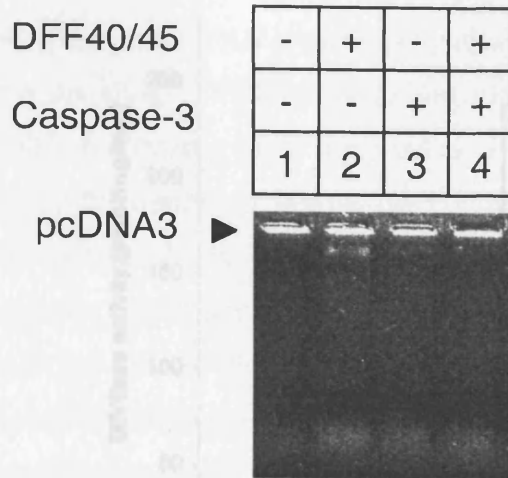


**Figure 6.15 *In vitro* assay for DFF40/45 activity.** pcDNA3 (0 $\mu$ g) was incubated with purified DFF40/45 fusion protein (1 $\mu$ g) and recombinant caspase-3 (500ng) in the (A) absence or (B) presence of histone H1 (2.5 $\mu$ g) for 2h at 37°C in BufferA. The DNA was then loaded onto a 2% agarose gel and stained with ethidium bromide as described in materials and methods.

A



B

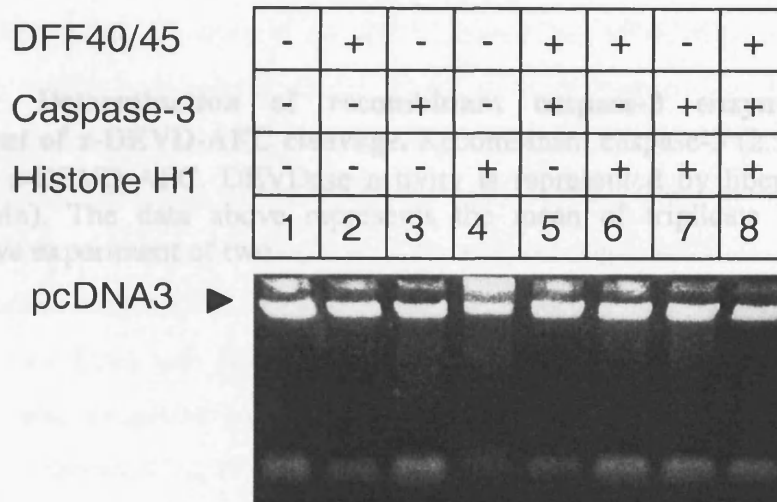


**Figure 6.15** *In vitro* assay for DFF40/45 activity. pcDNA3 (3 $\mu$ g) was incubated with purified DFF40/45 fusion protein (1 $\mu$ g) and recombinant caspase-3 (500ng) in the A) absence or B) presence of histone H1 (2.5 $\mu$ g) for 2h at 37°C in BufferA. The DNA was then loaded onto a 2% agarose gel and stained with ethidium bromide as described in materials and methods.

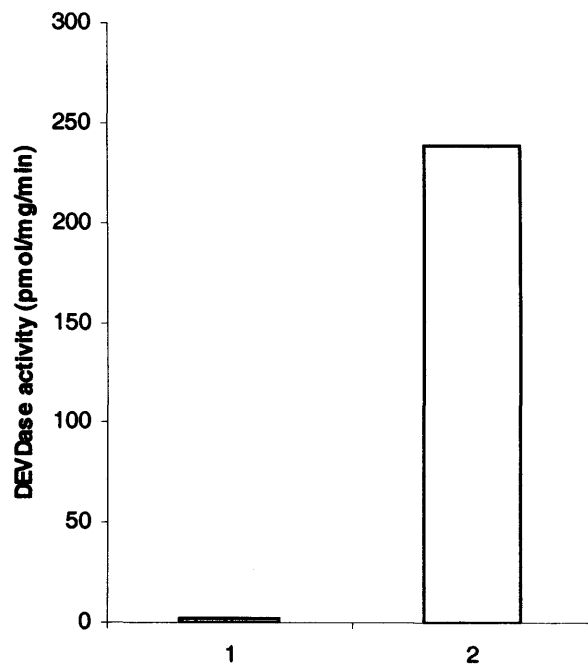


**Figure 6.16 Determination of recombinant caspase-3 enzymatic activity by measurement of z-DEVD-AFC cleavage.** Recombinant caspase-3 (2.5 $\mu$ g) was incubated with 40 $\mu$ M z-DEVD-AFC. DEVDase activity is represented by liberation of free AFC (pmol/mg/min). The data above represents the mean of triplicate samples from one representative experiment of two.

## 6.2 Discussion

During apoptosis genomic DNA is specifically cleaved at the linker regions between adjacent nucleosomes generating 180-200bp oligo/internucleosomal-length DNA fragments which appear as a laddering pattern when separated on a conventional agarose gel (Wyllie, 1980a; Wyllie et al., 1980b; Arends and Wyllie, 1991; Cohen et al., 1992; Compton, 1992). Prior to oligonucleosomal degradation, DNA is sequentially cleaved into distinct >700, 200-250 and 30-50kbp fragments which can be observed by FIGE (Brown et al., 1993; Oberhammer et al., 1993; Cohen et al., 1994). DNA fragmentation is thought to be the result of endonuclease activity(s), however a definitive identity for the endonuclease(s) involved in both HMW and oligonucleosomal-length DNA fragmentation remains elusive. Recent studies have identified DFF45/DFF40 as a key mediator of oligonucleosomal-length DNA fragmentation (Liu et al., 1997b; Enari et al., 1998) but its contribution to the formation of HMW DNA fragmentation is not clear. DFF45/40 is primarily activated by caspase-3 during apoptosis (Liu et al., 1997b; Tang and Kidd, 1998; Sakahira et al., 1998; Enari et al., 1998; Wolf et al., 1999). Using MCF-7 cells which lack caspase-3, the contribution of caspase-3 and DFF40/45 to both oligonucleosomal-length and HMW DNA fragmentation was first examined. In agreement with previous studies, (Tang and Kidd, 1998; Janicke et al., 1998b; Wolf et al., 1999) it was found that after induction of apoptosis with staurosporine, MCF-7 cells do not exhibit oligonucleosomal-length DNA fragmentation. However, analysis of the chromatin by FIGE revealed that the DNA was cleaved into HMW DNA fragments of 50-200kbp, confirming observations that apoptosis can occur in the absence of oligonucleosomal-length DNA fragmentation (Brown et al., 1993; Oberhammer et al., 1993). Furthermore, DFF45 was only partially cleaved to the 31kDa fragment, suggesting that DFF40 was not active. Taken together these results confirm that caspase-3 and DFF are dispensable for HMW DNA fragmentation during apoptosis.

A previous study by Weis et al, (1995) showed that the serine protease inhibitor, TPCK was an effective tool in dissecting HMW and oligonucleosomal-length DNA fragmentation in Jurkat T cells. TPCK has been shown to block DNA fragmentation at the HMW stage, thus preventing the appearance of oligonucleosomal-length DNA fragmentation although the precise mechanism by which it acts remains unclear. Possible targets for TPCK include  $\text{Ca}^{2+}/\text{Mg}^{2+}$  proteolytic activities which have been shown to be involved in DNA

fragmentation (Cohen and Duke, 1984; Cohen et al., 1994). However, TPCK could be acting on either DFF40/45 or caspase-3 to exert its effect on oligonucleosomal length DNA fragmentation. Therefore the effect of TPCK on DNA fragmentation and caspase-3 and DFF40/45 activity during Fas- and staurosporine-induced apoptosis in Jurkat T cells was examined. During both Fas- and staurosporine-mediated apoptosis, low to intermediate concentrations of TPCK caused a potentiation of HMW DNA fragmentation, caspase-3 processing and DFF45 cleavage, whilst completely inhibiting further degradation into oligonucleosomal-length fragments. Caspase-3 was judged to be active by the cleavage of PARP and the caspase-3 fluorogenic substrate z-DEVD-AFC. In addition DFF45 was also cleaved to the 11kDa fragment which is used to denote nuclease activity (Liu et al., 1997b). This was surprising, as the associated oligonucleosomal length DNA fragmentation was not observed.

Therefore, the results presented in this chapter imply that DFF40 and caspase-3 activity are not required for HMW DNA fragmentation and suggest that further caspase-independent protease activities may also play a role in the formation of HMW DNA fragments during apoptosis (Weiss et al., 1995; Hughes et al., 1998b). In addition, the serine protease inhibitor TPCK has been shown to inhibit oligonucleosomal-length DNA fragmentation by potentially inhibiting caspase-3 activity. These results suggest that DFF-dependent and -independent mechanisms may contribute to the formation of oligonucleosomal-length and HMW DNA fragment formation during receptor- and chemical-induced apoptosis.

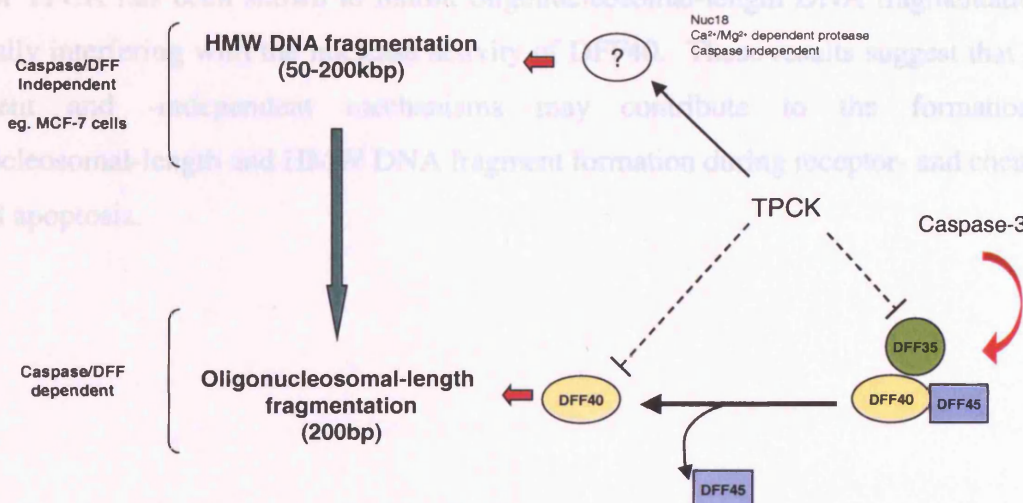


**Figure 6.17 Temporal scheme for the potential role of TPCK in the regulation of DFF40/45 activity and HMW and oligonucleosomal-length DNA fragmentation.** TPCK could prevent oligonucleosomal-length DNA fragmentation by directly inhibiting DFF40 nuclease activity and/or preventing the cleavage and release of inhibitory molecules such as DFF45/35 (dashed lines). In parallel, TPCK could also potentiate the cleavage of DNA into HMW fragments by acting on, an as yet unidentified, caspase-independent protease activity.

A number of explanations can be drawn from the presented data with regard to the action of TPCK on caspase-3 mediated DFF40 activity and HMW and oligonucleosomal-length DNA

fragmentation (Figure 6.17). TPCK could be acting on an as yet undefined protease to induce HMW DNA fragmentation during Fas- and staurosporine-induced apoptosis in Jurkat T cells, which based on the MCF-7 cell data, is likely to be independent of caspase-3 and DFF40 activity. In parallel, these results suggest that once released from DFF45, the nuclease activity of DFF40 may be a target of TPCK, thus preventing the cleavage of DNA into oligonucleosomal-length fragments. Alternatively, TPCK could be acting on a further protease activity(s) which acts in concert with, or downstream of DFF40/45 activation. Recently DFF35, a DFF45 isoform, has been shown to inhibit DFF40 nuclease activity in addition to DFF45. TPCK could potentially prevent the cleavage and inactivation of DFF35 by caspase-3, thus preventing complete DFF40 release and activation (Gu et al., 1999). The exact effect of TPCK on DFF40/45 activity could not be determined in this study. However, taken together, the results presented in this chapter imply that DFF40 and caspase-3 activity are not required for HMW DNA fragmentation and suggest that further caspase-independent protease activities may also play a role in the formation of HMW DNA fragment formation during apoptosis (Weis et al., 1995; Hughes et al., 1998b). In addition, the serine protease inhibitor TPCK has been shown to inhibit oligonucleosomal-length DNA fragmentation by potentially interfering with the nuclease activity of DFF40. These results suggest that DFF-dependent and -independent mechanisms may contribute to the formation of oligonucleosomal-length and HMW DNA fragment formation during receptor- and chemical-induced apoptosis.

## **CHAPTER SEVEN**

### **GENERAL DISCUSSION**

## 7.0 General Discussion

In order to understand the process of apoptosis the signalling events which occur downstream of the death inducing stimulus must be determined. Recent research has focused specifically upon one of two basic apoptotic pathways which signal via the mitochondria or through death receptors on the cell surface (Green, 1998a). Despite this divergence in upstream signalling, chemical and receptor-mediated apoptosis converge at the level of effector caspase activation and ultimately result in similar apoptotic morphologies. Chemical-mediated apoptosis often signals via the mitochondria in a cytochrome c dependent manner (Li et al., 1997) whilst receptor-mediated apoptosis results in direct activation of caspase-8 at the DISC, although this signal can also be amplified via the mitochondria (Medema et al., 1997; Kuwana et al., 1998). The results presented in this thesis provide an integrated view of the regulation of chemical and receptor-mediated apoptosis and their associated biochemical and morphological changes in Jurkat T cells using various inhibitors of apoptosis such as Bcl-2 and peptide-based caspase inhibitors.

In chapter three the effect of differential Bcl-2 overexpression on chemical and receptor-mediated apoptosis in Jurkat T cells was examined. Bcl-2 has been shown to be effective in the inhibition of apoptosis which signals via the mitochondria preventing cytochrome c release (Kluck et al., 1997; Yang et al., 1997; Bossy-Wetzler et al., 1998). However the ability of Bcl-2 to consistently inhibit receptor-mediated apoptosis remains controversial (Itoh et al., 1993; Armstrong et al., 1996; Chinnaiyan et al., 1996). One explanation for these effects could be the differential overexpression of Bcl-2 in the systems examined. Therefore, to test this hypothesis, a number of Bcl-2 overexpressing clones were generated which expressed Bcl-2 to various levels (between 3- and 7-fold) above control cells in order to study the effect of differential Bcl-2 overexpression on Fas and staurosporine-mediated apoptosis. There was an inhibition of both staurosporine and Fas-mediated apoptosis in a manner, which was to some extent, dependent upon the level of protein expressed. However, high levels of Bcl-2 expression such as those expressed in clone J-Bcl-2/A8, had no significant effect on apoptosis induced by either stimulus. The pattern of caspase processing was also examined in Bcl-2 overexpressing cells treated with either staurosporine or anti-Fas and revealed different caspase signalling pathways. During

staurosporine induced apoptosis, caspase-2, -3, -6 and -8 processing was reduced in clones J-Bcl-2/C6.1, J-Bcl-2/C4.1 and J-Bcl-2/C5.2, but less so in clone J-Bcl-2/A8. These observations are in agreement with studies which show that Bcl-2 can inhibit chemical-induced apoptosis at the level of cytochrome c release upstream of caspase activation (Kluck et al., 1997; Yang et al., 1997; Kluck et al., 1997). However, during Fas-mediated apoptosis Bcl-2 appeared to function at a point downstream of caspase-8 activation, as large amounts of caspase-8 processing were observed irrespective of the ability of each clone to inhibit apoptosis. Studies by Scaffidi et al., 1998, define Jurkat T cells as type II cells. Type II cells activate a small amount of caspase-8 at the DISC which is sufficient to stimulate the release of cytochrome c from the mitochondria to amplify the original signal, whereas type I cells signal directly from the death receptor (Scaffidi et al., 1998). Therefore Bcl-2 is proposed to be more effective in the inhibition of receptor-mediated apoptosis in type II cells which signal via the mitochondria (Scaffidi et al., 1999). The results presented in chapter three confirmed that caspase-8 was the apical caspase activated during receptor mediated apoptosis (Muzio et al., 1996; Boldin et al., 1996; Juo et al., 1998) and suggest that Bcl-2 acts at a point downstream of caspase-8 activation to exert its anti-apoptotic effect in the Jurkat T cell line used in this study, which is in agreement with previous findings (Boesen-de Cock et al., 1999). Another potential target for Bcl-2 is Bid, which is cleaved by caspase-8 during receptor-mediated apoptosis and translocates to the nucleus causing cytochrome c release and amplification of the original signal (Luo et al., 1998; Kuwana et al., 1998; Li et al., 1998). The mechanism by which Bcl-2 inhibits Fas-mediated apoptosis in the Jurkat T cell line could also involve the inhibition of cytochrome c release from the mitochondria (Kluck et al., 1997; Yang et al., 1997; Kluck et al., 1997). A number of studies have also shown that Bcl-2 can act downstream of cytochrome c release and delay apoptosis even when cytochrome c is present in the cytosol (Rosse et al., 1998; Zhivotovsky et al., 1998). Thus Bcl-2 appears to be acting at different control points to inhibit staurosporine- and Fas-mediated apoptosis. Furthermore, high expression levels of the Bcl-2 protein may not always be predictive of anti-apoptotic activity as clone J-Bcl-2/A8 did not significantly inhibit either staurosporine- or Fas-mediated apoptosis. This observation is not unique as similar findings have been reported in photoreceptor cells in Bcl-2 transgenic mice (Chen et al., 1996) and in 293 cells which have been enforced to overexpress Bcl-2 (Uhlmann.E.J. et al., 1998).

The effect of Bcl-2 was also examined in Jurkat cells stimulated to undergo AICD. Previous studies have shown that Bcl-2 is able to inhibit AICD induced by a number of stimuli by maintaining calcium homeostasis in the ER (He et al., 1997; Berridge et al., 1998). Bcl-2 significantly inhibited AICD and caspase-8 processing, suggesting that in this situation Bcl-2 may be acting at a point upstream of receptor trimerization and caspase-8 signalling. Indeed, it appeared that Bcl-2 was down regulating either the release or production of sFasL, as Bcl-2 overexpressing clones secreted less sFasL into the cell culture supernatants after treatment with either PHA, TPA or TPA and thapsigargin. Interestingly clone J-Bcl-2/A8 which expressed high levels of Bcl-2 inhibited AICD despite being unable to inhibit Fas- and staurosporine-mediated apoptosis. Therefore Bcl-2 may function at different points to inhibit apoptosis depending on the apoptosis-inducing stimuli. Taken together with the results from chapter three, these data suggest that the expression level of Bcl-2 can influence its function. Furthermore, the anti-apoptotic activity of Bcl-2 may not only be dependent upon overexpression *per se*, but could also be influenced by an intracellular Bcl-2 threshold level, beyond which the function and location of Bcl-2 may be altered.

In contrast to Bcl-2, the peptide based caspase inhibitor z-VAD-FMK has been shown to completely inhibit Fas-mediated apoptosis and even promote relatively long term cell survival (Longthorne and Williams, 1997; Ko et al., 2000) by directly blocking caspase-8 activation. However the ability of z-VAD-FMK to inhibit chemical-induced apoptosis which signals via the mitochondria appears to be less definitive (Borner and Monney, 1999). A number of studies have shown that z-VAD-FMK is unable to prevent the release of cytochrome c or the disruption of mitochondrial membrane potential (Zhuang et al., 1998; Benson et al., 1998; Green and Reed, 1998b; Susin et al., 1999; Borner and Monney, 1999), but is still able to inhibit many of the biochemical features of apoptosis. In this study, the effect of the peptide based caspase inhibitors z-VAD-FMK, Ac-YVAD-FMK and z-DEVD-FMK on chemical-induced apoptosis was studied in detail and related to both the biochemical and morphological features of apoptosis. Upon treatment with staurosporine in the absence or presence of caspase inhibitors a novel nuclear morphological change was observed which was characterized by partially condensed chromatin abutting into the nuclear envelope and dilatation of the nuclear envelope and ER. Furthermore, the nuclear morphological change occurred prior to externalisation of

PS, chromatin condensation and DNA laddering and could be dissociated from the formation of HMW DNA fragments and cell shrinkage. Examination of caspase processing revealed that caspase-2, -6, -7, and -8 processing was inhibited in cells displaying the partially condensed nuclear morphology although caspase-3 was processed to the p20 subunit. Further investigations revealed that the nuclear morphological change also occurred in the caspase-3-null cell line, MCF-7, when treated with staurosporine in the absence or presence of z-VAD-FMK. Therefore the appearance of the partially condensed nuclear morphology appeared to be independent of effector caspase activity. In agreement with previous studies, z-VAD-FMK did not prevent the release of cytochrome c or the perturbation of mitochondrial membrane potential in staurosporine-induced apoptosis, suggesting that the novel nuclear morphological change occurred downstream of these events.

When Bcl-2 overexpressing cells were treated with staurosporine the partially condensed nuclear morphology was not observed. Bcl-2 appeared to delay staurosporine-induced apoptosis, as the percentage of apoptosis increased between the 3h and 6h timepoints and viability decreased. However, in the presence of z-VAD-FMK, Bcl-2 delayed the appearance of the partially condensed nuclear morphology and overall cell viability remained high at the 6h timepoint. These results suggest that the partially condensed nuclear morphology occurs downstream of the Bcl-2 checkpoint, which is in agreement with the results showing cytochrome c release and decreased mitochondrial membrane potential in cells displaying this morphology. The data presented in chapter five suggests that a novel morphological change occurs early in the process of chemical-induced apoptosis and may be independent of effector caspase activity. A potential candidate for the mediation of this morphological change is caspase-9. Caspase-9 activation occurs downstream of the mitochondria and cytochrome c release and plays a central role in signalling from the mitochondria to downstream caspases during chemical-induced or mitochondrial-dependent apoptosis (Hakem et al., 1998; Kuida et al., 1998; Slee et al., 1999). Interestingly, caspase-9<sup>-/-</sup> ES cells also show incomplete chromatin condensation (Hakem et al., 1998). The results presented in chapter five suggest that caspase-9 could itself instigate some of the initial morphological changes associated with chemical-induced apoptosis independently of effector caspase activity, although within the confines of this

study the exact molecular cause of the partially condensed nuclear morphology could not be directly determined.

Recent evidence suggests that caspase-independent mechanisms may also play an important role in the co-ordinate appearance of an apoptotic morphology (Williams and Henkart, 1994). These may include the action of non-caspase proteases such as calpains (Squier and Cohen, 1996) cathepsins (Deiss et al., 1996), and serine proteases (Samejima et al., 1998; Hughes et al., 1998a). There is considerable evidence that the cleavage of chromatin into HMW fragments occurs independently of caspase-3 activation and DFF40/45 which degrades DNA into oligonucleosomal-length fragments (Chow et al., 1995; Weis et al., 1995; Kass et al., 1996; Hughes et al., 1998b). Therefore, to examine the involvement of caspase-3 and DFF40/45 in the formation of HMW DNA fragments, MCF-7 cells were utilized as they lack caspase-3. Treatment of MCF-7 cells with staurosporine resulted in apoptosis and a decrease in cell viability. Although no oligonucleosomal-length DNA fragmentation was observed, DNA was cleaved into HMW fragments of 50-300kbp which is in agreement with previous studies (Janicke et al., 1998; Tang and Kidd, 1998). Examination of DFF45 cleavage in these cells revealed that it was partially cleaved to a 31kDa fragment despite extensive caspase-7 processing. These results suggest that HMW DNA fragmentation can occur independently of caspase-3 and DFF40/45 activity and may be mediated by non-caspase dependent processes. Therefore to examine this possibility further, the involvement of non-caspase proteases in the degradation of chromatin during Fas- and staurosporine induced apoptosis was studied using the serine protease inhibitor TPCK. The results presented in chapter six suggest that TPCK inhibits oligonucleosomal length DNA fragmentation by potentially interfering with the nuclease activity of DFF40 whilst simultaneously potentiating the formation of HMW DNA fragments. Therefore, HMW DNA fragmentation appears to be independent of caspase-3 and DFF40/45 but could be regulated by a TPCK-sensitive protease which acts upstream of caspase-3. However the identity of the protease and the exact mechanism by which TPCK mediates HMW DNA fragmentation and inhibits oligonucleosomal-length DNA fragmentation could not be elucidated. Thus the results in chapters five and six suggest that effector caspase activation may not be the only mechanism by which the apoptotic features of apoptosis are mediated and implies a further level of complexity in

the apoptotic cascade as upstream initiator caspases and/or other protease activities may regulate some of the early biochemical and morphological features of apoptosis.

## 7.1 Future work

A number of approaches could be taken to clarify some of the work presented in this thesis. Firstly, the exact mechanism by which Bcl-2 inhibits AICD could be determined. The study of calcium fluxes in response to AICD and more specifically detailed analysis of the transcriptional regulation of FasL and potential interactions between Bcl-2 and calcineurin may provide the necessary answers. Furthermore, the intracellular localization of Bcl-2 in these clones, in response to AICD could be determined by immunofluorescence techniques. These experiments could provide an interesting insight into the action of Bcl-2 in this system. Following on from the work presented in chapter Five, it would be interesting to determine the exact cause of the partially condensed nuclear morphology at the molecular level. As caspase-9 appears to be a potential candidate for mediating this process during chemical-induced apoptosis, a more specific way of inhibiting caspase-9 must be first be established. A possible solution could be the use of antisense or dominant-negative caspase-9 followed by examination of nuclear morphological changes. It would also be important to determine the long-term destiny of staurosporine-treated cells in the presence of z-VAD-FMK. The results presented here show that upon withdrawal of z-VAD-FMK the cells go on to exhibit a fully apoptotic morphology. However, if z-VAD-FMK was maintained in the culture medium, the eventual outcome might not be typical of apoptosis and cells may eventually die by a necrotic-like process (Borner and Monney, 1999). As a continuation of the work presented in chapter six, the exact molecular mechanism of TPCK action during DNA fragmentation could be determined in order to identify the non-caspase proteases which may be involved in these processes.

## **CHAPTER EIGHT**

### **REFERENCES**

## 8.0 Reference List

Adachi, M., Watanabe-Fukunaga, R., and Nagata, S. (1993). Aberant transcription caused by the insertion of an early transposable element in an intron of the Fas antigen gene of lpr mice. *Proc.Natl.Acad.Sci.USA* 90, 1756-1760.

Adams, J.M. and Cory, S. (1998). The Bcl-2 Protein Family: Arbiters of Cell Survival. *Science* 281, 1322-1326.

Akao, Y., Otsuki, Y., Kataoka, S., Ito, Y., and Tsujimoto, Y. (1994). Multiple subcellular localization of bcl-2: detection in nuclear outer membrane, endoplasmic reticulum membrane, and mitochondria membranes. *Cancer Res.* 54, 2468-2471.

Alderson, M.R., Tough, T.W., DavisSmith, T., Braddy, S., Falk, B., Schooley, K.A., Goodwin, R.G., Smith, C.A., Ramsdell, F., and Lynch, D.H. (1995). Fas ligand mediates activation-induced cell death in human T lymphocytes. *Journal of Experimental Medicine* 181, 71-77.

Alles, A., Alley, K., Barrett, J. C., Buttyan, R., Columbano, A., Cope, F. O., Copelan, E. A., Duke, R. C., Farel, P. B., Gerschenson, L. E., Goldgaber, D., Green, D. R., Honn, K. V., Hully, J., Isaacs, J. T., Kerr, J. F. R., Krammer, P. H, Lockshin, R. A., Martin, D. P., McConkey, D. J., Michaelson, J., Schulte-Hermann, R., Server, A. C., Szende, B., Tomei, L. D., Tritton, T. R., Umansky, S. R., Valerie, K., and Warner, H. R. (1991). Apoptosis: a general comment. *FASEB J.* 5, 2127-2128.

Alnemri, E.S., Livingston, D.J., Nicholson, D.W., Salvesen, G.S., Thornberry, N.A., Wong, W.W., and Yuan, J. (1996). Human ICE/CED-3 protease nomenclature. *Cell* 87, 171-171.

Ambrosini, G., Adida, C., and Altieri, D. C. (1997). A novel anti-apoptosis gene, survivin, expressed in cancer and lymphoma. *Nature Medicine* 3, 917-921.

Antonsson, B., Conti, F., Ciavatta, A., Montessuit, S., Lewis, S., Martinou, I., Bernasconi, L., Bernard, A., Mermoud, J.-J., Mazzei, G, Maundrell, K., Gambale, F., Sadoul, R., and Martinou, J.-C. (1997). Inhibition of Bax channel-forming activity by Bcl-2. *Science* 277, 370-372.

Aravind, L., Dixit, V. M., and Koonin, E. V. (1999). The domains of death: evolution of the apoptosis machinery. *Trends in Biochemical Science* 24, 47-53.

Arends, M.J., Morris, R.G., and Wyllie, A.H. (1990). Apoptosis - The role of the endonuclease. *Am.J.Pathol.* 136, 593-608.

Arends, M.J. and Wyllie, A.H. (1991). Apoptosis: Mechanisms and Roles in Pathology. *Int.Rev.Exper.Pathol.* 32, 223-254.

Armstrong, R.C., Aja, T., Xiang, J., Gaur, S., Krebs, J.F., Hoang, K., Bai, X., Korsmeyer, S.J., Karanewsky, D.S., Fritz, L.C., and Tomaselli, K.J. (1996). Fas-induced activation of the cell death-related protease cpp32 is inhibited by bcl-2 and by ice family protease inhibitors. *J.Biol.Chem.* 271, 16850-16855.

- Ashkenazi, A. and Dixit, V. M. (1998). Death receptors: signalling and modulation. *Science* 281, 1305-1309.
- Bakhshi, A., Jensen, J. P., Goldman, P., Wright, J. J., McBride, O. W., Epstein, A. L., and Korsmeyer, S. J. (1995). Cloning the chromosomal breakpoint of t(14:18) human lymphomas: clustering around JH on chromosome 14 and near a transcriptional unit on 18. *Cell* 41, 899-906.
- Barry, M.A. and Eastman, A. (1993). Identification of deoxyribonuclease II as an endonuclease involved in apoptosis. *Arch.Biochem.Biophys.* 300, 440-445.
- Beere, H.M., Chresta, C.M., Alejo-Herberg, A., Skladanowski, A., Dive, C., Larsen, A.K., and Hickman, J.A. (1995). Investigation of the mechanism of higher order chromatin fragmentation observed in drug-induced apoptosis. *Mol.Pharmacol.* 47, 986-996.
- Benson, R. S. P., Dive, C., and Watson, A. J. M. (1998). Comparative effects of Bcl-2 over-expression and ZVAD.FMK treatments on dexamethasone and VP16-induced apoptosis in CEM cells. *Cell Death & Differentiation* 5, 432-439.
- Benson, R. S. P., Heer, S., Dive, C., and Watson, A. J. M. (1996). Characterization of cell volume loss in CEM-C7A cells during dexamethasone-induced apoptosis. *American Journal of Physiology - Cell Physiology* 270, 1190-1203.
- Berridge, M.J. (1987). Inositol trisphosphate and diacylglycerol: two interacting second messengers. *Annu.Rev.Biochem.* 56, 159-193.
- Berridge, M.J., Bootman, M. D., and Lipp, P. (1998). Calcium - a life and death signal. *Nature* 395, 645-648.
- Berridge, M.J. and Irvine, R. F. (1989). Inositol phosphates and cell signalling. *Nature* 341, 197-205.
- Bertrand, R., Solary, E., O'Connor, P., Kohn, K.W., and Pommier, Y. (1994). Induction of a common pathway of apoptosis by staurosporine. *Exp.Cell Res.* 211, 314-321.
- Bissonnette, R.P., Echeverri, F., Mahboubi, A., and Green, D.R. (1992). Apoptotic cell death induced by *c-myc* is inhibited by *bcl-2*. *Nature* 359, 552-554.
- Boesen-de Cock, J. G. R., Tepper, A. D, De Vries, E., van Blitterswijk, W. J, and Borst, J. (1999). Common regulation of apoptosis signalling induced by CD95 and the DNA-damaging stimuli etoposide and  $\gamma$ -radiation downstream of caspase-8 activation. *Journal of Biological Chemistry* 274, 14255-14261.
- Boldin, M.P., Goncharov, T.M., Goltsev, Y.V., and Wallach, D. (1996). Involvement of mach, a novel mort1/fadd-interacting protease, in Fas/APO-1- and TNF receptor-induced cell death. *Cell* 85, 803-815.
- Boldin, M.P., Varfolomeev, E.E., Pancer, Z., Mett, I.L., Camonis, J.H., and Wallach, D. (1995). A novel protein that interacts with the death domain of as/APO-1 contains a sequence motif related to the death domain. *J.Biol.Chem.* 270, 7795-7798.

- Borner, C. (1996). Diminished cell proliferation associated with the death-protective activity of Bcl-2. *J.Biol.Chem.* 271, (pp 12695-12698).
- Borner, C., Martinou, I., Mattmann, C., Irmeler, M., Schaerer, E., Martinou, J.-C., and Tschopp, J. (1994). The protein bcl-2 $\alpha$  does not require membrane attachment, but two conserved domains to suppress apoptosis. *J.Cell Biology* 126, 1059-1068.
- Borner, C. and Monney, L. (1999). Apoptosis without caspases: an inefficient molecular guillotine? *Cell Death & Differentiation* 6, 497-507.
- Bortner, C. D. and Cidlowski, J. A. (1999). Caspase independent/dependent regulation of K<sup>+</sup> cell shrinkage, and mitochondrial membrane potential during lymphocyte apoptosis. *Journal of Biological Chemistry* 274, 21953-21962.
- Bossy-Wetzell, E., Newmeyer, D.D., and Green, D.R. (1998). Mitochondrial cytochrome c release in apoptosis occurs upstream of DEVD-specific caspase activation and independently of mitochondrial transmembrane depolarization. *EMBO J.* 17, 37-49.
- Brady, H.J.M., Gil-Gomez, G., Kirberg, J., and Berns, A.J.M. (1996). Bax $\alpha$  perturbs T cell development and affects cell cycle entry of T cells. *EMBO J.* 15, 6991-7001.
- Brancolini, C., Benedetti, M., and Schneider, C. (1995). Microfilament reorganization during apoptosis: the role of gas2, a possible substrate for ice-like proteases. *EMBO J.* 14, 5179-5190.
- Brancolini, C., Lazarevic, D., Rodriguez, J., and Schneider, C. (1997). Dismantling cell-cell contacts during apoptosis is coupled to a caspase-dependent proteolytic cleavage of beta-catenin. *Journal of Cell Biology* 139, (pp 759-771).
- Broccoli, D., Young, J.W., and De Lange, T. (1995). Telomerase activity in normal and malignant hematopoietic cells. *Proceedings of the National Academy of Sciences of the United States of America* 92, 9082-9086.
- Brown, D.G., Sun, X.-M., and Cohen, G.M. (1993). Dexamethasone-induced apoptosis involves cleavage of DNA to large fragments prior to internucleosomal fragmentation. *J.Biol.Chem.* 268, 3037-3039.
- Brunner, T., Mogil, R.J., LaFace, D., Yoo, N.J., Mahboubi, A., Echeverri, F., Martin, S.J., Force, W.R., Lynch, D.H., Ware, C.F., and Green, D.R. (1995). Cell-autonomous Fas (CD95)/Fas-ligand interaction mediates activation-induced apoptosis in T-cell hybridomas. *Nature* 373, 441-444.
- Brustugun, O. T., Fladmark, K. E., Døskeland, S. O., Orrenius, S., and Zhivotovsky, B. (1998). Apoptosis induced by microinjection of cytochrome c is caspase-dependent and is inhibited by Bcl-2. *Cell Death & Differentiation* 5, 660-668.
- Buja, L.M., Eigenbrodt, M.L., and Eigenbrodt, E.H. (1993). Apoptosis and necrosis: Basic types and mechanisms of cell death. *Arch.Pathol.Lab.Med.* 1208-1214.
- Bump, N.J., Hackett, M., Hugunin, M., Seshagiri, S., Brady, K., Chen, P., Ferenz, C., Franklin, S., Ghayur, T., Li, P., Licari, P., Mankovich, J., Shi, L., Greenberg, A.H., Miller,

- L.K., and Wong, W.W. (1995). Inhibition of ice family proteases by baculovirus antiapoptotic protein p35. *Science* 269, 1885-1888.
- Cantrell, D. T (1996). Cell antigen receptor signal transduction pathways. *Annu.Rev.Immunol.* 14, 259-274.
- Cardone, M.H., Salvesen, G.S., Widmann, C., Johnson, G., and Frisch, S.M. (1997). The regulation of anoikis: MEKK-1 activation requires cleavage by caspases. *Cell* 90, 315-323.
- Carle and Olsen, (1986). *Gel Electrophoresis of nucleic acids -A practical approach*, Edited by D.Rickwood and B.D.Hames.
- Casciola-Rosen, L., Nicholson, D.W., Chong, T., Rowan, K.R., Thornberry, N.A., Miller, D.K., and Rosen, A. (1996). Apopain/ CPP32 cleaves proteins that are essential for cellular repair: A fundamental principle of apoptotic death. *Journal of Experimental Medicine* 183, 1957-1964.
- Cecconi, F., Alvarez-Bolado, G., Meyer, B. I., Roth, K. A., and Gruss, P. (1998). Apaf-1 (Ced-4 homolog) regulates programmed cell death in mammalian development. *Cell* 94, 727-737.
- Cerretti, D.P., Kozlosky, C.J., Mosley, B., Nelson, N., Van Ness, K., Greenstreet, T.A., March, C.J., Kronheim, S.R., Druck, T., Cannizzaro, L.A., Huebner, K., and Black, R.A. (1992). Molecular cloning of the interleukin-1beta converting enzyme. *Science* 256, 97-100.
- Chang, B.S., Minn, A.J., Muchmore, S.W., Fesik, S.W., and Thompson, C.B. (1997). Identification of a novel regulatory domain in Bcl-x(L) and Bcl-2. *EMBO J.* 16, 968-977.
- Chao, D.T. and Korsmeyer, S.J. (1998). BCL-2 family: Regulators of cell death. *Annual Review of Immunology* 16, 395-419.
- Chao, D.T., Linette, G.P., Boise, L.H., White, L.S., Thompson, C.B., and Korsmeyer, S.J. (1995). Bcl-x(L) and Bcl-2 repress a common pathway of cell death. *Journal of Experimental Medicine* 182, (pp 821-828).
- Chen-Levy, Z., Nourse, J., and Cleary, M.L. (1989). The bcl-2 candidate proto-oncogene product is a 24-kilodalton integral -membrane protein highly expressed in lymphoid cell lines and lymphomas carrying the t(14;18) translocation. *Mol.Cell.Biol.* 9, 701-710.
- Chen, J., Flannery, J.G., LaVail, M.M., Steinberg, R.H., Xu, J., and Simon, M.I. (1996). bcl-2 overexpression reduces apoptotic photoreceptor cell death in three different retinal degenerations. *Proceedings of the National Academy of Sciences of the United States of America* 93, 7042-7047.
- Cheng, E.H.-Y., Kirsch, D.G., Clem, R.J., Ravi, R., Kastan, M.B., Bedi, A., Ueno, K., and Hardwick, J.M. (1997). Conversion of Bcl-2 to a bax-like death effector by caspases. *Science* 278, 1966-1968.

- Cheng, E.H.-Y., Levine, B., Boise, L.H., Thompson, C.B., and Hardwick, J.M. (1996). Bax-independent inhibition of apoptosis by Bcl-x(L). *Nature* 379, 554-556.
- Chinnaiyan, A.M., Chaudhary, D., O'Rourke, K., Koonin, E.V., and Dixit, V.M. (1997). Role of CED-4 in the activation of CED-3. *Nature* 388, 728-729.
- Chinnaiyan, A.M., O'Rourke, K., Tewari, M., and Dixit, V.M. (1995). FADD, a novel death domain-containing protein, interacts with the death domain of FAS and initiates apoptosis. *Cell* 81, 505-512.
- Chinnaiyan, A.M., O'Rourke, K., Lane, B.R., and Dixit, V.M. (1997). Interaction of ced-4 with ced-3 and ced-9: a molecular framework for cell death. *Science* 275, 1122-1126.
- Chinnaiyan, A.M., Orth, K., O'Rourke, K., Duan, H., Poirier, G.G., and Dixit, V.M. (1996). Molecular ordering of the cell death pathway. Bcl-2 and Bcl-x(L) function upstream of the CED-3-like apoptotic proteases. *J.Biol.Chem.* 271, 4573-4576.
- Chittenden, T., Harrington, E.A., O'Connor, R., Flemington, C., Lutz, R.J., Evan, G.I., and Guild, B.C. (1995). Induction of apoptosis by the Bcl-2 homologue Bak. *Nature* 374, 733-736.
- Chiu, V.K., Walsh, C.M., Liu, C.C., Reed, J.C., and Clark, W.R. (1995). Bcl-2 blocks degranulation but not fas-based cell-mediated cytotoxicity. *Journal of Immunology* 154, 2023-2032.
- Chou, J. J., Matsuo, H., Duan, H., and Wagner, G. (1998). Solution structure of the RAIDD CARD and model for CARD/CARD interaction in caspase-2 and caspase-9 recruitment. *Cell* 94, 171-180.
- Chow, S. C., Slee, E. A., MacFarlane, M., and Cohen, G. M. (1999). Caspase-1 is not involved in CD95/Fas-induced apoptosis in Jurkat T cells. *Exp.Cell Res.* 246, 491-500.
- Chow, S.C., Weis, M., Kass, G.E.N., Holmström, T.H., Eriksson, J.E., and Orrenius, S. (1995). Involvement of multiple proteases during Fas-mediated apoptosis in T lymphocytes. *FEBS Lett.* 364, 134-138.
- Chu, J.L., Drappa, J., Parnassa, A., and Elkon, K.B. (1993). The defect in fas mRNA expression in mrl/lpr mice is associated with insertion of the retrotransposon, etn. *Journal of Experimental Medicine* 178, 723-730.
- Cleary, M. L., Smith, S. D., and Sklar, L. A. (1986). Cloning and structural analysis of cDNA's for bcl-2/immunoglobulin transcript resulting from the t(14:18) translocation. *Cell* 47, 19-28.
- Clem, R.J., Cheng, E.H.-Y., Karp, C.L., Kirsch, D.G., Ueno, K., Takahashi, A., Kastan, M.B., Griffin, D.E., Earnshaw, W.C., Veluona, M.A., and Hardwick, J.M. (1998). Modulation of cell death by Bcl-x(L) through caspase interaction. *Proceedings of the National Academy of Sciences of the United States of America* 95, 554-559.
- Clem, R.J., Fecheimer, M., and Miller, L.K. (1991). Prevention of apoptosis by a baculovirus gene during infection of insect cells. *Science* 254, 1388-1390.

- Clem, R. J. and Miller, L. K. (1994). Control of cell death by the baculovirus genes p35 and iap. *Molecular and Cellular Biology* 14, 5212-5222.
- Cohen, G.M. (1997). Caspases: The executioners of apoptosis. *Biochem.J.* 326, 1-16.
- Cohen, G.M., Sun, X.-M., Fearnhead, H., MacFarlane, M., Brown, D.G., Snowden, R.T., and Dinsdale, D. (1994). Formation of large molecular weight fragments of DNA is a key committed step of apoptosis in thymocytes. *J.Immunol.* 153, 507-516.
- Cohen, G.M., Sun, X.-M., Snowden, R.T., Dinsdale, D., and Skilleter, D.N. (1992). Key morphological features of apoptosis may occur in the absence of internucleosomal DNA fragmentation. *Biochem.J.* 286, 331-334.
- Cohen, G.M., Sun, X.-M., Snowden, R.T., Ormerod, M.G., and Dinsdale, D. (1993). Identification of a transitional preapoptotic population of thymocytes. *J.Immunol.* 151, 566-574.
- Cohen, J.J. (1993). Apoptosis. *Immunology Today* 14, 126-130.
- Cohen, J.J. and Duke, R.C. (1984). Glucocorticoid activation of a calcium-dependent endonuclease in thymocyte nuclei leads to cell death. *J.Immunol.* 132, 38-42.
- Cohen, P.L. and Eisenberg, R.A. (1992). The lpr and gld genes in systemic autoimmunity: life and death in the fas lane. *Immunology Today* 13, 427-428.
- Compton, M. (1999). The mitochondrial permeability transition pore and its role in cell death. *Biochemical Journal* 341, 233-249.
- Compton, M. M. (1992). A biochemical hallmark of apoptosis: Internucleosomal degradation of the genome. *Cancer and Metastasis Reviews* 11, 105-119.
- Conradt, B. and Horvitz, H. R. (1998). The *C.elegans* protein Egl-1 is required for programmed cell death and interacts with the Bcl-2-like protein CED-9. *Cell* 93, 519-529.
- Crook, N. E., Clem, R. J., and Miller, L. K. (1993). An apoptosis-inhibiting baculovirus gene with a zinc finger-like motif. *Journal of Virology* 67, 2168-2174.
- Cryns, V. and Yuan, J. (1998). Proteases to die for. *Genes & Development* 12, 1551-1570.
- D'Souza, S. D., Bonetti, B., Balasingham, V., Cashman, N. R., Barker, P. A., Troutt, A. B., Raine, C. S., and Antel, J. P. (1996). Multiple sclerosis: Fas signalling in oligodendrocyte cell death. *J.Exp.Med.* 184, 2361-2370.
- Datta, R., Kojima, H., Yoshida, K., and Kufe, D. (1997). Caspase-3-mediated cleavage of protein kinase C theta in induction of apoptosis. *J.Biol.Chem.* 272, 20317-20320.
- Debatin, K-M., Fähring-Faissner, A., Enenkel-Stoodt, S., Kreuz, W., Benner, A., and Krammer, P. H. (1994). High expression of APO-1 (CD95) on T lymphocytes from HIV-1-infected children. *Blood* 83, 3101-3105.

- Deiss, L.P., Galinka, H., Berissi, H., Cohen, O., and Kimchi, A. (1996). Cathepsin D protease mediates programmed cell death induced by interferon-gamma, Fas/APO-1 and TNF-alpha. *EMBO J.* 15, 3861-3870.
- Deng, G. and Podack, E. R. (1993). Suppression of apoptosis in a cytotoxic T-cell line by interleukin-1-mediated gene transcription and deregulated expression of the protooncogene bcl-2. *Proc.Natl.Acad.Sci.USA* 90, 2189-2196.
- Deveraux, Q.L., Roy, N., Stennicke, H.R., Van Arsdale, T., Zhou, Q., Srinivasula, S.M., Alnemri, E.S., Salvesen, G.S., and Reed, J.C. (1998). IAPs block apoptotic events induced by caspase-8 and cytochrome c by direct inhibition of distinct caspases. *EMBO J.* 17, 2215-2222.
- Deveraux, Q.L., Takahashi, R., Salvesen, G.S., and Reed, J.C. (1997). X-linked IAP is a direct inhibitor of cell-death proteases. *Nature* 388, 300-304.
- Devitt, A., Moffatt, O. D, Raykundalia, C D, Capra J, Simmons, D. L, and Gregory, C. D. (2000). Human CD14 mediates recognition and phagocytosis of apoptotic cells. *Nature* 392, 505-509.
- Dhein, J., Walczak, H., Bäumer, C., Debatin, K.-M., and Krammer, P.H. (1995). Autocrine T-cell suicide mediated by apo-1/(Fas/CD95). *Nature* 373, 438-441.
- Dowling, P., Shang, G., Ravel, S., Menonna, J., Cook, S., and Husar, W. (1996). Involvement of the CD95 (APO-1/Fas) receptor/ligand system in multiple sclerosis brain. *J.Exp.Med.* 184, 1513-1518.
- Duan, H., Chinnaiyan, A.M., Hudson, P.L., Wing, J.P., He, W.W., and Dixit, V.M. (1996). Ice-lap3, a novel mammalian homologue of the caenorhabditis elegans cell death protein ced-3 is activated during fas- and tumor necrosis factor- induced apoptosis. *J.Biol.Chem.* 271, 1621-1625.
- Duan, H. and Dixit, V.M. (1997). RAIDD is a new 'death' adaptor molecule. *Nature* 385, 86-89.
- Duan, H., Orth, K., Chinnaiyan, A.M., Poirier, G.G., Froelich, C.J., He W, W., and Dixit, V.M. (1996). Ice-lap6, a novel member of the ice/ced-3 gene family, is activated by the cytotoxic t cell protease granzyme b. *J.Biol.Chem.* 271, 16720-16724.
- Duckett, C.S., Nava, V.E., Gedrich, R.W., Clem, R.J., Van Dongen, J.L., Gilfillan, M.C., Shiels, H., Hardwick, J.M., and Thompson, C.B. (1996). A conserved family of cellular genes related to the baculovirus iap gene and encoding apoptosis inhibitors. *EMBO J.* 15, 2685-2694.
- Earnshaw, W.C. (1995). Apoptosis: lessons from *in vitro* systems. *Trends Cell Biol.* 5, 217-220.
- Eberstadt, M., Huang, B., Chen, Z., Meadows, R. P., Ng, S-C., Zheng, L., Lenardo, M. J., and Fesik, S. W. (1998). NMR structure and mutagenesis of the FADD (Mort1) death-effector domain. *Nature* 293, 941-945.

Ellis, H.M. and Horvitz, H.R. (1986). Genetic Control of Programmed Cell Death in the Nematode *C. Elegans*. *Cell* 44, 817-829.

Ellis, R. E, Yuan, J., and Horvitz, H. R. (1991). Mechanisms and functions of cell death. *Annual Review of Cell Biology* , 663-698.

Emoto, Y., Manome, Y., Meinhardt, G., Kisaki, H., Kharbanda, S., Robertson, M., Ghayur, T., Wong, W.W., Kamen, R., Weichselbaum, R., and Kufe, D. (1995). Proteolytic activation of protein kinase c delta by an ice-like protease in apoptotic cells. *EMBO J.* 14, 6148-6156.

Enari, M., Hug, H., and Nagata, S. (1995). Involvement of an ICE-like protease in Fas-mediated apoptosis. *Nature* 375, 78-81.

Enari, M., Sakahira, H., Yokoyama, H., Okawa, K., Iwamatsu, A., and Nagata, S. (1998). A caspase-activated DNase that degrades DNA during apoptosis, and its inhibitor ICAD. *Nature* 391, 43-50.

Enari, M., Talanian, R.V., Wong, W.W., and Nagata, S. (1996). Sequential activation of ice-like and cpp32-like proteases during fas-mediated apoptosis. *Nature* 380, 723-726.

Eriksson, J.E., Paatero, G.I.L., Meriluoto, J.A.O., Codd, G.A., Kass, G.E.N., Nicotera, P., and Orrenius, S. (1989). Rapid microfilament reorganization induced in isolated rat hepatocytes by microcystin-LR, a cyclic peptide toxin. *Exp.Cell Res.* 185, 86-100.

Estoppey, S., Rodriguez, I., Sadoul, R., and Martinou, J.-C. (1997a). Bcl-2 prevents activation of CPP32 cysteine protease and cleavage of poly (ADP-ribose) polymerase and U1-70 kD proteins in staurosporine-mediated apoptosis. *Cell Death & Differentiation* 4, 34-38.

Estoppey, S., Rodriguez, I., Sadoul, R., and Martinou, J.C. (1997b). Bcl-2 prevents activation of cpp32 cysteine protease and cleavage of poly (adp-ribose) polymerase and u1-70 kd proteins in staurosporine- mediated apoptosis. *Cell Death Different.* 4, 34-38.

Evan, G.I., Brown, L., Whyte, M., and Harrington, E. (1995). Apoptosis and the cell cycle. *Current Opinion in Cell Biology* 7, 825-834.

Evan, G.I., Wyllie, A.H., Gilbert, C.S., Littlewood, T.D., Land, H., Brooks, M., Waters, C.M., Penn, L.Z., and Hancock, D.C. (1992). Induction of Apoptosis in Fibroblasts by c-myc Protein. *Cell* 69, 119-128.

Fadok, V. A, Bratton, D. L, Rose, D. L, Pearson, A, Ezekewitz, A. B, and Hanson, P. M. (2000). A receptor for phosphatidylserine-specific clearance of apoptotic cells. *Nature* 405, 85-90.

Fadok, V. A, Voelker, D. R., Campbell, P. A., Cohen, J. J., Bratton, D. L, and Henson, P. M. (1992). Exposure of phosphatidylserine on the surface of apoptotic lymphocytes triggers specific recognition and removal by macrophages. *J.Immunol.* 148, 2207-2216.

- Faucheu, C., Blanchet, A.M., CollardDutilleul, C., Lalanne, J.L., and DiuHercend, A. (1996). Identification of a cysteine protease closely related to interleukin-1 $\beta$ -converting enzyme. *Eur.J.Biochem.* 236, 207-213.
- Faucheu, C., Diu, A., Chan, A.W.E., Blanchet, A.-M., Miossec, C., Hervé, F., Collard-Dutilleul, V., Gu, Y., Aldape, R.A., Su, M.S.S., Livingston, D.J., Hercend, T., and Lalanne, J.-L. (1995). A novel human protease similar to the interleukin-1 $\beta$  converting enzyme induces apoptosis in transfected cells. *EMBO J.* 14, 1914-1922.
- Fernandes-Alnemri, T., Armstrong, R.C., Krebs, J., Srinivasula, S.M., Wang, L., Bullrich, F., Fritz, L.C., Trapani, J.A., Tomaselli, K.J., Litwack, G, and Alnemri, E.S. (1996). In vitro activation of CPP32 and Mch3 by Mch4, a novel human apoptotic cysteine protease containing two FADD-like domains. *Proceedings of the National Academy of Sciences of the United States of America* 93, 7464-7469.
- Fernandes-Alnemri, T., Takahashi, A., Armstrong, R., Krebs, J., Fritz, L., Tomaselli, K.J., Wang, L., Yu, Z., Croce, C.M., Salvesen, G.S., Earnshaw, W.C., Litwack, G., and Alnemri, E.S. (1995). Mch3, a novel human apoptotic cysteine protease highly related to CPP32. *Cancer Res.* 55, 6045-6052.
- Fernandes Alnemri, T., Takahashi, A., Armstrong, R., Krebs, J.F., Fritz, L.C., Tomaselli, K.J., Wang, L., Yu, Z., Croce, C.M., Salvesen, G.S., Earnshaw, W.C., Litwack, G., and Alnemri, E.S. (1995). Mch3, a novel human apoptotic cysteine protease highly related to CPP32. *Cancer Res.* 55, 6045-6052.
- FernandesAlnemri, T., Litwack, G., and Alnemri, E.S. (1995). Mch2, a new member of the apoptotic ced-3/ice cysteine protease gene family. *Cancer Res.* 55, 2737-2742.
- Fernandez-Alnemri, T., Litwack, G., and Alnemri, E.S. (1994). CPP32, a novel human apoptotic protein with homology to *caenorhabditis elegans* cell death protein ced-3 and mammalian interleukin-1 $\beta$ -converting enzyme. *J.Biol.Chem.* 269, 30761-30764.
- Fine, A., Anderson, N.L., Rothstein, T.L., Williams, M.C., and Gochuico, B.R. (1997). Fas expression in pulmonary alveolar type II cells. *American Journal of Physiology - Lung Cellular & Molecular Physiology* 273, L64-L71.
- Finucane, D. M., Bossy-Wetzel, E., Waterhouse, N. J., Cotter, T. G., and Green, D. R. (1999). Bax-induced caspase activation and apoptosis via cytochrome c release from mitochondria is inhibitable by Bcl-xL. *Journal of Biological Chemistry* 274, 2225-2233.
- Fisher, G. H., Rosenberg, F. J., Straus, S. E., Dale, J. K., Middleton, L. A., Lin, A. Y., Strober, W., Lenardo, M. J., and Puck, J. M. (1995). Dominant interfering Fas gene mutations impair apoptosis in a human autoimmune lymphoproliferative syndrome. *Cell* 81, 935-946.
- Fruman, D.A., Klee, C.B., Bierer, B.E., and Burakoff, S.J. (1992). Calcineurin phosphatase activity in T lymphocytes is inhibited by FK 506 and cyclosporin A. *Proc.Natl.Acad.Sci.USA* 89, 3686-3690.

- Gagliardini, V., Fernandez, P.-A., Lee, R.K.K., Drexler, H.C.A., Rotello, R.J., Fishman, M.C., and Yuan, J. (1994). Prevention of vertebrate neuronal death by *crmA* gene. *Science* 263, 826-828.
- Galle, P.R. (1997). Apoptosis in liver disease. *Journal of Hepatology* 27, 405-412.
- Garcia-Calvo, M., Peterson, E., Leiting, B., Ruel, R., Nicholson, D. W., and Thornberry, N. A. (1998). Inhibition of human caspases by peptide-based and macromolecular inhibitors. *Journal of Biological Chemistry* 273, 32608-32613.
- Garcia-Cozar, F. J, Okamura, H., Aramburu, J. F, Shaw, K. T. Y., Pelletier, L. A., Showalter, R. E., Villafranca, E., and Rao, A. (1998). Two-site interaction of Nuclear Factor of Activated T cells with activated Calcineurin. *Journal of Biological Chemistry* 273, 23877-23883.
- Gerschenson, L.E. and Rotello, R.J. (1992). Apoptosis: a different type of cell death. *FASEB J.* 6, 2450-2455.
- Gil-Gomez, G., Berns, A., and Brady, H. J. M. (1998). A link between cell cycle and cell death: Bax and Bcl-2 modulate Cdk2 activation during thymocyte apoptosis. *Embo Journal* 17, 7209-7218.
- Gillis, S. and Watson, J. (1980). Biochemical and biological characterization of lymphocyte regulatory molecules. V. Identification of an interleukin-2 producing human leukaemic T cell line. *Journal of Experimental Medicine* 152, 1709.
- Glucksmann, A. (1951). Cell death in normal vertebrate ontogeny. *Biol Rev* 26, 59-86.
- Goodwin, C. J., Holt, S. J., Riley, P. A., Downes, S., and Marshall, N. J. (1996). Growth hormone-responsive DT-diaphorase-mediated bioreduction of tetrazolium salts. *Biochem.Biophys.Res.Commun.* 226, 935-941.
- Goping, I. S., Gross, A., Lavoie, J. N., Nguyen, M., Jemmerson, R., Roth, K., Korsmeyer, S. J., and Shore, G. C. (1998). Regulated targeting of BAX to mitochondria. *J.Cell Biol.* 143, 207-215.
- Grandgirard, D., Studer, E., Monney, L., Belser, T., Fellay, I., Borner, C., and Michel, M.R. (1998). Alphaviruses induce apoptosis in Bcl-2-overexpressing cells: Evidence for a caspase-mediated, proteolytic inactivation of Bcl-2. *EMBO J.* 17, 1268-1278.
- Green, D. R. (1998). Apoptotic pathways: The roads to ruin. *Cell* 94, 695-698.
- Green, D. R. (2000). Apoptotic pathways: Paper wraps stone blunts scissors. *Cell* 102, 1-4.
- Green, D. R. and Reed, J. C. (1998). Mitochondria and apoptosis. *Science* 281, 1309-1312.
- Green, D.R. and Scott, D.W. (1994). Activation-induced apoptosis in lymphocytes. *Curr.Opin.Immunol.* 6, 476-487.
- Gross, A., Yin, X-M., Wang, K., Wei, M. C., Jockel, J., Milliman, C., Erdjument-Bromage, H., Tempst, P., and Korsmeyer, S. J. (1999). Caspase cleaved BID targets

mitochondria and is required for cytochrome c release, while BCL-X<sub>L</sub> prevents this release but not tumour necrosis factor-R1/Fas death. *Journal of Biological Chemistry* 274, 1156-1163.

Gross, A. T., Jockel, J., Wei, M. C., and Korsmeyer, S. J. (1998). Enforced dimerization of Bax results in its translocation, mitochondrial dysfunction and apoptosis. *EMBO Journal* 17, 3878-3885.

Gu, J., Dong, R-P., Zhang, C., McLaughlin, D. F., Wu, M. X., and Schlossman, S. F. (1999). Functional interaction of DFF35 with caspase-activated DNA Fragmentation Nuclease DFF40. *Journal of Biological Chemistry* 274, 20759-20762.

Gu, Y., Kuida, K., Tsutsui, H., Ku, G., Hsiao, K., Fleming, M. A., Hayashi, N., Higashino, K., Okamura, H., Nakanishi, K., Kurimoto, M., Tanimoto, T., Flavell, R. A., Sato, V., Harding, M. W., Livingston, D. J., and SuM.S. (1997). Activation of interferon-gamma inducing factor mediated by interleukin-1-beta converting enzyme. *Science* 275, 206-209.

Gueth-Hallonet, C., Weber, K., and Osborn, M. (1997). Cleavage of the nuclear matrix protein NuMA during apoptosis. *Experimental Cell Research* 233, 21-24.

Guo, M. W., Mori, E., Xu, J. P., and Mori, T. (1994). Identification of Fas antigen associated with apoptotic cell death in murine ovary. *Biochem.Biophys.Res.Commun.* 203, 1438-1446.

Gurtu, V., Kain, S. R., and Zhang, G. (1997). Fluorometric and colorimetric detection of caspase activity associated with apoptosis. *Biochem.* 251, 98-102.

Hague, A., Moorghen, M., Hicks, D., Chapman, M., and Paraskeva, C. (1994). Bcl-2 expression in human colorectal adenomas and carcinomas. *Oncogene* 9, 3367-3370.

Hahne, M., Peitsch, M.C., Irmier, M., Schroter, M., Lowin, B., Rousseau, M., Bron, C., Renno, T., French, L., and Tschopp, J. (1995). Characterization of the non-functional fas ligand of gld mice. *Int.Immunol.* 7, 1381-1386.

Hahne, M., Rimoldi, D., Schroter, M., Romero, P., Schreier, M., French, L.E., Schneider, P., Bornand, T., Fontana, A., Lienard, D., Cerottini, J.C., and Tschopp, J. (1996). Melanoma cell expression of fas(apo-1/cd95) ligand: implications for tumor immune escape. *Science* 274, 1363-1366.

Hakem, R., Hakem, A., Duncan, G. S., Henderson, J. T., Woo, M., Soengas, M. S., Elia, A. J., de la Pompa, J. L., Kagi, D., Khoo, W., Potter, J., Yoshida, R., Kaufman, S. A., Lowe, S. W., Penninger, J. M., and Mak, T. W. (1998). Differential requirement for caspase-9 in apoptotic pathways invivo. *Cell* 94, 339-352.

Hammar, S. P and Mottet, N. K. (1971). Tetrazolium salt and electron-microscopic studies of cellular degeneration and necrosis in the interdigital areas of the developing chick limb. *Science* 8, 229-251.

Han, Z., Hendrickson, E.A., Bremner, T.A., and Wyche, J.H. (1997). A sequential two-step mechanism for the production of the mature p17:p12 form of caspase-3 in vitro. *J.Biol.Chem.* 272, 13432-13436.

- Hanabuchi, S., Koyanagi, M., Kawasaki, A., Shinohara, N., Matsuzawa, A., Nishimura, Y., Kobayashi, Y., Yonehara, S., Yagita, H., and Okumura, K. (1994). Fas and its ligand in a general mechanism of T-cell-mediated cytotoxicity. *Proc.Natl.Acad.Sci.USA* 91, 4930-4934.
- Hanada, M., Aime-Sempe, C., Sato, T., and Reed, J.C. (1995). Structure-function analysis of Bcl-2 protein. Identification of conserved domains important for homodimerization with Bcl-2 and heterodimerization with bax. *J.Biol.Chem.* 270, 11962-11969.
- Hara, H., Friedlander, R.M., Gagliardini, V., Ayata, C., Fink, K., Huang, Z., Shimizu-Sasamata, M., Yuan, J., and Moskowitz, M.A. (1997). Inhibition of interleukin 1beta converting enzyme family proteases reduces ischemic and excitotoxic neuronal damage. *Proceedings of the National Academy of Sciences of the United States of America* 94, 2007-2012.
- Hay, B. A., Wassermann, D. A., and Rubin, G. M. (1995). Drosophila homologs of baculovirus inhibitor of apoptosis proteins function to block cell death. *Cell* 83, 1253-1262.
- Hay, B. A., Wolff, T., and Rubin, G. M. (1994). Expression of baculovirus p35 prevents cell death in drosophila. *Development* 120, 2121-2129.
- He, H., Lam, M., McCormick, T. S., and Distelhorst, C. W. (1997). Maintenance of calcium homeostasis in the endoplasmic reticulum by Bcl-2. *J.Cell Biol.* 138:6, 1219-1228.
- Hengartner, H. and Horvitz, H.R. (1994). C. elegans cell survival gene *ced-9* encodes a functional homolog of the mammalian proto-oncogene *bcl-2*. *Cell* 76, 665-676.
- Hengartner, M.O. (1997). CED-4 is a stranger no more. *Nature* 388, 714-715.
- Hengartner, M. O. (1998). Death cycle and swiss army knives. *Nature* 391, 441-442.
- Hengartner, M.O., Ellis, R.E., and Horvitz, H.R. (1992). *Caenorhabditis elegans* gene *ced-9* protects cells from programmed cell death. *Nature* 356, 494-499.
- Hengartner, M.O. and Horvitz, H.R. (1994). C. elegans cell survival gene *ced-9* encodes a functional homolog of the mammalian proto-oncogene *bcl-2*. *Cell* 76, 665-676.
- Hirata, H., Takahashi, A., Kobayashi, S., Yonehara, S., Sawai, H., Okazaki, T., Yamamoto, K., and Sasada, M. (1998). Caspases are activated in a branched protease cascade and control distinct downstream processes in Fas-induced apoptosis. *Journal of Experimental Medicine* 187, 587-600.
- Hirotsu, M., Zhang, Y., Fujita, N., Naito, M., and Tsurou, T. (1999). NH<sub>2</sub>-terminal BH4 domain of Bcl-2 is functional for heterodimerization with Bax and inhibition of apoptosis. *Journal of Biological Chemistry* 274, 20415-20420.
- Hockenbery, D.M., Nunez, G., Millman, C., Schreiber, R.D., and Korsmeyer, S.J. (1990). Bcl-2 is an inner mitochondrial membrane protein that blocks programmed cell death. *Nature* 348, 334-336.

Howard, A. D., Kostura, M. J., Thornberry, N., Ding, G. J., Limjuco, G., Weidner, J., Salley, J. P., Hogquist, K. A., Chaplin, D. D., Mumford, R. A., Schmidt, J. A., and Tocci, M. J. (1991). IL-1-converting enzyme requires an aspartic acid residues for processing of the IL-1 $\beta$  precursor at two distinct sites and does not cleave 31kDa IL-1 $\alpha$ . *J.Immunol.* *147*, 2964-2969.

Howard, A.D., Palyha, O.C., Griffin, P.R., Peterson, E.P., Lenny, A.B., Ding, G., Pickup, D.J., Thornberry, N.A., Schmidt, J.A., and Tocci, M.J. (1995). Human IL-1beta processing and secretion in recombinant baculovirus-infected Sf9 cells is blocked by the cowpox virus serpin crm. *Journal of Immunology* *154*, 2321-2332.

Hsu, H., Shu, H.-B., Pan, M.-G., and Goeddel, D.V. (1996). TRADD-TRAF2 and TRADD-FADD interactions define two distinct TNF receptor 1 signal transduction pathways. *Cell* *84*, 299-308.

Hsu, H., Xiong, J., and Goeddel, D.V. (1995). The TNF receptor 1-associated protein TRADD signals cell death and NF-kappaB activation. *Cell* *81*, 495-504.

Hu, S., Snipas, S., Vincenz, C., Salvesen, G. S., and Dixit, V. M. (1998). Caspase-14 is a novel developmentally regulated protease. *Journal of Biological Chemistry* *273*, 29648-29653.

Hu, Y., Benedict, M. A., Ding, L., and Nunez, G. (1999). Role of cytochrome c and dATP/ATP hydrolysis in Apaf-1-mediated caspase-9 activation and apoptosis. *EMBO J.* *18*, 3586-3595.

Hu, Y., Benedict, M.A., Wu, D., Inohara, N., and Nunez, G. (1998a). Bcl-X(L) interacts with Apaf-1 and inhibits Apaf-1-dependent caspase-9 activation. *Proceedings of the National Academy of Sciences of the United States of America* *95*, 4386-4391.

Hu, Y., Ding, L., Spencer, D. M., and Nunez, G. (1998). WD-40 repeat region regulates Apaf-1 self-association and procaspase-9 activation. *Journal of Biological Chemistry* *273*, 33489-33494.

Huang, D.C.S., Adams, J.M., and Cory, S. (1998). The conserved N-terminal BH4 domain of Bcl-2 homologues is essential for inhibition of apoptosis and interaction with CED-4. *EMBO J.* *17*, 1029-1039.

Huang, D.C.S., O'Reilly, L.A., Strasser, A., and Cory, S. (1997). The anti-apoptosis function of: Bcl-2 can be genetically separated from its inhibitory effect on cell cycle entry. *EMBO J.* *16*, 4628-4638.

Hueber, A.-O., Zornig, M., Lyon, D., Suda, T., Nagata, S., and Evan, G.I. (1997). Requirement for the CD95 receptor-ligand pathway in c-Myc-induced apoptosis. *Science* *278*, 1305-1309.

Hughes, F. M., Evans-Storms, R. B., and Cidlowski, J. A. (1998). Evidence that non-caspase proteases are required for chromatin degradation during apoptosis. *Cell Death & Differentiation* *5*, 1017-1027.

- Hughes, F. M., Evans-Storms, R. B., and Cidlowski, J. A. (1998). Evidence that non-caspase proteases are required for chromatin degradation during apoptosis. *Cell Death & Differentiation* 5, 1017-1027.
- Humke, E. W., Ni, J., and Dixit, V. M. (1998). ERICE, a novel FLICE-activatable caspase. *Journal of Biological Chemistry* 273, 15702-15707.
- Hunter, J.J., Bond, B.L., and Parslow, T.G. (1996). Functional dissection of the human Bcl2 protein: Sequence requirements for inhibition of apoptosis. *Molecular & Cellular Biology* 16, 877-883.
- Ikegaki, N., Katsumata, M., Minna, J., and Tsujimoto, Y. (1994). Expression of bcl-2 in small cell lung carcinoma cells. *Cancer Research* 54, 6-8.
- Inohara, N., Gourley, S., Carrio, R., Muniz, M., Merino, J., Garcia, I., Koseki, T., Hu, Y., Chen, S., and Nunez, G. (1998). Diva, a Bcl-2 homologue that binds directly to Apaf-1 and induces BH2-independent cell death. *Journal of Biological Chemistry* 273, 32479-32486.
- Inohara, N., Koseki, T., Chen, S., Benedict, M. A., and Nunez, G. (1999). Identification of Regulatory and catalytic domains in the apoptosis nuclease DFF40/CAD. *Journal of Biological Chemistry* 274, 270-274.
- Itoh, N. and Nagata, S. (1993a). A novel protein domain required for apoptosis. *J.Biol.Chem.* 268, 10932-10937.
- Itoh, N., Tsujimoto, Y., and Nagata, S. (1993b). Effect of bcl-2 on Fas antigen-mediated cell death. *J.Immunol.* 151, 621-627.
- Itoh, N., Yonehara, S., Ighui, A., Yonehara, M., Mitzushima, S., Sameshine, S., Maye, A., Seto, Y., and Mayala, S. (1991). The polypeptide encoded by the DNA for human cell surface antigen Fas can mediate apoptosis. *Cell* 66, 233-243.
- Jaattela, M., Benedict, M., Tewari, M., Shayman, J.A., and Dixit, V.M. (1995). Bcl-x and Bcl-2 inhibit TNF and Fas-induced apoptosis and activation of phospholipase A2 in breast carcinoma cells. *Oncogene* 10, 2297-2305.
- Jacobson, M. D. (1997). Programmed cell death: a missing link is found. *Trends in Cell Biology* 7, 467-469.
- Jacobson, M.D., Weil, M., and Raff, M.C. (1997b). Programmed cell death in animal development. *Cell* 88, (pp 347-354).
- Jain, J., McCaffrey, P.G., Miner, Z., Kerppola, T.K., Lambert, J.N., Verdine, G.L., Curran, T., and Rao, A. (1993). The T-cell transcription factor NFAT(p) is a substrate for calcineurin and interacts with fos and jun. *Nature* 365, 352-355.
- Janicke, R.U., Ng, P., Sprengart, M.L., and Porter, A.G. (1998a). Caspase-3 is required for alpha-fodrin cleavage but dispensable for cleavage of other death substrates in apoptosis. *J.Biol.Chem.* 273, 15540-15545.

- Janicke, R.U., Sprengart, M.L., Wati, M.R., and Porter, A.G. (1998b). Caspase-3 is required for DNA fragmentation and morphological changes associated with apoptosis. *J.Biol.Chem.* 273, 9357-9360.
- Janicke, R.U., Walker, P.A., Yu Lin, X., and Porter, A.G. (1996). Specific cleavage of the retinoblastoma protein by an ICE-like protease in apoptosis. *EMBO J.* 15, 6969-6978.
- Jäättelä, M., Benedict, M., Tewari, M., Shayman, J.A., and Dixit, V.M. (1995). Bcl-x and Bcl-2 inhibit TNF and Fas-induced apoptosis and activation of phospholipase A<sub>2</sub> in breast carcinoma cells. *Oncogene* 10, 2297-2305.
- Jäättelä, M. (1999). Escaping cell death: survival proteins in cancer. *Exp.Cell Res.* 248, 30-43.
- Jiang, S., Chow, S.C., Nicotera, P., and Orrenius, S. (1994). Intracellular Ca<sup>2+</sup> signals activate apoptosis in thymocytes: studies using the Ca<sup>2+</sup>-ATPase inhibitor thapsigargin. *Experimental Cell Research* 212, 84-92.
- Jiang, S., Zhivotovsky, B., Burgess, D. H., Gahm, A., Chow, S. C., and Orrenius, S. (1997). The role of proteolysis in T cell apoptosis triggered by chelation of intracellular Zn<sup>2+</sup>. *Cell Death and Differentiation* 4, 39-50.
- Ju, S.-T., Panka, D.J., Cui, H., Ettinger, R., El-Khatib, M., and Marshak-Rothstein, A. (1995). Fas(CD95)/FasL interactions required for programmed cell death after T-cell activation. *Nature* 373, 444-448.
- Juo, P., Kuo, C. J., Yaun, J., and Blenis, J. Essential requirement for caspase-8/FLICE in the initiation of the Fas-induced apoptotic cascade. *Current Biology* 8, 1001-1008. 1998.
- Jurgensmeier, J.M., Xie, Z., Deveraux, Q., Ellerby, L., Bredesen, D., and Reed, J.C. (1998). Bax directly induces release of cytochrome c from isolated mitochondria. *Proceedings of the National Academy of Sciences of the United States of America* 95, 4997-5002.
- Kamens, J., Paskind, M., Hugunin, M., Talanian, R.V., Allen, H., Banach, D., Bump, N., Hackett, M., Johnston, C.G., Li, P., Mankovich, J.A., Terranova, M., and Ghayur, T. (1995). Identification and characterization of ICH-2, a novel member of the interleukin-1 $\beta$ -converting enzyme family of cysteine proteases. *J.Biol.Chem.* 270, 15250-15256.
- Kass, G.E.N., Eriksson, J.E., Weis, M., Orrenius, S., and Chow, S.C. (1996). Chromatin condensation during apoptosis requires atp. *Biochem.J.* 318, 749-752.
- Katsikis, P. D., Wunderlich, E. S., Smith, C. A, and Herzenberg, L. A. (1995). Fas antigen stimulation induces marked apoptosis of T lymphocytes from HIV-1-infected individuals. *J.Exp.Med.* 181, 2029-2036.
- Kaufmann, S.H. (1989). Induction of endonucleolytic DNA cleavage in human acute myelogenous leukemia cells by etoposide, camptothecin, and other cytotoxic anticancer drugs: a cautionary note. *Cancer Res.* 49, 5870-5878.

Kaufmann, S.H., Desnoyers, S., Ottaviano, Y., Davidson, N.E., and Poirier, G.G. (1993). Specific proteolytic cleavage of poly(ADP-ribose) polymerase: An early marker of chemotherapy-induced apoptosis. *Cancer Res.* 53, 3976-3985.

Kayagaki, N., Kawasaki, A., Ebata, T., Ohmoto, H., Ikeda, S., Inoue, S., Yoshino, K., Okumura, K., and Yagita, H. (1995). Metalloproteinase-mediated release of human fas ligand. *Journal of Experimental Medicine* 182, 1777-1783.

Kerr, J. F. R. (1971). Shrinkage necrosis: a distinct mode of cellular death. *Journal of Pathology* 105, 13-20.

Kerr, J.F.R., Wyllie, A.H., and Currie, A.R. (1972). Apoptosis: a basic biological phenomenon with wide ranging implications in tissue kinetics. *Br.J.Cancer* 26, 239-257.

Kharbanda, S., Pandey, P., Schofield, L., Israels, S., Roncinske, R., Yoshida, K., Bharti, A., Yuan, Z.M., Saxena, S., Weichselbaum, R., Nalin, C., and Kufe, D. (1997). Role for bcl-x(l) as an inhibitor of cytosolic cytochrome c accumulation in dna damage-induced apoptosis. *Proceedings of the National Academy of Sciences of the United States of America* 94, 6939-6942.

King, K. L. and Cidlowski, J. A. (1995). Cell cycle and apoptosis: common pathways to life and death. *Journal of Cellular Biochemistry* 58, 175-180.

Kischkel, F.C., Hellbardt, S., Behrmann, I., Germer, M., Pawlita, M., Krammer, P.H., and Peter, M.E. (1995). Cytotoxicity-dependent apo-1 (fas/cd95)-associated proteins form a death-inducing signaling complex (disc) with the receptor. *EMBO J.* 14, 5579-5588.

Kluck, R.M., BossyWetzel, E., Green, D.R., and Newmeyer, D.D. (1997a). The release of cytochrome c from mitochondria: a primary site for bcl- 2 regulation of apoptosis. *Science* 275, 1132-1136.

Kluck, R.M., Martin, S.J., Hoffman, B.M., Zhou, J.S., Green, D.R., and Newmeyer, D.D. (1997b). Cytochrome c activation of CPP32-like proteolysis plays a critical role in a *Xenopus* cell-free apoptosis system. *EMBO J.* 16, 4639-4649.

Ko, S. C. W., Johnson, V. L., and Chow, S. C. (2000). Functional characterization of Jurkat T cells rescued from CD95/Fas-induced apoptosis through the inhibition of caspases. *Biochem.Biophys.Res.Commun.* 270, 1009-1015.

Komiyama, T., Ray, C.A., Pickup, D.J., Howard, A.D., Thornberry, N.A., Peterson, E.P., and Salvesen, G.S. (1994). Inhibition of interleukin-1beta converting enzyme by the cowpox virus serpin CrmA. An example of cross-class inhibition. *J.Biol.Chem.* 269, 19331-19337.

Koopman, G., Reutelingsperger, C.P.M., Kuijten, G.A.M., Keehnen, R.M.J., Pals, S.T., and Van Oers, M.H.J. (1994). Annexin V for flow cytometric detection of phosphatidylserine expression on B cells undergoing apoptosis. *Blood* 84, 1415-1420.

Korsmeyer, S.J. (1992). Bcl-2 initiates a new category of oncogenes: Regulators of cell death. *Blood* 80, 879-886.

- Kothakota, S., Azuma, T., Reinhard, C., Klippel, A., Tang, J., Chu, K., McGarry, T.J., Kirschner, M.W., Kohts, K., Kwiatkowski, D.J., and Williams, L.T. (1997). Caspase-3-generated fragment of gelsolin: Effector of morphological change in apoptosis. *Science* 278, 294-298.
- Krajewski, S., Tanaka, S., Takayama, S., Schibler, M. J., Fenton, W., and Reed, J. C. (1993). Investigation of the subcellular distribution of the bcl-2 oncoprotein: residence in nuclear envelope, endoplasmic reticulum, and outer mitochondrial membranes. *Cancer Research* 53, 4701-4714.
- Kroemer, G. (1997). The proto-oncogene Bcl-2 and its role in regulating apoptosis. *Natural Medicines* 3, 614-620.
- Kroemer, G., Dallaporta, B., and Resche-Rigon, M. (1998). The mitochondrial death/life regulator in apoptosis and necrosis. *Annual Review of Physiology* 60, 619-642
- Kuida, K., Haydar, T. F., Kuan, C. Y., Gu, Y., Taya, C., Karasuyama, H., Su, M. S-S., Rakic, P., and Flavell, R. A. (1998). Reduced apoptosis and cytochrome c-mediated caspase activation in mice lacking caspase-9. *Cell* 94, 325-337.
- Kuida, K., Lippke, J.A., Ku, G., Harding, M.W., Livingston, D.J., Su, M.S.S., and Flavell, R.A. (1995). Altered cytokine export and apoptosis in mice deficient in interleukin-1 $\beta$  converting enzyme. *Science* 267, 2000-2003.
- Kuida, K., Zheng, T. S., Na, S., Kuan, C. Y., Karasuyama, H., Rakic, P., and Flavell, R. A. (1996). Decreased apoptosis in the brain and premature lethality in CPP32-deficient mice. *Nature* 384, 368-372.
- Kumar, S., Kinoshita, M., Noda, M., Copeland, N.G., and Jenkins, N.A. (1994). Induction of apoptosis by the mouse *Nedd2* gene, which encodes a protein similar to the product of the *Caenorhabditis elegans* cell death *ced-3* and the mammalian IL-1 $\beta$ -converting enzyme. *Gene Dev.* 8, 1613-1526.
- Kuwana, T., Smith, J. J., Muzio, M., Dixit, V. M., Newmeyer, D. D., and Kornbluth, S. (1998). Apoptosis induction by caspase-8 is amplified through the mitochondrial release of cytochrome c. *Journal of Biological Chemistry* 273, 16589-16594.
- Lam, M., Dubyak, G., Chen, L., Nuñez, G., Miesfeld, R.L., and Distelhorst, C.W. (1994). Evidence that bcl-2 represses apoptosis by regulating endoplasmic reticulum-associated Ca<sup>2+</sup> fluxes. *Proc.Natl.Acad.Sci.USA* 91, 6569-6573.
- Latinis, K.M., Norian, L.A., Eliason, S.L., and Koretzky, G.A. (1997). Two NFAT transcription factor binding sites participate in the regulation of CD95 (Fas) ligand expression in activated human T cells. *J.Biol.Chem.* 272, (pp 31427-31434).
- Lazebnik, Y.A., Cole, S., Cooke, C.A., Nelson, W.G., and Earnshaw, W.C. (1993). Nuclear events of apoptosis *in vitro* in cell-free mitotic extracts: a model system for analysis of the active phase of apoptosis. *J.Cell Biology* 123, 7-22.

- Lazebnik, Y.A., Kaufmann, S.H., Desnoyers, S., Poirier, G.G., and Earnshaw, W.C. (1994). Cleavage of poly(ADP-ribose) polymerase by a proteinase with properties like ICE. *Nature* 371, 346-347.
- Lazebnik, Y.A., Takahashi, A., Moir, R.D., Goldman, R.D., Poirier, G.G., Kaufmann, S.H., and Earnshaw, W.C. (1995). Studies of the lamin proteinase reveal multiple parallel biochemical pathways during apoptotic execution. *Proceedings of the National Academy of Sciences of the United States of America* 92, 9042-9046.
- Lee, N., MacDonald, H., Reinhard, C., Halenbeck, R., Roulston, A., Shi, T., and Williams, L.T. (1997). Activation of hPAK65 by caspase cleavage induces some of the morphological and biochemical changes of apoptosis. *Proceedings of the National Academy of Sciences of the United States of America* 94, 13642-13647.
- Leek, R. D., Kaklamanis, L., Pezzella, F., Gatter, K. C., and Harris, A. L. (1994). bcl-2 in normal human breast and carcinoma, association with oestrogen receptor-positive, epidermal growth factor receptor-negative tumours and in situ cancer. *British Journal of Cancer* 69, 135-139.
- Leist, M., Single, B., Naumann, H., Fava, E., Simon, B., Kühnle, S., and Nicotera, P. (1999). Inhibition of mitochondrial ATP generation by nitric oxide switches apoptosis to necrosis. *Exp.Cell Res.* 249, 396-403.
- Leithauser, F, Dhein, J, Mechttersheiner, G, Koretz, K, Bruderlein, S, Henne, C, Schmidt, A, Debatin, K. M, Krammer, P. H, and Moller, P. (1993). Constitutive and induced expression of APO-1, a new member of the NGF/TNF receptor superfamily in normal and neoplastic cells. *Laboratory Investigation* 69, 415-421.
- Li-Weber, M., Laur, O., Hekele, A., Coy, J., Walczak, H., and Krammer, P. H. (1998). A regulatory element in the CD95 (APO-1/Fas) ligand promoter is essential for responsiveness to TCR-mediated activation. *European Journal of Immunology* 28, 2373-2383.
- Li, F., Ambrosini, G., Chu, E. Y., Plescia, J., Tognin, S., Marchisio, P. C., and Altieri, D. C. (1998). Control of apoptosis and mitotic spindle checkpoint by survivin. *Nature* 396, 580-584.
- Li, H. and Yuan, J. (1999). Deciphering the pathways of life and death. *Current Opinion in Cell Biology* 11, 261-266.
- Li, H., Zhu, H., Xu, C., and Yuan, J. (1998). Cleavage of BID by caspase-8 mediates the mitochondrial damage in the Fas pathway of apoptosis. *Cell* 94, 491-501.
- Li, K., Li, Y., Shelton, J. M., Richardson, J. A., Spencer, E., Chen, Z., Wang, X., and Williams, R. S. (2000). Cytochrome c deficiency causes embryonic lethality and attenuates stress-induced apoptosis. *Cell* 101, 389-399.
- Li, P., Allen, H., Banerjee, S., Franklin, S., Herzog, L., Johnston, C., McDowell, J., Paskind, M., Rodman, L., Salfeld, J., Towne, E., Tracey, D., Wardwell, S., Wei F, Y., Wong, W., Kamen, R., and Seshadri, T. (1995). Mice deficient in il-1beta-converting

enzyme are defective in production of mature il-1beta and resistant to endotoxic shock. *Cell* 80, 401-411.

Li, P., Nijhawan, D., Budlhardjo, I., Srinivasula, S.M., Ahmad, M., Alnemri, E.S., and Wang, X. (1997). Cytochrome c and dATP-dependent formation of Apaf-1/caspase-9 complex initiates an apoptotic protease cascade. *Cell* 91, 479-489.

Linette, G.P., Li, Y., Roth, K., and Korsmeyer, S.J. (1996). Cross talk between cell death and cell cycle progression: bcl-2 regulates nfat-mediated activation. *Proceedings of the National Academy of Sciences of the United States of America* 93, 9545-9552.

Ling, Y., Tornos, C., and Perez-Soler, R. (1998). Phosphorylation of Bcl-2 is a marker of M phase events and not a determinant of apoptosis. *Journal of Biological Chemistry* 273, 18984-18991.

Liston, P., Roy, N., Tamai, K., Lefebvre, C., Baird, S., Cherton-Horvat, G., Farahani, R., Mclean, M., Ikeda, J. E., MacKenzie, A., and Korneluk, R. G. (1996). Suppression of apoptosis in mammalian cells by NAIP and a related family of IAP genes. *Nature* 379, 349-352.

Liu, J., Farmer, J.D., Jr., Lane, W.S., Friedman, J., Weissman, I., and Schreiber, S.L. (1991). Calcineurin is a common target of cyclophilin-cyclosporin A and FKBP-FK506 complexes. *Cell* 66, 807-815.

Liu, X., Kim, C.N., Yang, J., Jemmerson, R., and Wang, X. (1996). Induction of apoptotic program in cell-free extracts: requirement for datp and cytochrome c. *Cell* 86, 147-157.

Liu, X., Li, P., Widlak, P., Zou, H., Luo, X., Garrard, W.T., Wang, and X. (1998). The 40-kDa subunit of DNA fragmentation factor induces DNA fragmentation and chromatin condensation during apoptosis. *Proceedings of the National Academy of Sciences of the United States of America* 95, 8461-8466.

Liu, X., Zou, H., Slaughter, C., and Wang, X. (1997a). DFF, a heterodimeric protein that functions downstream of caspase-3 to trigger DNA fragmentation during apoptosis. *Cell* 89, 175-184.

Liu, X., Zou, H., Slaughter, C., and Wang, X. (1997b). DFF, a heterodimeric protein that functions downstream of caspase-3 to trigger DNA fragmentation during apoptosis. *Cell* 89, 175-184.

Liu, X., Zou, H., Widlak, P., Garrard, W., and Wang, X. (1999). Activation of the apoptotic endonuclease DFF40 (caspase- activated DNase or nuclease). Oligomerization and direct interaction with histone H1. *J.Biol.Chem.* 274, 13836-13840.

Longthorne, V.L. and Williams, G.T. (1997). Caspase activity is required for commitment to fas-mediated apoptosis. *EMBO J.* 16, 3805-3812.

Los, M., Van de Craen, M., Penning, L.C., Schenk, H., Westendorp, M., Baeuerle, P.A., Dröge, W., and Schulze-Osthoff, K. (1995). Requirement of an ICE/CED-3 protease for Fas/APO-1-mediated apoptosis. *Nature* 375, 81-83.

- Luo, X., Budlhardjo, I., Zou, H., Slaughter, C., and Wang, X. (1998). Bid, a Bcl-2 interacting protein, mediates cytochrome c release from the mitochondria in response to activation of cell surface death receptors. *Cell* 94, 481-490.
- Lynch, D.H. (1995). Biology of Fas. *Circ.Shock* 44, 63-66.
- MacFarlane, M., Cain, K., Sun, X.M., Alnemri, E.S., and Cohen, G.M. (1997). Processing/activation of at least four interleukin-1beta converting enzyme-like proteases occurs during the execution phase of apoptosis in human monocytic tumor cells. *Journal of Cell Biology* 137, 469-479.
- Maggi, C. A. (1998). Therapeutic opportunities from the pharmacological manipulation of the Fas system. *Pharmacological Research* 38:1, 1-34.
- Mancini, M., Nicholson, D.W., Roy, S., Thornberry, N.A., Peterson, EP, Casciola-Rosen, L.A., and Rosen, A. (1998). The caspase-3 precursor has a cytosolic and mitochondrial distribution: Implications for apoptotic signaling. *Journal of Cell Biology* 140, 1485-1495.
- Mantal, M., Maggirwar, S.B., Sharma, N., Kaufmann, S.H., Sun, S.-C., and Kumar, R. (1996). Bcl-2 prevents CD95 (Fas/APO-1)-induced degradation of lamin B and poly(ADP-ribose) polymerase and restores the NF-kappaB signaling pathway. *J.Biol.Chem.* 271, 30354-30359.
- Marchetti, P., Castedo, M., Susin, S.A., Zamzami, N., Hirsch, T., Macho, A., Haeffner, A., Hirsch, F., Geuskens, M., and Kroemer, G. (1996). Mitochondrial permeability transition is a central coordinating event of apoptosis. *Journal of Experimental Medicine* 184, 1155-1160.
- Mariani, S. M., Matiba, B., Bäumlner, C., and Krammer, P. H. (1995). Regulation of cell surface APO-1/Fas (CD95) ligand expression by metalloproteases. *European Journal of Immunology* 25, 2303-2307.
- Marin, M., Fernandez, A., Bick, R. J., Brisbay, S., Buja, L. M., Snuggs, M., McConkey, D. J., von Eschenbach, A. C., Keating, M. J., and McDonnell, T. J. (1996). Apoptosis suppression by bcl-2 is correlated with the regulation of nuclear and cytosolic Ca<sup>2+</sup>. *Oncogene* 12, 2259-2266.
- Marsters, S. A., Sheridan, J. P., Pitti, R. M., Brush, J., Goddard, A. D., and Ashkenazi, A. (1998). Identification of a ligand for the death-domain-containing receptor Apo-3. *Current Biology* 8, 525-528.
- Martin, S.J., Finucane, D.M., Amarante-Mendes, G.P., O'Brien, G.A., and Green, D.R. (1996). Phosphatidylserine externalization during CD95-induced apoptosis of cells and cytoplasts requires ICE/CED-3 protease activity. *J.Biol.Chem.* 271, 28753-28756.
- Martin, S.J., Reutelingsperger, C.P.M., McGahon, A.J., Rader, J.A., Van Schie, R.C.A., LaFace, D.M., and Green, D.R. (1995). Early redistribution of plasma membrane phosphatidylserine is a general feature of apoptosis regardless of the initiating stimulus: Inhibition by overexpression of Bcl-2 and Abl. *Journal of Experimental Medicine* 182, 1545-1556.

Martinez-Lorenzo, M.J., Alava, M.A., Anel, A., Pineiro, A., and Naval, J. (1996). Release of preformed Fas ligand in soluble form is the major factor for activation-induced death of Jurkat cells. *Immunology* 89, 511-517.

Martinou, J-C., Desagher, S., and Antonsson, B. (2000). Cytochrome c release from mitochondria: all or nothing. *Nature Cell Biology* 2, 41-43.

Martins, L.M., Mesner, P.W., Kottke, T.J., Basi, G.S., Sinha, S., Tung, J.S., Svingen, PA, Madden, B.J., Takahashi, A., McCormick, D.J., Earnshaw, W.C., and Kaufmann, S.H. (1997). Comparison of caspase activation and subcellular localization in HL-60 and K562 cells undergoing etoposide-induced apoptosis. *Blood* 90, 4283-4296.

Marzo, I., Brenner, C., Zamzami, N., Susin, S.A., Beutner, G., Brdiczka, D., Remy, R., Xie, Z.-H., Reed, J.C., and Kroemer, G. (1998a). The permeability transition pore complex: A target for apoptosis regulation by caspases and Bcl-2-related proteins. *Journal of Experimental Medicine* 187, 1261-1271.

Marzo, I., Susin, S.A., Petit, P.X., Ravagnan, L., Brenner, C., Larochette, N., Zamzami, N., and Kroemer, G. (1998b). Caspases disrupt mitochondrial membrane barrier function. *FEBS Lett.* 427, 198-202.

Matsuyama, S., Schendel, S., Xie, Z., and Reed, J. C. (1998). Cytoprotection by Bcl-2 requires the pore-forming  $\alpha 5$  and  $\alpha 6$  helices. *Journal of Biological Chemistry* 273, 30995-31001.

Mayo, M. W., Wang, C., Drouin, S. S., Madrid, L. V., Marshall, A. F., Reed, J. C., Weissman, B. E., and Baldwin, A. S. (1999). WT1 modulates apoptosis by transcriptionally upregulating the bcl-2 proto-oncogene. *Embo Journal* 18, 3990-4003.

Mazel, S., Burtrum, D., and Petrie, H.T. (1996). Regulation of cell division cycle progression by bcl-2 expression: A potential mechanism for inhibition of programmed cell death. *Journal of Experimental Medicine* 183, 2219-2226.

McCaffrey, P. G., Perrino, B. A., Soderling, T. R., and Rao, A. (1993). NF-AT<sub>p</sub>, a T-lymphocyte DNA-binding protein that is a target for calcineurin and immunosuppressive drugs. *Journal of Biological Chemistry* 268:5, 3747-3752.

McCarthy, N.J., Whyte, M.K.B., Gilbert, C.S., Evan, and GI. (1997). Inhibition of Ced-3/ICE-related proteases does not prevent cell death induced by oncogenes, DNA damage, or the Bcl-2 homologue bak. *Journal of Cell Biology* 136, 215-227.

McDonnell, T. J. and Korsmeyer, S. J. (1991). Progression from lymphoid hyperplasia to high-grade malignant lymphoma in mice transgenic for the t(14:18). *Nature* 349, 254-256.

Medema, J.P., Scaffidi, C., Kischkel, F.C., Shevchenko, A., Mann, M., Krammer, P.H., and Peter, M.E. (1997). Flice is activated by association with the cd95 death-inducing signaling complex (disc). *EMBO J.* 16, 2794-2804.

Memon, S.A., Moreno, M.B., Petrak, D., and Zacharchuk, C.M. (1995). Bcl-2 blocks glucocorticoid- but not fas- or activation-induced apoptosis in a t cell hybridoma. *Journal of Immunology* 155, 4644-4652.

- Mignotte, B. and Vayssiere, J.-L. (1998). Mitochondria and apoptosis. *Eur.J.Biochem.* 252, 1-15.
- Minn, A. J., Kettlun, C. S., Liang, H., Kelekar, A., Vander Heiden, M. G., Chang, B. S., Fesik, S. W., Fill, M., and Thompson, C. B. (1999). Bcl-xL regulates apoptosis by heterodimerization-dependent and -independent mechanisms. *Embo Journal* 18, 632-643.
- Minn, A.J., Velez, P., Schendel, S.L., Liang, H., Muchmore, S.W., Fesik, S.W., Fill, M., and Thompson, C.B. (1997). Bcl-X(L) forms an ion channel in synthetic lipid membranes. *Nature* 385, 353-356.
- Miura, M., Zhu, H., Rotello, R., Hartwig, E.A., and Yuan, J. (1993). Induction of apoptosis in fibroblasts by IL-1 $\beta$ -converting enzyme, a mammalian homolog of the *C. elegans* cell death gene *ced-3*. *Cell* 75, 653-660.
- Montague, J. W., Hughes, F. M., and Cidlowski, J. A. (1997). Native recombinant cyclophilins A, B and C degrade DNA independently of peptidylprolyl cis-trans isomerase activity: Potential roles of cyclophilins in apoptosis. *Journal of Biological Chemistry* 272, 6677-6684.
- Moriishi, K., Huang, D. C. S., Cory, S., and Adams, J. A. (1999). Bcl-2 family members do not inhibit apoptosis by binding the caspase activator Apaf-1. *Proc.Natl.Acad.Sci.USA* 96, 9683-9688.
- Muchmore, S.W., Sattler, M., Liang, H., Meadows, R.P., Harlan, J.E., Yoon, H.S., Nettesheim, D., Chang, B.S., Thompson, C.B., Wong, S.-L., Ng, S.-C., and Fesik, S.W. (1996). X-ray and NMR structure of human Bcl-x(L), an inhibitor of programmed cell death. *Nature* 381, 335-341.
- Munday, N.A., Vaillancourt, J.P., Ali, A., Casano, F.J., Miller, D.K., Molineaux, S.M., Yamin, T.-T., Yu, V.L., and Nicholson, D.W. (1995). Molecular cloning and the pro-apoptotic activity of ICE<sub>rel</sub>II and ICE<sub>rel</sub>III, members of the ICE/CED-3 family of cysteine proteases. *J.Biol.Chem.* 270, 15870-15876.
- Muzio, M., Chinnaiyan, A.M., Kischkel, F.C., O'Rourke, K., Shevchenko, A., Ni, J., Scaffidi, C., Bretz, J.D., Zhang, M., Gentz, R., Mann, M., Krammer, P.H., Peter, M.E., and Dixit, V.M. (1996). Flice, a novel fadd-homologous ice/ced-3-like protease, is recruited to the cd95 (fas/apo-1) death-inducing signaling complex. *Cell* 85, 817-827.
- Muzio, M., Salvesen, G.S., and Dixit, V.M. (1997). Flice induced apoptosis in a cell-free system. cleavage of caspase zymogens. *J.Biol.Chem.* 272, 2952-2956.
- Muzio, M., Stockwell, B.R., Stennicke, H.R., Salvesen, G.S., and Dixit, V.M. (1998). An induced proximity model for caspase-8 activation. *J.Biol.Chem.* 273, 2926-2930.
- Mysler, E., Bini, P., Drappa, J., Ramos, P., Friedman, S. M., Krammer, P. H., and Elkon, K. B. (1994). The Apoptosis-1/Fas protein in human systemic lupus erythematosus. *J.Clin.Invest.* 93, 1029-1034.

- Nagata, S. (1994). Apoptosis regulated by a death factor and its receptor: Fas ligand and Fas. *Philosophical Transactions of the Royal Society of London Series B-Biological* 345, 281-287.
- Nagata, S. (1997). Apoptosis by death factor. *Cell* 88, 355-365.
- Nakagawa, T., Zhu, H., Morishima, N., Li, E., Xu, J., Yankner, B. A., and Yuan, J. (2000). Caspase-12 mediates endoplasmic-reticulum specific apoptosis and cytotoxicity by amyloid- $\beta$ . *Nature* 403, 98-103.
- Ng, F.W.H., Nguyen, M., Kwan, T., Branton, P.E., Nicholson, D.W., Cromlish, J.A., Shore, and GC. (1997). p28 Bap31, a Bcl-2/Bcl-X(L)- and procaspase-8-associated protein in the endoplasmic reticulum. *Journal of Cell Biology* 139, 327-338.
- Nicholson, D.W. (1996). Ice/ced3-like proteases as therapeutic targets for the control of inappropriate apoptosis. *Nature Biotechnology* 14, 297-301.
- Nicholson, D.W., Ali, A., Thornberry, N.A., Vaillancourt, J.P., Ding, C.K., Gallant, M., Gareau, y., Griffin, P.R., Labelle, M., Lazebnik, Y.A., Munday, N.A., Raju, S.R., Smulson, M.E., Yamin, T.-T., Yu, V.L., and Miller, D.K. (1995). Identification and inhibition of the ICE/CED-3 protease necessary for mammalian apoptosis. *Nature* 376, 37-43.
- Nicholson, D.W. and Thornberry, N.A. (1997). Caspases: Killer proteases. *Trends in Biochemical Sciences* 22, 299-306.
- Nishizuka, Y. (1988). The molecular heterogeneity of protein kinase C and its implications for cellular regulation. *Nature* 334, 661-665.
- Northrop, J.P., Ho, S.N., Chen, L., Thomas, D.J., Timmerman, L.A., Nolan, G.P., Admon, A., and Crabtree, G.R. (1994). NF-AT components define a family of transcription factors targeted in T-cell activation. *Nature* 369, 497-502.
- Nosseri, C., Coppola, S., and Ghibelli, L. (1994). Possible involvement of ploy(ADP-ribose) polymerase in triggering stress-induced apoptosis. *Exp.Cell Res.* 212, 367-373.
- Nunez, G., London, L., Hockenbery, D.M., Alexander, M., McKeaon, J.P., and Korsmeyer, S.J. (1990). Deregulated Bcl-2 gene expression selectively prolongs survival of growth factor-deprived hemopoietic cell lines. *J.Immunol.* 144, 3602-3610.
- O'Reilly, L.A., Huang, D.C.S., and Strasser, A. (1996). The cell death inhibitor BCL-2 and its homologues influence control of cell cycle entry. *EMBO J.* 15, 6979-6990.
- Oberhammer, F., Wilson, J.W., Dive, C., Morris, I.D., Hickman, J.A., Wakeling, A.E., Walker, P.R., and Sikorska, M. (1993). Apoptotic death in epithelial cells: cleavage of DNA to 300 and/or 50 kb fragments prior to or in the absence of internucleosomal fragmentation. *EMBO J.* 12, 3679-3684.
- Oberhammer, F.A., Hochegger, K., Fröschl, G., Tiefenbacher, R., and Pavelka, M. (1994). Chromatin condensation during apoptosis is accompanied by degradation of lamin A+B, without enhanced activation of cdc2 kinase. *J.Cell Biology* 126, 827-837.

- Oehm, A., Behrmann, I., Falk, W., Pawlita, M., Maier, G., Klaus, C., Li-Weber, M., Richard, S., Dhein, J., Trauth, B.C., Ponsting, H., and Krammer, P.H. (1992). Purification and molecular cloning of the APO-1 cell surface antigen, a member of the Tumor Necrosis Factor/Nerve Growth Factor receptor superfamily. *J.Biol.Chem.* 267, 10709-10715.
- Oltvai, Z.N. and Korsmeyer, S.J. (1994). Checkpoints of dueling dimers foil death wishes. *Cell* 79, 189-192.
- Oltvai, Z.N., Milliman, C., and Korsmeyer, S.J. (1993). Bcl-2 heterodimerizes *in vivo* with a conserved homolog, bax, that accelerates programmed cell death. *Cell* 74, 609-619.
- Otter, I., Conus, S., Ravn, U., Rager, M., Olivier, R., Monney, L., Fabbro, D., and Borner, C. (1998). The binding properties and biological activities of Bcl-2 and Bax in cells exposed to apoptotic stimuli. *Journal of Biological Chemistry* 273, 6110-6120.
- Pan, G., Humke, E.W., and Dixit, V.M. (1998). Activation of caspases triggered by cytochrome c *in vitro*. *FEBS Lett.* 426, 151-154.
- Pan, G., Ni, J., Wei, Y.-F., Yu, G.-I., Gentz, R., and Dixit, V.M. (1997). An antagonist decoy receptor and a death domain-containing receptor for TRAIL. *Science* 277, 815-818.
- Pan, G., O'Rourke, K., and Dixit, V.M. (1998). Caspase-9, Bcl-X(L), and Apaf-1 form a ternary complex. *J.Biol.Chem.* 273, 5841-5845.
- Peitsch, M.C., Mannherz, H.G., and Tschopp, J. (1994). The apoptosis endonucleases: cleaning up after cell death? *Trends Cell Biol.* 4, 37-41.
- Perry, D.K., Smyth, M.J., Wang, H.G., Reed, J.C., Duriez, P., Poirier, G.G., Obeid, L.M., and Hannun, Y.A. (1997). Bcl-2 acts upstream of the parp protease and prevents its activation. *Cell Death Different.* 4, 29-33.
- Peter, M.E., Kischkel, F.C., Hellbardt, S., Chinnaiyan, A.M., Krammer, P.H., and Dixit, V.M. (1996). CD95 (APO-1/Fas)-associating signalling proteins. *Cell Death & Differentiation* 3, 161-170.
- Peter, M.E., Kischkel, F.C., Scheuerpflug, C.G., Medema, J.P., Debatin, K.M., and Krammer, P.H. (1997). Resistance of cultured peripheral t cells towards activation-induced cell death involves a lack of recruitment of flice (mach/caspase 8) to the cd95 death-inducing signaling complex. *Eur.J.Immunol.* 27, 1207-1212.
- Pezzella, F., Tse, A.G.D., Cordell, J.L., Pulford, K.A.F., Gatter, K.C., and Mason, D.Y. (1990). Expression of the bcl-2 oncogene protein is not specific for the 14;18 chromosomal translocation. *Am.J.Pathol.* 137, 225-232.
- Porter, A.G. and Janicke, R.U. (1999). Emerging roles of caspase-3 in apoptosis. *Cell Death & Differentiation* 6, 99-104.
- Pratt, R.M. and Martin, G.R. (1975). Epithelial cell death and cyclic AMP increase during palatal development. *Proc.Natl.Acad.Sci.USA* 72, 874-877.

- Rabizadeh, S., LaCount, D. J., Friesen, P. D., and Bredesen, D. E. (1993). Expression of baculovirus p35 gene inhibits mammalian cell death. *Journal of Neurochemistry* *61*, 2318-2321.
- Raff, M. C. (1992). Social controls on cell survival and cell death. *Nature* *356*, 397-400.
- Rao, A., Luo, C., and Hogan, P.G. (1997). Transcription factors of the NFAT family: regulation and function. *Annual Review of Immunology* *15*, 707-747.
- Rao, L., Perez, D, and White, E. (1996). Lamin proteolysis facilitates nuclear events during apoptosis. *J.Cell Biol.* *135*, 1441-1455.
- Ray, C.A., Black, R.A., Kronheim, S.R., Greenstreet, T.A., Sleath, P.R., Salvesen, G.S., and Pickup, D.J. (1992). Viral inhibition of inflammation: Cowpox virus encodes an inhibitor of the interleukin-1beta converting enzym. *Cell* *69*, 597-604.
- Raynal, P. and Pollard, H. B. (1994). Annexins: the problem of assessing the biological role for a gene family of multifunctional calcium- and phospholipid-binding proteins. *Biochim.Biophys.Acta* *1197*, 63-93.
- Reed, J.C. (1994). Bcl-2 and the regulation of programmed cell death. *Journal of Cell Biology* *124*, 1-6.
- Reed, J.C. (1997). Double identity for proteins of the bcl-2 family. *Nature* *387*, 773-776.
- Reed, J. C., Miyashita, T., Takayama, S., Wang, H-G., Sato, T., Krajewski, S., Aime-Sempe, C., Bodrug, S., Kitada, S., and Hanada, M. (1996). Bcl-2 family proteins: Regulators of cell death involved in the pathogenesis of cancer and resistance to therapy. *J Chem Biochem* *60*, 23-32.
- Reipert, S., Reipert, B.M., Hickman, J.A., and Allen, T.D. (1998). Nuclear pore clustering is a consistent feature of apoptosis in vitro. *Cell Death and Differentiation*, *3*(1) 131-139.
- Richter, C., Schweizer, M., Cossarizza, A., and Franceschi, C. (1996).Control of apoptosis by the cellular ATP level. *FEBS Letters* *378*, 107-110.
- RieuxLaucat, F., Le Deist, F., Hivroz, C., Roberts, I. A. G., Debatin.K.M., Fischer, A., and De Villartay, J. P. (1995).Mutation in Fas associated with human lymphoproliferative syndrome and autoimmunity. *Science* *268*, 1347-1349.
- Rosse, T., Olivier, R., Monney, L., Rager, M., Conus, S., Fellay, I., Jansen, B., and Borner, C. (1998). Bcl-2 prolongs cell survival after Bax-induced release of cytochrome c. *Nature* *391*, 496-499.
- Rostovtseva, T. and Columbini, M. (1997). VDAC channels mediate and gate flow of ATP: implications for the regulation of mitochondrial function. *J.Biophys* *72*, 1954-1962.
- Rothe, M., Pan, M.-G., Henzel, W.J., Ayres, T.M., and Goeddel, D.V. (1995). The TNFR2-TRAF signaling complex contains two novel proteins related to baculoviral inhibitor of apoptosis proteins. *Cell* *83* , 1243-1252.

- Roy, N., Deveraux, Q.L., Takahashi, R., Salvesen, G.S., and Reed, J.C. (1997). The c-IAP-1 and c-IAP-2 proteins are direct inhibitors of specific caspases. *EMBO J.* 16, 6914-6925.
- Roy, N., Mahadevan, M. S., Mclean, M., Shutler, G., Yaraghi, Z., Farahani, R., Baird, S., Besner-Johnston, A., Lefebvre, C., Kang, X., Salih, M., Aubrey, H., Tamai, K., Guan, X., Ioannou, P., Crawford, T. O., de Jong, P. J., Surh, H., Ideda, J. E., Korneluk, R. G., and MacKenzie, A. (1995). The gene for neuronal apoptosis inhibitory protein is partially deleted in individuals with spinal muscular atrophy. *Cell* 80, 167-178.
- Rudel, T. and Bokoch, G.M. (1997). Membrane and morphological changes in apoptotic cells regulated by caspase-mediated activation of PAK2. *Science* 276, 1571-1574.
- Russell, J. H. (1995). Activation induced cell death of mature T cells in the regulation of immune responses. *Current Opinion in Immunology* 7, 382.
- Sakahira, H., Enari, M., and Nagata, S. (1998). Cleavage of CAD inhibitor in CAD activation and DNA degradation during apoptosis. *Nature* 391, 96-99.
- Samali, A., Cai, J., Zhivotovsky, B., Jones, D. P., and Orrenius, S. (1999). Presence of a pre-apoptotic complex of pro-caspase-3, Hsp60 and Hsp10 in the mitochondrial fraction of Jurkat T cells. *Embo Journal* 18, 2040-2048.
- Samejima, K., Tone, S., Kottke, T.J., Enari, M., Sakahira, H., Cooke, C.A., Durrieu, F, Martins, L.M., Nagata, S., Kaufmann, S.H., and Earnshaw, W.C. (1998). Transition from caspase-dependent to caspase-independent mechanisms at the onset of apoptotic execution. *Journal of Cell Biology* 143, 225-239.
- Sattler, M., Liang, H., Nettekheim, D., Meadows, R.P., Harlan, J.E., Eberstadt, M., Ho Sup Yoon, Shuker, S.B., Chang, B.S., Minn, A.J., Thompson, C.B., and Fesik, S.W. (1997). Structure of Bcl-x(1)-Bak peptide complex: Recognition between regulators of apoptosis. *Science* 275, 983-986.
- Saunders J.W (1966). Death in the embryonic systems. *Science* 154, 604-612.
- Savill, J.S., Fadok, V., Henson, P., and Haslett, C. (1993). Phagocyte recognition of cells undergoing apoptosis. *Immunol.Today* 14, 131-136.
- Scaffidi, C., Fulda, S., Srinivasan, A., Friesen, C., Li, F., Tomaselli, K.J., Debatin, K.-M., Krammer, P.H., and Peter, M.E. (1998). Two CD95 (APO-1/Fas) signaling pathways. *EMBO J.* 17, 1675-1687.
- Scaffidi, C., Medema, J.P., Krammer, P.H., and Peter, M.E. (1997). FLICE is predominantly expressed as two functionally active isoforms, caspase-8/a and caspase-8/b. *J.Biol.Chem.* 272, 26953-26958.
- Scaffidi, C., Schmitz, I., Zha, J., Korsmeyer, S. J., Krammer, P. H, and Peter, M. E. (1999). Differential modulation of apoptosis sensitivity in CD95 type I and type II cells. *Journal of Biological Chemistry* 274, 22532-22538.

- Schendel, S.L., Xie, Z., Montal, M.O., Matsuyama, S., Montal, M., and Reed, J.C. (1997). Channel formation by antiapoptotic protein bcl-2. *Proceedings of the National Academy of Sciences of the United States of America* 94, 5113-5118.
- Schlesinger, P. H., Gross, A., Yin, X-M., Yamamoto, K., Saito, M., Waksman, G., and Korsmeyer, S. J. (1997). Comparison of the ion channel characteristics of proapoptotic Bax and antiapoptotic Bcl-2. *Proc.Natl.Acad.Sci.USA* 94, 11357-11362.
- Schmeiser, K., Hammond, E. M., Roberts, S., and Grand, R. J. A. (1998). Specific cleavage of  $\gamma$  catenin by caspases during apoptosis. *FEBS Letters* 433, 51-57.
- Schneider, P., Bodmer, J.-L., Holler, N., Mattmann, C., Scuderi, P., Terskikh, A., Peitsch, M.C., and Tschopp, J. (1997). Characterization of Fas (Apo-1, CD95)-Fas ligand interaction. *J.Biol.Chem.* 272, 18827-18833.
- Schneider, U., Schwenck, H., and BornKamm, G. (1977). Characterization of EBV-genome negative "null" and "T" cell lines derived from children with acute lymphoblastic leukaemia and leukaemia transformed non-hodgkins lymphoma. *Int.J.Cancer* 19, 621.
- Schulze-Osthoff, K. (1994). The Fas/APO-1 receptor and its deadly ligand. *Trends in Cell Biology* 4, 421-427.
- Schulze-Osthoff, K., Krammer, P.H., and Dröge, W. (1994b). Divergent signalling via APO-1/Fas and the TNF receptor, two homologous molecules involved in physiological cell death. *EMBO J.* 13, 4587-4596.
- Sentman, C.L., Shutter, J.R., Hockenbery, D.M., Kanagawa, O., and Korsmeyer, S.J. (1991). Bcl-2 inhibits multiple forms of apoptosis but not negative selection in thymocytes. *Cell* 67, 879-888.
- Shen, Y. and Shenk, T. E. (1995). Viruses and apoptosis. *Current Biology* 5, 105-111.
- Shi, L., Nishioka, W.K., Th'ng, J., Bradbury, E.M., Litchfield, D.W., and Greenberg, A.H. (1994). Premature p34<sup>cdc2</sup> activation required for apoptosis. *Science* 263, 1143-1145.
- Shi, Y., Bissonnette, R.P., Parfrey, N., Szalay, M., Kubo, R.T., and Green, D.R. (1991). *In vivo* administration of monoclonal antibodies to the CD3 T cell receptor complex induces cell death (apoptosis) in immature thymocytes. *J.Immunol.* 146, 3340-3346.
- Shibasaki, F., Kondo, E., Akagi, T., and McKeon, F. (1997). Suppression of signalling through transcription factor nf-at by interactions between calcineurin and bcl-2. *Nature* 386, 728-731.
- Shibasaki, F. and McKeon, F. (1995). Calcineurin functions in ca<sup>2+</sup>-activated cell death in mammalian cells. *Journal of Cell Biology* 131, 735-743.
- Shimizu, S., Narita, M., and Tsujimoto, Y. (1999). Bcl-2 family proteins regulate the release of cytochrome c by the mitochondrial channel VDAC. *Nature* 399, 483-487.
- Simbulan-Rosenthal, C., Rosenthal, D. S., Iyer, S., Boulares, A. H., and Smulson, M. E. (1998). Transient poly(ADP-ribosyl)ation of nuclear proteins and role of poly(ADP-ribose)

polymerase in the early stages of apoptosis. *Journal of Biological Chemistry* 273, 13703-13712.

Simonian, P.L., Grillot, D.A.M., Merino, R., and Nunez, G. (1996). Bax can antagonize Bcl-X(L) during etoposide and cisplatin- induced cell death independently of its heterodimerization with Bcl-X(L). *J.Biol.Chem.* 271, 22764-22772.

Singer, G. G and Abbas, A. K. (1994). The Fas antigen is involved in peripheral but not thymic deletion of T lymphocytes in T cell receptor transgenic mice. *Immunity* 1, 365-371.

Sleath, P. R., Hendrickson, R. C, Kronheim, S. R, March, C. J, and Black, R. A. (1990). Substrate specificity of the protease that processes human interleukin-1 $\beta$ . *Journal of Biological Chemistry* 265, 14526-14528.

Slee, E. A., Harte, M., Kluck, R. M., Casiano, C. A., Newmeyer, D. D., Wang, H-G., Reed, J. C., Nicholson, D. W., Alnemri, E. S., Green, D. R., and Martin, S. J. (1999). Ordering the cytochrome c-initiated caspase cascade: Hierarchical activation of caspases-2, -3, -6, -7, -8 and -10 in a caspase-9-dependent manner. *Journal of Cell Biology* 144, 281-292.

Slee, E.A., Zhu, H., Chow, S.C., MacFarlane, M., Nicholson, D.W., and Cohen, G.M. (1996). Benzylloxycarbonyl-val-ala-asp (ome) fluoromethylketone (z- vad.fmk) inhibits apoptosis by blocking the processing of cpp32. *Biochem.J.* 315, 21-24.

Smith, C.A., Williams, G.T., Kingston, R., Jenkinson, E.J., and Owen, J.J.T. (1989). Antibodies to CD3/T-cell receptor complex induce death by apoptosis in immature T cells in thymic cultures. *Nature* 337, 181-184.

Smith.C.A., Farrah, T., and Goodwin, R. G. (1994). The TNF receptor superfamily of cellular and viral proteins-activation, costimulation and death. *Cell* 76, 959-962.

Song, Q., Lees-Miller, S. P, Kumar, S., Zhang, Z., Chan, D. W., Smith, G. C., Jackson, S. P., Alnemri, E. S., Litwack, G., Khanna, K. K., and Lavin, M. F. (1996). DNA-dependent protein kinase catalytic subunit: A target for an ICE-like protease in apoptosis. *EMBO J.* 15, 3238-3246.

Spector, M.S., Desnoyers, S., Hoepfner, D.J., and Hengartner, M.O. (1997). Interaction between the *C. elegans* cell-death regulators CED-9 and CED- 4. *Nature* 385, 653-656.

Squier, M.K.T. and Cohen, J.J. (1996). Calpain and cell death. *Cell Death Different.* 3, 275-283.

Srinivasula, S. M., Ahmad, M., Fernandes-Alnemri, T., and Alnemri, E. S. (1998). Autoactivation of procaspase-9 by Apaf-1 mediated oligomerization. *Molecular Cell* 1, 949-957.

Srinivasula, S.M., Ahmad, M., FernandesAlnemri, T., Litwack, G., and Alnemri, E.S. (1996a). Molecular ordering of the fas-apoptotic pathway: the fas/apo-1 protease mch5 is a crma-inhibitable protease that activates multiple ced-3/ice-like cysteine proteases. *Proceedings of the National Academy of Sciences of the United States of America* 93, 14486-14491.

Srinivasula, S.M., FernandesAlnemri, T., Zangrilli, J., Robertson, N., Armstrong, R.C., Wang, L., Trapani, J.A., Tomaselli, K.J., Litwack, G., and Alnemri, E.S. (1996b). The ced-3/interleukin 1beta converting enzyme-like homolog mch6 and the lamin-cleaving enzyme mch2alpha are substrates for the apoptotic mediator cpp32. *J.Biol.Chem.* *271*, 27099-27106.

Stanger, B.Z., leder, P., Lee, T.-H., kim, E., and Seed, B. (1995). RIP: A novel protein containing a death domain that interacts with FAS/APO-1 (CD95) in yeast and causes cell death. *Cell* *81*, 513-523.

steller, H. (1995). Mechanisms and genes of cellular suicide. *Science* *267*, 1445-1449.

Stennicke, H. R., Jurgensmeier, J. M., Shin, H., Deveraux, Q., Wolf, B. B, Yang, X., Zhou, Q., Ellerby, L. M., Bredesen, D., Green, D. R., Reed, J. C., Froelich, C. J., and Salvesen, G. S. (1998). Pro-caspase-3 is a major physiologic target of caspase-8. *Journal of Biological Chemistry* *273*, 27084-27090.

Stennicke, H. R. and Salvesen, G. S. (1998). Properties of the caspases. *Biochim.Biophys.Acta* *1387*, 17-31.

Strand, S., Hoffman, W. J., Hug, H., Muller, M., Otto, G., Strand, D., Mariani, S. M., Stremmel, W., Krammer, P. H, and Galle, P. R. (1996).Lymphocyte apoptosis induced by CD95 (APO-1/Fas) ligand expressing tumor cells- A mechanism of immune evasion. *Nature Medicine* *2*, 1361-1366.

Strasser, A. (1995). Death of a T cell. *Nature* *373*, 385-386.

Strasser, A., Harris, A.W., and Cory, S. (1991). *bcl-2* transgene inhibits T cell death and perturbs thymic self- censorship. *Cell* *67*, 889-899.

Strasser, A., Harris, A.W., Huang, D.C.S., Krammer, P.H., and Cory, S. (1995). Bcl-2 and Fas/APO-1 regulate distinct pathways to lymphocyte apoptosis. *EMBO J.* *14*, 6136-6147.

Suda, T., Okazaki, T., Naito, Y., Yokota, T., Arai, A., Ozaki, S., Nakao, K., and Nagata, S. (1995). Expression of the Fas ligand in cells of T cell lineage. *J.Immunol.* *154*, 3806-3813.

Suda, T., Takahashi, T., Golstein, P., and Nagata, S. (1993). Molecular cloning and expression of the Fas Ligand, a novel member of the tumor necrosis factor family. *Cell* *75*, 1169-1178.

Sugimoto, A., Friesen, P. D., and Rothman, J. H. (1994). Baculovirus p35 prevents developmentally programmed cell death and rescues a ced-9 mutant in the nematode *Caenorhabditis elegans*. *EMBO J.* *13*, 2023-2028.

Sun, X.-M. and Cohen, G.M. (1994). Mg<sup>2+</sup>-dependent cleavage of DNA into kilobase pair fragments is responsible for the initial degradation of DNA in apoptosis. *J.Biol.Chem.* *269*, 14857-14860.

Sun, X.-M., MacFarlane, M., Zhuang, J., Wolf, B. B, Green, D. R., and Cohen, G. M. (1999). Distinct caspase cascades are initiated in receptor-mediated and chemical induced apoptosis. *Journal of Biological Chemistry* *274*, 5053-5060.

Susin, S. A., Lorenzo, H. K., Zamzami, N., Marzo, I., Brenner, C., Larochette, N., Prevost, M. C., Alzari, P. M., and Kroemer, G. (1999). Mitochondrial release of caspase-2 and -9 during the apoptotic process. *J.Exp.Med.* 189, 381-394.

Susin, S. A., Lorenzo, H. K., Zamzami, N., Marzo, I., Snow, B. E., Brothers, G. M., Mangion, J., Jacotot, E., Costantini, P., Loeffler, M., Larochette, N., Goodlet, D. R., Aebersold, R., Siderovski, D. P., Penninger, J. M., and Kroemer, G. (1999). Molecular characterization of mitochondrial apoptosis inducing factor. *Nature* 397, 441-446.

Susin, S.A., Zamzami, N., Castedo, M., Hirsch, T., Marchetti, P., Macho, A., Daugas, E., Geuskens, M., and Kroemer, G. (1996). Bcl-2 inhibits the mitochondrial release of an apoptogenic protease. *Journal of Experimental Medicine* 184, 1331-1341.

Tait, J. F., Gibson, D., and Fujikawa, K. (1989). Phospholipid binding properties of human placental anticoagulant protein -I, a member of the lipocortin family. *Journal of Biological Chemistry* 264, 7944-7949.

Takahashi, A., Alnemri, E.S., Lazebnik, Y.A., FernandesAlnemri, T., Litwack, G., Moir, R.D., Goldman, R.D., Poirier, G.G., Kaufmann, S.H., and Earnshaw, W.C. (1996). Cleavage of lamin a by mch2alpha but not cpp32: multiple interleukin 1beta- converting enzyme-related proteases with distinct substrate recognition properties are active in apoptosis. *Proceedings of the National Academy of Sciences of the United States of America* 93, 8395-8400.

Takahashi, A., GoldschmidtClermont, P.J., Alnemri, E.S., FernandesAlnemri, T., YoshizawaKumagaya, K., Nakajima, K., Sasada, M., Poirier, G.G., and Earnshaw, W.C. (1997a). Inhibition of ice-related proteases (caspases) and nuclear apoptosis by phenylarsine oxide. *Experimental Cell Research* 231, 123-131.

Takahashi, A., Hirata, H., Yonehara, S., Imai, Y., Lee, K.K., Moyer, R.W., Turner, P.C., Mesner, P.W., Okazaki, T., Sawai, H., Kishi, S., Yamamoto, K., Okuma, M., and Sasada, M. (1997b). Affinity labeling displays the stepwise activation of ice- related proteases by fas, staurosporine, and crma-sensitive caspase-8. *Oncogene* 14, 2741-2752.

Takahashi, R., Deveraux, Q., Tamm, I., Welsh, K., Assa-Munt, N., Salvesen, G.S., and Reed, J.C. (1998). A single BIR domain of XIAP sufficient for inhibiting caspases. *J.Biol.Chem.* 273, 7787-7790.

Takahashi, T., Tanaka, M., Brannan, C.I., Jenkins, N.A., Copeland, N.G., Suda, T., and Nagata, S. (1994). Generalized lymphoproliferative disease in mice, caused by a point mutation in the fas ligand. *Cell* 76, 969-976.

Talanian, R.V., Quinlan, C., Trautz, S., Hackett, M.C., Mankovich, J.A., Banach, D., Ghayur, T., Brady, K.D., and Wong, W.W. (1997). Substrate specificities of caspase family proteases. *J.Biol.Chem.* 272, 9677-9682.

Tanaka, M., Suda, T., Takahashi, T., and Nagata, S. (1995). Expression of the functional soluble form of human Fas ligand in activated lymphocytes. *EMBO J.* 14, 1129-1135.

Tang, D. and Kidd, V.J. (1998). Cleavage of DFF-45/ICAD by multiple caspases is essential for its function during apoptosis. *J.Biol.Chem.* 273, 28549-28552.

- Tartaglia, L. A., Weber, R. F., Figari, I. S., Reynolds, C., Palladino, M. A., and Goeddel, D. V. (1991). Two different receptors for tumour necrosis factor mediate distinct cellular responses. *Proc.Natl.Acad.Sci.USA* 88, 9292-9296.
- Tedeschi, G., Chen, S., and Massey, V. (1995). Active site studies of DT-diaphorase employing artificial flavins. *Journal of Biological Chemistry* 270, 2512-2516.
- Tewari, M. and Dixit, V.M. (1995a). Fas- and tumor necrosis factor-induced apoptosis is inhibited by the poxvirus *crmA* gene product. *J.Biol.Chem.* 270, 3255-3260.
- Tewari, M., Quan, L.T., O'Rourke, K., Desnoyers, S., Zeng, Z., Beidler, D.R., Poirier, G.G., Salvesen, G.S., and Dixit, V.M. (1995b). Yama/ CPP32 $\beta$ , a mammalian homolog of CED-3, is a CrmA-inhibitable protease that cleaves the death substrate poly(ADP-ribose) polymerase. *Cell* 81, 801-809.
- Thastrup, O., Cullen, P.J., Dröbak, B.K., Hanley, M.R., and Dawson, A.P. (1990). Thapsigargin, a tumor promoter, discharges intracellular Ca<sup>2+</sup> stores by specific inhibition of the endoplasmic reticulum Ca<sup>2+</sup>-ATPase. *Proc.Natl.Acad.Sci.USA* 87, 2466-2470.
- Thome, M., Schneider, P., Hofmann, K., Fickenscher, H., Meini, E., Neipel, F., Mattmann, C., Burns, K., Bodmer, J.L., Schroter, M., Scaffidi, C., Krammer, P.H., Peter, M.E., and Tschopp, J. (1997). Viral flc-inhibitory proteins (flips) prevent apoptosis induced by death receptors. *Nature* 386, 517-521.
- Thompson, C.B. (1995). Apoptosis and the pathogenesis and treatment of disease. *Science* 267, 1456-1462.
- Thornberry, N.A., Bull, H.G., Calaycay, J.R., Chapman, K.T., Howard, A.D., Kostura, M.J., Miller, D.K., Molineaux, S.M., Weidner, J.R., Aunins, J., Elliston, K.O., Ayala, J.M., Casano, F.J., Chin, J., Ding, G.J.F., Egger, L.A., Gaffney, E.P., Limjuco, G., Palyha, O.C., and et, a. (1992). A novel heterodimeric cysteine protease is required for interleukin-1 $\beta$  processing in monocytes. *Nature* 356, 768-774.
- Thornberry, N. A. and Lazebnik, Y. (1998). Caspases: Enemies within. *Science* 281, 1312-1316.
- Thornberry, N.A. and Molineaux, S.M. (1995). Interleukin-1 $\beta$  converting enzyme: a novel cysteine protease required for il-1 $\beta$  production and implicated in programmed cell death. *Protein Science* 4, 3-12.
- Thornberry, N.A., Peterson, E.P., Zhao, J.J., Howard, A.D., Griffin, P.R., and Chapman, K.T. (1994). Inactivation of interleukin-1 $\beta$  converting enzyme by peptide (acyloxy)methyl ketones. *Biochemistry (USA)* 33, 3934-3940.
- Thornberry, N.A., Rano, T.A., Peterson, E.P., Rasper, D.M., Timkey, T., Garcia-Calvo, M., Houtzager, V.M., Nordstrom, P.A., Roy, S., Vaillancourt, J.P., Chapman, K.T., and Nicholson, D.W. (1997). A combinatorial approach defines specificities of members of the caspase family and granzyme B: Functional relationships established for key mediators of apoptosis. *J.Biol.Chem.* 272, 17907-17911.

- Toh, S.Y., Wang, X., and Li, P. (1998). Identification of the nuclear factor HMG2 as an activator for DFF nuclease activity. *Biochemical & Biophysical Research Communications* 250, 598-601.
- Trauth, B.C., Klas, C., Peters, A.M.J., Matzku, S., Moller, P., Falk, W., Debatin, K., and Krammer, P.H. (1989). Monoclonal antibody-mediated tumor regression by induction of apoptosis. *Science* 245, 301-305.
- Tsujimoto, Y. (1997). Apoptosis and necrosis intracellular ATP as a determinant for cell death modes. *Cell Death & Differentiation* 4, 429-434.
- Tsujimoto, Y., Gorham, J., Cossman, J., Jaffe, E., and Croce, C.M. (1985). The t(14;18) chromosome translocations involved in B-cell neoplasms result from mistakes in VDJ joining. *Science* 229, 1300-1303.
- Uhlmann, E.J., Subramanian, T., Vater, C. A., Lutz, R., and Chinnadurai, G. (1998). A potent cell death activity associated with transient high level expression of Bcl-2. *Journal of Biological Chemistry* 273, 17926-17932.
- Vairo, G., Innes, K.M., and Adams, J.M. (1996). Bcl-2 has a cell cycle inhibitory function separable from its enhancement of cell survival. *Oncogene* 13, 1511-1519.
- Van de Craen, M., Van Loo, G., Pype, S., Van Crielinge, W., Van den Brande, I., Molemans, F., Fiers, W., Declercq, W., and Vandenabeele, P. (1998). Identification of a new caspase homologue: caspase-14. *Cell Death & Differentiation* 5, 838-846.
- Van de Craen, M., Vandenabeele, P., Declercq, W., Van den Brande, I., Van Loo, G., Molemans, F., Schotte, P., Van Crielinge, W., Beyaert, R., and Fiers, W. (1997). Characterization of seven murine caspase family members. *FEBS Lett.* 403, 61-69.
- Vance, B.A., Zacharchuk, C.M., and Segal, D.M. (1996). Recombinant mouse Bcl-2((1-203)): Two domains connected by a long protease-sensitive linker. *J.Biol.Chem.* 271, 30811-30815.
- Vander Heiden, M., Chandel, N. S., Williamson, E. K., Schumacker, P. T., and Thompson, C. B. (1997). Bcl-xL regulates the membrane potential and volume homeostasis of mitochondria. *Cell* 91, 627-637.
- Vander Heiden, M. and Thompson, C. B. (1999). Bcl-2 proteins: regulators of apoptosis or of mitochondrial homeostasis? *Nature Cell Biology* 1, 209-215.
- Varfolomeev, E.E., Boldin, M.P., Goncharov, T.M., and Wallach, D. (1996). A potential mechanism of 'cross-talk' between the p55 tumor necrosis factor receptor and Fas/APO1: Proteins binding to the death domains of the two receptors also bind to each other. *Journal of Experimental Medicine* 183, 1271-1275.
- Vaux, D.L. (1997). CED-4 - The third horseman of apoptosis. *Cell* 90, 389-390.
- Vaux, D.L., Cory, S., and Adams, J.M. (1988). Bcl-2 gene promotes haemopoietic cell survival and cooperates with c-myc to immortalize pre-B cells. *Nature* 335, 440-442.

- Verhoven, B., Schlegel, R.A., and Williamson, P. (1995). Mechanisms of phosphatidylserine exposure, a phagocyte recognition signal, on apoptotic T lymphocytes. *Journal of Experimental Medicine* 182, 1597-1601.
- Vincenz, C. and Dixit, V.M. (1997). Fas-associated death domain protein interleukin-1beta-converting enzyme 2 (flice2), an ice/ced-3 homologue, is proximally involved in cd95- and p55- mediated death signaling. *J.Biol.Chem.* 272, 6578-6583.
- Walczak, H., Degli-Esposti, M.A., Johnson, R.S., Smolak, P.J., Waugh, J.Y., Boiani, N., Timour, M.S., Gerhart, M.J., Schooley, K.A., Smith, C.A., Goodwin, R.G., and Rauch, C.T. (1997). TRAIL-R2: A novel apoptosis-mediating receptor for TRAIL. *EMBO J.* 16, 5386-5397.
- Walker, N.P.C., Talanian, R.V., Brady, K.D., Dang, L.C., Bump, N.J., Ferez, C.R., Franklin, S., Ghayur, T., Hackett, M.C., Hammill, L.D., Herzog, L., Hugunin, M., Houy, W., Mankovich, J.A., McGuinness, L., Orlewicz, E., Paskind, M., Pratt, C.A., Reis, P., and et, a. (1994). Crystal structure of the cysteine protease interleukin-1beta- converting enzyme: a (p20/p10)<sub>2</sub> homodimer. *Cell* 78, 343-352.
- Walker, P.R., Weaver, V.M., Lach, B., Leblanc, J., and Sikorska, M. (1994). Endonuclease activities associated with high molecular weight and internucleosomal DNA fragmentation in apoptosis. *Exp.Cell Res.* 213, 100-106.
- Wallach, D., Boldin, M., Varfolomeev, E., Beyaert, R., Vandenabeele, P., and Fiers, W. (1997). Cell death induction by receptors of the TNF family: Towards a molecular understanding. *FEBS Lett.* 410, 96-106.
- Wang, H.-G., Miyashita, T., Takayama, S., Sato, T., Torigoe, T., Krajewski, S., Tanaka, S., Hovey, I.I.L., Troppmair, J., Rapp, U.R., and Reed, J.C. (1994). Apoptosis regulation by interaction of Bcl-2 protein and Raf-1 kinase. *Oncogene* 9, 2751-2756.
- Waring, P., Kos, F.J., and Millbacher, A. (1991). Apoptosis or programmed cell death. *Med.Res.Rev.* 11, 219-236.
- Watanabe-Fukunaga, R., Brannan, C.I., Copeland, N.G., Jenkins, N.A., and Nagata, S. (1992). Lymphoproliferation disorder in mice explained by defects in Fas antigen that mediates apoptosis. *Nature* 356, 314-316.
- WatanabeFukunaga, R., Brannan, C.I., Copeland, N.G., Jenkins, N.A., and Nagata, S. (1992). Lymphoproliferation disorder in mice explained by defects in fas antigen that mediates apoptosis. *Nature* 356, 314-317.
- Watson, A. J. M, Merritt, A. J., Jones, L. S., Askew, J. N., Anderson, E., Becciolini, A., Balzi, M., Potten, C. S., and Hickman, J. A. (1996). Evidence of reciprocity of bcl-2 and p53 expression in human colorectal adenomas and carcinomas. *Br.J.Cancer* 73, 889-895.
- Weis, M., Schlegel, J., Kass, G.E.N., Holmstrom, T.H., Peters, I., Eriksson, J., Orrenius, S., and Chow, S.C. (1995a). Cellular events in fas/apo-1-mediated apoptosis in jurkat t lymphocytes. *Experimental Cell Research* 219, 699-708.

- Weis, M., Schlegel, J., Kass, G.E.N., Holmström, T.H., Peters, I., Eriksson, J.E., Orrenius, S., and Chow, S.C. (1995b). Cellular events in Fas/APO-1-mediated apoptosis in JURKAT T lymphocytes. *Exp.Cell Res.* 219, 699-708.
- Weiss, A and Littman, D. R. (1994). Signal transduction by lymphocyte antigen receptors. *Cell* 76, 263-274.
- Whyte, M. (1996). A link between cell-surface receptors and ICE proteases. *Trends Cell Biol.* 6, 418.
- Williams, G.T., Smith, C.A., McCarthy, N.J., and Grimes, E.A. (1992). Apoptosis: Final control point in cell biology. *Trends Cell Biol.* 2, 263-267.
- Williams, M.S. and Henkart, P.A. (1994). Apoptotic cell death induced by intracellular proteolysis. *J.Immunol.* 153, 4247-4255.
- Wilson, K.P., Black, J.A.F., Thomson, J.A., Kim, E.E., Griffith, J.P., Navia, M.A., Murcko, M.A., Chambers, S.P., Aldape, R.A., Raybuck, S.A., and Livingston, D.J. (1994). Structure and mechanism of interleukin-1beta converting enzyme. *Nature* 370, 270-275.
- Wolf, B. B and Green, D. R. (1999). Suicidal tendencies: Apoptotic cell death by caspase family proteinases. *Journal of Biological Chemistry* 274, 20049-20052.
- Wolf, B. B, Schuler, M, Echeverri, F., and Green, D. R. (1999). Caspase-3 is the primary activator of apoptotic DNA fragmentation via DNA fragmentation factor-45/Inhibitor of caspase-activated DNase inactivation. *Journal of Biological Chemistry* 274, 30651-30656.
- Woo, M., Hakem, R., Soengas, M.S., Duncan, G.S., Shahinian, A., Kagi, D., Hakem, A., McCurrach, M., Khoo, W., Kaufman, S.A., Senaldi, G., Howard, T., Lowe, S.W., and Mak, T.W. (1998). Essential contribution of caspase 3/CPP32 to apoptosis and its associated nuclear changes. *Genes & Development* 12, 806-819.
- Wöhrl, W. and Häcker, G. (1999). Extent and limitation of the control of nuclear apoptosis by DNA-fragmentation factor. *Biochem.Biophys.Res.Comm.* 254, 552-558.
- Wu, D., Wallen, H.D., Inohara, N., and Nunez, G. (1997a). Interaction and regulation of the *Caenorhabditis elegans* death protease CED-3 by CED-4 and CED-9. *J.Biol.Chem.* 272, 21449-21454.
- Wu, D., Wallen, H.D., and Nunez, G. (1997b). Interaction and regulation of subcellular localization of CED-4 by CED-9. *Science* 275, 1126-1129.
- Wu, J., Wilson, J., He, J., Xiang, L., Schur, P. H., and Mountz, J. D. (1996). Fas ligand mutation in a patient with systemic lupus erythematosus and lymphoproliferative disease. *J.Clin.Invest.* 98, 1107-1113.
- Wyllie, A.H. (1980a). Glucocorticoid-induced thymocyte apoptosis is associated with endogenous endonuclease activation. *Nature* 284, 555-556.
- Wyllie, A.H., Kerr, J.F.R., and Currie, A.R. (1980b). Cell death: The significance of apoptosis. *Int.Rev.Cytol.* 68, 251-306.

Xiang, J., Chao, D.T., and Korsmeyer, S.J. (1996). Bax-induced cell death may not require interleukin 1beta- converting enzyme-like proteases. *Proceedings of the National Academy of Sciences of the United States of America* 93, 14559-14563.

Xue, D. and Horvitz, H.R. (1995). Inhibition of the *Caenorhabditis elegans* cell-death protease CED-3 by a CED-3 cleavage site in baculovirus p35 protein. *Nature* 377, 248-251.

Yakovlev, A.G., Knoblach, S.M., Fan, L., Fox, G.B., Goodnight, R., and Faden, A.I. (1997). Activation of CPP32-like caspases contributes to neuronal apoptosis and neurological dysfunction after traumatic brain injury. *J.Neurosci.* 17, 7415-7424.

Yang, J., Liu, X., Bhalla, K., Kim, C.N., Ibrado, A.M., Cai, J., Peng, T.I., Jones, D.P., and Wang, X. (1997). Prevention of apoptosis by bcl-2: release of cytochrome c from mitochondria blocked. *Science* 275, 1129-1132.

Yin, X.-M., Oltvai, Z.N., and Korsmeyer, S.J. (1994). BH1 and BH2 domains of bcl-2 are required for inhibition of apoptosis and heterodimerization with bax. *Nature* 369, 321-323.

Yonehara, S., Ishii, A., and Yonehara, M. (1989). A cell-killing monoclonal antibody (anti-fas) to a cell surface antigen co-downregulated with the receptor of tumor necrosis factor. *Journal of Experimental Medicine* 169, 1747-1756.

Yoshida, H., Kong, Y. Y., Yoshida, R., Elia, A. J., Hakem, A., Hakem, R., Penninger, J. M., and Mak, T. W. (1998). Apaf-1 is required for mitochondrial pathways of apoptosis and brain development. *Cell* 94, 739-750.

Yuan, J. (1996). Evolutionary conservation of a genetic pathway of programmed cell death. *J.Cell.Biochem.* 60, 4-11.

Yuan, J. (1997). Transducing signals of life and death. *Current Opinion in Cell Biology* 9, 247-251.

Yuan, J., Shaham, S., Ledoux, S., Ellis, H.M., and Horvitz, H.R. (1993). The *C. Elegans* cell death gene *ced-3* encodes a protein similar to mammalian interleukin-1  $\beta$ -converting enzyme. *Cell* 75, 641-652.

Zamzami, N., Marchetti, P., Castedo, M., Zanin, C., Vayssi re, J.-L., Petit, P.X., and Kroemer, G. (1995). Reduction in mitochondrial potential constitutes an early irreversible step of programmed lymphocyte death *in vivo*. *J.Exp.Med.* 181, 1661-1672.

Zha, H., AimeSempe, C., Sato, T., and Reed, J.C. (1996). Proapoptotic protein bax heterodimerizes with bcl-2 and homodimerizes with bax via a novel domain (BH3) distinct from BH1 and BH2. *J.Biol.Chem.* 271, 7440-7444.

Zha, H. and Reed, J.C. (1997). Heterodimerization-independent functions of cell death regulatory proteins Bax and Bcl-2 in yeast and mammalian cells. *J.Biol.Chem.* 272, 31482-31488.

- Zhang, H., Saeed, B., and Ng, S.C. (1995). Combinatorial interaction of human bcl-2 related proteins: mapping of regions important for bcl-2-bcl-x-s interaction. *Biochemical and Biophysical Research Communications* 208, 950-956.
- Zhang, J., Cado, D., Chen, A., Kabra, N. H., and Winoto, A. (1998). Fas-mediated apoptosis and activation-induced T-cell proliferation are defective in mice lacking FADD/Mort-1. *Nature* 392, 296-300.
- Zheng, T. S., Schlosser, S. F., Dao, T, Hingorani, R., Crispe, N., Boyer, J. L, and Flavell, R. A. (1998). Caspase-3 controls both cytoplasmic and nuclear events associated with Fas-mediated apoptosis *in vivo*. *Proc.Natl.Acad.Sci.USA* 95, 13618-13623.
- Zhivotovsky, B., Orrenius, S., Brustugun, O. T., and Døskeland, S. O. (1998). Injected cytochrome c induces apoptosis. *Nature* 391, 449-450.
- Zhou, B., Li, H., Yuan, J., and Kirschner, M. W. (1998). Caspase-dependent activation of cyclin-dependent kinases during Fas-induced apoptosis in Jurkat cells. *Proc.Natl.Acad.Sci.USA* 95, 6785-6790.
- Zhou, Q., Snipas, S., Orth, K., Muzio, M., Dixit, V.M., and Salvesen, G.S. (1997). Target protease specificity of the viral serpin crma. analysis of five caspases. *J.Biol.Chem.* 272, 7797-7800.
- Zhu, W., Cowie, A., Wasfy, G.W., Penn, L.Z., Leber, B., and Andrews, D.W. (1996). Bcl-2 mutants with restricted subcellular location reveal spatially distinct pathways for apoptosis in different cell types. *EMBO J.* 15, 4130-4141.
- Zhuang, J., Dinsdale, D., and Cohen, G. M. (1998). Apoptosis, in human monocytic THP-1 cells, results in the release of cytochrome c from mitochondria prior to their ultracondensation, formation of outer membrane discontinuities and reduction in inner membrane potential. *Cell Death & Differentiation* 5, 953-962.
- Zhuang, J., Ren, Y., Snowden, R.T., Zhu, H., Gogvadze, V., Savill, J.S., and Cohen, G.M. (1998b). Dissociation of Phagocyte Recognition of Cells Undergoing Apoptosis from Other Features of the Apoptotic Program. *J.Biol.Chem.* 273, 15628-15632.
- Zou, H., Henzel, W.J., Liu, X., Lutschg, A., and Wang, X. (1997). Apaf-1, a human protein homologous to *C. elegans* CED-4, participates in cytochrome c-dependent activation of caspase-3. *Cell* 90, 405-413.
- Zou, H., Li, Y., Liu, X., and Wang, X. (1999). An APAF-1-Cytochrome c multimeric complex is a functional apoptosome that activates procaspase-9. *Journal of Biological Chemistry* 274, 11549-11556.
- Zutter, M., Hockenbery, D., Silverman, G.A., and Korsmeyer, S.J. (1991). Immunolocalization of the Bcl-2 protein within hematopoietic neoplasms. *Blood* 78, 1062-1068.